UNIVERSITY OF ALBERTA

Functional assessment of the human copper transporter, ATP7B

By

Gloria Hsi 

A thesis submitted to the Faculty of Graduate Studies and Research
in partial fulfillment of the requirements for the degree of

Doctor of Philosophy

in

Medical Sciences – Medical Genetics

Edmonton, Alberta

Spring 2006

Your file Votre référence
ISBN: 0-494-13990-0
Our file Notre référence
ISBN: 0-494-13990-0

ABSTRACT

ATP7B encodes a copper transporter, ATP7B, which is essential for delivering copper to ceruloplasmin and for excreting excess copper into bile. Mutations in *ATP7B* result in Wilson disease (WND), with patients exhibiting copper accumulation. This thesis focused on the identification of specific residues and regions in ATP7B critical for its biochemical function in copper homeostasis.

The WND mutation spectrum was compared with mutations in *ATP7A* to identify similarly altered residues. Since *ATP7A* encodes a copper transporter, ATP7A, that also acts in copper delivery and export and shows 56% amino acid similarity to ATP7B, such a comparison would highlight areas important for ATP7B function. Both spectra revealed higher mutation frequencies within the transmembrane and conserved domains, and comparatively fewer mutations in the N- and C-termini. Missense mutations accounted for the majority of *ATP7B* mutations; whereas the *ATP7A* spectrum depicted similar proportions of all mutation types examined, with *ATP7A* having more splice-site mutations relative to *ATP7B*.

Two assays are used in our laboratory to identify residues required for overall ATP7B function: 1) expression in yeast to examine copper transport, and 2) expression in mammalian cells to investigate copper-dependent localization. The yeast assay identified four residues within the conserved ATP-binding domain important for copper transport, and showed that the three examined residues in the N-terminus were not critical for the

transport function. A deletion of the entire C-terminus completely abolished copper transport, likely due to a disruption of protein stability. This region may also be critical for subcellular distribution, as it contains a motif found to be responsible for the localization of several proteins, including ATP7A. Thus, to ascertain the full effect of a mutation and to contribute to the functional analysis of variants showing normal transport, a reliable assay for examining localization is required. The necessary components for a higher throughput and biologically relevant system have been delineated to improve upon our current method.

This thesis has, therefore, characterized the role of selected specific regions and residues in ATP7B copper transport, which is invaluable for predicting phenotypic consequences of patient mutations and for further advancing our understanding of this essential transporter.

ACKNOWLEDGEMENTS

There are many individuals to whom I owe thanks, and without whom this thesis would not have come to fruition.

I am indebted to my supervisor, Dr. Diane Cox, for her constant encouragement and enthusiasm for scientific discovery. She allowed me to follow my own research path in order to become an independent and critical thinker. I also thank Diane for her support and guidance as I completed my thesis while attending law school in Victoria, B.C.

I would like to thank the past and present members of the Cox Lab, who made the lab an enjoyable place to work. I am grateful for all that I have learned from every Cox lab member. I would especially like to thank David, Gina, Lara and Veronica for their intellectual contributions, friendship and support.

I thank the members of my committee, Dr. Moira Glerum and Dr. Susan Andrew, for all their time, advice and scientific contributions. I thank them for all their encouragement over the years; I could not have made it to the end without them. I would also like to thank everyone in the department of Medical Genetics, many of whom have become good friends.

I would like to thank my family, for without their support, encouragement and confidence in my abilities, I would not have accomplished this goal. There are also many friends to whom I will be forever grateful: David, Karen, Tanya, Anna, Pamela, Denise, Susan, Michael and Jess, have all contributed to the success of this thesis.

TABLE OF CONTENTS

LIST OF TABLES

LIST OF FIGURES

LIST OF ABBREVIATIONS, SYMBOLS AND NOMENCLATURE

-Cu	low copper conditions
+Cu	high copper conditions
3D	3-dimensional
-MEM	Alpha modified eagles medium
AP	adaptor protein
ATP-BD	ATP-binding domain
BCS	bathocuproine disulfonic acid
bp	base pair
CCS	copper chaperone for superoxide dismutase
cDNA	complementary DNA
CHO	Chinese hamster ovary cell line
COS-7	African green monkey kidney cell line
Cp	ceruloplasmin
CT	copper toxicosis
C-terminal	carboxy-terminal
Cu	copper
CuBD	copper-binding domain
Cu/Zn-SOD1	copper/zinc-superoxidase dismutase
Cys	cysteine
DAPI	4', 6-Diamidino-2-phenylindole
DMEM	Dulbecco's modified eagles medium
DNA	deoxyribonucleic acid
DTT	dithiothreitol
ECFP	enhanced cyan fluorescent protein
ER	endoplasmic reticulum
FCS	fetal calf serum
Fe	iron
GFP	green fluorescent protein
H-bond	hydrogen-bond
kb	kilo base
kDa	kilo Dalton
HEK293	human embryonic kidney cell line
KF ring	Kayser-Fleischer ring
LB	Luria broth
LEC rat	Long-Evans Cinnamon rat
LF	Lipofectamine 2000 reagent

MBS	metal-binding site
MDCK	Madin-Darby canine kidney
MNK	Menkes disease
MRE	metal-responsive element
mRNA	messenger RNA
MRP2	Multidrug Resistance-associated Protein 2
MT	metallothionein
N-ATP7B	N-terminal domain of ATP7B
NCBI	National Center for Biotechnology Information
N-terminal	amino-terminal
OHS	occipital horn syndrome
PAGE	polyacrylamide gel electrophoresis
PBS	phosphate-buffered saline
PBS-X	PBS and 0.05% Triton X-100
PBS-X/BSA	PBS and 0.05% Triton X-100 and 5% BSA
PCR	polymerase chain reaction
PINA	pineal night-specific ATPase
PM	plasma membrane
PVDF	polyvinylidine difluoride
RNA	ribonucleic acid
ROS	reactive oxygen species
RT-PCR	reverse transcriptase PCR
S. cerevisiae	*Saccharomyces cerevisiae*
SD medium	synthetic dextrose medium
SDS	sodium dodecyl sulphate
SSC	standard sodium citric acid
TBS	Tris-buffered saline
TBS-T	TBS containing 0.1% Tween-20
TGN	*trans*-Golgi network
TM	transmembrane
tx mouse	toxic milk mouse
WND	Wilson disease
Zn	zinc

CHAPTER 1:
Introduction

I. INTRODUCTION TO COPPER

To sustain life, organisms require a balanced diet containing adequate amounts of protein, carbohydrates, fat, vitamins and minerals, including trace metals. Certain trace metals are non-essential with adverse health effects (e.g. lead (Pb), cadmium (Cd) and mercury (Hg)); whereas, others, such as copper (Cu), iron (Fe), manganese (Mn), and zinc (Zn), are essential for maintaining important biological functions. These essential trace metals can be toxic in excess and thus are under strict homeostatic control. Various mechanisms are used to maintain the balance between their essentiality and toxicity, including uptake, transport, storage and excretion; reviewed in (Pena *et al.* 1999; Wijmenga and Klomp 2004).

A. BIOCHEMICAL BASIS FOR THE REQUIREMENT OF COPPER

The essential nature of Cu has been demonstrated in all living organisms from bacterial cells to humans. The biological function of Cu stems from its unique chemistry and ability to adopt distinct oxidation states, with Cu^{2+} being its most stable form (Linder 1991). As such, Cu is capable of cycling between these different states and transferring electrons, thus serving as an integral part of several enzymes and necessary for survival (Pena *et al.* 1999). Cu can affect the enzymatic potential of proteins in different ways: as an electron transfer intermediate during the catalytic cycle, as a major component of the catalytic centre of the enzyme, or as an allosteric component conferring the correct tertiary structure for catalytic activity (Uauy *et al.* 1998).

Cu has also been shown to be a vital effector element in activating and repressing gene expression in eukaryotic organisms; reviewed in (Uauy *et al.* 1998). As demonstrated in yeast, Cu binds to certain transcription factors, notably Ace1 and Mac1, which affects their tertiary structure and induces their interaction with specific metal-responsive elements (MREs) in the 5' end of MRE-regulated genes. These Cu-dependent transcription factors act as components of metal-responsive genetic switches and are often associated with the expression of genes that affect several physiologic processes, including Cu storage, superoxide dismutation, reduction of Cu^{2+} and Fe^{3+}, and detoxification of hydrogen peroxide, making Cu an indispensable element (Gross *et al.* 2000).

B. Biochemical basis for copper toxicity

The facile release and acceptance of one electron is part of the basic chemistry of Cu that, in addition to making it essential, causes it to become a particularly potent cytotoxin when allowed to accumulate in excess of cellular needs. Free Cu can react with poorly reactive oxygen species (ROS) to produce highly reactive radicals. For example, trace amounts of Cu^{+} can catalyze the generation of hydroxyl radicals from hydrogen peroxide via the Fenton reaction; reviewed in (Halliwell and Gutteridge 1984; Tapiero *et al.* 2003). Hydroxyl radicals are responsible for cellular damage, such as lipid peroxidation in membranes, cleavage of DNA and RNA molecules, and oxidation of proteins; reviewed in (Halliwell and Gutteridge 1990; Pena *et al.* 1999). The production and action of ROS play an important role in disease pathologies, with free radicals being major contributing factors to the development of cancer, neurodegenerative disorders and aging (Halliwell and Gutteridge 1990).

Cu may also manifest its toxicity by displacing other metal cofactors from their natural ligands (Pena *et al.* 1999). Cu can potentially associate with many adventitious sites and replace metal ions in a number of catalytic or structural motifs, thus negatively affecting several biological pathways. Due to its ability to disturb a wide range of cellular processes, precise regulatory mechanisms are crucial to prevent the accumulation of Cu ions to toxic levels.

C. Homeostatic control of copper

The essential, yet toxic nature of Cu dictates the need for intricate mechanisms to monitor and regulate its status in organisms. This is achieved by strict homeostatic control at different points of Cu regulation: at uptake and absorption, transport through blood plasma and interstitial fluid, during intracellular distribution and metabolism of Cu, and through detoxification and excretion (Pena *et al.* 1999). Cu is generally not stored due to the relative ease in absorbing and excreting the metal; thus, most of the Cu found in organisms is functional (Linder *et al.* 1998).

i. Dietary copper uptake and absorption

Cu normally enters mammals through the alimentary tract. The concentrations of Cu in foods are highly variable, with organ meats, shellfish and chocolate being among the richest sources of Cu; reviewed in (Linder and Hazegh-Azam 1996). The average diet in Western countries affords 0.6 to 1.6 mg Cu per day, with 55-75% being absorbed and actively recycled between certain tissues (particularly the liver), the circulation and the digestive tract (Figure 1-1).

Of the dietary Cu that is absorbed, most is passed across the mucosal membrane into cells that line the stomach and small intestine, primarily being absorbed by cells of the small intestine. Cu^{2+} is transported across the brush border of enterocytes of the intestinal mucosa using a non-energy-dependent saturable carrier at low Cu^{2+} concentrations and diffusion at high concentrations. Subsequent transport of the Cu^{2+} across the basolateral membrane into the blood and interstitial fluid is mediated by a rate-limiting, saturable, energy-dependent mechanism; reviewed in (Tapiero *et al.* 2003).

ii. Copper transport in blood plasma and interstitial fluid

In the general circulation, specific carrier proteins with a high-affinity for Cu are responsible for transporting Cu to its requisite sites. After Cu enters the blood, it follows two phases of distribution: entry into the liver and kidney from the blood, and Cu delivery to other tissues following reemergence in the plasma from the liver (Figure 1-1) (Linder *et al.* 1998).

The initial movement of Cu from intestinal cells to the liver and kidney is orchestrated by albumin (Linder and Hazegh-Azam 1996). Albumin is part of the exchangeable Cu pool and is able to directly bind or incorporate the metal when exposed to Cu ions. Cu in the plasma can also be bound by components of low molecular weight, such as histidine or other amino acid chelates (Linder and Hazegh-Azam 1996).

Ceruloplasmin (Cp) is a major carrier of Cu in the plasma. Unlike albumin, Cp is not considered to be part of the exchangeable Cu pool. Seven Cu atoms are instead incorporated during the biosynthesis and maturation of Cp in the secretory pathway, primarily in the liver.

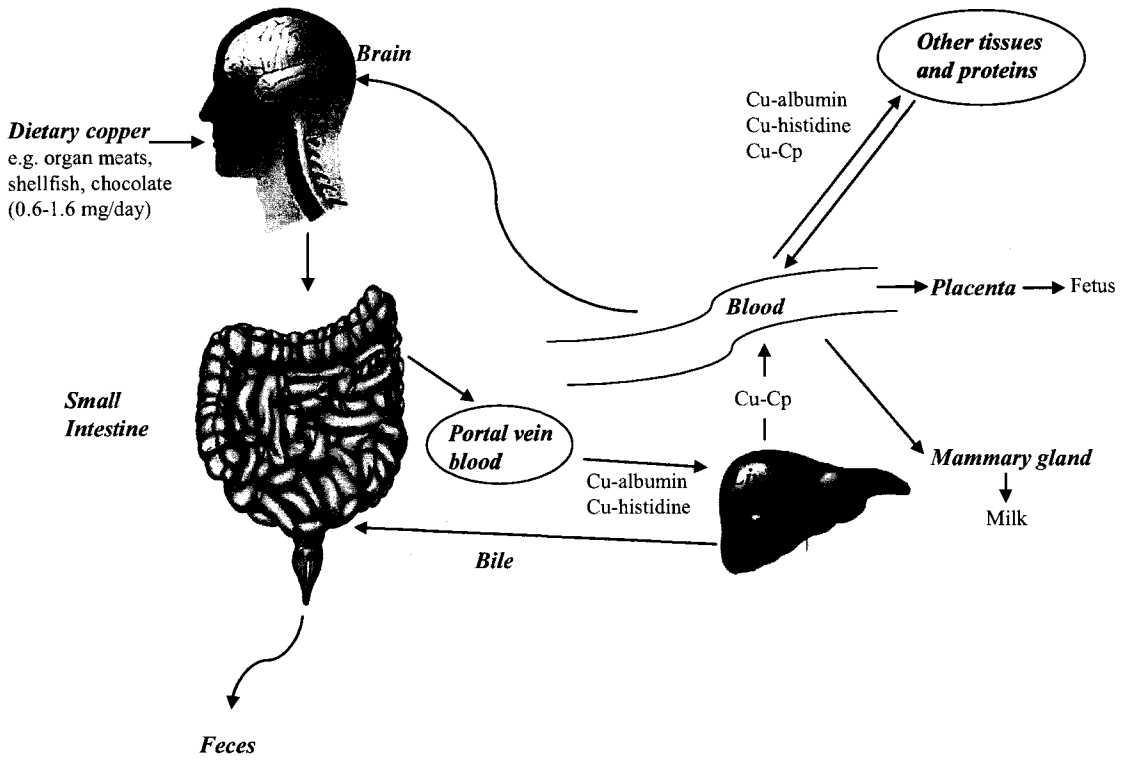

Figure 1-1. A model of the physiologic flow of copper through the body in mammals.

The flow of copper through the system is shown by arrows. Ingested copper is absorbed by the enterocytes of the small intestine and effluxed across the basolateral surface of these cells into the portal circulation. Most of the newly absorbed copper is usually taken up by the liver. In situations of copper overload, excess copper is excreted in the bile. Copper in the liver is incorporated into ceruloplasmin (Cp) and delivered to the blood. Other forms of Cu, such as Cu-histidine and Cu-albumin, are important sources of copper for tissues. Transport of Cu to the fetus and neonate is vital for normal development. (Adapted from Mercer and Llanos 2003).

Under normal dietary conditions, much of the Cu that reemerges from the liver and kidney into plasma is Cp-bound. Thus, Cp is a carrier of Cu during the second phase of Cu distribution to non-hepatic tissues (Linder and Hazegh-Azam 1996; Harris 2000).

iii. Intracellular distribution of copper

The main protein responsible for Cu^{+} uptake in human cells is CTR1, a 190 amino acid protein with three transmembrane (TM) domains and rich in methionine and histidine residues for the binding of Cu (Zhou and Gitschier 1997). Consistent with its role in Cu influx, CTR1 resides predominantly in the plasma membrane (PM) (Klomp *et al.* 2002).

Once Cu enters the cell through CTR1, a network of trafficking pathways exists for moving the metal through the cytosol (Figure 1-2). These pathways are designed either to detoxify and sequester the metal or to escort the ion to its cognate site in a metalloprotein (Pena *et al.* 1999). In doing so, the concentration of free ionic Cu is maintained at a low level. The total cytoplasmic free Cu concentration has been estimated to be less than 10^{-18} M, which represents many orders of magnitude less than one atom of "free" Cu per cell and is much less than the total Cu concentration (micromolar range) in a living cell (Rae *et al.* 1999).

The phrase "Cu chaperone" was coined to describe a family of soluble metal receptor proteins that spare Cu from detoxification factors and guide the metal to specific cellular targets (Pufahl *et al.* 1997). Their role in intracellular trafficking also prevents cytoplasmic exposure to free Cu ions in transit. Only a few Cu chaperones have been identified, but they are conserved across plant, bacterial and animal species, indicating their importance for Cu routing in the majority of living systems.

Cu chaperones are highly specific, with each interacting with only one Cu-requiring target (Field *et al.* 2002). An interaction between the chaperone and target protein is necessary for Cu to be transferred onto the metalloenzyme, and likely involves a transient docking of the donor and acceptor sites. The interaction could be achieved by a network of electrostatic and hydrogen bonding interactions and facilitated by similar protein folds (Harrison *et al.* 1999).

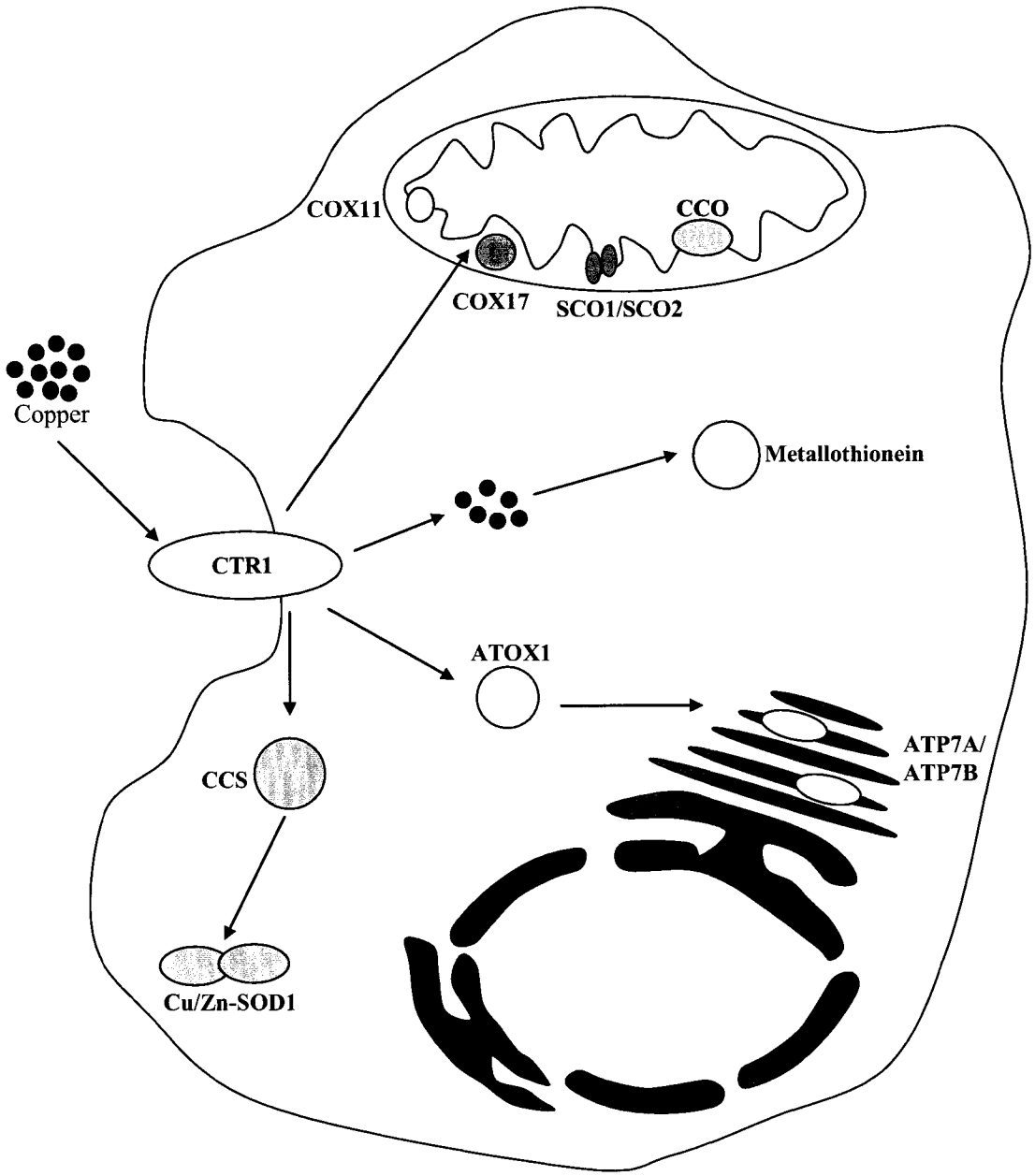

Figure 1-2. A model for human copper uptake and distribution at the cellular level.

Tissue copper uptake is mediated by the CTR1 Cu transporter. Once transported into the cytosol by CTR1, Cu chaperones are involved in distributing Cu to specific cellular compartments for the incorporation of Cu into Cu-requiring proteins. COX17 delivers Cu to the mitochondrial protein CCO through SCO1 and COX11; ATOX1 delivers Cu to ATP7A/ATP7B in the secretory compartment, and CCS delivers Cu to Cu/Zn-SOD1 in the cytosol. Excess Cu is effluxed by the ATPases ATP7A and ATP7B, and if the efflux capacity is exceeded, metallothioneins are induced to sequester excess Cu. (Adapted from Peña *et al.* 1999).

Three-dimensional structures of the human CCS domain II, a bacterial Cu chaperone (CopZ), and the yeast orthologs of ATOX1 (Atx1) and CCS (Lys7) have revealed remarkable structural similarities between chaperones and target proteins (Rosenzweig and O'Halloran 2000).

These Cu chaperone-target protein interactions are invaluable for Cu movement within the cell. There are at least three pathways utilizing different chaperones that are employed to reserve and transfer available intracellular Cu to specific enzymes: (a) trafficking to the secretory pathway to activate cuproenzymes destined for the cell surface or extracellular milieu; (b) delivery to the mitochondria for incorporation into cytochrome-*c*-oxidase; and (c) incorporation into Cu/Zn-superoxide dismutase (SOD1) in the cytoplasm.

a. Copper trafficking to the secretory pathway

All cuproenzymes that transit through the secretory pathway to their final destinations are bound with Cu in a compartment of the Golgi apparatus. This process is assisted by the small soluble Cu chaperone in the cytoplasm, ATOX1. ATOX1 specifically shuttles Cu to an intracellular membrane-bound Cu-transporting P-type ATPase (ATP7A or ATP7B) located in the Golgi compartment that is ultimately responsible for translocating the metal ion into the lumen of the Golgi for subsequent insertion into Cu-requiring enzymes, such as ceruloplasmin (Cp) (Klomp *et al.* 1997).

b. Copper delivery to the mitochondria for incorporation into cytochrome-c-oxidase

Cytochrome-*c*-oxidase is a key mitochondrial enzyme in the respiratory chain and requires a total of three Cu ions to be inserted into two subunits. The assembly of the Cu sites occurs on the inner mitochondrial membrane and involves a series of accessory proteins. COX17 is a small soluble Cu-binding protein found in both the cytoplasm and intermembrane space of mitochondria. Accordingly, this chaperone was originally proposed to escort Cu through the outer membrane and into the intermembranous space. Recent data, however, indicate COX17 is not required to shuttle Cu across the outer membrane and is instead metalled in the intermembranous space to function (Maxfield *et al.* 2004), together with COX11 and SCO1, in the assembly of cytochrome-c-oxidase ; reviewed in (Carr and Winge 2003).

c. Copper delivery to the cytoplasm for incorporation into Cu/Zn-SOD1

The cytosolic protein Cu/Zn-SOD1 protects cells against oxidative damage by scavenging toxic superoxide anion radicals and converting them to hydrogen peroxide and oxygen. This reaction relies on the redox cycling of the bound Cu ions in SOD1. Cu is known to be inserted into SOD1 through the action of the Cu chaperone CCS (Copper Chaperone for SOD1) (Culotta *et al.* 1997). This trafficking pathway is unique in that the activation of SOD1 appears to require just CCS to directly insert Cu into the cuproenzyme; reviewed in (O'Halloran and Culotta 2000; Luk *et al.* 2003; Prohaska and Gybina 2004).

d. General copper chaperone: glutathione

Glutathione may behave as a general chaperone for Cu ions. Cu ions complex with glutathione almost immediately upon entering a cell and before binding to other proteins. Due to the chemistry and ability of glutathione to reduce disulphide bonds to cysteines within cytoplasmic proteins, this general chaperone could facilitate Cu binding to Cu-dependent proteins, and may ensure the Cu ions are in their correct physiological state to bind; however, glutathione lacks distinguishable target-specific domains and may not be needed directly for Cu distribution; reviewed in (Tapiero *et al.* 2003).

iv. Detoxification and excretion

Two common detoxification mechanisms are involved in the mammalian system: the chelation or sequestration of Cu ions into relatively innocuous complexes, and the exportation of excess metal ions by a cation-translocating P-type ATPase; reviewed in (Dameron and Harrison 1998).

The regulation of Cu excretion appears to be the main mechanism for preserving Cu homeostasis. Dietary Cu intake is approximately 0.6-1.6 mg daily, and approximately half of this Cu is absorbed (Linder *et al.* 1998). Of the Cu retained from the diet, approximately 15% is transported to various tissues, while the remaining is excreted, primarily via bile (Linder *et al.* 1998). This highlights the significance of the liver in attaining whole-body Cu homeostasis.

a. Biliary excretion of copper

Hepatocytes are polarized into an apical (canalicular) domain and a basolateral domain, with the canalicular membrane housing a plethora of transport proteins responsible for cellular elimination of physiological and toxic compounds via biliary excretion. The rate of biliary Cu efflux is enhanced in response to a rise in dietary Cu intake and as Cu concentration in the liver increases; reviewed in (Wijmenga and Klomp 2004). Excretion of Cu is facilitated by ATP7B, a member of a highly conserved family of heavy-metal-transporting P-type ATPases. The exact role of ATP7B in Cu efflux across the canalicular membrane and into the biliary system has not been clearly defined.

b. Sequestration of copper

Metallothioneins (MTs) are a family of small, cysteine-rich proteins responsible for sequestering excess Cu ions (Hamer 1986). They act as scavengers of any unbound metal and toxic by-products, and are induced by transition metals other than Cu. In mammals, MTs predominantly bind Zn, but Zn ions can be easily displaced by Cu or Cd (Shaw *et al.* 1991). Excess Cu can therefore be immediately bound by any available MT upon entry into the cell. The Cu is sequestered into a solvent-shielded cluster by binding to the Cys residues in MT, preventing the Cu from causing cellular damage (Hamer 1986). The Cu-MT complexes can be oxidized to generate nontoxic insoluble polymers, which accumulate in lysosomes and are eventually secreted in bile (Coyle *et al.* 2002), thus excreting excess Cu. The metal ions in Cu-MT complexes can be donated, *in vitro*, to higher affinity ligands on other proteins, such as Cu/Zn-SOD1 (Coyle *et al.* 2002).

Glutathione is important in modulating the presence of excess Cu, with multiple roles in intracellular Cu metabolism and detoxification, including: (i) rapid binding of Cu following uptake and subsequent transfer to Cu-requiring proteins; (ii) amelioration of Cu toxicity by directly chelating Cu and maintaining it in a reduced state; and (iii) acting as a substrate for several enzymes that remove reactive oxygen species; reviewed in (Harris 2000).

v. Consequences of altered copper homeostasis

The dual aspect of Cu demands a crucial balance of the metal ion in biological systems. An alteration of homeostasis leads to errors of metabolism and damage to cells, which

ultimately results in pathological conditions if not resolved. This is exemplified by two classic Cu metabolism disorders, Menkes disease (MNK) and Wilson disease (WND).

II. MENKES DISEASE

A. PHENOTYPE OF MENKES DISEASE

MNK is a relatively rare X-linked recessive Cu deficiency disorder with an incidence of 1 in 100,000 live births to 1 in 250,000. The disease was originally described in 1962, with the report of five male infants affected with a distinctive syndrome of neurological degeneration, peculiar hair and failure to thrive (Menkes *et al.* 1962). The infants appeared normal at birth and for the first several months, but became progressively worse and died between the ages of 7 months and 3½ years. The underlying cause remained unknown until a link between Cu metabolism and MNK was identified. The connection was based on the observation that the brittle and depigmented hair characteristic of patients resembled the wool of sheep raised on Cu-deficient soil (Danks *et al.* 1972). The symptoms in sheep resulted from the decreased activity of Cu-dependent enzymes. As expected, the MNK patients demonstrated low serum Cu concentrations and subnormal serum concentrations of Cp, a Cu-requiring enzyme (Danks *et al.* 1973).

i. Clinical phenotype

As an X-linked disease, MNK typically affects males. Babies are usually born prematurely, but their birth weights are appropriate to gestation and they appear normal externally. However, by 2-3 months of age, affected patients show loss of previously obtained developmental milestones and progressive deterioration ensues until death, usually around 3 years of age (Danks *et al.* 1983).

The most distinctive features of MNK include: unusually coarse, twisted and sparse hair that feels like steel wool ("kinky hair") and progresses into fragile, lusterless and hypopigmented scalp and eyebrow hair; connective tissue abnormalities that typically present as loose, hypopigmented and hyperextensible skin (cutis laxa); hypermobile joints; bones that show osteoporosis; elongated, tortuous and tangled blood vessels; as well as

severe neurological symptoms, such as profound truncal hypotonia, poor head control, and impaired visual fixation and tracking (Danks *et al.* 1983); reviewed in (Kaler 1998a; Kaler 1998b; Harrison and Dameron 1999).

ii. Biochemical phenotype

The biochemical phenotype in Menkes disease involves low concentrations of Cu in plasma, liver and brain, and Cu accumulation in certain other tissues (duodenum, kidney, spleen, pancreas, skeletal muscle and placenta) (Kaler 1998b). The primary defect is in Cu transport, with the cultured cells from MNK patients showing Cu retention and reduced Cu expulsion (Horn 1976; Horn and Jensen 1980). In patients, this defect leads to generalized Cu deficiency within the system, and impaired incorporation of Cu into Cu-requiring enzymes. Certain clinical features of MNK can be due to the deficient activity of cuproenzymes, including: dopamine - hydroxylase, peptidlyglycine -amidating monooxygenase, cytochrome-*c*-oxidase, protein-lysine-6-oxidase (lysyl oxidase), Cu/Zn-SOD1, and tyrosinase. The pleiotropic symptoms of MNK can be largely attributed to the inefficient distribution of Cu into these enzymes that require Cu to be functional; reviewed in (Kaler 1998b).

iii. Clinical heterogeneity of Menkes disease

Three Cu deficiency disease variants of MNK have been recognized: classic MNK, mild MNK and occipital horn syndrome (OHS, or X-linked cutis laxa/Ehlers-Danlos type IX) (Kaler *et al.* 1994; Das *et al.* 1995; Tumer and Horn 1997). Even though these disorders are due to allelic mutations of the gene affected in MNK (*ATP7A*), they have distinguishing features.

Classic MNK has the most severe clinical phenotype, with marked neurodegeneration, mental retardation and death by the age of 3 or 4 years. Most patients, approximately 90-95%, present with this more severe clinical course (Tumer *et al.* 1999). Mild MNK patients exhibit moderate developmental delay and cerebellar ataxia. The symptoms normally associated with classic MNK are present but with diminished severity (Danks 1988). The clinical phenotype of OHS patients comprises primarily connective tissue abnormalities, with the other hallmarks of classic MNK absent or minimal (Proud *et al.*

1996). This suggests that lysyl oxidase, a cuproenzyme critical for cross-linking structurally essential proteins, collagen and elastin, may be particularly sensitive to an imbalance in intracellular Cu levels relative to other cuproenzymes. In fact, the lysyl oxidase activity in skin biopsies of OHS patients was comparable to that found in cultured cells from patients with classic MNK (Byers *et al.* 1980).

B. Treatment of Menkes disease

The main treatment for classic MNK has been Cu replacement therapy (Kaler 1998a). Parenteral Cu administration seems to be immediately beneficial for most patients, improving hair abnormalities, serum Cp levels and Cu levels in the serum, cerebrospinal fluid and liver (Grover and Scrutton 1975; Kollros *et al.* 1991; Kreuder *et al.* 1993; Sarkar *et al.* 1993). Cu replacement therapy, however, does not correct all MNK symptoms, such as connective tissue problems, as Cu deficiency is present at birth. Furthermore, in classic MNK disease patients older than one month of age, Cu treatment does not improve the neurological degeneration (Kaler *et al.* 1995).

C. Menkes disease gene, *ATP7A*

Three independent research groups identified a gene localized at X chromosome Xq13.3 as the disease-causing gene in MNK patients (Chelly *et al.* 1993; Mercer *et al.* 1993; Vulpe *et al.* 1993). The gene is designated as *ATP7A*, and is organized into 23 exons and spans approximately 140-kb of genomic DNA (Dierick *et al.* 1995). Different *ATP7A* transcripts have been identified as a result of alternative splicing of exon 10 in several normal tissues, including lymphoblast, fibroblast, cerebellar and cortical brain (Dierick *et al.* 1995).

The full-length *ATP7A* transcript is approximately 8.5-kb, and by Northern analysis, the mRNA shows strong expression in fibroblasts and lymphoblasts, and in muscle, kidney, lung, heart and brain, with weaker expression in placenta and pancreas and only trace amounts in the liver (Mercer *et al.* 1993; Vulpe *et al.* 1993). *ATP7A* expression was demonstrated to be abnormal in a rare female translocation patient and other severely affected individuals (Chelly *et al.* 1993; Mercer *et al.* 1993; Vulpe *et al.* 1993), verifying that alterations in *ATP7A* are likely responsible for MNK.

D. MENKES DISEASE PROTEIN, ATP7A

The *ATP7A* gene codes for a 1500 amino acid residue protein, ATP7A, which is predicted to be a member of the family of cation-translocating P-type ATPases (Vulpe *et al.* 1993). The ATPases are a group of membrane proteins that function to transport ions across biological membranes and have characteristic elements that distinguish them as a family. ATP7A contains eight membrane-spanning regions, which are clustered together to form a channel through which Cu can pass. The intervening loops contain functional domains required to couple ATP hydrolysis with the transport of ions through the channel, including: (1) an ATP-binding site (GDGIND), (2) a phosphorylation domain that contains a conserved phosphorylated aspartic acid residue (DKTG), and (3) a phosphatase domain (TGEA/S) that removes the phosphate from aspartic acid as part of the reaction cycle. The designation "P-type" ATPase is employed to distinguish the members as a subfamily of ATPases that use the conserved aspartic acid residue to form an aspartyl phosphate intermediate during their reaction cycle (Harrison and Dameron 1999).

ATP7A also has six putative metal binding sites (MBSs) located in the N-terminal domain of the protein. The core binding motif has the consensus sequence Gly-Met-Thr-Cys-X-X-Cys (where X is an unspecified amino acid), which is highly conserved among heavy metal transport proteins. In addition, ATP7A contains a proline in its sixth TM domain that is thought to be important for the conformational changes associated with cation transport in P-type ATPases. The proline in ATP7A is flanked by two cysteines, which are presumed to bind the metal as it traverses the channel. These flanking residues are possibly involved in determining metal specificity. There is also a conserved SEHPL motif in ATP7A in the large cytoplasmic loop between the conserved aspartic acid and ATP-binding site (Solioz and Vulpe 1996; Solioz 1998; Harrison and Dameron 1999).

i. ATP7A protein function

The ATP7A protein has two critical functions. First, the protein functions as an efflux pump to export excess intracellular Cu out of many extrahepatic cells (Mercer 1998). ATP7A is critical for transporting Cu from the gut epithelial cells into the portal circulation, and thus for maintaining general systemic Cu levels. ATP7A also functions in Cu efflux within the kidney and the reabsorption of Cu back into circulation (Mercer 1998),

which is consistent with the *in situ* localization of the mouse orthologue (*Atp7a*) to the glomerulus of the kidney (Moore and Cox 2002) and localization within the proximal and distal tubules (Grimes *et al.* 1997). The Cu efflux function of ATP7A is also present within the brain, transporting Cu across the cells that constitute the blood-brain barrier (Mercer 1998). Second, ATP7A is crucial for the provision of Cu to Cu-dependent enzymes in different cell types (Harrison and Dameron 1999). An orthologous gene in *Saccharomyces cerevisiae* exists and has a similar Cu transport function in the yeast cell, providing Cu to a Cu-dependent enzyme involved in Fe transport (Yuan *et al.* 1995), as discussed in section IX.A.i.a.

E. MUTATIONS IN THE *ATP7A* GENE

Over 160 different mutations in the *ATP7A* gene have been identified, including the four types of point mutations, which account for approximately 120 of the mutations (deletions/insertions, missense and nonsense mutations, splice site mutations), and gross deletions of *ATP7A*, which are causative in about fifteen percent of all patients. Chromosomal abnormalities have also been reported in at least seven MNK patients (Tumer *et al.* 1999).

A comparison of mutations seen in classic MNK with those of OHS patients has suggested that mutations resulting in some normal transcript being produced and/or in a protein product with some residual Cu transport are associated with lower disease severity (Das *et al.* 1995; Moller *et al.* 2000; Dagenais *et al.* 2001). Most classic MNK patients have greatly reduced or absent *ATP7A* mRNA. The disease-causing changes are usually nonsense mutations, large deletions, frameshifts, or mutations at invariant splice sites that likely render any resultant products nonfunctional. Missense mutations associated with MNK often affect critical regions, leading to inactive proteins (Das *et al.* 1995; Mercer 1998). Mutations resulting in the milder MNK variants, such as OHS, often lead to reduced expression of functional *ATP7A* mRNA. Presumably, a milder phenotype will result provided that enough functional protein is present for incorporation of Cu into cuproenzymes (Moller *et al.* 2000; Dagenais *et al.* 2001).

F. Animal models of Menkes disease

A murine model for human MNK, the mottled mouse (*Atp7a*^{mo}), has been described. *Atp7a*^{mo} mice exhibit impaired Cu export with concomitant cytosolic Cu accumulation. Systemic Cu deficiency is manifested in these mutants due to Cu accumulation in the intestines and kidneys leading to a failure of Cu delivery to other tissues (Harrison and Dameron 1999).

A series of mottled mice result from allelic mutations of the murine orthologue of the human MNK gene, *Atp7a*, such as *mottled*, *pewter*, *mosaic*, *brindled*, *viable brindled*, *blotchy*, *tortoiseshell*, and *dappled* (Mercer *et al.* 1994; Cecchi *et al.* 1997; Grimes *et al.* 1997). All of the mouse mutations leave the majority of the coding region intact and there are no frameshift or nonsense mutations (Cunliffe *et al.* 2001). These mouse mutants present with many pathological features that closely resemble classic MNK, such as depigmentation, kinky hair, skeletal abnormalities and defective elastin and collagen. As with MNK, there is substantial phenotypic variation among the mottled mutations (Das *et al.* 1995; Cecchi *et al.* 1997; Levinson *et al.* 1997; Reed and Boyd 1997), ranging from coat color changes in *pewter*, connective tissues defects in *blotchy* and viable *brindled*, severe neurologic impairment and perinatal death in *brindled* and *macular*, to prenatal death in *dappled* and *tortoiseshell* (Harrison and Dameron 1999). A new deletion mutation with aberrant mRNA splicing and removal of most of the cytoplasmic C-terminus of the *Atp7a* protein, has recently been described (*tohoku*). *Tohoku* has been reported as the most severe model of human MNK in mottled mice identified to date, with embryonic lethality at day E11 of male mice hemizygous for *tohoku*.

III. WILSON DISEASE

A. Phenotype of Wilson Disease

WND is an autosomal recessive disorder of Cu metabolism that presents with a prevalence of approximately 1 in 30,000 in most populations. It was first recognized in 1912 as a familial disorder of liver disease and/or progressive neurological abnormalities often associated with a corneal change (Wilson 1912), known as the Kayser-Fleischer (KF) ring

(Kayser 1902; Fleischer 1903; Fleischer 1912). Cu overload was soon implicated, yet the aetiological role of Cu was not firmly established until 1948 when the presence of excess Cu in the tissues of affected patients was detected (Cumings 1948); reviewed in (Brewer and Yuzbasiyan-Gurkan 1992; Houwen *et al.* 1993).

i. Clinical Phenotype

The clinical presentation of WND is highly variable; WND can present as liver disease, as a progressive neurological disorder without clinically evident hepatic dysfunction (hepatic dysfunction being less apparent or occasionally absent), or as a psychiatric illness (Roberts and Schilsky 2003). Liver disease is the most common presentation of patients with WND (Kitzberger *et al.* 2005). Phenotypic presentation typically occurs between the ages of 6 and 45 years; however, WND has been diagnosed in children as young as 3 years with extensive hepatic involvement (Roberts and Cox 1998), and in patients in their eighth decade (Ala *et al.* 2005).

a. Hepatic Presentation

Hepatic involvement may be acute, subacute or chronic, and the liver disease may also be progressive or, apparently, self-limiting (Walshe 2005). In the majority of patients presenting with liver disease, hepatic injury develops gradually and will proceed to cirrhosis if untreated. Some WND patients will occasionally present with fulminant hepatic failure, accompanied by the sudden release of excess Cu into the bloodstream and hemolytic anemia. WND presents with hepatic disease more commonly in children and younger adult patients than in older adults (Roberts and Schilsky 2003).

b. Neurological Presentation

WND patients who present with neurological disease are usually older teenagers or adults, although some have shown earlier onset. Neurological involvement is generally of two types: Parkinsonian disturbances and movement disorders, or rigid dystonia and choreic patterns. The most common symptoms seen are speech defects, drooling, hand tremors and gait disturbances; reviewed in (Roberts and Cox 1998).

c. Psychiatric Presentation

Patients presenting with purely psychiatric symptoms may go undiagnosed unless specific investigations relating to WND, such as liver function tests, are performed. Psychiatric symptoms are highly variable and include a spectrum of symptoms from behavioral abnormalities and personality changes to psychosis. Patients with psychiatric presentation are typically older and the symptoms are often subtle (Dening and Berrios 1989).

d. Ocular Involvement

The most common ocular finding in WND is the KF ring, an asymptomatic corneal Cu deposition in the Decemet's membrane. KF rings are present in only 50-62% of patients with mainly hepatic involvement at the time of diagnosis (Steindl *et al.* 1997; Gow *et al.* 2000; Roberts and Schilsky 2003), and are usually absent in children presenting within liver disease (Sanchez-Albisua *et al.* 1999). KF rings are found in nearly all WND patients presenting with neurological or psychiatric complications (Steindl *et al.* 1997); but, KF rings may be absent in 5% of these patients (Demirkiran *et al.* 1996).

ii. Biochemical Phenotype

Reduced biliary Cu excretion is typically recognized as the primary cause of hepatic Cu overload. All WND patients, irrespective of initial disease presentation, have abnormalities on liver biopsy, abnormal routine liver function tests and high liver Cu concentrations; reviewed in (Roberts and Cox 1998).

Cu overload in the liver and secondary accumulation in other tissues may be partly attributed to reduced incorporation of Cu into apo-Cp. In fact, low serum Cp is a hallmark of WND, since in most patients, serum Cp is greatly reduced and non-Cp bound Cu is increased (Roberts and Cox 1998). The effect of decreased holo-Cp in the serum, however, may be trivial. In hereditary aceruloplasminemia and hypoceruloplasminea, where patients lack or have an almost complete absence of Cp in their serum, no evidence of Cu deficiency or a defect in Cu transport has been seen, indicating that abrogation of Cp biosynthesis may be of minor importance to Cu homeostasis (Miyajima *et al.* 1987; Shim and Harris 2003).

B. WILSON DISEASE GENE, *ATP7B*

The gene defective in WND, *ATP7B*, was identified by two independent research groups (Bull *et al.* 1993; Tanzi *et al.* 1993). *ATP7B* shows strong similarity to the MNK gene *ATP7A* (approximately 60% overall similarity), and this similarity was exploited to isolate the WND-causing gene in our laboratory (Bull *et al.* 1993). A probe from the proposed copper-binding domain (CuBD) of *ATP7A* was used to select yeast artificial chromosomes and cosmids containing sequences hybridizing to the probe. A cDNA selection strategy was then used to identify cDNA fragments from human liver and kidney cDNA libraries to assemble a complete *ATP7B* gene.

The *ATP7B* gene, which is located on chromosome 13q14.3 (Bowcock *et al.* 1987; Bowcock *et al.* 1988; Yuzbasiyan-Gurkan *et al.* 1988), spans approximately 80-kb of genomic DNA and contains 21 exons (Bull *et al.* 1993; Tanzi *et al.* 1993). The exons range in size from 77-bp (exon 6) to 2,355-bp (exon 21), with the ATG start codon in the first exon (Petrukhin *et al.* 1994; Thomas *et al.* 1995). The splice sites conform to the published consensus splice site sequences (Petrukhin *et al.* 1994). The 5' flanking region contains four MRE sites and six MRE-like sequences, similar to those in MT promoters, and not found in *ATP7A* (Oh *et al.* 1999).

The expression patterns of *ATP7A* and *ATP7B* are very different, with *ATP7B* being expressed mainly in the liver and kidney where ATP7A is scarcely detectable (Bull *et al.* 1993; Tanzi *et al.* 1993). Slight expression is also seen in the placenta, heart, brain, lung, muscle and pancreas. This expression complements the clinical and biochemical features of WND as the liver is the predominant site of Cu accumulation and renal damage is a common symptom in WND patients.

An alternative transcript, which lacks exons 5 and 11, is present in the brain (Tanzi *et al.* 1993). Further RT-PCR experiments on poly(A^+)- RNA isolated from liver and brain tissue identified additional brain splicing variants that lacked a combination of exons including: exon 17; exon 13; exons 6, 7 and 8; and exon 12. Some of these splicing variants are also present in human kidney and placenta (Petrukhin *et al.* 1994).

A unique alternatively spliced form of *ATP7B*, which uses a promoter in intron 8 and produces a 665 amino acid polypeptide designated as pineal night-specific ATPase (PINA), also exists. The protein is expressed in the pineal gland and exhibits a diurnal rhythm in both the pineal gland and retina, with selective expression at night (Borjigin *et al.* 1999). PINA is identical to the C-terminal portion of ATP7B, and also contains a 5' 300-bp stretch that is pineal-specific and part of the intron sequence immediately upstream of exon 9 of *ATP7B* (Li *et al.* 1998). Despite the loss of four ATP7B TM segments and the Cu-binding domain found in the N-terminus of ATP7B, PINA showed limited restoration of Cu transport activity in yeast deficient in the homologous Cu-transporting ATPase, Ccc2p (Borjigin *et al.* 1999). No additional work has been performed to analyze the Cu transport ability of PINA; therefore, further studies are required to confirm and define any function that PINA may have as a Cu transporter in rat pinealocytes.

C. Wilson Disease Protein, ATP7B

The *ATP7B* gene is predicted to encode a 1465-amino acid Cu-translocating P-type ATPase, similar to ATP7A, which translocates Cu ions across cell membranes, using the energy of ATP hydrolysis (Lutsenko and Kaplan 1995; Scarborough 1999). The cation-transporting P-type ATPase family consists of more than 200 members with representatives in all living organisms, including bacteria, yeast, plants and mammals (Palmgren and Axelsen 1998). ATP7A and ATP7B are the first P-type ATPases shown to be involved in the transport of Cu, with homologues found in a wide range of species.

ATP7B has the signature features distinctive of the P-type ATPase family members (Bull *et al.* 1993; Bull and Cox 1994), including a transduction/phosphatase domain (TGEA/S) and an ATP-binding domain (ATP-BD, AMXGDGNVD), as well as an aspartic acid in the conserved sequence DKTG (phosphorylation domain). These motifs are necessary for ATP-binding and hydrolysis and for conformational changes associated with these processes. ATP7B also has conserved sequences characteristic of Cu-transporters, such as six MBSs within the N-terminal Cu-binding domain (CuBD), an intramembranous CPC motif, and a conserved SEHPL sequence, which lies 34–43 amino acids C-terminal to the CPC motif within the ATP-BD cytoplasmic loop (Figure 1-3) (Bull and Cox 1994; Solioz and Vulpe 1996).

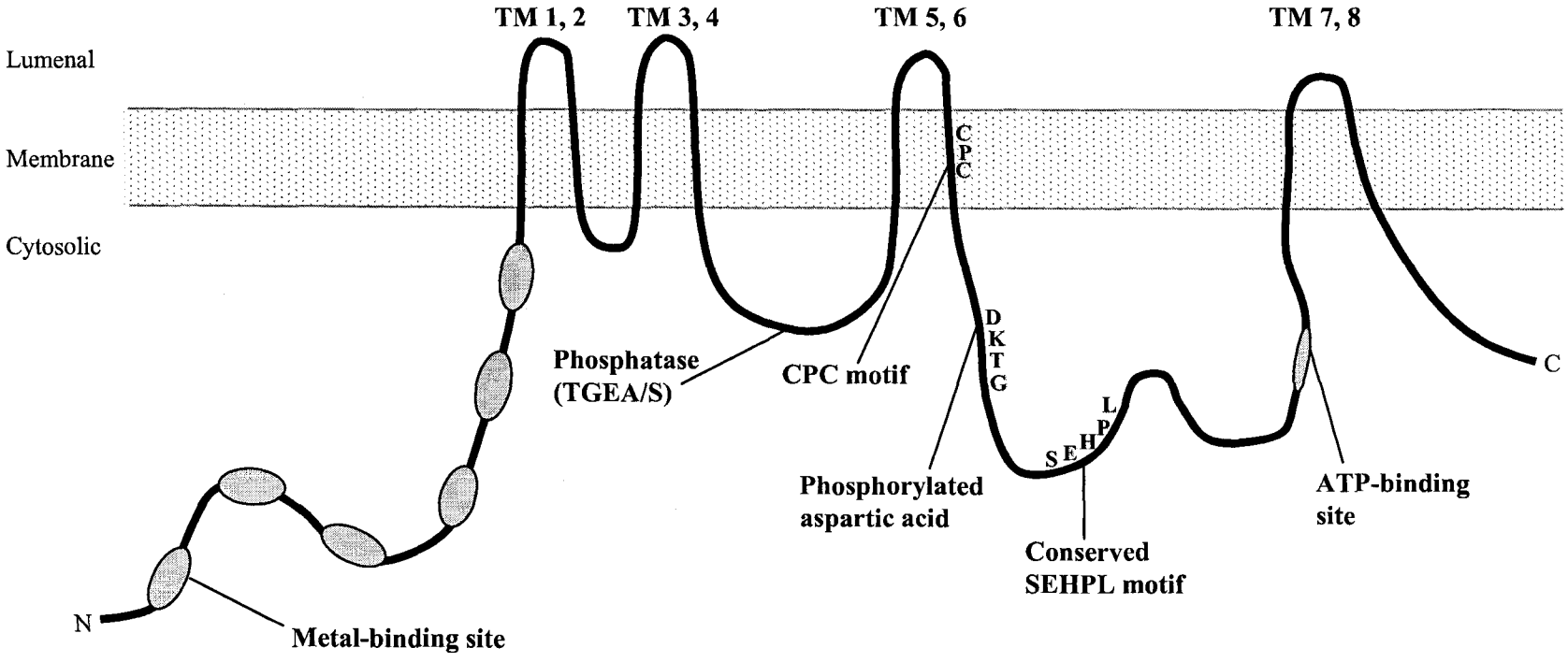

Figure 1-3. Two-dimensional representation of the MNK and WND Cu-transporting P-type ATPases.

Both ATP7A and ATP7B are predicted to have eight transmembrane (TM) domains. The predicted protein has an ATP-binding site, a phosphatase domain and an invariant aspartic acid. The N-terminal region has 6 metal-binding sites (the copper-binding domain), and the sixth TM has a CPC motif as an intramembranous metal-binding site. Between TM 6 and TM 7, there is a conserved SEHPL motif.
(Adapted from Mercer 2001).

i. ATP7B Protein Function

Analogous to MNK, WND appears to stem from an underlying defect in Cu efflux. This is supported by studies that have demonstrated complementation of the defective Cu efflux in MNK fibroblasts with the expression of recombinant *ATP7B* (La Fontaine *et al.* 1998b; Payne and Gitlin 1998).

ATP7B has two primary functions in the hepatocyte that are critical for maintaining Cu homeostasis within the system. First, ATP7B is involved in the excretion of excess intracellular Cu via bile, and second, ATP7B is involved in the mobilization of Fe and the distribution of Cu to non-hepatic tissues by delivering Cu to apo-Cp. In WND, the hepatic Cu content is elevated, while the Cu concentration in the bile is decreased.

D. Mutations in the ATP7B Gene

A mutation in the *ATP7B* gene is responsible for manifestation of WND. Molecular analysis of the gene in affected patients and families has detected more than 260 distinct mutations, which are mainly confined to well-defined consensus motifs and TM domains (http://www.medicalgenetics.med.ualberta.ca/wilson/index.php – accessed May 2005); (Cox and Moore 2002). Approximately half of all the mutations are missense, with the other three types of point mutations represented to a lesser extent. Gross deletions are rare, with one patient deletion of 2144-bp covering exon 20 and parts of the flanking introns recently reported (Moller *et al.* 2005); however, a comprehensive analysis aimed at uncovering large chromosomal deletions in WND patients has not been undertaken.

Most WND patients are compound heterozygotes (Schilsky 1994; Figus *et al.* 1995; Thomas *et al.* 1995; Loudianos *et al.* 1996; Shah *et al.* 1997; Loudianos *et al.* 1998b; Loudianos *et al.* 1999). Many disease-causing mutations have been identified, with each showing a low frequency in WND patients. There are a few mutations that are more prevalent in the population. The most common mutation, His1069Gln, accounts for over 70% of WND chromosomes in Polish patients (Czlonkowska *et al.* 1997), 60% in Austrian patients (Maier-Dobersberger *et al.* 1997), and for between 10 and 40% of all mutations identified in patients of other European and North American origin (Figus *et al.* 1995; Houwen *et al.* 1995; Thomas *et al.* 1995; Waldenstrom *et al.* 1996; Shah *et al.* 1997;

Loudianos *et al.* 1998b). His1069Gln, along with four other mutations, also accounts for 74% of WND alleles in the Greek population (Loudianos *et al.* 1998a). In contrast, the most common mutation in patients of Asian descent is the Arg778Leu mutation in the fourth TM domain. The allele frequency of Arg778Leu was 37.9% in Korean WND patients (Kim *et al.* 1998; Yoo 2002), 27% in Japanese patients (Nanji *et al.* 1997; Shimizu *et al.* 1999; Kusuda *et al.* 2000; Okada *et al.* 2000; Takeshita *et al.* 2002), 28-44% in Chinese (Chuang *et al.* 1996; Tsai *et al.* 1998; Fan *et al.* 2000; Lee *et al.* 2000; Wu *et al.* 2000; Wu *et al.* 2001; Xu *et al.* 2001), and 45.6% in the Han Chinese population (Liu *et al.* 2004). The molecular characterization of approximately 80% of mutated WND chromosomes is routinely seen in patient groups of a particular population (Gu *et al.* 2003; Margarit *et al.* 2005; Vrabelova *et al.* 2005), with one study reporting the detection of 95% of disease-causing mutations in 89 Bulgarian index cases (Todorov *et al.* 2005). However, over half of all known mutations occur only rarely in any given population (Petrukhin *et al.* 1994; Figus *et al.* 1995; Thomas *et al.* 1995; Loudianos *et al.* 1996; Shah *et al.* 1997; Loudianos *et al.* 1998a; Loudianos *et al.* 1998b; Loudianos *et al.* 1999).

Despite the high mutation detection rates in certain populations, genotype-phenotype correlations have been difficult due to extensive allelic heterogeneity. Some phenotypic variation can be explained on a genetic basis. For example, in a cohort of European, British, Middle Eastern and Asian families studied, mutations predicted to destroy the function of the gene usually presented as hepatic disease with an average age of onset of 7.2 years and as early as 3; whereas, patients with less severe abnormalities, had ages of onset approximately 10 years later and presented mainly with neurological symptoms (Thomas *et al.* 1995). The common Caucasian mutation, H1069Q, causes "mild" WND, with a later age of onset and predominantly neurological symptoms (Figus *et al.* 1995; Houwen *et al.* 1995; Thomas *et al.* 1995; Waldenstrom *et al.* 1996; Czlonkowska *et al.* 1997; Shah *et al.* 1997; Tarnacka *et al.* 2000; Firneisz *et al.* 2002; Panagiotakaki *et al.* 2004). A recent study of the His1069Gln genotype in 70 Dutch patients for its association with clinical presentation, as well as a meta-analysis performed on all patients available from the literature, has confirmed the His1069Gln genotype-phenotype correlation (Stapelbroek *et al.* 2004).

There have been general genotype-phenotype correlations recognized, where mutations that completely prevent function of *ATP7B* produce a more severe phenotype than certain types of missense mutations (Cox 1996; Wu *et al.* 2001); however, other studies done on patients homozygous for specific alleles have shown only slight correlations between a given mutation and the age of onset, clinical features, biochemical parameters or disease severity. This is consistent with the marked clinical variability often observed between affected sibs with WND (Riordan and Williams 2001; Panagiotakaki *et al.* 2004; Gupta *et al.* 2005). Thus, at least some phenotypic variability in WND is due to additional genetic and environmental factors, such as dietary Cu intake, intestinal MT inducibility, and capacity for countering Cu stress at the cellular level via glutathione, superoxide dismutase and heat shock proteins (Riordan and Williams 2001; Panagiotakaki *et al.* 2004).

E. Wilson Disease Diagnosis

i. Challenges with Wilson disease diagnosis

Because of the tremendous variability in clinical presentation, correct clinical diagnosis is often difficult and sometimes delayed. Diagnosis is complicated by the fact that no specific combination of clinical or biochemical features is necessarily definitive.

Establishing the diagnosis of WND is generally unambiguous if the major clinical and laboratory features are present. Difficulties arise when patients do not have associated clinical manifestations such as KF rings and low serum Cp. In fact, KF rings are often absent early in the disease, and not all patients show signs of KF rings (Gow *et al.* 2000).

Although low serum Cp is often a hallmark of WND in most patients, it is not always reliable as a diagnostic measure. The challenge with using Cp levels is that Cp is an acute-phase protein, the serum levels of which are increased due to infection or inflammation, including active liver involvement (Steindl *et al.* 1997). Cp levels are, in fact, within the normal range in 15% or more of WND patients (Cauza *et al.* 1997; Steindl *et al.* 1997; Yuce *et al.* 1999; Riordan and Williams 2001). Exogenous administration of estrogens and pregnancy can also increase the Cp level, possibly raising actual low serum Cp levels to within the normal range (Ferenci *et al.* 2003). A low serum Cp is also not specific for WND, as Cp synthesis can be reduced with acute liver failure or cirrhosis of any aetiology,

as well as in patients with severe Cu deficiency, in patients with significant protein-losing nephropathy or enteropathy, and patients with hypoceruloplasminemia or aceruloplasminemia (Gow *et al.* 2000; Schilsky 2002). Furthermore, low Cp levels are found in at least 10% of heterozygotes for WND (Gibbs and Walshe 1979; Roberts and Cox 1998; Gaffney *et al.* 2000).

The level of "free" Cu in the serum (i.e. not bound to Cp) can also be measured, and is useful in identifying whether the serum Cp level has been overestimated. An overestimation of the Cp level would result in lower than expected serum Cu concentrations and thus a false negative (Ferenci 2004a). Measuring the serum "free" Cu is not generally performed as a diagnostic tool, however, it has been used as an adjunct to diagnosis and is often employed when monitoring the success of treatment (Ferenci 2004b).

Although urinary Cu excretion is a valuable parameter when diagnosing WND, it is only useful to the extent that the collection is accurate and the container free from Cu contamination (Ferenci *et al.* 2003). Urinary Cu excretion is also increased in any disease with extensive hepatocellular necrosis, and can be normal in WND children and presymptomatic sibs (Gow *et al.* 2000; Ferenci *et al.* 2003).

Measurement of hepatic Cu content is the most reliable biochemical test for diagnosis of WND (Roberts and Cox 1998), but its use in diagnosis is still problematic. Hepatic Cu content may be normal or borderline in patients with unquestionable WND, and in later stages of WND, Cu is distributed unevenly in the liver and measurement of Cu concentration is not as accurate (McDonald *et al.* 1992). Non-Wilsonian patients with chronic liver disease may also have elevated liver Cu (Frommer 1981; McDonald *et al.* 1992).

The discovery of the gene responsible for WND (Bull *et al.* 1993; Tanzi *et al.* 1993) has facilitated the molecular identification of the disease by haplotype analysis around the disease locus. Direct mutational analysis is also performed, and is the most reliable method for WND diagnosis; however, screening of patients is difficult given the number of mutations that are scattered throughout the coding region. Prior to advancements in DNA sequencing technology, extensive time and costs associated with screening all mutations

limited its utility, and the failure to detect the mutation of both alleles was an issue (Schilsky 2002). The previous lack of resources also meant that screening of introns and regulatory regions for mutations had not been widespread, thus resulting in an incomplete analysis. Recent scientific advances in technology, however, have enabled higher-throughput and more complete screening in our laboratory (Cox, DW *et al.*, personal communication) and should soon permit the *de novo* identification of suspected WND patients.

ii. Treatment of Wilson Disease

WND treatments aim to prevent the accumulation of Cu or reverse its toxic effects by reducing the absorption of Cu, inducing synthesis of endogenous cellular proteins such as MT, and/or promoting the excretion of Cu in the urine or bile. Early diagnosis is important since medical therapy is effective, and most patients demonstrate improvement of liver function within 6-12 months of treatment (Schilsky 2002).

Several Cu chelating agents, including D-penicillamine, trientine, and tetrathiomolybdate, are used to promote the solubilization of Cu-rich particles in lysosomes and prevent the formation of more, hence facilitating urinary Cu excretion. Some chelators may also induce tissue MTs and/or interfere with intestinal absorption of Cu (Roberts and Cox 1998; Fatemi and Sarkar 2002a). D-penicillamine has been used as first-line therapy since 1956 (Walshe 1956; Durand *et al.* 2001); however, its utility is sometimes limited due to its serious adverse side-effects (Roberts and Cox 1998).

Zn therapy is the easiest regimen for long-term maintenance. Zn interferes with the absorption of Cu from the gastrointestinal tract by stimulating MTs in enterocytes, which have greater affinity for Cu than for Zn (Walshe 1984; Hill *et al.* 1987; Hoogenraad *et al.* 1987). The bound Cu is excreted in feces as enterocytes are shed. Zinc treatment may also induce hepatocellular MTs to deal with Cu absorbed from internal secretions (Schilsky *et al.* 1989).

Liver transplantation can correct the WND phenotype and provide excellent long-term survival for patients with acute hepatic failure. Recurrence of Cu-associated liver damage has not, as of yet, been reported in a WND transplant patient (Langner and Denk 2004).

Renal function in patients with associated kidney dysfunction also recovers following liver transplantation (Schilsky 2002). Although transplantation corrects the underlying metabolic defect in the hepatocytes of patients, the outcome of neurological disease is unclear (Ferenci 2004b). It is thus uncertain whether this procedure is beneficial in the management of patients with neurological WND, in the absence of hepatic insufficiency (Ferenci 2004b). There would still be the consequential effects of mutant ATP7B protein being produced in the brain and tissues other than the transplanted liver.

F. Animal Models of Wilson Disease

i. The Toxic Milk Mouse

The naturally occurring toxic milk (*tx*) mouse is a rodent strain that is likely a murine model for WND. *Tx* is an autosomal recessive disorder that causes hepatic accumulation of Cu and liver damage similar to that seen in patients with WND (Rauch 1983). Hepatic Cu accumulation commences in the third postnatal week (Theophilos *et al.* 1996), with Cu levels 14-fold higher than in normal mice (DL inbred strain) 7 weeks after birth (Rauch 1983) and 55-fold higher in adult *tx* mice compared with controls (Howell and Mercer 1994). Cu levels can reach 100-fold greater than that of a normal adult by 6 months of age, which resembles the gradual Cu accumulation observed in the livers of WND patients (Theophilos *et al.* 1996). In addition, pups born to homozygous mutant dams with the *tx* phenotype are born Cu-deficient and show retarded growth. Cu levels are reduced in the milk produced by the mutant mothers, resulting in the death of pups (Rauch 1983). Weaning the same progeny with normal mothers corrects the Cu deficiency, and symptoms of the infant syndrome are much milder or do not develop.

The *tx* mouse has a single nucleotide change from the DL mouse, which alters a methionine residue to a valine in the eighth TM domain (Theophilos *et al.* 1996). The affected methionine is conserved in all Cu ATPases, including those from bacteria and yeast. The *tx* mutation has been mapped to the same region of chromosome 8 as the murine homologue of human *ATP7B*, consistent with a mutation in murine *Atp7b* being responsible for the *tx* phenotype (Rauch and Wells 1995; Reed *et al.* 1995).

There is an additional *tx* strain (tx^J) that arose in a different background strain (C3H/HeJ animal resources colony) in the Jackson Laboratory, which shows a similar phenotype to the *tx* mouse (Sweet and Davisson 1989). The causative mutation of the tx^J mouse is a glycine to aspartate substitution (Gly712Asp) resulting from a single missense mutation in the second putative TM segment (Coronado *et al.* 2001).

A mouse strain has been generated that is homozygous null for murine *Atp7b* (Buiakova *et al.* 1999). The mutation in the null mice led to alternative splicing of exon 2 and the creation of a frameshift mutation at the exon2/intron3 splice junction, resulting in the lack of expression on Western blot. The *Atp7b* homozygous null mice accumulated Cu in their livers, kidney, brain, placenta and lactating mammary glands, and morphological abnormalities resembling cirrhosis were also evident. The cirrhotic liver disease was phenotypically similar to that seen in the *tx* mice.

ii. The Long-Evans Cinnamon Rat

The Long-Evans Cinnamon (LEC) rat is an inbred strain that was originally established in 1975 from the non-inbred Long-Evans parental strain. The LEC rat shares many of the clinical and biochemical characteristics of WND (Yoshida *et al.* 1987). These rats spontaneously develop acute hepatitis about four months after birth, with clinical features similar to human fulminant hepatitis seen in some WND patients. LEC rats which survive the acute hepatitis continue to suffer from chronic liver disease and some lines develop hepatocellular carcinoma (Yoshida *et al.* 1987; Masuda *et al.* 1988). Cu accumulation in the liver occurs prior to the development of the hepatitis, which can be prevented by treatment with Cu chelating agents such as D-penicillamine (Li *et al.* 1991). In addition, serum Cp and Cu levels are significantly lower in LEC rats as compared with normal rats, and hepatic Cu content is significantly higher in LEC rats than control rats (Kodama *et al.* 1998). Cu excretion into bile is also reduced in LEC rats (Schilsky *et al.* 1994).

The LEC rat has a partial deletion of the rat homologue of human *ATP7B* (*Atp7b*) gene found on rat chromosome 16. The proximal deletion breakpoint is in intron 15, with the deletion removing at least 900-bp of coding region and approximately 400-bp of the 3' UTR (Wu *et al.* 1994). The truncated protein product lacks the conserved ATP-binding

domain, leading to inactivation of Cu transport function, which supports the hypothesis that the LEC rat is an animal model for human WND (Wu *et al.* 1994).

IV. COPPER TRANSPORT FUNCTION OF ATP7B

The basal subcellular location of both ATP7A and ATP7B is in the membrane of the final compartment of the Golgi apparatus, the *trans*-Golgi network (TGN) (Petris *et al.* 1996; Yamaguchi *et al.* 1996; Dierick *et al.* 1997; Hung *et al.* 1997). A key physiological function of both proteins in the TGN is a biosynthetic one of delivering Cu into the secretory pathway to enzymes that require Cu for function.

In order to be incorporated into cuproenzymes, Cu needs to be acquired from cytosolic carriers and transported into the Golgi lumen. The general mechanism of Cu transport across the TGN membrane by ATP7B is presumed to resemble the mechanism used by other P-type ATPases: the cytosolic side of ATP7B binds Cu and ATP; ATP is hydrolyzed with its -phosphate being transferred to the invariant Asp residue in the DKTG sequence motif in ATP7B; Cu is released into the TGN lumen, the Asp becomes dephosphorylated, and ATP7B returns to its initial state (Lutsenko *et al.* 2002).

This reaction cycle is critical for the biosynthetic role of ATP7B in transferring Cu to Cp. The LEC rat has been used to illustrate this Cu transport function of ATP7B. LEC rat studies have demonstrated that the process of Cu incorporation into Cp is disturbed in the livers of affected rats (Sato and Gitlin 1991; Yamada *et al.* 1993; Terada *et al.* 1995), leading to impaired secretion of functional Cp into plasma. Introduction of a wild-type human *ATP7B* cDNA into these rats restored synthesis of holo-Cp, which was then secreted into plasma with Cu bound in its ferroxidase-active state (Terada *et al.* 1998; Meng *et al.* 2004).

A. ATOX1 AND COPPER TRANSPORT

i. Delivery of copper to the ATP7B homologue in yeast

The molecular components of Cu trafficking have largely been identified in *S. cerevisiae*, and studies have since demonstrated high conservation between the yeast and human Cu metabolism pathways. In *S. cerevisiae*, once Cu^{+} is taken up by the cell through the action of Cu transporters Ctr1p and Ctr3p (Dancis *et al.* 1994a; Knight *et al.* 1996), the Cu is bound by Cu chaperones and delivered to target enzymes (Figure 1-4) (Yuan *et al.* 1995; Yuan *et al.* 1997).

Biochemical evidence, confirmed by a yeast-two hybrid study, was used to demonstrate an interaction between the Atx1p chaperone (orthologue of human ATOX1) and Ccc2p (orthologue of human ATP7A and ATP7B), from which it was suggested that Atx1p functions as a cytoplasmic Cu carrier protein that delivers Cu from Ctr1p to Ccc2p (Lin *et al.* 1997; Pufahl *et al.* 1997). Furthermore, yeast strains lacking *ATX1* are deficient in high-affinity Fe uptake, yet expression of human *ATOX1* in these strains permitted growth on Fe-depleted media and restored Cu incorporation into newly-synthesized Fet3p through the function of Ccc2p (Klomp *et al.* 1997).

ii. Role of ATOX1 in ATP7B function

Human ATOX1 (previously known as HAH1) was postulated to play a role in Cu homeostasis, based on the yeast *ATX1* knock-out studies (Klomp *et al.* 1997; Hung *et al.* 1998). ATOX1, a 63 amino acid, 8-kDa cytosolic protein with a single metal-binding site (Met-X-Cys-X-X-Cys), was proposed to act as the Cu-donor for ATP7B. In fact, ATOX1 binds 0.85 ± 0.1 Cu atoms/ATOX1 (Walker *et al.* 2002), by coordinating the Cu between the cysteine residues of the metal-binding site (Wernimont *et al.* 2000). Docking of ATOX1 with ATP7B is likely facilitated by electrostatic interactions between the positively charged face of the chaperone and the negatively charged area on the analogous segment of ATP7B. Indeed ATOX1 and two metal-binding sites (MBSs) of ATP7A (MBS 2 and MBS 4) have been shown to have a similar ferredoxin-like -fold (Gitschier *et al.* 1998; Jones *et al.* 2003).

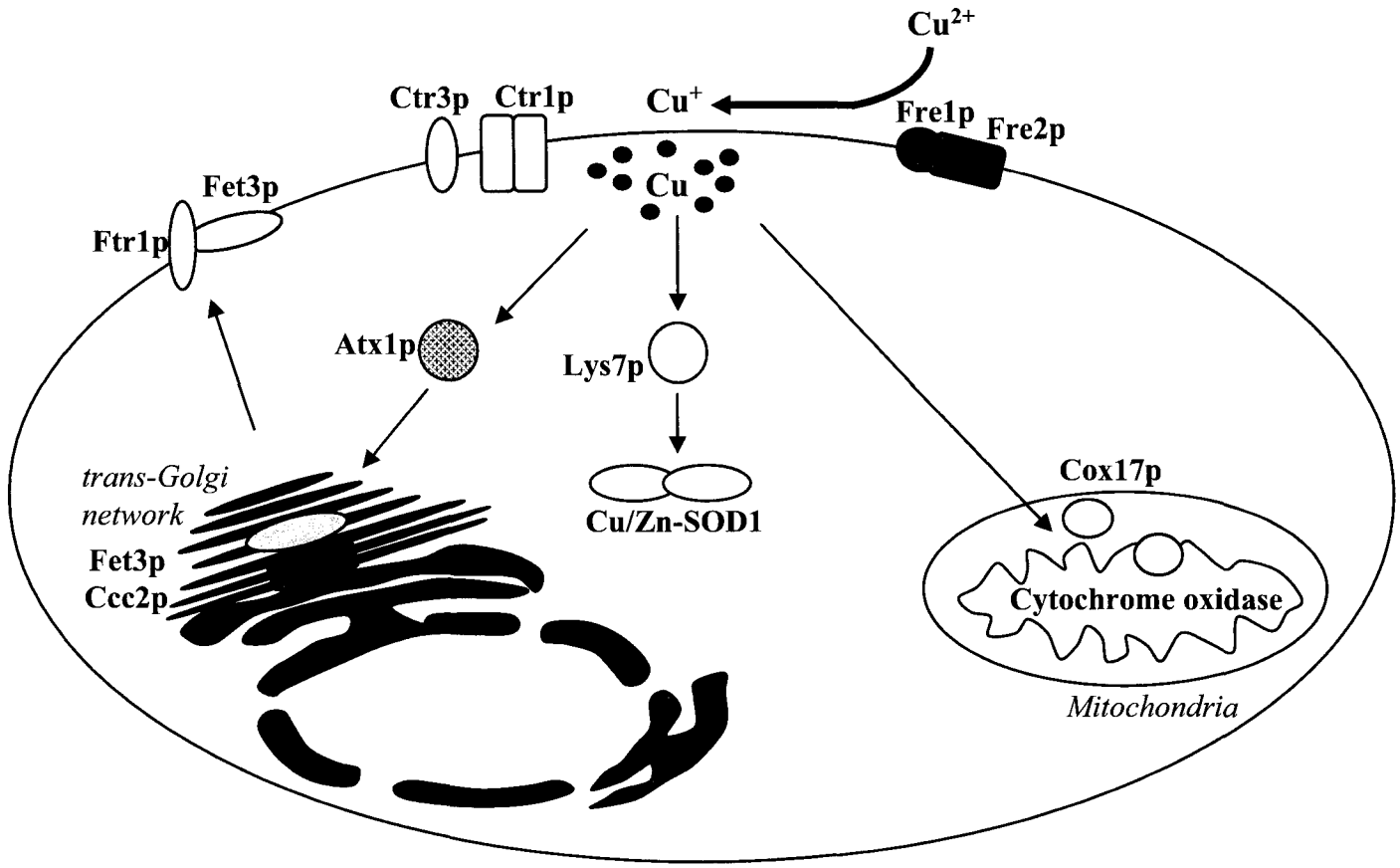

Figure 1-4. Copper transport and distribution in *Saccharomyces cerevisiae*.
Copper is first reduced from Cu^{2+} to Cu^{+} by cell surface reductases Fre1p/Fre2p prior to cell uptake. High affinity Cu uptake is mediated by Ctr1p and Ctr3p, and once within the cell, Cu chaperones (Atx1p, Lys7p, Cox17p) bind the metal and deliver it to specific proteins in the secretory pathway, cytosolic Cu/Zn-SOD1, and mitochondria. Within the secretory pathway, Ccc2p accepts Cu from Atx1p, followed by Cu incorporation into the multicopper ferroxidase Fet3p. Holo-Fet3p, complexed with the iron permease Ftr1p, is responsible for high affinity iron uptake at the plasma membrane. Cu-Cox17p delivers Cu to cytochrome oxidase in the mitochondrion, which involves the inner membrane protein Sco1p and possibly its homologue, Sco2p. (Adapted from Peña et al. 1999).

Interactions between ATOX1 and the N-terminal domains of ATP7A and ATP7B have been demonstrated *in vivo* and *in vitro*, and shown to be dependent on the presence of Cu (Larin *et al.* 1999; Lockhart and Mercer 2000; Hamza *et al.* 2001). This transient interaction could be disrupted by WND patient mutations and by mutation of the conserved cysteines in ATOX1, suggesting that the interaction is essential for normal Cu homeostasis and Cu may be necessary for the process (Hamza *et al.* 2001).

Biochemical studies have established that the protein-protein interaction results in the Cu transfer from ATOX1 to ATP7A or ATP7B (Walker *et al.* 2002). ATOX1 transferred Cu to fill all six N-terminal MBSs upon incubation of the N-terminal domain of ATP7B (N-ATP7B), bound to amylose resin, with increasing amounts of purified Cu-ATOX1. Incubation with Cu-ATOX1 also resulted in the catalytic phosphorylation of membrane-bound full-length ATP7B. This activation of ATP7B was not apparent with apo-ATOX1. Furthermore, apo-ATOX1 can remove Cu from Cu-bound N-ATP7B and full-length Cu-bound ATP7B, and consequently, down-regulate the activity of membrane-bound ATP7B (Walker *et al.* 2002); therefore, ATOX1 can presumably control ATP7B function by regulating the amount of Cu bound to the transporter.

Reversal of Cu-binding by apo-ATOX1 does not strip all of the Cu atoms from a fully-loaded N-ATP7B. Three to four Cu atoms were easily removed from ATP7B *in vitro* using a small excess of apo-ATOX1 over N-ATP7B, but 1.11 ± 0.11 Cu atoms remained bound even with a large excess of apo-ATOX1 (Walker *et al.* 2002). Despite this Cu removal, ATP7B still retained substantial activity (~ 50%), indicating that occupation of all metal-binding sites is not necessary to support function (Walker *et al.* 2002), and that Cu was only removed from the regulatory binding sites (Lutsenko *et al.* 2002). These studies have thus elucidated a critical role for ATOX1 in the regulation of ATP7B activity and its Cu transport function.

B. Role of the N-terminal domain in copper transport

The N-terminal domains of ATP7A and ATP7B contain six metal binding sites (MBSs). Each N-terminal MBS contains a metal-binding GMxCxxCxxxIE motif within a 70 amino acid residue sequence that is evolutionarily conserved in heavy metal-binding proteins

(DiDonato *et al.* 1997; Lutsenko *et al.* 1997). This N-terminal Cu-binding domain (CuBD) plays an essential role in the Cu transport function and activity of the proteins. Importantly, Cu has been shown to bind to the N-ATP7B in the Cu^{+}-form (reduced state) with a Cu:protein ratio of 6.5-7.3:1 (DiDonato *et al.* 1997; Sarkar 2000).

The N-terminal domain of ATP7B is critical for acquiring Cu from ATOX1, as the MBS in ATOX1 binds specifically to the ATP7B CuBD. A single MBS of ATP7B is capable of interaction with ATOX1, and all six of the binding sites are capable of being occupied by Cu, as indicated by the Cu:protein ratio (Larin *et al.* 1999).

Recent results suggest that ATOX1 delivers Cu specifically to the second MBS (Walker *et al.* 2004) even though the chaperone was capable of interacting with several ATP7B MBSs in yeast two-hybrid experiments (Larin *et al.* 1999). The specific delivery to MBS 2 was not due to a unique binding ability of the site, since several of the MBSs were sufficiently exposed and available for Cu-binding, and the apparent affinities of the MBSs, including MBS 2, did not differ significantly (Walker *et al.* 2004). In the *in vitro* experiments performed by Walker, it appeared that specific protein-protein interactions with ATOX1 may be responsible for the preferential delivery of Cu to MBS 2. It is possible that in the *in vivo* situation the N-terminus may form intramolecular bonds and interact with other domains of ATP7B, thereby limiting the accessibility of the N-terminal MBSs to ATOX1 and making the transfer of Cu to these motifs strongly dependent on the initial binding of Cu to MBS2. In fact, conformational changes were apparent following the binding of one Cu *in vitro*, as the proteolytic pattern of N-ATP7B changed as a result (Walker *et al.* 2004). Circular dichroism and X-ray absorption studies have indeed shown that Cu-binding to a purified ATP7B CuBD product induces a series of subtle secondary and tertiary structural changes in the domain, which result in more substantial tertiary structure changes (DiDonato *et al.* 2000). Recent data also support the idea that Cu-binding to the N-terminus causes conformational changes, as the binding of an exogenous ligand resulted in the Cu^{+} centres in different subdomains moving into proximity (Ralle *et al.* 2004). This change in conformation was suggested to correlate with either a low- or high-affinity Cu-binding state of the enzyme.

The N-terminal conformational changes may be transmitted to the catalytic domains of the transporter and affect the interaction between the ATP-BD and the N-terminal CuBD of ATP7B. This has been demonstrated *in vitro*, with the interaction between the domains being altered by Cu binding to the MBSs (Tsivkovskii *et al.* 2001). Experimental evidence has indicated that Cu-free and Cu-bound forms of N-ATP7B induce distinct and specific conformational changes. The ATP-BD associated more tightly with a Cu-free form of N-ATP7B as compared with the Cu-bound form. It is possible that the Cu-free N-terminal CuBD holds the ATP-BD in a certain conformation to prevent the transport of Cu; whereas, Cu-binding by the CuBD triggers conformational changes in the N-terminus, resulting in decreased domain-domain interactions and allowing the ATP-BD to adopt a different conformation with a higher affinity for ATP and initiation of the transport cycle (DiDonato *et al.* 2000; Tsivkovskii *et al.* 2001).

Based on zinc binding experiments, Cu-binding by the CuBD of ATP7B may be cooperative (DiDonato *et al.* 1997; Sarkar 2000). The cooperative activation indicates that transition of these proteins from a low affinity Cu-binding state to a high affinity state involves binding of Cu to more than one site (Huster and Lutsenko 2003). This property enables ATP7B to have a more sensitive response to Cu concentration, which facilitates the retrieval of this scarcely available metal ion in the cytosol, provides efficient transport even under low intracellular Cu conditions, and enables effective responses to small changes in metal concentration. For ATP7B, both MBS 5 and MBS 6 may be required for the cooperative effect of Cu, as mutation of these sites results in non-cooperative activation. This implied that these two MBSs occupy similar positions within the CuBD, and that binding of Cu to one allows Cu-binding to the other (Huster and Lutsenko 2003). Importantly, however, either motif 5 or 6 alone is sufficient for the Cu transport function of ATP7B, as discussed below (Forbes *et al.* 1999; Cater *et al.* 2004).

The delivery of Cu from the cytosolic N-terminus to the intramembrane Cu-binding site(s) is critical for catalytic phosphorylation and thus the translocation of Cu. MBS 5 and MBS 6 have also been implicated in this process, as either of these MBSs are necessary for the Cu transport function of ATP7B (Iida *et al.* 1998; Forbes *et al.* 1999). Furthermore, MBS 5 and MBS 6 regulate the affinity of intramembrane site(s) for Cu, since mutation of these

MBSs result in mutant proteins with an increased affinity for Cu and decreased inhibition by BCS (Huster and Lutsenko 2003). Possibly the motifs nearer to the TM domains are important for Cu delivery and Cu-binding in the channel.

In contrast to MBS 5 and MBS 6 of ATP7B, the role of the first four MBSs is unclear and appears to be more regulatory in nature. These motifs have been postulated to regulate the access of Cu to the functionally important MBSs, and to increase the efficacy of cytoplasmic Cu scavenging or Cu delivery to the transduction channel (Huster and Lutsenko 2003; Cater *et al.* 2004; Walker *et al.* 2004). These MBSs may be important under certain cellular conditions and necessary for additional functional aspects of ATP7B.

C. Role of additional residues in copper transport

The residues Cys-980, Cys-983 and Cys-985 in the sixth TM domain of ATP7B have been shown to be essential for Cu transport. This may be due to their ability to provide a suitable coordination geometry for Cu^+ ion binding. Importantly, Cys-983 and Cys-985 are part of the CPC motif in TM 6 thought to be critical for formation of the transduction channel. Mutations of the CPC residues result in non-functional proteins (Forbes and Cox 1998; Yoshimizu *et al.* 1998), and the motif has been demonstrated to interact with Cu^+ (Myari *et al.* 2004). The involvement of the CPC motif in Cu transport is not surprising given its location within the transduction channel and the binding property of cysteine residues (i.e. free sulfhydryl groups). In fact, both of the cysteine residues are essential for interacting with Cu^+, as the interaction is abolished when one of the two cysteines of the CPC motif is mutated (Myari *et al.* 2004). The role of the Pro residue is unclear as proline mutation studies have not been reported; however, given its conservation in heavy metal-transporting ATPases, the proline is likely important. Nuclear magnetic resonance data has demonstrated a significant shift for proline protons in response to Cu-binding; thus supporting a role for the proline in Cu transport. The proline may regulate transport channel opening and closing, as the Cys-Pro cis peptide bond is energetically accessible, allowing conversion of H-bonding patterns and resulting in different conformational states (Myari *et al.* 2004).

Single amino acid substitutions in the conserved DKTG motif, such as Asp1027Ala and Thr1029Ala, have also been introduced into the ATP7B coding region and analyzed in yeast mutant for *CCC2*. Both variants were unable to rescue the *ccc2* mutant, suggesting that the DKTG motif is also essential for the manifestation of ATP7B Cu transport function (Iida *et al.* 1998). This is likely due to the role of the conserved aspartic acid residue in the catalytic cycle as it is phosphorylated during Cu transport.

V. ACYL-PHOSPHORYLATION AND THE CATALYTIC TRANSPORT CYCLE

The catalytic transport cycle of classical P-type ATPases is characterized by the coupled reactions of cation translocation and ATP hydrolysis with a transient aspartyl phosphate formed as a part of the reaction cycle. The binding of a phosphate results in the enzyme changing its conformation from the high affinity cation (i.e. binding of Cu) and nucleotide binding state (i.e. binding of ATP), E1, to the low affinity, E2 state. Binding of ATP and catalytic phosphorylation are the key steps in ATP7B-mediated Cu transport.

The expression of ATP7B in insect cells has been useful in displaying some of the catalytic properties of ATP7B that are characteristic of P-type ATPases (Tsivkovskii *et al.* 2002). Experiments have confirmed that the transport of Cu by either ATP7A or ATP7B requires ATP (Voskoboinik *et al.* 1998; Voskoboinik *et al.* 2001a). Furthermore, incubation of ATP7B with 1-2 μM of radioactive -ATP results in the transfer of the -phosphate of ATP to the invariant Asp residue in the DKTG motif and formation of a phosphorylated intermediate which can be monitored following separation of the protein on an acidic gel. The aspartyl-phosphate intermediate that is formed is transient in nature, reversible in the presence of ADP, and sensitive to treatment with hydroxylamine (Tsivkovskii *et al.* 2002). The sensitivity to hydroxylamine distinguishes this product of catalytic phosphorylation from the products of phosphorylation by kinases.

The formation of an acyl-phosphate was shown to depend on the presence of the transported Cu ion, and to be Cu concentration-dependent and Cu-specific. A trace amount of Cu was sufficient for the formation of an acyl-phosphate intermediate of ATP7B, as the presence of 1-1.5 μM Cu was adequate to fully activate ATP7B. As expected, the addition

of a Cu chelator, bathocuproine disulphonic acid (BCS), was able to decrease the level of catalytic phosphorylation; however, a concentration of chelator much greater than that needed to just sequester the Cu present in the system was necessary in order to inactivate ATP7B. This indicated that the BCS was required to both sequester the Cu in the buffers and to compete with ATP7B for the Cu tightly bound to its metal-binding sites (MBSs). Furthermore, removal of Cu from ATP7B caused a decrease in the apparent affinity of BCS-treated ATP7B for Cu, as more Cu had to be added to BCS-treated ATP7B to obtain a comparable level of activity than before the BCS treatment (Tsivkovskii *et al.* 2002). From these results, it has been suggested that prior to BCS treatment, Cu bound to the N-terminus of ATP7B confers a high affinity state of ATP7B, where Cu can bind efficiently to the intramembrane site(s) and induce catalytic phosphorylation. Upon Cu removal from the N-terminus, the conformation of ATP7B is altered which results in a decreased affinity for Cu and down-regulation of the protein (Lutsenko *et al.* 2002).

A. Role of the N-terminal domain

Studies analyzing the regulation of the catalytic activity of ATP7A in the yeast *ccc2* system have revealed an ATP7A variant with MBSs 1-6 mutated from Cys-X-X-Cys to Ser-X-X-Ser, that was catalytically active yet possessed a decreased affinity for Cu (Voskoboinik *et al.* 2001b). It is possible that under conditions of increased Cu concentrations, the catalytic cycle of the mutant protein is similar to wild-type ATP7A, whereas under physiological Cu concentrations, the mutant protein is unable to perform its catalytic function. This indicated that the N-terminal MBSs may be internal regulators of ATP7A activity. The CuBD may provide the enzyme with high affinity Cu sensors that, upon binding of Cu, increase the proportion of ATP7A in the E1 state and thus facilitate initiation of catalysis. Under physiological conditions where bioavailable Cu is found at very low concentrations, Cu may be delivered to the MBSs via the high-affinity Cu chaperone ATOX1, and permit the initiation of catalysis and Cu translocation. Thus, the N-terminus is particularly critical given its role in providing Cu to the intramembrane MBS.

B. Role of copper binding sites in the cation channel

The cation channel appears be important during the catalytic cycle as the cycle begins with the binding of Cu to intramembrane MBSs in the channel (Voskoboinik *et al.* 2001b). Disruption of these high affinity MBSs probably prevents ATP binding and thus phosphorylation. In fact, mutation of a highly conserved methionine residue within TM 8 (*tx* mutation) resulted in lost Cu-translocating activity and an inability to become transiently phosphorylated (Voskoboinik *et al.* 2001a). This implied the methionine may constitute a part of the Cu channel and binding of Cu to the putative intramembrane site(s) is required for ATP hydrolysis. Mutation of a residue in the bacterial Zn^{2+}-transporter, ZntA, which corresponds to the WND mutation Pro992Leu and located between the MBS and the phosphorylation domain, caused low ATPase activity and poor phosphorylation and dephosphorylation (Okkeri *et al.* 2002). It was suggested that the effect was due to a defect in the communication between the metal binding and phosphorylation sites, thus supporting the idea that high affinity Cu binding within the cation channel may be a prerequisite for acyl-phosphorylation.

C. Function of the ATP-binding domain in catalysis

The three-dimensional (3D) structure of the ATP-binding domain (ATP-BD) of ATP7B has been modeled (Fatemi and Sarkar 2002b; Lutsenko *et al.* 2002; Tsivkovskii *et al.* 2003; Efremov *et al.* 2004; Morgan *et al.* 2004) based upon the high resolution crystal structure of the Ca^{2+}-transporting P-type ATPase of the sarcoplasmic reticulum, SERCA1a (Toyoshima *et al.* 2000). As with SERCA1a, the ATP-BD of ATP7B consists of two structural sub-domains: the P-domain, which contains the site of catalytic phosphorylation, and the N-domain, which may form a binding site for ATP.

The modeling data have predicted that the overall catalytic reaction, which occurs within the conserved P-domain, is likely to be similar for ATP7B and SERCA. The nucleotide-binding properties of the N-domains, on the other hand, could be different as the homology between the two proteins in this region was lower. Unfortunately, the residues known to be involved in ATP binding in SERCA and the Na^+, K^+-ATPase are not conserved in the structure of ATP7B (Lutsenko *et al.* 2002).

The structures of the P- and N-domains in SERCA have also suggested that domain motion plays a central role in the catalytic activity of P-type ATPases (Toyoshima *et al.* 2000; Toyoshima and Nomura 2002). As noted previously, Cu loading of the N-terminus of ATP7B weakens the interaction between the ATP-BD and the CuBD, causing the domains to dissociate (Tsivkovskii *et al.* 2001). This dissociation would facilitate the nucleotide-binding affinity of the N-domain, thereby allowing the binding of ATP to the site. The binding of ATP to the metal-bound E1 state could induce movement of the N-domain towards the P-domain, resulting in the formation of the high-affinity site for ATP and subsequent phosphorylation of the aspartate residue and initiation of catalysis; however, it is also possible that the domain movement results from large-scale thermal motions independent of ATP binding. Regardless of the order of events, the conformational changes are predicted to be transmitted to the translocation domain, thereby changing the accessibility of the channel to the cytosolic and lumenal spaces (Fatemi and Sarkar 2002b). The hydrolysis of the acyl-phosphate requires the release of Cu from the transduction channel into the lumen, which thus allows the cycle to repeat itself.

Using computational modeling and simulations of the ATP-BD of ATP7B, large-scale movements of the P- and N-sub-domains have been demonstrated (Efremov *et al.* 2004). The dynamics seemed to mainly consist of a narrowing of the space separating the sub-domains, which subsequently induced significant changes in the distances between several key residues. The adenosine moiety of ATP was shown to be buried in a cleft near residues His-1069, Arg-1151 and Asp-1164. The carboxy group of Asp-1164 appeared to play a critical role in forming an H-bond with the amino group of the ATP; whereas, Arg-1151, along with Lys-1028 and Asp-1222 seemed to stabilize and anchor the -phosphate moiety of the bound ATP in the E1 state and orient it toward the functionally important Asp-1027 residue. Upon conformational transition towards the E2 state, the -phosphate appeared to reach the carboxy group of Asp-1027 in the simulation experiments, with the phosphate tail of the ligand being stabilized by H-bonds with Asp-1027, Lys-1028 and Thr-1029.

Experimental evidence has confirmed some of the findings from the molecular modeling. The site of the most frequent WND mutation, His-1069, was analyzed for its role in enzymatic activity. Mutations of His-1069 suggested that His-1069 plays a key role in

binding and positioning ATP, either directly or indirectly, with respect to the catalytic aspartate, thus allowing phosphorylation to occur (Okkeri and Haltia 1999; Okkeri *et al.* 2002; Tsivkovskii *et al.* 2003; Morgan *et al.* 2004; Okkeri *et al.* 2004). The residue Glu-1064 may also be important for catalytic activity and nucleotide coordination, as the mutation Glu1064Ala drastically reduced ATP affinity (Okkeri and Haltia 1999; Morgan *et al.* 2004; Okkeri *et al.* 2004). On the other hand, mutation of Arg-1151 only slightly reduced the domain's affinity for ATP (Morgan *et al.* 2004). This was surprising as the molecular model predicted a significant role for Arg1151 in anchoring the bound ATP (Efremov *et al.* 2004). Studies using ZntA also suggest that there may be a glycine motif (Gly-1099 to Val-1106) in ATP7B involved in forming the nucleotide binding site (Okkeri *et al.* 2004).

Mutation of the invariant aspartate residue in ATP7B within the DKTG motif had no affect on ATP7B expression in insect cells, but did prevent its catalytic phosphorylation, affirming its role as the acceptor of the -phosphate during ATP hydrolysis. This was also demonstrated in ATP7A, where a Asp1044Glu mutation was unable to form an acylphosphate intermediate and resulted in a loss of Cu-translocating activity (Voskoboinik *et al.* 2001b). These results confirmed that the invariant aspartate within these Cu transporters is most likely the residue phosphorylated during the catalytic cycle.

Several amino acids within the conserved hinge domain of ATP7A (MVGDGINDSP MVAAAINDSP), an essential catalytic domain in the ATP-BD, were also mutated. This variant remained unphosphorylated and lacked Cu-transport activity. The sequence change probably prevented the binding of ATP and subsequent acyl-phosphorylation (Voskoboinik *et al.* 2001b). The important role of the hinge domain has been supported by mutations in ZntA (Okkeri *et al.* 2002). In particular, mutation of the aspartic acid residue and proline residue, which correspond to WND mutations Asp1267Ala and Pro1273Leu, showed that the Asp-1267 has an important role in the phosphorylation site of ATP7B and that Pro-1273 is critical for the transition between the E1and E2 states.

Preliminary data has also identified a novel cytosolic motif in the ATP-BD of ATP7A, Asp-X-X-Lys-1233, which may play a unique role in catalysis by coupling ATP-related events and conformational changes with the Cu transport function (Voskoboinik *et al.*

2003b). Mutation of Asp-1230 resulted in a variant with increased affinity for ATP and highly efficient Cu-dependent phosphorylation, but a significantly impaired ability to translocate Cu.

Clearly, several amino acid residues are critical for formation of the phosphorylated intermediate and completion of the catalytic cycle. ATP-binding to the ATP-BD of ATP7B and transfer of the -phosphate seemingly involves a complex network of H-bonds between conserved residues and both the adenosine and phosphate moieties of ATP. Furthermore, requisite spatial juxtaposition of binding sites is necessary and results from coordinated movements of different domains of the protein.

VI. COPPER EXCRETION FUNCTION OF ATP7B

A. ROLE OF ATP7B IN BILIARY EXCRETION OF COPPER

The liver plays a critical role in Cu metabolism, serving as the site of storage for the metal and being the primary determinant regulating biliary Cu excretion. Hepatocytes are able to sense the Cu status in their cytoplasm and regulate excretion depending upon the intracellular Cu concentration. ATP7B is the key protein accomplishing this metal regulation in the liver, being responsible for the excretion of excess Cu via bile. Biliary excretion of Cu is essential since it is the only physiological route for Cu elimination in humans, with 98% of Cu excretion via the bile and only 2% via the urine; reviewed in (Wijmenga and Klomp 2004).

The function of ATP7B in Cu export has been demonstrated by transfecting a Cu transporter-deficient *mottled* fibroblast cell line defective in Cu export with a wild-type *ATP7B* cDNA construct. Expression of ATP7B rescued the *mottled* phenotype as there was a reduction in the accumulation of Cu in the cell and cell viability was restored, indicating that ATP7B is capable of transporting Cu out of the cell and is important in maintaining cellular Cu homeostasis (Payne *et al.* 1998). *ATP7B* cDNA was also expressed in an immortalized human skin fibroblast cell strain from a patient with classical MNK disease, which restored Cu efflux and reduced the Cu accumulation phenotype of the MNK cells (La Fontaine *et al.* 1998b).

Direct evidence of the role of ATP7B in Cu excretion has also been provided by experiments in the LEC rat (Terada *et al.* 1999; Meng *et al.* 2004). Introduction of wild-type human *ATP7B* into the LEC rat has shown that expression of *ATP7B* decreased cytosolic Cu concentrations, elevated levels of Cu content in the lysosomal fractions, and increased excretion of Cu into the bile relative to control LEC rats. The cytosolic Cu may have been reduced by its discharge into bile through the lysosomal fractions. ATP7B did not associate with the accumulated Cu in the lysosomes, but was instead detected in the microsomal fraction which contains the Golgi apparatus, the site where ATP7B resides under normal basal conditions.

B. Possible role of COMMD1 (MURR1)

Canine Cu toxicosis (CT) is an autosomal recessive disorder with a high frequency in Bedlington terriers (Twedt *et al.* 1979; Johnson *et al.* 1980). Dietary intake of Cu in these animals is normal, but biliary Cu excretion is markedly reduced compared with control animals (Su *et al.* 1982). The excess Cu is stored in the lysosomes of hepatocytes, which leads to liver cirrhosis and death if not treated. The CT locus was localized to canine chromosome region 10q26 (van de Sluis *et al.* 1999), with the CT region further refined to a ~9 MB region (van de Sluis *et al.* 2000) and then to <500 kb (van De Sluis *et al.* 2002). The gene, *COMMD1* (previously known as *MURR1*), was first implicated in Cu homeostasis in 2002 by positional cloning (van De Sluis *et al.* 2002), and it was established that CT is associated with a deletion of exon 2 of the *COMMD1* gene (van De Sluis *et al.* 2002; Coronado *et al.* 2003). The deletion causes complete absence of detectable COMMD1 protein in the livers of affected terriers, whereas expression of *COMMD1* is clearly evident as a 23-kDa polypeptide in normal animals (Klomp *et al.* 2003). *COMMD1* is ubiquitously expressed, suggesting that it may have a pleiotropic function in various organs, not necessarily linked to Cu metabolism (Klomp *et al.* 2003). Studies on the function of COMMD1 have revealed that (i) COMMD1 restricts HIV-1 replication in resting CD4+ lymphocytes by inhibiting NF- B activity (Ganesh *et al.* 2003); (ii) COMMD1 regulates the human epithelial sodium channel (Biasio *et al.* 2004); and (iii) XIAP, a suppressor of apoptosis, may regulate the proteasomal degradation of COMMD1 (Burstein *et al.* 2004). COMMD1 appears to be mainly a cytosolic protein, with a small

portion found in the membranous fraction either bound to membranes or interacting with membrane-associated proteins (Klomp *et al.* 2003).

In terms of its role in Cu metabolism, COMMD1 may function in the ATP7B-mediated pathway of Cu excretion, most likely downstream of ATP7B. This is supported by the *in vitro* and *in vivo* demonstration of a direct interaction between COMMD1 and the N-terminal domain of ATP7B (Tao *et al.* 2003). Remarkably, this interaction is specific for ATP7B, and not ATP7A (Tao *et al.* 2003), consistent with the observation that the phenotype of affected Bedlington terriers is confined to the liver and may be significant for the role of the liver in Cu excretion. A recent study has also demonstrated that a deficiency in COMMD1 results in a slight accumulation of Cu in cultured cells (Burstein *et al.* 2004). The involvement of COMMD1 may be limited to a Cu excretory role as a defective COMMD1 does not completely inactivate ATP7B function. *COMMD1*-deficient Bedlington terriers present with normal plasma holo-Cp activity in spite of their elevated lysosomal Cu content and reduced biliary Cu excretion. A comparison of the *COMMD1* sequence with other fully-sequenced genomes has suggested that the gene is restricted to vertebrates because of their unique ability to excrete toxic compounds via bile (van De Sluis *et al.* 2002).

Indirect immunofluorescence studies in certain cell lines have also demonstrated localization of COMMD1 in intracellular vesicular compartments, with partial overlap with early endosomal and lysosomal markers (Klomp *et al.* 2003), supporting the hypothesis that COMMD1 has a role in Cu excretion into bile during Cu overload. Despite the experimental evidence supporting the involvement of COMMD1 in biliary excretion of Cu, the specific function of COMMD1 in Cu metabolism is still unknown. The role of COMMD1 is particularly questionable since some dogs affected with canine CT do not have the exon 2 deletion of *COMMD1* (Coronado *et al.* 2003; Hyun *et al.* 2004).

VII. ROLE IN REGULATING PLATINUM DRUGS

Recent studies have demonstrated that Cu transporters are involved in the regulation of platinum-containing drugs used in the treatment of cancers, such as cisplatin, carboplatin

and oxaliplatin. The interconnection between platinum drugs and Cu transport was recognized when studying the cellular mechanisms behind the resistance of cells to these drugs following continued therapy. Attention was focused on the transport of the drugs since decreased accumulation was the single most commonly observed defect found in resistant cells; reviewed in (Safaei *et al.* 2004a; Safaei and Howell 2005).

The Cu uptake protein CTR1 plays a role in mediating the transport and sensitivity of cells to the platinum drugs (Ishida *et al.* 2002; Lin *et al.* 2002). In both yeast and mammalian cells lacking CTR1, the cells were resistant to the cytotoxic effect of cisplatin and accumulated less of the platinum drug. The platinum drugs and Cu were found to inhibit each other's uptake in a concentration-dependent manner (Ishida *et al.* 2002; Lin *et al.* 2002), and both caused degradation of CTR1 in yeast cells (Ishida *et al.* 2002). In mammalian cells, the same factors that influenced the uptake of the platinum drugs affected uptake of Cu via CTR1 (Safaei and Howell 2005). Furthermore, Cu and platinum transport showed parallel changes in several studies; different cross-resistant cell lines demonstrated lower levels of both Cu and the platinum drugs than their drug-sensitive counterparts when analyzed following drug exposure (Katano *et al.* 2002; Safaei *et al.* 2004b). Thus, CTR1 appears to be important in regulating the cellular uptake of the platinum drugs and a major route of drug entry.

Several studies have also demonstrated parallel changes in the efflux of Cu and the platinum drugs, suggesting a role for the Cu efflux proteins ATP7A and ATP7B. In fact, research has shown that transfection of an *ATP7B* expression construct into various cancer cell lines either rendered the cell lines resistant to the platinum drugs or enhanced their resistance (Komatsu *et al.* 2000; Samimi *et al.* 2004a). ATP7B-transfected ovarian carcinoma cells accumulated significantly lower levels of Cu and carboplatin following incubation with Cu or the platinum drug, and increased expression of ATP7B heightened the rate of efflux of cisplatin and carboplatin (Katano *et al.* 2003). Furthermore, immunohistochemical and mRNA analyses have illustrated that higher expression of ATP7B is correlated with an unfavourable response to platinum drug treatment (Kanzaki *et al.* 2002; Nakayama *et al.* 2002). Therefore, the data published thus far provide strong evidence that ATP7B mediates resistance to the platinum drugs by regulating drug efflux.

A similar role for ATP7A in drug efflux has also been elucidated (Samimi *et al.* 2004b; Safaei and Howell 2005).

VIII. INTRACELLULAR LOCALIZATION OF ATP7B

Before the assessment of the intracellular localization of ATP7B, the way in which the dual functions of ATP7B were accomplished was puzzling: (i) ATP7B is required to transfer Cu across the TGN membrane and deliver it to the Cu-dependent enzyme Cp, and (ii) ATP7B is critical for the excretion of Cu via bile, presumably near the bile canalicular membrane. Studies have since established that in order to facilitate its activity, ATP7B reacts to modulations in Cu concentration by trafficking from the TGN to an undefined cytosolic vesicular compartment localized toward the hepatocyte canalicular membrane (Figure 1-5) (Hung *et al.* 1997; Schaefer *et al.* 1999a; Schaefer *et al.* 1999b; Suzuki and Gitlin 1999). This response is a posttranslational mechanism of Cu homeostasis that is clearly consistent with the proposed function of ATP7B in holo-Cp biosynthesis and excretion.

A. COPPER-DEPENDENT TRAFFICKING OF ATP7B

Under steady-state conditions, ATP7B is expressed specifically in hepatocytes of the liver, with detection of its intracellular localization in the TGN as a single 165-kDa protein (Hung *et al.* 1997; Yang *et al.* 1997; Schaefer *et al.* 1999a; Schaefer *et al.* 1999b). Cu-dependent trafficking from this basal TGN location is independent of new protein synthesis (Hung *et al.* 1997) and steady-state levels of ATP7B are unaffected by hepatic Cu concentrations (Schaefer *et al.* 1999a). The movement out of the TGN is reversible, as chelation of excess Cu resulted in restoration of the perinuclear localization reminiscent of the TGN. This trafficking process was specific for Cu, as increasing concentrations of zinc, Fe, cadmium, or cobalt had no effect, and was specific for ATP7B, as the general reorganization of the structure and distribution of subcellular organelles was undisturbed (Hung *et al.* 1997).

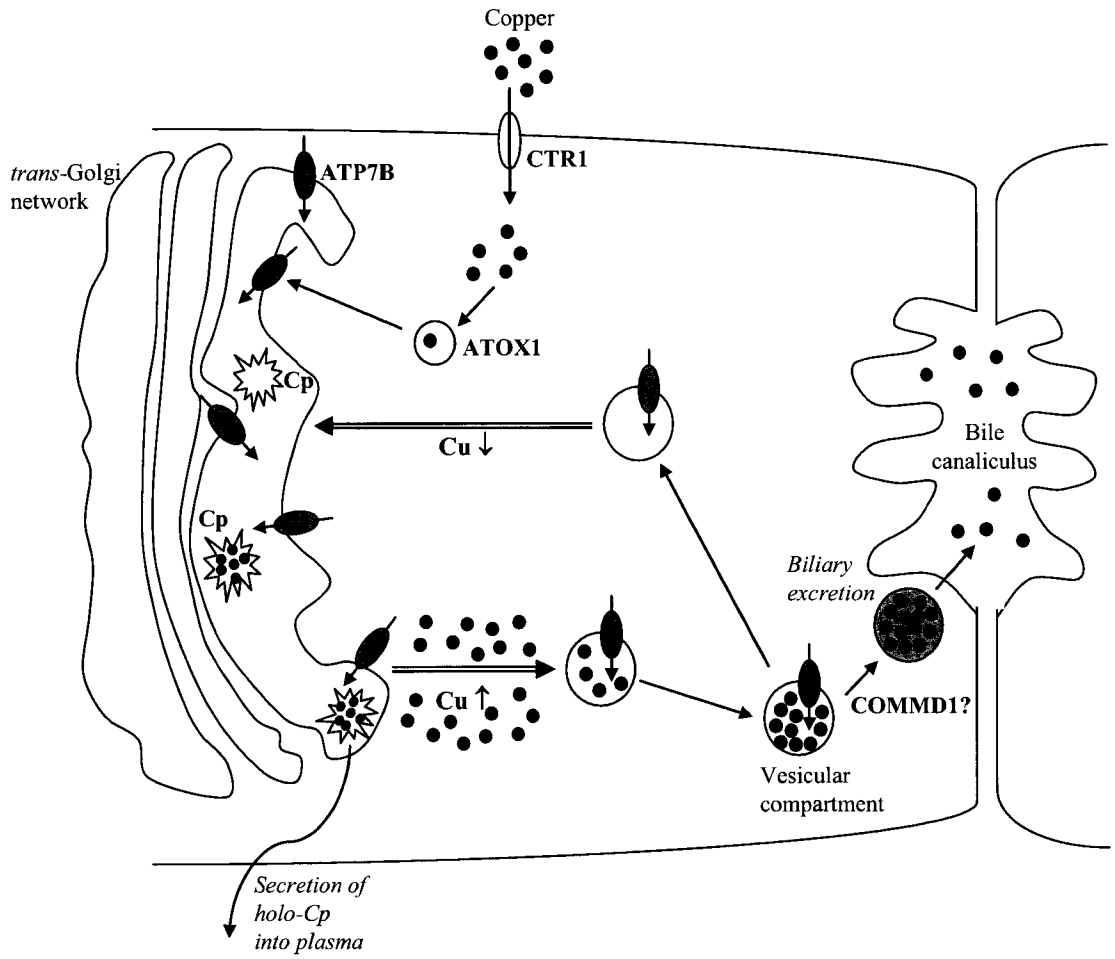

Figure 1-5. Model of the function and copper-induced redistribution of ATP7B within the hepatocyte.

Following Cu entry into the cell via the plasma membrane Cu transporter (CTR1), Cu is delivered to Cu chaperones, including ATOX1. ATOX1 transfers its Cu to ATP7B, which is essential for Cu deliver to ceruloplasmin (Cp). Cu-loaded Cp (holo-Cp) is secreted into the plasma. When copper concentration is elevated, the ATP7B protein redistributes to a pericanalicular vesicular compartment or the apical/canalicular membrane of polarized hepatocyte cells. The biliary excretion of Cu is still ill-defined. It is unknown whether ATP7B fuses with the apical membrane and is itself involved in the biliary excretion, or whether it involves Cu-loading of a vesicle that fuses with the membrane. Research suggests a role for COMMD1 in the biliary excretion of Cu. ATP7B is retrieved to the TGN following a reduction in cellular Cu levels.
(Adapted from Schaefer *et al.* 1999).

Furthermore, ATP7B is continuously recycled between the two intracellular locations; however, ATP7B is localized predominantly to the TGN under low hepatic Cu concentrations, and is localized mainly in a vesicular compartment in the presence of elevated Cu (Hung *et al.* 1997; Schaefer *et al.* 1999a).

Studies using the *tx* mutation have also been performed, demonstrating perinuclear localization of the protein in cells in the mammary gland and movement of wild-type murine Atp7b to a more diffuse distribution upon lactation (Michalczyk *et al.* 2000). The *tx* mouse did not display this redistribution; Atp7b remained in the TGN, which is consistent with the *tx* phenotype where lactating dams homozygous for the mutation produce Cu-deficient milk (Rauch 1983). This indicated that ATP7B localization and trafficking in response to stimuli is critical in cells other than the hepatocytes.

The basal TGN localization has been confirmed by different research groups in various cell lines: endogenous ATP7B in HepG2 (liver) cells (Hung *et al.* 1997; Yang *et al.* 1997), in ATP7B-transfected HTB9 (human bladder carcinoma) cells (Yang *et al.* 1997), in ATP7B-transfected LEC rat hepatocytes (Nagano *et al.* 1998), in ATP7B-transfected murine *mottled* fibroblasts (Payne *et al.* 1998), in ATP7B-transfected fibroblasts from patients with MNK (La Fontaine *et al.* 1998b), endogenous ATP7B in rat hepatocytes (Schaefer *et al.* 1999a; Huster *et al.* 2003), endogenous ATP7B in human hepatocytes (Schaefer *et al.* 1999b), in ATP7B-transfected CHO cells (Forbes and Cox 2000; La Fontaine *et al.* 2001; Cater *et al.* 2004), endogenous ATP7B in polarized hepatic cells (Roelofsen *et al.* 2000; Guo *et al.* 2005), and in GFP-ATP7B-transfected Huh7 (liver) and HepG2 cells (Huster *et al.* 2003).

Intracellular trafficking of a Cu transporter was first observed by Petris et al., who studied the redistribution of ATP7A (Petris *et al.* 1996). Hung et al. (Hung *et al.* 1997) were the first to demonstrate the Cu-induced relocalization of ATP7B in hepatocytes. Besides the usual concentrated perinuclear location indicative of the TGN, a variable degree of ATP7B-specific signal was also shown in a punctate expression pattern in some cells. This varied expression was similarly evident in normal human liver sections, where some ATP7B was detected in vesicular structures at the canalicular membrane of hepatocytes;

the majority of the staining, however, was still in the TGN of hepatocytes, confirming the TGN as the steady-state location of ATP7B (Schaefer *et al.* 1999b). Rat liver sections also demonstrated a small proportion of ATP7B in a punctate pattern in the cytoplasm not co-localized with the TGN (Schaefer *et al.* 1999a). These findings are consistent with the experimental evidence showing that ATP7B continuously recycles between the TGN and a vesicular cytoplasmic compartment.

In HepG2 cells, the effect of Cu was saturable with respect to Cu concentration and time, with movement from the TGN detected within 15 min and found in >95% of all cells within 2 hr (Hung *et al.* 1997). The redistribution occurred at a minimal concentration of 40 μM of $CuSO_4$ (Hung *et al.* 1997). A lower Cu concentration and less time were required for the Cu-dependent trafficking in primary rat hepatocytes (Schaefer *et al.* 1999a). Studies in rats also indicated that there may be a threshold Cu concentration necessary to trigger redistribution, since Cu excretion in a Cu-deficient rat re-introduced to a Cu-loaded diet was only measurable once the level of hepatic Cu reached a specific threshold necessary to initiate relocalization (Owen and Hazelrig 1966). Requirement for a certain threshold seems reasonable, given a recent study illustrating a significant role for ATOX1 in Cu efflux (Hamza *et al.* 2003). At lower levels of Cu (between 0.1 and 10 μM of Cu), ATOX1 was essential for Cu-mediated movement of ATP7A out of the Golgi; however, the protein was dispensable under conditions of higher Cu concentrations (i.e. 100 μM Cu).

To establish a possible Cu threshold and outline the possible anterograde and retrograde pathway of ATP7B, Cu- and time-dependent studies have been performed in a polarized hepatoma cell line (HepG2) (Roelofsen *et al.* 2000). TGN localization was observed only when extracellular Cu concentrations were low (<1 μM). Within 30 min after the addition of 20 μM $CuSO_4$, ATP7B was distributed in the cytosol in vesicular structures, and after 4 hours, much of the ATP7B had accumulated in apical vacuoles close to bile canaliculi. Even in the presence of only 1 μM Cu, a significant percentage of apical vacuoles were positive for ATP7B within 4 hours. Interestingly, it was found that the percentage of positive apical vacuoles reached a plateau of around 60% after a few hours of incubation. Prolonged incubations or higher concentrations of Cu did not further increase this

percentage, and not all apical vacuoles became positive for ATP7B after Cu treatment. Following the removal of extracellular Cu, most apical vacuoles were devoid of ATP7B after three hours, and by the 16 hour mark, the majority of ATP7B had returned to the TGN in virtually all polarized cells examined. The redistribution process of ATP7B thus appears to be quite sensitive to Cu, and initiated and completed in a time-sensitive manner.

The intracellular site to which ATP7B trafficks in response to increased Cu levels has not been fully clarified. Cu-induced movement from the TGN is normally associated with redistribution to an undefined cytoplasmic vesicular compartment. *In vitro* studies have reported the specific trafficking to a novel cytoplasmic vesicular compartment in HepG2 cells (Hung *et al.* 1997), in CHO cells (Forbes and Cox 2000; Cater *et al.* 2004) and in a polarized hepatic cell line, WIF-B (Guo *et al.* 2005). The introduction of wild-type ATP7B-GFP (green fluorescent protein) expression plasmids in HepG2 and Huh7 cells also resulted in the trafficking of the protein from the TGN to a diffuse vesicular distribution in the cell periphery (Huster *et al.* 2003). However, other *in vitro* studies in primary rat hepatocytes (Schaefer *et al.* 1999a) and polarized hepatic cells (Roelofsen *et al.* 2000; Guo *et al.* 2005), have further established relocalization of ATP7B to the apical PM, in addition to cytoplasmic vesicles. Studies performed *in vivo* have also demonstrated the presence of ATP7B both at the TGN and at or near the PM of hepatocytes following the injection of an ATP7B expression construct into LEC rats (Nagano *et al.* 1998). Furthermore, a predominance of ATP7B-containing vesicular structures near the bile canalicular membrane in the liver sections from a Cu-loaded normal rat has been noted (Schaefer *et al.* 1999a). Thus, it still remains unclear whether ATP7B trafficks and is localized to the bile canalicular membrane or if it only redistributes to vesicular structures within the cytoplasm or to vesicular structures near the membrane. From the studies in polarized hepatic cells, it may be that ATP7B continuously recycles between a subapical vesicular compartment and the apical membrane when Cu levels are increased (Roelofsen *et al.* 2000), making the localization of ATP7B to one site or the other difficult to assess. In fact, endogenous ATP7B has been shown to overlap in expression with Rab11 (Guo *et al.* 2005), which has been localized to apical recycling compartments in polarized cells (Wang *et al.* 2001).

Despite the experimental evidence establishing the intracellular localization and Cu-dependent trafficking properties of ATP7B, controversy still exists over the steady-state location of the protein and whether or not the protein changes its intracellular localization in response to a change in the environmental Cu concentrations. An earlier report indicated that ATP7B in HepG2 cells did not re-distribute in response to elevated Cu levels (200 μM Cu for 1 or 24 h), and instead remained localized in the perinuclear regions, thought to be the TGN, similar to that seen in basal Cu conditions (Yang *et al.* 1997). A more current report illustrated Cu-induced relocalization in the polarized hepatic WIF-B cell line; however, the data also indicated that incubation in Cu chelator resulted in localization to a post-TGN compartment containing syntaxin 6, which has been implicated in retrograde trafficking (Guo *et al.* 2005).

More recent studies have been even more controversial, suggesting that ATP7B is not localized in the TGN but rather in late endosomes, and is observed at this intracellular location in either Cu-depleted or Cu-loaded conditions. This late endosomal localization of ATP7B has been demonstrated by transfecting Huh7 cells (Harada *et al.* 2000a; Harada *et al.* 2000b; Harada *et al.* 2001; Harada *et al.* 2005), isolated rat hepatocytes (Harada *et al.* 2000b), HEK293 cells (Harada *et al.* 2001; Harada *et al.* 2003), Hep3B cells, a highly polarized human hepatocyte cell line OUMS29 (Harada *et al.* 2003; Harada *et al.* 2005), and Madin-Darby canine kidney (MDCK) cells (Harada *et al.* 2005), with *ATP7B* tagged with GFP. These researchers have proposed that the late endosome localization is favourable given the role of ATP7B in Cu homeostasis in the hepatocyte. ATP7B may translocate Cu from the cytosol into the late endosomal lumen, and then Cu in the late endosomes may be transported to lysosomes and excreted to the bile by a process referred to as biliary lysosomal excretion (Gross *et al.* 1989; Harada *et al.* 1993). Cu in the late endosomes may be transported to the TGN by mannose-6-phosphate receptor recycling vesicles and incorporated into apo-Cp at the TGN to fulfil ATP7B's biosynthetic role (Harada *et al.* 2003).

Regardless of the localization of ATP7B in the TGN or late endosomes, it is evident that wherever ATP7B resides, the protein must be able to carry out its dual functional role in

the hepatocytes or traffick to the correct intracellular compartment in order to perform its biosynthetic function or excretory function.

i. Copper-dependent localization studies on ATP7A

ATP7A also displays this unique system of protein distribution whereby the ligand directly and specifically stimulates the trafficking of its own transporter (Petris *et al.* 1996). In fact, ATP7A was the first Cu transporter to show this type of Cu-dependent relocalization, and many of the trafficking studies of the Cu transporters were performed on ATP7A before the trafficking of ATP7B had been defined. The Cu-dependent movement of ATP7A is similar to ATP7B except that ATP7A moves from its basal localization in the TGN (Yamaguchi *et al.* 1996; Dierick *et al.* 1997) to the PM following stimulation with Cu (Petris *et al.* 1996). ATP7A was also identified in association with intracellular vesicles, supporting the hypothesis that either ATP7A transports Cu into vesicles en route to the PM and the Cu is then released from the cell upon fusion of the vesicles with the membrane, or that the vesicles simply serve to carry ATP7A to the PM where Cu is effluxed from the cell (La Fontaine *et al.* 1998a). Studies have indicated that trafficking occurs in a constitutive fashion, does not require new protein synthesis, and is reversible, as for ATP7B (Petris *et al.* 1996; La Fontaine *et al.* 1998a; Petris and Mercer 1999). Given the constitutive recycling of the protein, the effect of elevated extracellular Cu levels is to increase exocytic movement of ATP7A from the TGN, rather than to reduce retrieval from the PM (Petris and Mercer 1999), thus resulting in a shift of the steady state of the protein toward the PM in conditions of high Cu. This is consistent with the results from experiments using biotin labeling of cell surface proteins, where Cu did not exert a significant effect on ATP7A endocytosis from the PM as the rate of internalization was similar in the presence and absence of added extracellular Cu (Pase *et al.* 2004).

Current information on ATP7A and ATP7B trafficking suggests that there may be several, potentially interrelated, mechanisms controlling the steady-state localization and Cu-induced trafficking of these human Cu transporters.

B. Factors regulating localization and trafficking of ATP7B

i. Targeting motifs in ATP7A and ATP7B

a. N-terminal exocytic signal

Several protein domains and signals involved in ATP7A trafficking and subcellular localization have been identified. Researchers have identified a possible exocytic signal, showing that one N-terminal CXXC MBS is necessary and sufficient for the Cu-induced redistribution of ATP7A from the TGN to the PM (Goodyer *et al.* 1999; Strausak *et al.* 1999). In one study, researchers found that any one of the MBSs alone was capable of sustaining the trafficking ability of ATP7A (Goodyer *et al.* 1999); however, other research has shown that mutation of MBSs 4-6 resulted in an ATP7A mutant variant that remained localized to the TGN even when exposed to 300 μM Cu (Strausak *et al.* 1999). It was further demonstrated in this second study that either MBS 5 or MBS 6, within a maximum distance of ~170 amino acids from the proposed transduction channel was necessary and sufficient for Cu-induced movement from the TGN (Strausak *et al.* 1999). On the other hand, amino acids 8-495 of the ATP7A N-terminus, which includes MBSs 1-4, were not necessary for trafficking to the PM, which suggested that this region of the protein did not contain a critical Cu-sensing or Cu-responsive targeting signal (Strausak *et al.* 1999). Evidence also suggests that the 27 amino acid sequence linking MBS 6 to the first TM of ATP7A is important for localization (Das *et al.* 1995; Kim *et al.* 2003). In fact, a Menkes patient mutation in exon 8, which encodes the linker region, has been shown to have normal Cu transport function but failed to traffick out of the TGN in high Cu conditions (Kim *et al.* 2003).

Although studies on the signals responsible for ATP7B trafficking have not been as extensive as they have been for ATP7A, recent reports have indicated similar, yet distinct, results in regards to the role of the N-terminus of ATP7B in Cu-induced relocalization. Of the six N-terminal MBSs, only MBS 5 or MBS 6 is required for the trafficking process, with either MBS being necessary to support the redistribution of ATP7B to vesicular compartments (Cater *et al.* 2004). Interestingly, these are the same MBSs that have been shown to be significant for the Cu transport function of ATP7B, indicating that the ability to traffick correctly correlates with the ability to transport Cu. In addition to either MBS 5

or MBS 6, the first 63 amino acids of the N-terminus are also required for correct trafficking of ATP7B (Guo *et al.* 2005). Amino acids 64-540, which encompasses MBS1-5, could be deleted with no effect on the trafficking capability of ATP7B (Cater *et al.* 2004; Guo *et al.* 2005), suggesting that amino acids 1-63 contain necessary information for the Cu responsiveness and correct targeting of ATP7B. The importance of these N-terminal 63 amino acids in Cu transport has not been specifically analyzed. The requisite 63 amino acids at the very N-terminus are not necessary in ATP7A (Strausak *et al.* 1999), which may explain the different destinations of the two proteins; Cu efflux by ATP7A in the intestine is into the basolateral space (i.e. interstitium), whereas that of ATP7B in hepatocytes is into the apical space (i.e. bile) (Roelofsen *et al.* 2000; Mercer *et al.* 2003).

b. Golgi retention signal

Extensive analysis on the trafficking of ATP7A has elucidated additional sequence motifs that may be significant for localization. A stretch of amino acids containing TM 3 may be responsible for Golgi retention of the MNK protein (Francis *et al.* 1998). Alternatively spliced forms, which lack the sequence for TM 3 and TM 4 encoded by exon 10, were shown to localize to the endoplasmic reticulum instead of the TGN (Francis *et al.* 1998; Qi and Byers 1998), and a 38 amino acid sequence containing TM 3 fused to a non-Golgi reporter molecule was shown to be sufficient for localization to the Golgi (Francis *et al.* 1998).

Under elevated Cu conditions, it is plausible that this TGN retention signal is not capable of retaining the protein in the TGN and thus redistribution ensues. Conformational changes, as a result of Cu binding to the N-terminus and ATP binding to the ATP-BD, may also play a role in reducing the efficiency of the TM 3 retention signal, or it may reveal a targeting motif, such as the di-leucine motif present in the C-terminus of ATP7A (described below), to be recognized by vesicular sorting machinery.

c. The di-leucine targeting motif

Given that both ATP7A and ATP7B constitutively recycle between the TGN and the cell surface/cytoplasmic vesicles, it is reasonable that TGN localization of the proteins will depend on retrieval from the surface/cytoplasmic vesicles into the endocytic pathway for

recycling to the TGN. The Golgi retention signal that is responsible for retaining ATP7A in the TGN and those signals in the N-terminus that are possibly responsible for exocytosis are not sufficient for recycling ATP7A back to the TGN once it is localized to the cell surface; therefore, the Cu-dependent trafficking of ATP7A and ATP7B necessitates the presence of specific endocytic signals.

Endocytic signals are generally on the cytosolic side of proteins and consist of short amino acid sequences. The cytoplasmic signals responsible for internalization mainly fall into two common types: (i) the tyrosine-based motifs, which contain a critical tyrosine residue within the consensus sequences, NPXY or YXXØ (where Ø represents an amino acid with a bulky hydrophobic group), and (ii) the di-leucine (or isoleucine-leucine) signals (Trowbridge *et al.* 1993). Both of these motifs generally function by concentrating proteins into clathrin-coated pits at the cell surface prior to endocytosis. In addition to its major role in endocytosis, the di-leucine motif is also important in the targeting of proteins to endosomes and lysosomes (Letourneur and Klausner 1992; Dittrich *et al.* 1994; Dittrich *et al.* 1996; Garippa *et al.* 1996; Morrison *et al.* 1996; Tan *et al.* 1998).

The tyrosine-based and di-leucine motifs, found in several proteins, are essential for conferring the steady-state TGN localization by surface retrieval. They are found in many recycling proteins, including TGN38 (Bos *et al.* 1993), the endopeptidase, furin (Schafer *et al.* 1995; Voorhees *et al.* 1995), the virus envelope protein, gp1 (Alconada *et al.* 1996), and GLUT4 (Corvera *et al.* 1994; Verhey and Birnbaum 1994).

Adaptor proteins (AP), including AP-1, AP-2, AP-3 and AP-4 (Simpson *et al.* 1997; Hirst and Robinson 1998; Robinson and Bonifacino 2001), are involved in the organelle targeting by the tyrosine and di-leucine motifs (Figure 1-6). These adaptor proteins are important for linking the clathrin-coated vesicles, which help move proteins through the endocytic pathway, to the organelles, such as the TGN (via AP-1) or the PM (via AP-2). The recognition and binding of the targeting signals by the APs has been shown to enable clathrin-coated vesicle transport of the protein (Robinson 1994). The role of AP-3 and AP-4 are still uncertain, but have been implicated in protein sorting at the TGN and/or endosomes (Robinson and Bonifacino 2001).

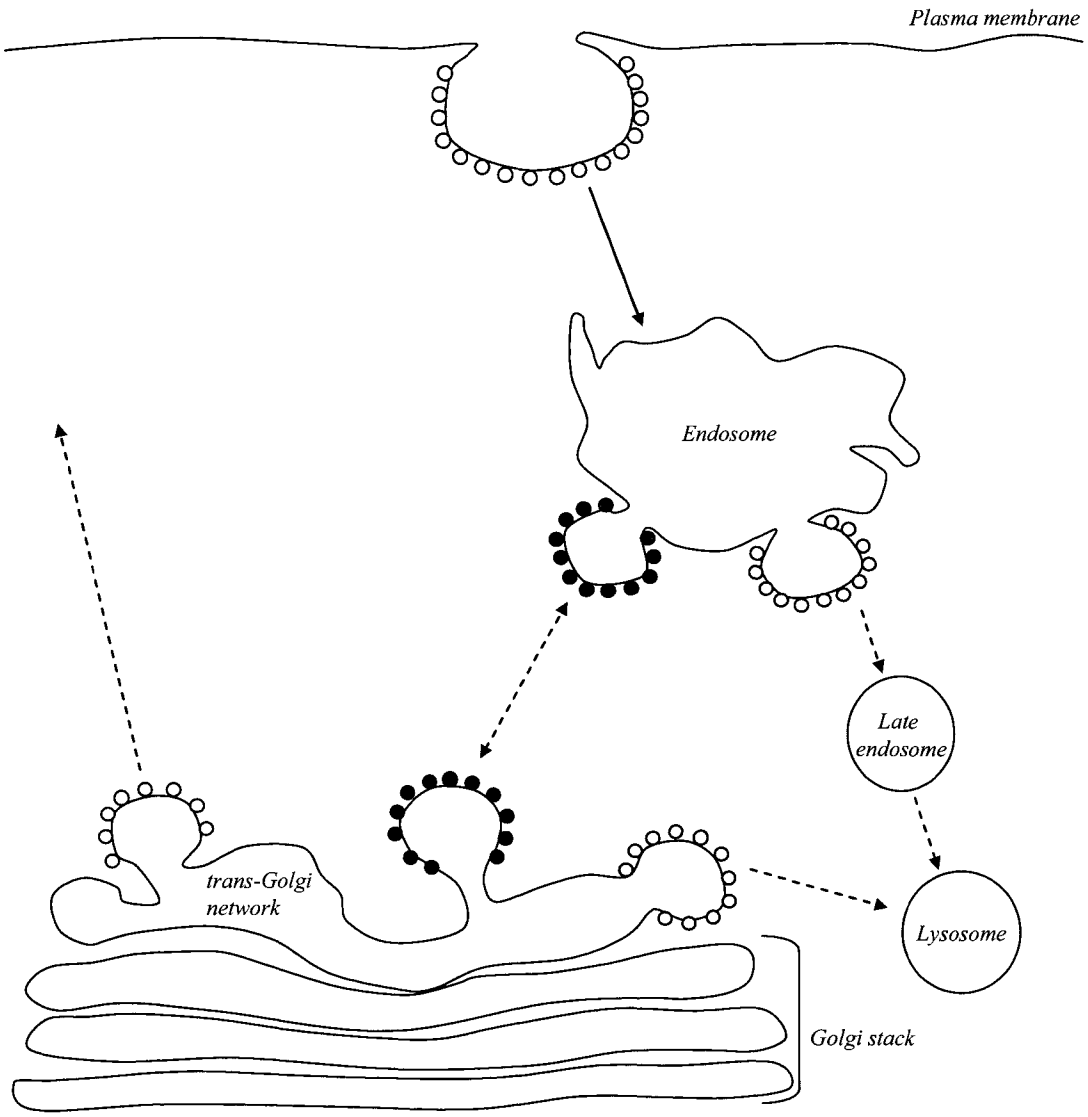

Figure 1-6. Adaptor proteins involved in trafficking pathways.

Purple, AP-1; blue, AP-2; green, AP-3; and yellow, AP-4. For simplicity, not all adaptor proteins and pathways involved in trafficking are shown. The dotted lines indicate pathways where there is still some question about directionality and/or the identity of the acceptor compartment; e.g. whether AP-1 is involved in TGN-to-endosome traffic, endosome-to-TGN traffic, or both; whether AP-3 coated vesicles deliver their cargo to a lysosome or to a late endosome; how AP-4 is involved in trafficking through the cell. (Adapted from Robinson 2004).

A di-leucine Leu-1487/Leu-1488 motif at the C-terminal end of ATP7A has been shown to be instrumental in mediating the protein endocytosis of the protein from the PM (Petris *et al.* 1998; Francis *et al.* 1999; Petris and Mercer 1999). Mutation of the di-leucine internalization motif led to an accumulation of the protein at the cell surface in basal medium but did not affect Cu efflux (Petris *et al.* 1998; Francis *et al.* 1999). The di-leucine motif could possibly interact with the AP-2 adaptor at the PM, prior to clathrin-coated vesicle transport through the endocytic pathway. This interaction may be direct or indirect via an additional cytosolic protein(s), and could occur via other adaptor-related proteins.

ATP7A TGN localization may occur via two steps: the first involving direct retention in the TGN via the TM region, and the second by retrieval of recycling ATP7A from the PM via the di-leucine signal (Petris *et al.* 1998). The TM 3 Golgi retention signal may also play a role in endocytosis, as suggested by studies done with a TGN resident protein (TGN38), which demonstrated that the TM domain of TGN38 was important for sorting the protein from endosomal compartments to the TGN (Reaves *et al.* 1998). Moreover, experimental evidence has indicated that the di-leucine motif may be sufficient for endocytosis to the recycling endosomes, but not sufficient for retrieving ATP7A directly to the TGN (Francis *et al.* 1999). This is consistent with research on the endocytic pathway followed by internalized ATP7A from the cell surface, which indicated that newly internalized ATP7A is initially targeted to peripheral and perinuclear endosomes, and is then sorted from these transferrin-containing compartments to the TGN (Petris and Mercer 1999).

The di-leucine motif in ATP7A also acts as a basolateral targeting motif, as is often seen with internalization signals (Greenough *et al.* 2004). In polarized MDCK cells, wild-type ATP7A relocalized to the basolateral membrane after elevated Cu treatment. Mutation of the di-leucine resulted in mislocalization of the protein to an apical or subapical position and failure to redistribute to the TGN upon return to basal medium (Greenough *et al.* 2004).

Downstream of the di-leucine in ATP7A is a putative PDZ binding motif, Asp-1497-Thr-Ala-Leu-1500, which may also play a role in ATP7A trafficking. This C-terminal motif

was shown to be important for stabilization and retention of ATP7A at the basolateral membrane (Hung and Sheng 2002). A novel protein with a single PDZ domain, AIPP1 (ATPase-interacting PDZ protein), has been demonstrated to interact with the last 15 amino acids of ATP7A, which contains the PDZ binding motif (Stephenson *et al.* 2005). This protein likely is important for ATP7A localization since PDZ proteins, which bind to specific C-terminal motifs such as that found in ATP7A, have an essential role in targeting protein complexes to distinct subcellular locations, and in organizing and maintaining these complexes in these locations.

d. Additional residues critical for localization and trafficking

For both WND and MNK mutations, research has been performed to analyze additional critical residues for localization. Some studies have found that certain sequence alterations in *ATP7A* and *ATP7B* result in incorrect localization of the mutant proteins or an inability to traffick in response to elevated levels of Cu (Hung *et al.* 1997; Payne *et al.* 1998; Qi and Byers 1998; Forbes and Cox 2000; Kim *et al.* 2002; Huster *et al.* 2003; Kim *et al.* 2003). These studies demonstrate that, in addition to the sequence motifs important for signaling localization, certain MNK and WND mutations may affect the intracellular distribution of the proteins and contribute to the pathogenesis of these diseases.

A thorough investigation of the localization of several WND patient mutations under high and low Cu conditions in our laboratory revealed that some amino acids within the transmembrane domains of ATP7B are required for localization within the TGN and/or for trafficking (Forbes and Cox 2000). Mutant variants of Asp-765, Leu-776 and Arg-778 within TM 4, were all largely mislocalized through the cell, likely due to misfolding of the proteins. These proteins were, thus, expected to be unable to mediate effective Cu efflux, even if they possessed Cu transport activity, thereby causing WND as seen in patients carry the mutations. The Gly943Ser variant, located within TM 5, resulted in a protein unable to redistribute from the Golgi to cytoplasmic vesicles, indicating that effective biliary Cu efflux would be prevented. Likewise, mutation of the conserved Cys-Pro-Cys motif in TM 6 showed negligible Cu-dependent redistribution, suggesting that the motif may be required as a trafficking initiation signal or that mutation of the motif may prevent critical TM domain conformation changes necessary for responding to increased Cu levels. Therefore,

studying the affects of different mutations is valuable and will elucidate additional residues critical for localization and provide some explanation for the clinical heterogeneity seen with the diseases.

ii. Relation between copper transport and copper-dependent localization

Trafficking of ATP7A and ATP7B has been hypothesized to be dependent on Cu transport activity, with some mutations indirectly preventing trafficking by affecting catalysis (Petris *et al.* 2002). This proposition implies that a variant defective in Cu transport would also be unable to traffick in response to Cu stimulation (La Fontaine *et al.* 2001; Petris *et al.* 2002). In fact, mutations of the conserved CPC motif in ATP7A (Petris *et al.* 2002) and ATP7B (Forbes and Cox 1998; Forbes and Cox 2000), and the conserved histidine within the SEHPL motif in ATP7A impair Cu transport and disable Cu-induced trafficking (Forbes and Cox 1998; Forbes and Cox 2000; Petris *et al.* 2002). Other research analyzing the significance of the MBSs in Cu-dependent relocalization has also shown that the ability of ATP7A and ATP7B to transport Cu and confer resistance to Cu is directly linked to its ability to undergo Cu-induced redistribution (Strausak *et al.* 1999; Cater *et al.* 2004). CHO cells transfected with either an ATP7A mutant for MBS 4-6 or an ATP7B mutant for MBS 4-6 were defective in trafficking (Strausak *et al.* 1999), causing the ATP7A-transfected cells to accumulate significantly more Cu than control cells (Voskoboinik *et al.* 1999) and the ATP7B mutant unable to complement a *ccc2* yeast (Forbes and Cox 1998; Cater *et al.* 2004). Even though this mutant was still capable of transporting Cu and retained its catalytic activity *in vitro*, it could not perform its full physiological role *in vivo* since both of its functions were not intact (Voskoboinik *et al.* 1999).

Although the ability to traffick may depend on the Cu transport capacity of the protein, it does not seem that the reverse is necessary; that is, that the Cu transport ability requires correct trafficking of the protein. The mutant protein product of an *ATP7A* splice site mutation that deletes exon 8 of the gene localized correctly to the TGN and was able to transport Cu to tyrosinase, a Cu-dependent enzyme synthesized within secretory compartments; however, the protein failed to relocalize to the PM when exposed to increased Cu (Kim *et al.* 2003).

iii. Relation between formation of a phosphorylated intermediate and copper-dependent localization

Recent results have also indicated that Cu-induced trafficking of ATP7A from the TGN to the PM required the formation of the phosphorylated catalytic intermediate (Petris *et al.* 2002). This suggested that mutations which prevent the formation of an acyl-phosphate intermediate may inhibit movement from the TGN. Mutation of the conserved aspartate (Asp1044Glu) abolished the formation of the phosphoenzyme, and consequently inhibited the Cu-dependent trafficking response of the protein, whereas mutation of the conserved phosphatase domain (Thr-Gly-Glu Ala-Ala-Ala) resulted in hyperphosphorylation and constitutive PM localization under basal and elevated Cu conditions (Petris *et al.* 2002). The finding that the double mutant (Asp1044Glu/ Ala-Ala-Ala) inhibited Cu-regulated trafficking from the TGN confirmed that trafficking of ATP7A requires formation of a phosphorylated catalytic intermediate. The link between these two events was further demonstrated in ATP7B, where a mutation in the phosphatase domain caused constitutive relocalization in a vesicular distribution under basal conditions, reminiscent of the distribution seen in elevated Cu conditions (Petris *et al.* 2002). These results also suggest that a similar mechanism for Cu-induced trafficking exists for both ATP7A and ATP7B, and is one that involves the formation of an acyl-phosphate intermediate during catalysis. It is important to note that this model does not suggest that ATP7A and ATP7B will undergo trafficking from the TGN with every catalytic cycle (Petris *et al.* 2002), as exocytic trafficking depends on several factors. Furthermore, a pool of ATP7A and ATP7B is likely required in the TGN to continue with the biosynthetic function of delivering Cu to secreted cuproenzymes.

The deleterious effect of certain mutations could be explained if formation of a phosphorylated intermediate during catalysis is the critical trigger for exocytic trafficking. For example, the brindled mouse mutation (Ala799_Leu800del) (La Fontaine *et al.* 1999), a missense mutation (Ala1362Val) that causes mild Menkes disease (Ambrosini and Mercer 1999), and the *tx* mouse mutation (Met1356Val) (La Fontaine *et al.* 2001), were all localized to the TGN and demonstrated a defect in their abilities to traffick in response to varying Cu conditions. The sequence changes found in these mutants may disrupt a specific conformation associated with the acyl-phosphate intermediate. Since a specific

quaternary structure of ATP7A and ATP7B may be required for trafficking, any disturbance of this intermediate by exposing or occluding a localization signal may result in defective trafficking.

Further studies have reported that only completely catalytically inactive ATP7A mutants would be unable to undergo Cu-stimulated relocalization (Voskoboinik *et al.* 2003b). The ability of ATP7A to exocytose was proposed to be a function of ATP-binding and concomitant conformational changes, and/or be triggered by the accumulation of a certain threshold concentration of Cu; thus, retention of some catalytic activity would permit Cu-induced trafficking. As such, mutation of the histidine residue of the conserved SEHPL motif, which produced a mutant with low affinity for ATP and reduced catalytic activity, was still able to relocalize to the PM with higher intracellular Cu concentrations (300 μM). Therefore, it is possible that mutants with considerably compromised catalytic activity (such as, Asp1230Ala and Lys1233Met) may be able to traffick normally and result in a less severe ATP7A disease phenotype.

iv. Copper-dependent exocytic trafficking pathway

Studies done on the Cu-dependent transport of ATP7A from the Golgi to the PM (exocytic pathway) illustrate that ATP7A follows a novel membrane traffic event in response to elevated levels of Cu, which is independent from the constitutive secretion from the TGN (Cobbold *et al.* 2002).

The specialized movement of ATP7A from the TGN to the PM in elevated extracellular Cu conditions occurred in a Cdc42-dependent manner; however, the trafficking was independent of protein kinase D (PKD) activity, which is a major component regulating constitutive secretion from the TGN to the PM (Cobbold *et al.* 2002). Furthermore, the exocytic pathway followed by ATP7A was dependent on both actin and microtubule networks (Cobbold *et al.* 2002; Cobbold *et al.* 2004), whereas constitutive transport is actin-independent.

The trafficking of ATP7A may not involve all synthesized ATP7A, as a distinct pool of ATP7A in the cell has been demonstrated to be specifically responsive to Cu by trafficking to the PM (Pase *et al.* 2004). This pool of ATP7A was able to rapidly recycle to the cell

surface at an almost 15-fold more rapid pace than those trafficking from the TGN to the PM, suggesting that the fast-recycling pathway does not involve transport through the TGN (Pase *et al.* 2004). The presence of excess Cu may operate in diverting ATP7A to a rapid recycling pathway for more efficient Cu efflux.

Exocytic trafficking of ATP7B in polarized hepatic cells was shown to involve lipid rafts (cholesterol-enriched domains) for transport (Slimane *et al.* 2003). ATP7B was associated with specific lipid microdomains at the TGN and remained tightly associated with these domains following direct transport from the TGN to the apical bile canalicular membrane. Since lipid rafts in polarized HepG2 cells are active in both the transport of proteins to the apical membrane and the transport of proteins to the basolateral membrane, it is likely that these rafts are not sufficient for sorting to a particular location (Slimane *et al.* 2003); therefore, additional molecular mechanisms underlying this raft-mediated trafficking probably exist. The 63 amino acid N-terminal targeting sequence shown to play a specific role in trafficking of ATP7B in response to elevated Cu levels may be recognized by COMMD1, which interacts with the N-terminal ~653 amino acid region of ATP7B (Tao *et al.* 2003; Guo *et al.* 2005).

v. Copper-dependent endocytic trafficking pathway

Studies have been undertaken to elucidate the mechanism by which ATP7A and ATP7B, multiple TM domain proteins, are internalized from the PM into the mammalian cell (endocytic pathway). As many proteins with di-leucine motifs are efficiently internalized via clathrin-coated pits and vesicles, it was expected that ATP7A may follow this route. However, several studies have established the existence of clathrin-independent internalization pathways, such as specialized cholesterol-rich domains on the cell surface, called caveolae, or lipid rafts for endocytosis from the cell surface.

Preliminary data indicate that a novel pathway exists for targeting the MNK transporter from the cell surface to the endosome-lysosome network (Cobbold *et al.* 2003). ATP7A internalization from the PM has been demonstrated to occur via a clathrin- and caveolae-independent process, but does depend on Rac1, a small Rho GTPase involved in the regulating actin cytoskeleton dynamics (Cobbold *et al.* 2003). The role of the di-leucine

motif is unknown, but may be recognized by factors distinct from the AP-2/clathrin route. The pathway followed by ATP7B has not been thoroughly examined; however, syntaxin 6 may play a functional role in the movement of the protein from the canalicular membrane to the TGN (Guo *et al.* 2005).

Once ATP7A is internalized from the PM or ATP7B is internalized from the bile canalicular membrane, ATP7A and ATP7B follow intracellular routes to the TGN. The intracellular pathways followed by ATP7A and ATP7B, however, are ill-defined. As indicated above, there may be a distinct, rapid recycling pool of ATP7A that does traffick back to the TGN from the PM. This distinct pathway from the PM may be important for Cu efflux once Cu conditions are elevated (Pase *et al.* 2004).

To elucidate the intracellular route from the cell surface to the TGN, Rab proteins were exploited to identify the vesicular compartments involved in ATP7A and ATP7B trafficking. Rab proteins are organelle-specific GTPases that are markers of different endosomal compartments, and are assumed to participate in the processes by which transport vesicles identify and fuse with their target membranes (Figure 1-7). Through co-localization experiments and sucrose gradients, ATP7A retrieval from the PM has been shown to involve endosomes containing the Rab5 and Rab7 proteins (Pascale *et al.* 2003). Rab5 controls transport from the PM to the early endosome and regulates the dynamics of early endosome fusion (Bucci *et al.* 1992; Nielsen *et al.* 1999), and Rab7 governs membrane flux into and out of late endosomes (Feng *et al.* 1995). Rab7 has, in fact, been demonstrated to co-localize with ATP7B (Harada *et al.* 2005), suggesting that both ATP7A and ATP7B may cycle through early and late endosome compartments.

vi. Role of copper-dependent phosphorylation on intracellular trafficking

In many eukaryote ATPases, including the Na/K-ATPase, the Ca-ATPases, and the cystic fibrosis transmembrane conductance regulator, protein kinase-dependent phosphorylation is important in regulating catalytic activity and subcellular localization. Recent data indicate that this regulatory mechanism may also operate for Cu-transporting ATPases.

The regulation by protein kinase-dependent phosphorylation of ATP7B is unique in that it is Cu-dependent and involved in determining the intracellular distribution of ATP7B.

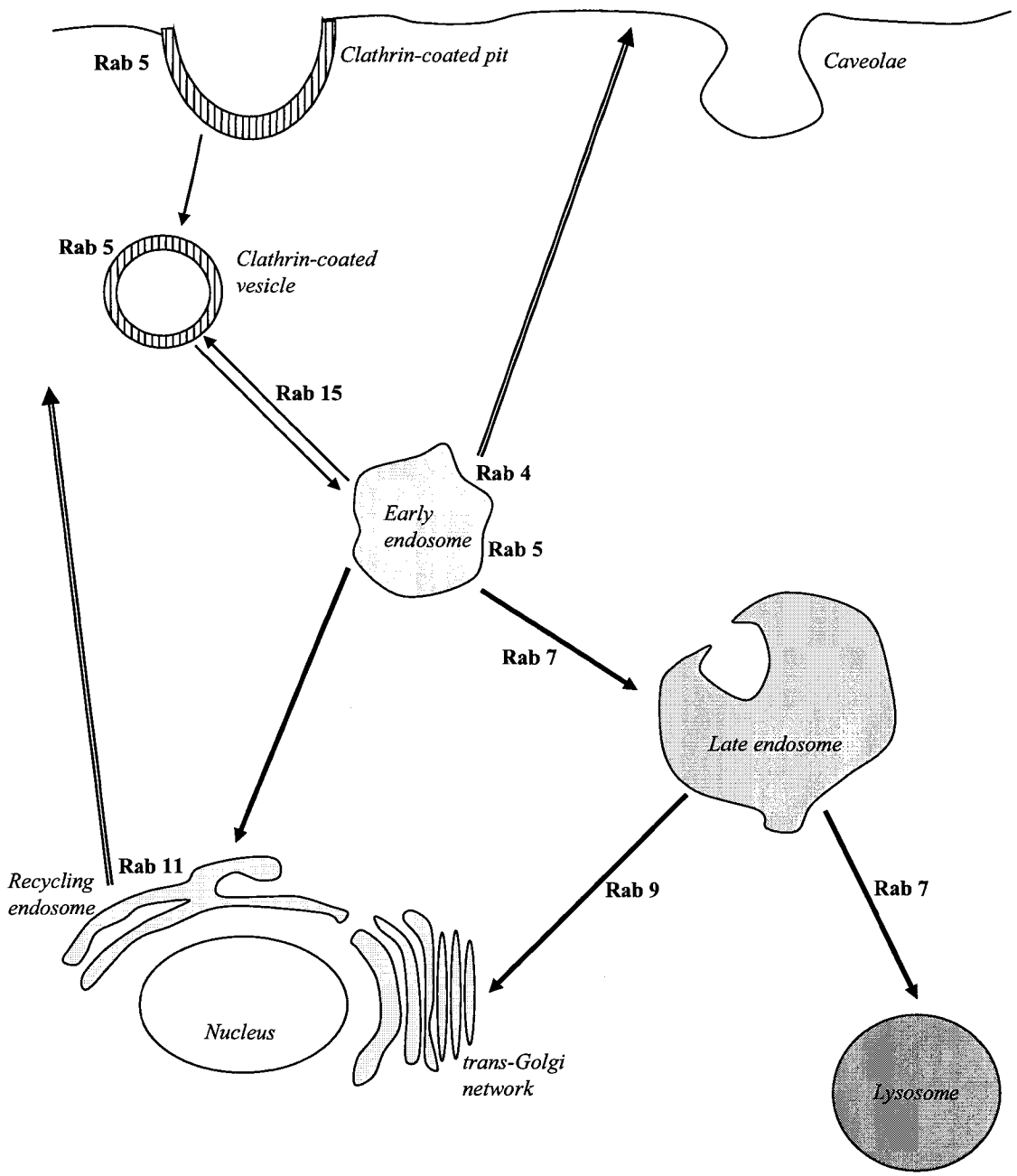

Figure 1-7. Illustration of specific Rab proteins involved in the endocytic pathway.

Molecules internalized by endocytosis are initially transported to early endosomal compartments that are characterized by the presence of Rab 5 and Rab 4. Some molecules are sorted into Rab 5-containing microdomains, resulting in transport either to perinuclear localized recycling compartments or toward lysosomes for degradation. Transport to perinuclear recycling endosomes leads to Rab 11-mediated recycling to the plasma membrane. Transport from early to late endosomes is facilitated by Rab 7, and cycling of molecules from late endosome to the TGN is mediated by Rab 9. Transport to lysosomes for degradation is mediated by Rab 7. (Adapted from Stein *et al.* 2003).

In fact, phosphorylation levels of ATP7B coincide with the intracellular location of the protein (Vanderwerf *et al.* 2001). A hyperphosphorylated ATP7B is associated with vesicular compartmentalization in elevated Cu conditions, whereas upon Cu depletion, ATP7B is basally phosphorylated and localized in the TGN. Studies done using the baculovirus system indicated that the Cu-dependent phosphorylation occurred on serine residues (Vanderwerf and Lutsenko 2002). Thus, kinase-dependent phosphorylation may be a mechanism for controlling intracellular distribution of ATP7B.

This regulatory mechanism is also evident with ATP7A. *In vitro* and *in vivo* evidence has demonstrated that ATP7A is basally phosphorylated in low levels of Cu; however, upon the addition of Cu, phosphorylation is rapidly induced, exclusively on serine residues, by an upstream protein kinase (Voskoboinik *et al.* 2003a). The event was reversible and shown to be Cu-specific and independent of *de novo* protein synthesis. Similar to ATP7B, the Cu-induced phosphorylation coincided with relocalization of ATP7A from the TGN to the PM. The stability of the phosphorylated form was also increased in the presence of Cu suggesting that Cu may also inhibit the dephosphorylation of ATP7A. Significantly, a non-trafficking ATP7A mutant variant did not exhibit the Cu-dependent induction of phosphorylation, yet the basal sites were phosphorylated (Voskoboinik *et al.* 2003a). It is unknown whether the protein-kinase is activated by Cu and leads to trafficking, or whether Cu-induced trafficking allows association with a kinase, and/or whether Cu-dependent conformational changes permit subsequent phosphorylation and trafficking.

IX. ASSESSMENT OF ATP7B FUNCTION

The functional characterization of mutant variants of ATP7B is valuable in fully understanding the protein and its role in Cu homeostasis. This allows the determination of residues and regions of ATP7B critical for Cu transport and excretion. Furthermore, the analysis of WND patient mutations is significant in delineating the effect of sequence changes on function and the clinical presentation of the patient. A useful system for analyzing ATP7B variants should be technically simple, sensitive, accurate and high-throughput in order to facilitate the production of reliable and rapid results.

Characterization of endogenously expressed ATP7B in human cells is difficult because of its very low level of expression (~0.005% of total membrane protein), as well as its predominant localization in intracellular membranes (Tsivkovskii *et al.* 2002). Given the large number of WND patient mutations and the over-representation of missense sequence changes, there are very few patients homozygous for a particular mutation; hence, assessing the consequence of a specific mutation endogenously is not practical in most cases. Therefore, alternative methods requiring exogenous expression are necessary to examine the function of ATP7B and its various mutants.

A. COPPER TRANSPORT FUNCTIONAL ASSAYS

A few assays have been created to assess the Cu transport ability of exogenous ATP7B and its variants in heterologous systems. Studies have been performed by expression of ATP7B constructs in a *ccc2* yeast strain, where their ability to complement the deleted yeast Cu-transporting ATPase Ccc2p was monitored (Iida *et al.* 1998; Forbes *et al.* 1999). Various patient mutations (both WND and MNK mutations) have been introduced into the homologous *Enterococcus hirae* CopB gene at the corresponding sequence positions, and their abilities to confer Cu resistance, form an acylphosphate intermediate and demonstrate ATPase activity were examined (Bissig *et al.* 2001). This has also been done with the Zn^{2+}-transporting P-type ATPase (Okkeri *et al.* 2002; Okkeri *et al.* 2004).

The murine orthologoue of ATP7B and mouse model systems were also used to examine the function of ATP7B. Expression of mouse *Atp7b* cDNA in an immortalized fibroblast cell line from a MNK patient (La Fontaine *et al.* 1998b), and expression of wild-type and mutant human ATP7B in a murine *mottled* fibroblast cell line (Payne *et al.* 1998) were performed to investigate the Cu translocating activity of the protein. Recent experiments have also used expression of wild-type mouse *Atp7b* and *tx* mouse *Atp7b* in mammalian cells to measure ATP-dependent Cu transport. The enzymatic steps associated with Cu transport, however, could not be analyzed using this system because ATP7B was only expressed at very low levels (Voskoboinik *et al.* 2001a).

A baculovirus-mediated expression system in insect cells has been designed to enable robust expression of ATP7B for study (Tsivkovskii *et al.* 2002). The protein yield using

this system is approximately 20-fold higher than the amount of ATP7B expressed in COS cells and about 400-fold higher than the amount of endogenous ATP7B in HepG2 cells (Lutsenko *et al.* 2002). ATP7B expression in the insect cells is mainly in the Golgi fraction, similar to its known primary localization in mammalian cells. This system has been useful in evaluating the ability of variants to form acyl-phosphate intermediates and their level of catalytic activity.

i. A functional assay using *Saccharomyces cerevisiae* as a model system

The yeast assay has been one of the predominant functional assays used to examine the Cu transport function of WND mutant variants. The marked evolutionary conservation of the Cu trafficking pathways in yeast and humans is invaluable and allows the use of yeast genetics to identify and characterize the proteins involved in Cu metabolism.

The yeast functional assay designed in our laboratory specifically analyzes the ability of ATP7B variants to transport Cu through the membrane and deliver it to the yeast orthologue of apo-Cp, apo-Fet3p (Forbes and Cox 1998). The assay is based on complementation of *S. cerevisiae* lacking *ccc2* by human ATP7B (Yuan *et al.* 1995). Ccc2p, along with a yeast chloride channel protein Gef1p (Gaxiola *et al.* 1998), is necessary for Cu incorporation into apo-Fet3p. Thus, *ccc2* yeast are unable to grow in Fe-limited media since the provision of Cu to apo-Fet3p is necessary for Fe homeostasis under low Fe conditions (Yuan *et al.* 1995). This impairment can be restored by human wild-type ATP7B; hence, an ATP7B variant capable of Cu transport will inferably permit survival in such conditions as well (Figure 1-8) (Forbes and Cox 1998; Iida *et al.* 1998; Forbes *et al.* 1999).

This yeast system has been invaluable as an indirect assay for examining the Cu delivery function of ATP7B variants. We have successfully used the heterologous expression system for studying the effect of mutations and deletions within the CuBD of ATP7B (Forbes *et al.* 1999), and in assessing the degree to which disease mutations in the TM segments affect protein function (Forbes and Cox 1998).

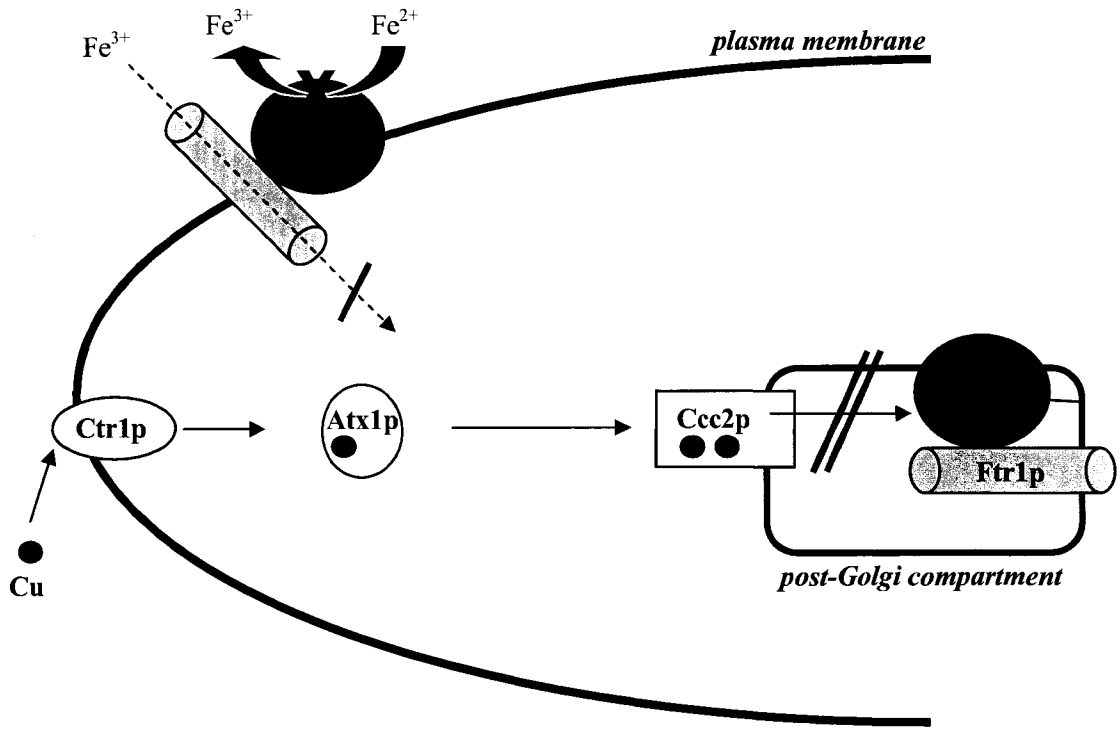

Figure 1-8. Model of yeast copper and iron homeostasis on which the yeast complementation assay is based.

Cytoplasmic Cu is bound by the Cu chaperone Atx1p, which is responsible for delivering Cu to Ccc2p in a post-Golgi compartment. Ccc2p supplies Cu to the plasma membrane ferroxidase Fet3p, which functions with the high affinity iron transporter Ftr1p to import iron. When yeast cells lack Ccc2p, Cu is not incorporated into Fet3p, and consequently, the cells lack high affinity iron uptake. In the absence of high affinity iron uptake, *ccc2* mutant yeast cells are unable to grow in iron-limiting conditions. Wild-type human ATP7B is able to complement *ccc2* mutant yeast, and restore Cu incorporation into Fet3p and growth on iron-limited medium. The double-line indicates where the breakdown in the Cu pathway occurs upon mutation of *CCC2*, the red X represents the inactive apo-Fet3p at the membrane, and the single red line shows the loss of high affinity Fe uptake that results from the *ccc2* mutation and lack of Fet3p ferroxidase activity. (Adapted from Forbes *et al.* 1998).

Other groups have also used yeast as a model system to examine the N-terminus of ATP7B (Iida *et al.* 1998; Cater *et al.* 2004), the His1069Gln mutation (Hung *et al.* 1997; Iida *et al.* 1998) and the mutations Asp1027Ala, Thr1029Ala and Asn1270Ser (Iida *et al.* 1998). Functional studies on the related protein ATP7A have also been performed using *ccc2* mutant yeast (Payne and Gitlin 1998).

a. The iron and copper connection

The utility of the yeast model system as a functional assay has depended upon the relationship between the Fe and Cu transport pathways. The physiological link between Cu and Fe is now well understood at the molecular level and exploited to analyze the main players involved in Cu homeostasis. The central component that metabolically links these two essential metal ions is a multicopper ferroxidase: ceruloplasmin (Cp) in mammals and Fet3p in the yeast *S. cerevisiae*. These ferroxidases bind Cu atoms, which is necessary for the biological activity of the ferroxidases in Fe homeostasis; thus, the proper functioning of the enzymes relies upon components of the Cu pathway. A defect in any of these Cu proteins would directly impact the Cu transfer to the multicopper ferroxidases, leading to a secondary effect on Fe homeostasis.

The epistatic relation between Cu and Fe in eukaryotes was first suggested 50 years ago, with the identification of a link between Cu deficiency and anemia in swine (Cartwright *et al.* 1956). The Cu-deficient anemia was unresponsive to Fe supplementation but could be corrected with Cp (Lee *et al.* 1968); accordingly, the animals showed very low Cp activity and profound alterations in Fe metabolism. The ferroxidase activity of Cp was characterized, demonstrating that Cp could play a critical role in catalyzing the trafficking of Fe^{2+} to apo-transferrin for transport of Fe through the plasma (Osaki *et al.* 1966; Osaki and Johnson 1969; Frieden and Osaki 1974). Cp functions enzymatically to mediate Fe mobilization by converting Fe^{2+} to Fe^{3+} that is then bound by transferrin. Fe^{2+} can be oxidized spontaneously; however, the presence of Cp accelerates the rate. Without Cp activity, 80% of the Fe released from erythrocyte turnover would accumulate as non-transferrin-bound and would be Fe^{2+} unavailable for reabsorption. Furthermore, the free Fe^{2+} could catalyze the formation of reactive oxygen species via the Fenton reaction and

result in disease. These data have been confirmed in yeast, supporting the close relation between these two metal pathways.

In yeast, the unveiling of the relation between Fe and Cu was serendipitous. Researchers were studying Fe transport in yeast, and instead of identifying ferrous Fe transporters, they successfully characterized human Cu transporters (Askwith *et al.* 1994; Dancis *et al.* 1994b). High-affinity Fe transport in yeast depends upon the Cu-containing ferroxidase, Fet3p, the yeast homologue of Cp. Analogous to Cp, Fet3p is responsible for mediating Fe transport by converting Fe^{2+} to Fe^{3+} which is then transported by Ftr1p into the yeast cell (De Silva *et al.* 1995). Although they have comparable functions, Fet3p mediates Fe transport into cells, whereas Cp mediates cellular Fe release and Fe transport throughout the body. The high-affinity Fe transport system in yeast is also unique in that the Fe uptake is dependent on both Fet3p and Ftr1p in the PM. In the presence of Fe^{2+}, the cell will exhibit no Ftr1p-dependent Fe uptake if the Fet3p in the PM is inactive as a ferroxidase. The Fe^{2+} must undergo an obligate oxidation by Fet3p prior to transport, and exogenous Fe^{3+} is not competent for uptake. Thus, Fe uptake through Ftr1p is strictly coupled to the Fet3p ferroxidase reaction.

The yeast studies have emphasized the epistatic relation between the gene products involved in the Cu transport pathway and the importance of Cu delivery to Fet3p for Fe homeostasis. Fe homeostasis in yeast requires the activities of other proteins, all with identified human counterparts, which either transport Cu or are activated by Cu. Ctr1p, the Cu permease (Dancis *et al.* 1994a); Atx1p, the Cu chaperone (Lin *et al.* 1997); and Ccc2p, the Cu transporter (Yuan *et al.* 1995) are necessary for the provision of Cu, whereas Fet3p and Fet5p are the Cu-activated proteins that are essential for the normal Fe trafficking into and within the yeast cell. A disruption in function of any one of these is correctable by the addition of sufficient Cu to bypass the specific step supported by the particular protein; however, loss of Fet3p cannot be corrected in this way, consistent with the pathway placing the active Fet3p as the end-product of Cu delivery. Thus, it is evident that using Cu incorporation into Fet3p as a biochemical measure of ATP7B functional activity was a rational and reasonable method and has been proven to be a valid and useful assay for analyzing ATP7B variants.

b. Limitations of the yeast functional assay

The yeast model system, however, is not without its limitations. By its nature, the yeast complementation assay is restricted in its use since it is reliable only under conditions where the introduced mutation affects the ATP-related function of the protein, i.e. its catalytic and Cu-translocating activity. The yeast system, as an assay, is only functional under basal or near Cu-deficient conditions by the addition of a Cu chelator and does not have the capability to assess the affect of a mutation on the affinity of the variant for Cu (Voskoboinik *et al.* 2001b; Voskoboinik and Camakaris 2002). The reduced affinity of a mutant for Cu may be manifested as the inability to complement the growth of *ccc2* yeast under Cu-/Fe-depleted conditions; therefore, the assay is not sensitive enough to distinguish between a defect in an ATP-related function or an impaired affinity for Cu. Perhaps the greatest limitation of the yeast system is its inability to evaluate the capacity of the variants to localize correctly within the cell and to traffick from the TGN prior to biliary excretion in response to an increase in the Cu concentration.

B. ATP7B LOCALIZATION AND TRAFFICKING ASSAYS

The recognition of intracellular relocalization of ATP7B in response to changing Cu environments has resulted in the development of methods for determining the distribution of ATP7B in varied Cu conditions. Original studies were aimed at localization of wild-type ATP7B under basal conditions, primarily in HepG2 cells (Hung *et al.* 1997; Yang *et al.* 1997; Lutsenko and Cooper 1998) and in human and rat liver sections and primary rat hepatocytes (Schaefer *et al.* 1999a; Schaefer *et al.* 1999b). Some studies furthered the characterization by examining movement of ATP7B in response to elevated extracellular Cu conditions in hepatoma cell lines (Hung *et al.* 1997; Harada *et al.* 2000a; Harada *et al.* 2003; Harada *et al.* 2005), primary rat hepatocytes (Schaefer *et al.* 1999a), polarized hepatic cells (Roelofsen *et al.* 2000; Harada *et al.* 2003; Guo *et al.* 2005), and MDCK cells (Harada *et al.* 2005).

Work has since been extended to the evaluation of mutant variants of ATP7B to understand the affect of different mutations on ATP7B function. A mutation may result in a variant still capable of translocating Cu, yet unresponsive to changing Cu conditions and unable to redistribute. As most WND patients are heterozygous for mutations, these studies have

primarily been performed in cultured cells, by transient or stable transfection, including CHO cells (Forbes and Cox 2000; La Fontaine *et al.* 2001; Cater *et al.* 2004) and hepatoma cell lines (Harada *et al.* 2001; Huster *et al.* 2003), with one study analyzing the affect of the His1069Gln mutation in the liver tissue of a WND patient harbouring the homozygous mutation (Huster *et al.* 2003).

The localization and trafficking assays have mainly been comprised of subcellular fractionation studies and co-localization of *ATP7B* expression with proteins of known localization (Hung *et al.* 1997; Schaefer *et al.* 1999b), or immunofluorescence studies often confirmed by co-localization with antibodies against specific organelle proteins (Hung *et al.* 1997; Yang *et al.* 1997; Lutsenko and Cooper 1998; Forbes and Cox 2000; Roelofsen *et al.* 2000; Cater *et al.* 2004). Similar methods have also been used in the study of ATP7A and its subcellular distribution.

Characterization of ATP7B *in situ* in rat and human liver sections has been aided by the detection of ATP7B by immunohistochemistry and alkaline-phosphate (Schaefer *et al.* 1999b) or immunogold labeling (Huster *et al.* 2003), or by double-label confocal scanning laser microscopy of the liver tissue and co-localization with organelle markers (Schaefer *et al.* 1999a; Schaefer *et al.* 1999b).

Some recent studies have used GFP-tagged ATP7B constructs to examine the immunofluorescent distribution of ATP7B and ATP7B variants, either in the absence or presence of specific organellar markers for co-localization (Harada *et al.* 2000a; Harada *et al.* 2000b; Harada *et al.* 2001; Harada *et al.* 2003; Huster *et al.* 2003; Guo *et al.* 2005; Harada *et al.* 2005). This method has been more favourable to the study of multiple mutant variants as the GFP can be directly detected under fluorescence without the use of an additional antibody; however, there is always a concern with introducing such a large tag and the possible confounding effects resulting from its addition.

C. Homology modeling of ATP7B functional domains

The 3D structure of ATP7B would be useful to fully appreciate the function of the protein in the hepatocyte; however, technical challenges have thus far hindered the experimental determination of the 3D structure of ATP7B by X-ray crystallography or NMR

spectroscopy (Fatemi and Sarkar 2002b). Thus, homology modeling (also known as comparative protein modeling) has been used in place of an actual 3D structure. This method takes advantage of known, solved structures of homologous proteins to derive a structure for a protein of unknown structure. Research groups are using the 2.6 Å crystal structure of the calcium pump of sarcoplasmic reticulum, SERCA1a (Toyoshima *et al.* 2000), as the template for modeling the core P-type ATPase components of ATP7B (Fatemi and Sarkar 2002b; Lutsenko *et al.* 2002; Tsivkovskii *et al.* 2003; Efremov *et al.* 2004; Morgan *et al.* 2004). A significant target-template sequence identity is useful in generating an accurate model since the sequence alignment between the two proteins is used to predict the secondary structure and 3D model. ATP7B and SERCA1a show an overall sequence identity of only 5% (Lutsenko *et al.* 2002), and generally sequences with such a low homology to the template protein (<30% sequence identity) are more difficult to model and of lower accuracy (Saqi *et al.* 1998; Rost 1999); however, higher identity between these two transporters is found in the functionally conserved regions.

A low resolution 3D model of the entire ATP7B molecule has been generated, depicting a rough spatial organization of the various domains and conserved sequence motifs (Fatemi and Sarkar 2002b). The multiple domains had to be modeled separately, and some insertions and deletions were incorporated into nonconserved regions where they were least likely to disrupt the overall structure. Because of the low target-template sequence, the alignment was continuously modified and improved in order to obtain a 3D structure of ATP7B. It is still possible that this model is inaccurate; however, the overall fold could be correct and may be useful in predicting the biochemical function of the protein (Fatemi and Sarkar 2002b).

Since the ATP-BDs of ATP7B and SERCA1a share a much higher degree of similarity, a model of the ATP7B ATP-BD was generated (Lutsenko *et al.* 2002; Tsivkovskii *et al.* 2003; Efremov *et al.* 2004; Morgan *et al.* 2004). Segments of the ATP-BD of ATP7B (Val997-Ala1065, Asp1185-Ile1236, Phe1240-Ile1311), mainly in the P-subdomain, shared significant homology to the SERCA1a ATP-BD sequence. The alignment of sequences and secondary structures generated by a software program (GenTHREADER) served as the basis for the ATP-BD model (Tsivkovskii *et al.* 2003). Numerous optimization steps were

performed to create a model with a predicted overall fold that agreed with the SERCA1a and Na^+, K^+-ATPase ATP-BD crystal structures (Efremov *et al.* 2004). The quality of the 3D model was evaluated using statistical analysis and programs (Profiles_3D program and 3D-profile algorithm) that assessed how well the model satisfied the general principles of folding for globular proteins.

The ATP-BD model has been drawn upon to better understand the potential effects of various mutations identified in WND patients, including the common His1069Gln mutation, Glu1064Ala, Arg1151His, and Cys1104Phe (Tsivkovskii *et al.* 2003; Morgan *et al.* 2004). The model has also been employed to confirm the functional importance of highly conserved residues, including Lys-1028, Thr-1029, Asp-1222 and the catalytically phosphorylated Asp-1027 in the P-subdomain. Thus, molecular modeling has proven to be beneficial in the analysis of disease mutations and dissecting the functional properties of the ATP-BD of ATP7B, and will likely be an important asset in further characterization of ATP7B.

X. AIMS OF THESIS

The overall aim of this thesis was to use various techniques to analyze ATP7B for regions and amino acids critical for its biochemical and physiological function in maintaining Cu homeostasis. The specific goals of my project were as follows:

1) To determine whether there are particular amino acid residues and regions of ATP7B and ATP7A that are similarly affected by mutation, in order to uncover areas that may be important for the role of ATP7B in the Cu transport pathway and to aid in the process of mutation recognition in WND patients. This would also provide information for developing a hierarchical plan for selecting future regions of ATP7B to analyze using functional assays.

2) To study the effect of select WND patient mutations within the N-terminal CuBD and the ATP-BD on ATP7B Cu transport function using the yeast functional assay,

in order to gain insight into the function of these conserved domains and the significance of the residues analyzed.

3) To study the role of the C-terminal domain of ATP7B in Cu transport and delivery to Cp and in correct intracellular distribution using the yeast functional assay and by immunofluorescence, in order to determine which amino acids, if any, are significant for ATP7B function, and to develop a better system for assessing the localization and trafficking properties of multiple ATP7B variants.

CHAPTER 2:
Determination of functionally significant regions by analyzing the mutation spectrum of Wilson disease

Results presented in this chapter have been published in:

> Hsi, G. and Cox, D.W. (2004). A comparison of the mutation spectra of Menkes disease and Wilson disease. Hum Genet 114(2): 165-72.

Exon 20 sequencing results in this chapter have been published in:

> Cox, D.W., Prat, L., Walshe, J.M., Heathcote, J., and Gaffney, D. (2005). Twenty-four novel mutations in Wilson disease patients of predominantly European ancestry. Hum Mutat 26(3): 280-286.

Ms. WenWen Shan (University of Alberta) contributed to the sequencing of exons 20 and 21 of *ATP7B*.

I. INTRODUCTION

The genes that are mutated in human MNK and WND, *ATP7A* and *ATP7B*, and their predicted protein products, share many of the same characteristic features. Our hypothesis has been that a comparison of the mutation spectra of WND and MNK could elucidate regions of importance since the two proteins are members of the same P-type ATPase family, having similar protein structures and similar roles in Cu metabolism (Vulpe *et al.* 1993; Bull and Cox 1994; Petrukhin *et al.* 1994). Both ATP7A and ATP7B play two critical functions within the cell: (1) export of Cu from cells, and (2) delivery of Cu into the secretory pathway for incorporation into Cu-dependent enzymes. Further, the two transporters display similar Cu-dependent trafficking in the cell (Petris *et al.* 1996; Hung *et al.* 1997; La Fontaine *et al.* 1998a; Payne and Gitlin 1998; Schaefer *et al.* 1999a; Schaefer *et al.* 1999b; Suzuki and Gitlin 1999).

ATP7A and *ATP7B* show complementary expression profiles that are consistent with the clinical and biochemical features of MNK and WND. Their differences in expression provide some explanation for their discrete functions, such as export into circulation instead of bile, incorporation of Cu into dopamine -hydroxylase rather than Cp. A comparison of the mutation spectra should be useful in identifying those sequences responsible for the specific function of each protein in Cu export and delivery to cuproenzymes, as well as identifying additional sequences responsible for expression.

The conserved functional domains of heavy metal P-type ATPases are necessary for Cu transport and for the distribution of the proteins in the cell. Besides these domains, additional regions not common to this class of proteins may be critical for ATP7B function in the hepatocyte. Analyzing the *ATP7B* mutation spectrum and comparing it with the *ATP7A* mutation spectrum will reveal regions of particular importance to both, and may also expose areas that are distinct for ATP7B function. Determination of these functional regions is central for fully understanding the role of ATP7B in maintaining Cu homeostasis and may aid in elucidating any intracellular functions exclusive to ATP7B. Furthermore, the identification of regions or specific amino acids essential for function could simplify the mutation detection process for molecular diagnosis by identifying certain regions in

ATP7A and/or ATP7B which are particularly prone to mutation and should be screened in the DNA of WND patients. A comparative analysis will also aid in clarifying whether certain sequence changes are disease-causing alterations.

II. MATERIALS AND METHODS

A. Comparison of amino acids

Amino acid sequences of ATP7A, ATP7B, and their orthologues were obtained from the National Center for Biotechnology Information (NCBI) database (http://www.ncbi.nlm.nih.gov/). NCBI accession numbers for the amino acid sequences used were as follows: *Homo sapiens* ATP7B: AAB52902; *Homo sapiens* ATP7A: NP_000043; *Mus musculus* Atp7b: NP_031537; *Mus musculus* Atp7a: AAB37301; *Rattus norvegicus* Atp7b: NP_036643; *Rattus norvegicus* Atp7a: P70705; *Ovis aries* ATP7B: AAB94620; *Arabidopsis thaliana* Ran-1: AAD29115; *Caenorhabditis elegans* CUA-1: BAA20550; *Saccharomyces cerevisiae* Ccc2p: L36317.

An overall comparison between all sequences was performed by using the ClustalW amino acid alignment program provided by the European Bioinformatics Institute (http://www.ebi.ac.uk/clustalw/). To facilitate the comparison, similar amino acids were shaded by using the BoxShade server program (http://www.ch.embnet.org). These sequence alignments are found in Appendix A.

B. Mutation comparison

A total of 316 ATP7B mutations were used in our comparisons. WND patient mutations are publicly available as a database on-line at http://www.medicalgenetics.med.ualberta.ca /wilson/index.php (September 2004 version). Over 200 disease-causing variants have been identified in MNK patients. A literature search was performed to assemble the various ATP7A mutations available (up-to-date as of May 2005) (Kapur *et al.* 1987; Tumer *et al.* 1992; Chelly *et al.* 1993; Vulpe *et al.* 1993; Beck *et al.* 1994; Das *et al.* 1994; Kaler *et al.* 1994; Tumer *et al.* 1994b; Das *et al.* 1995; Kaler *et al.* 1995; Levinson *et al.* 1996; Tumer *et al.* 1996; Ronce *et al.* 1997; Tumer *et al.* 1997; Qi and Byers 1998; Ambrosini and

Mercer 1999; Ogawa *et al.* 1999a; Ogawa *et al.* 1999b; Moller *et al.* 2000; Ogawa *et al.* 2000; Dagenais *et al.* 2001; Gu *et al.* 2001; Hahn *et al.* 2001; Ozawa *et al.* 2001; Mak *et al.* 2002; Borm *et al.* 2004; Tumer *et al.* 2004; Watanabe and Shimizu 2005). 91 MNK patient point mutations were obtained for use in our comparisons. The *ATP7A* mutations were assembled into a mutation database (Appendix B).

The sequence variations were recorded according to the guidelines of the Human Genome Variation Society (http://www.HGVS.org/mutnomen/), using the reference sequence L06133 for the *ATP7A* coding sequence and the reference sequence NM_000053 for the *ATP7B* coding sequence. The nucleotide +1 is the A of the ATG-translation initiation codon and the ATG-translation initiation codon is also the first codon in quoting the mutations used. The collected mutations were compiled into four different types of point mutations (small deletions, insertions or duplications, missense mutations, nonsense mutations, and splice-site mutations). These mutations were plotted onto the human ATP7A/ATP7B alignment.

C. Mutation screening of exons 20 and 21 in ATP7B

The genomic DNA of 23 WND patients was screened for exon 20 sequence variations, and 16 suspected WND patients were screened for exon 21 sequence variations. The patients were selected from our series of over 200 patients because there had been extensive mutation screening performed on their genomic DNA with either no *ATP7B* mutations yet identified or only one WND causative mutation detected. Since the majority of their genomic DNA had already been sequenced, there was a high probability of finding a sequence change in the remaining exons to be sequenced, including exons 20 and 21.

Primers were designed to amplify, by polymerase chain reaction (PCR), exons 20 and 21 of the *ATP7B* gene of WND patient genomic DNA (primer 20F #2988: 5'-GTGCCTGAAGC CCTCTCC-3'; primer 20R #2989: 5'-CCACTGTGCTAAGCATGCAG-3'; primer 21F: 5'-GAGGCCTTCACCAGGCTTAG-3' and, primer 21R: 5'-GCTAGCTCAGCCCATC CTG-3'). The PCR amplification of exon 20 was carried out as follows. The reaction mix consisted of reaction buffer, 2 mM each of dATP, dCTP, dTTP and dGTP nucleotides, 1 mM magnesium chloride, 100ng of each oligonucleotide primer (primer 20F and primer

20R), 0.2-0.5 units of Taq (Sigma), and template DNA. Reactions were typically carried out in a 50 L total volume and the template DNA was amplified under the following conditions: 3 minutes at 94 C, followed by 30 cycles of 30 seconds of 94 C denaturation, 30 seconds of 62 C primer annealing, and 45 seconds of 72 C extension. The PCR was completed with a final extension at 72 C for 5 minutes and then held at 4 C.

The reaction mix for exon 21 PCR amplification consisted of reaction buffer, 2 mM each of dATP, dCTP, dTTP and dGTP nucleotides, 1 mM magnesium chloride, 50 ng of each oligonucleotide primer (primer 21F and primer 21R), 0.2-0.5 units of Taq (Sigma), and template DNA. The reactions were carried out in a 25 L total volume and the same thermocycler conditions as those used for exon 20.

The exon 20 and 21 PCR products were gel-purified using a Qiagen Gel Purification Kit. The exon 20 products were cycle sequenced using the Li-COR automated sequencer with a fluorescently-labeled forward primer 20F, according to the manufacturer's protocol (Li-COR). The exon 21 products were manually cycle sequenced using [-33P]-dideoxynucleotide terminators, primer 21R, and Thermo Sequenase DNA polymerase, according to manufacturer's protocol (USB Corporation). The sequences derived from WND patient DNA were compared with a normal control to identify any patient mutations.

III. RESULTS

A. CONSERVATION AMONG ATP7A AND ATP7B HOMOLOGUES

A comparison of ATP7A and ATP7B and their orthologues was performed (Appendix A). Comparative analysis of the two human Cu transporters displayed an overall amino acid identity of 56%. An examination of the sequence comparison revealed that the similarity between the paralogues was striking within the conserved heavy metal and P-type ATPase domains.

A comparison of human ATP7B with its orthologues demonstrated overall amino acid identities of 82% with *Mus musculus* (mouse), *Rattus norvegicus* (rat), and *Ovis aries* (sheep). Comparison with more evolutionarily distant organisms, such as *Caenorhabditis*

elegans (worm), *Arabidopsis thaliana* (plant), and *Saccharomyces cerevisiae* (baker's yeast), showed lower overall amino acid identities of 41%, 39%, and 33%, respectively. Similar pairwise BLAST comparisons were performed between human ATP7A and its orthologues. Overall amino acid identities of 89%, 88%, 55%, 43%, 40%, and 34% with mouse, rat, sheep, worm, plant, and yeast were seen, respectively.

As anticipated, ATP7A/ATP7B sequence conservation in the lower species (yeast and worm) was limited to the characteristic heavy metal P-type ATPase domains: the nucleotide-binding subdomain (referred to in this chapter as the ATP-BD), the transduction domain, the conserved DKTG motif in the P-subdomain, the SEHPL motif, and the invariant CPC sequence in TM 6. Since the majority of these conserved motifs are located within the central portion of the protein sequence, the yeast and worm orthologues were expected to show more similarity to human ATP7A and ATP7B in this region rather than at the extreme 5' and 3' ends. Within the 5' region, however, there was significant conservation of the GMT/HCXXC sequence motif, which is a motif identifiable in all MBSs and Cu-binding proteins. Outside of these MBSs, the 5' ends of the genes showed little conservation of sequence.

In addition to the 5' end, other regions of non-conservation that warrant further investigation were identified. In the mouse, rat and sheep alignments, amino acid sequences corresponding to segments of *ATP7B* exons 2, 3, 15, 16, 20 and 21 are not well conserved. These sequences all coincide with regions positioned between the functional domains. Non-conservation was even more pronounced when comparing human ATP7A with human ATP7B. Several regions displayed dissimilarity in sequence, including the amino acids representing *ATP7B* exons 1-4, portions of 7, 14, 15 and 21. These non-conserved exons may be indicative of regions and amino acid residues either important for distinct ATP7A and ATP7B functions, or not important for function at all. This type of information may be useful when screening patients for mutations, as variants of non-conserved amino acids are less likely to result in disease while mutation of a conserved residue would be more apt to lead to disease.

B. Comparison of ATP7A and ATP7B mutation spectra

The mutation spectra of human ATP7A and ATP7B were focused on to detect functionally significant amino acid residues. Since these paralogues have a high degree of similarity and both are copper delivery and export proteins, their mutation spectra was compared for amino acids affected in each disorder. A large number of mutations are associated with both WND and MNK; thus, a determination of causative mutations similar for both diseases could be indicative of amino acids and regions that are functionally important.

The exonic structures of *ATP7A* and *ATP7B* display remarkable similarity (Figure 2-1), with the last 19 exons of each of the genes having almost identical boundaries (Tumer *et al.* 1995). Only one intron throughout these 19 exons, intron 17 of *ATP7A* and intron 15 of *ATP7B*, does not interrupt the aligned coding regions at the same position. Of the 19 concurring exons, 15 have the same number of nucleotides, with only *ATP7B* exons 3, 7, 15, and 16 (*ATP7A* exons 5, 9, 17, and 18) differing. The genes are most dissimilar at their 5' ends, where the first four exons of *ATP7A* correspond to the first two exons of *ATP7B*. These 5'-most exons encode the first four copper-binding motifs of both protein products. Notwithstanding the disparate 5' ends, the close similarity in the remaining exonic structures reiterates the strong conservation between the two genes and leads to the possibility that many of the sequence alterations in the exons or at the intron-exon boundaries may also be similar.

Separate plots were generated for missense, nonsense, splice-site, and small insertion/duplication/deletion mutations (Figure 2-1 A-D). Only those mutations within the coding region were included; the variants that have been identified within regulatory regions, such as in the promoter and in the intronic sequences, were omitted from this analysis. Likewise, large genomic deletions identified in MNK patients, which account for approximately 15%–20% of all MNK mutations (Chelly *et al.* 1993; Tumer *et al.* 1994a; Tumer *et al.* 1994b; Poulsen *et al.* 2002; Tumer *et al.* 2003), were excluded. There is an apparent scarcity of large genomic deletions among WND patients, which may be attributable to a difference in the chromosomal localization of *ATP7A* (X chromosome) and *ATP7B* (chromosome 13) and the general genomic stability and chromosomal contexts of each (Tumer *et al.* 1999).

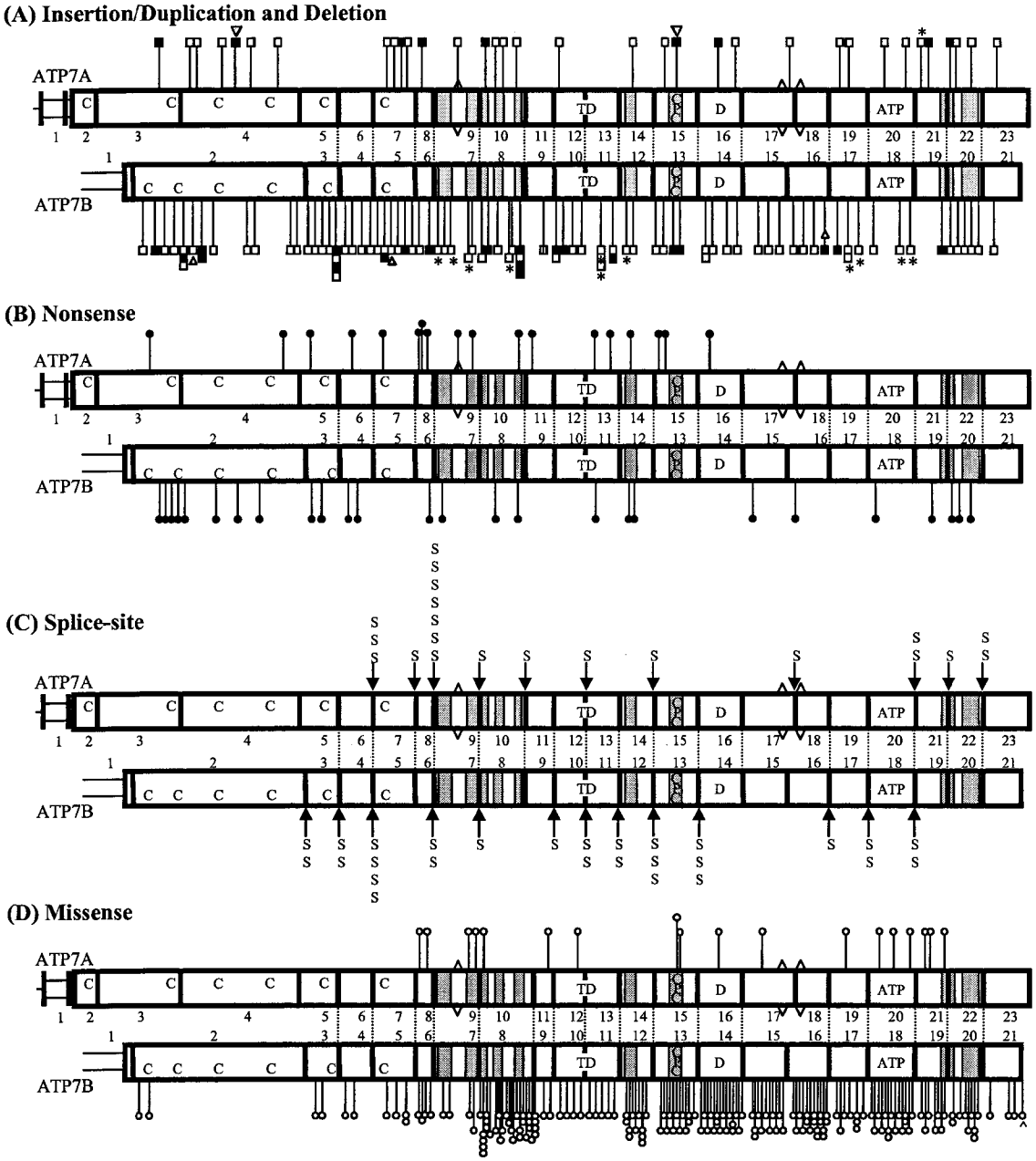

Figure 2-1. Comparison of MNK and WND patient mutations.

(A) Insertions/duplications, filled squares. Deletions, open squares. Striped square, indel mutation – deletion followed by insertion. Triangles, mutation creates termination codon. *, deletions of one or a few amino acids (in-frame). All others result in frameshifts. (B) Single bp substitutions that create termination codons (nonsense), filled circles. (C) Splice-site mutations, represented by "S" at specific exon-intron boundary. (D) Single bp substitutions that change an amino acid (missense), open circles. ^, stop codon of the gene replaced by an amino acid codon. "C", metal-binding site; "TD", transduction domain; "CPC", CPC motif in TM 6; "D", phosphorylated Asp; "ATP", ATP-binding site; shaded grey bars, TM segments; exons labeled by number.

To date, a large deletion of *ATP7B* (29-bp) in exon 8 (Nanji *et al.* 1997), and a partial gene deletion covering exons 20 and 21 (genomic deletion of 2144 bp) (Moller *et al.* 2005) have been identified. A more extensive search for large genomic deletions in WND patient DNA is needed to determine whether these really are not as common in *ATP7B* when compared with *ATP7A*.

To analyze the distribution of disease mutations within *ATP7A* and *ATP7B*, the genes were divided into different segments, corresponding to the various functional regions of the proteins, and the number of mutations within each segment was summed (Table 2-1). The number of mutations was examined with respect to the basepair size of the segment (% of the total coding sequence) being analyzed.

An analysis of the percentages of mutations lying within each segment (Table 2-1, "% of Total"), showed that most of the MNK mutations fell within exon 8 (sequence between MBS 6 and TM 1), exons 9-11 (TM 1-4) and exons 17-22 (includes the ATP-BD and TM 7 and TM 8). The last *ATP7A* exon, exon 23, which codes for the C-terminus, had the least. The WND mutation spectrum depicted a similar distribution, with the majority in exons 7-9 (TM 1-4) and exon 15-18 (ATP-BD). The major differences between the MNK and WND mutation spectra were in the region between MBS 6 and TM 1 (exon 8, *ATP7A* and exon 6, *ATP7B*), with fewer WND mutations in this segment, and with most of the *ATP7B* mutations in this region being missense compared with the abundance of *ATP7A* splice-site mutations. ATP7B also had proportionately more mutations within the transduction domain and TM 5. Significantly, both genes had the least number of mutations in their last exons, which code for the C-termini of both proteins, and a strong bias for the conserved domains and membrane-spanning portions.

To normalize the mutation frequencies seen within each segment, the number of mutations was considered in view of the basepair length per section of the gene (Table 2-1, "Normalized mutation frequency" = # of mutations/% of total gene length). The results were consistent with the actual percentages of mutations lying within each segment. With MNK, the frequency was greatest in exon 8 and exons 21/22 of *ATP7A*, which encode the region between MBS 6 and TM 1, and TM 7 and TM 8, respectively.

Table 2-1. Distribution of mutations in regions of the proteins and normalized mutation frequencies in the regions.

Exons	Region of Protein	Size of region (coding sequence)				*ATP7A* Mutations			*ATP7B* Mutations		
(*ATP7A*/ *ATP7B*)		# of nucleotides *ATP7A*	# of nucleotides *ATP7B*	% of total length *ATP7A*	% of total length *ATP7B*	# of Mutations	% of Total	Normalized mutation frequency (# mut/% total length)	# of Mutations	% of Total	Normalized mutation frequency (# mut/% total length)
Exon 1-4/ 1-2	MBS 1-4	1336	1285	29.7	29.2	9	9.9	0.3	27	8.5	0.92
Exon 5-7/ 3-5	MBS 5, 6	533	584	11.8	13.3	11	12.1	0.93	37	11.7	2.78
Exon 8/ 6	Between MBS 6 and TM 1	77	77	1.7	1.8	13	14.3	7.65	8	2.5	4.44
Exon 9-11/ 7-9	TM 1-4	552	501	12.3	11.4	15	16.5	1.22	58	18.4	5.09
Exon 12-14/ 10-12	Transduction domain, TM 5	418	418	9.3	9.5	8	8.8	0.86	42	13.3	4.42
Exon 15/13	TM 6 including CPC motif	195	195	4.3	4.4	6	6.6	1.4	19	6	4.32
Exon 16/14	Phosphorylation domain (including Asp)	183	183	4.1	4.2	4	4.4	0.98	21	6.6	5
Exon 17-20/ 15-18	ATP binding domain (N-subdomain)	711	660	15.8	15	12	13.2	0.76	73	23.1	4.87
Exon 21,22/ 19,20	TM 7, 8	221	221	4.9	5	12	13.2	2.45	26	8.2	5.2
Exon 23/21	C-terminal domain	274	271	6.1	6.2	1	1.1	0.16	5	1.6	0.81
TOTAL		4500	4395			91			316		

Exons 1-4 and exon 23 of *ATP7A*, which encode the N-terminal MBSs 1-4 and the C-terminus, showed the lowest mutation frequency. An analysis of the WND mutations revealed similar results, with exons 1-2 (MBSs 1-4) and exon 21 (C-terminus), the extreme 5' and 3' ends, having the lowest frequencies. In the WND spectrum, the normalized values indicated that exons 6-20 have comparable mutation frequencies, with each exon having a frequency between 4.3 and 5.2. None of the *ATP7B* exons had a mutation frequency as high as the mutation frequency seen in exon 8 of *ATP7A* (frequency of 7.65).

The mutation profiles of each disease are summarized in Table 2-2. The comparison of the different types of mutations associated with the mutation spectrum of MNK showed that there was relatively equal representation of all four types of mutations analyzed in *ATP7A*, with a slightly higher presence of small deletions, insertions and duplications in the mutations examined. With WND however, there was a definite bias in the spectrum towards missense mutations, as well as a higher incidence of small deletions, insertions and duplications. The splice-site mutations and nonsense mutations appear to be proportionately less prevalent amongst WND patients.

i. Small deletions and insertions, and duplications

Small (1–29 bp) insertions, duplications and deletions are spread throughout *ATP7B* and most of *ATP7A* (Figure 2-1A). The deletions and insertion/duplications that create termination codons at the mutation site are included in this plot, as are those that solely remove or add one or a few amino acids (in-frame mutations). The in-frame deletions are of particular use for our purposes, since they presumably identify amino acids that are necessary for normal function or structure. There are a few in-frame deletions in exons 7 (TM 1 and TM 2), 8, 11 (transduction domain), 12 (TM 5), 17 and 18 (ATP-BD) in *ATP7B*. Of these deletions, 30 of the 37 deleted amino acids are conserved among the mammalian ATP7B orthologues and also conserved in human ATP7A. An in-frame deletion has also been identified in a MNK patient. The deletion occurs just following the ATP-BD in exon 21; this deletes a conserved leucine residue. Interestingly, this leucine residue is also affected in a WND patient (missense mutation: Leu1305Pro), suggesting that the amino acid may be critical for function.

Table 2-2. Representation of the different types of mutations within each gene.

Type of Mutation	***ATP7A* Mutations**		***ATP7B* Mutations**	
	# of Mutations	% of Total	# of Mutations	% of Total
Splice-site mutations	21	23.1	27	8.5
Insertions/deletions/duplications	34	37.4	93	29.4
Nonsense mutations	18	19.8	26	8.2
Missense mutations	18	19.8	170	53.8
Total	91		316	

The majority of the small insertion/duplication and deletion mutations, for both ATP7A and ATP7B, result in frameshift mutations leading to premature truncations. Small deletions, as compared with insertions/duplications, are more predominant in both the MNK and WND genes, with deletions accounting for 27.5% and 22.8% and insertions/duplications accounting for 9.9% and 6.6% of all MNK and WND mutations, respectively.

ii. Nonsense mutations

The single basepair substitutions that generate termination codons are designated as nonsense mutations in Figure 2-1B. For MNK, the 3'-most nonsense mutation is found in exon 16, immediately following the invariant aspartic acid. This results in the disruption of the ATP-BD, which is necessary for catalytic activity. Further, TM 7 and TM 8, as well as the C-terminal domain are removed from the protein product.

Nonsense mutations for WND have been identified further downstream, with the 3'-most mutation lying in exon 20, making the termination codon fall in TM 8. Thus, the mutation leaves all conserved domains intact, only removing the last TM helix (TM 8) and the C-terminal cytoplasmic tail. The presence of this mutation indicates that TM 8 and/or the C-terminus are functionally important. In addition, more WND nonsense mutations are present at the 5' end of *ATP7B* than in *ATP7A*, and comparatively more MNK than WND nonsense mutations lie within the conserved domains in the mid-region.

iii. Splice-site mutations

The mutations labeled as splice-site mutations include those point mutations or small deletions and insertion/duplications that occur near splice-site junctions (Figure 2-1C). These mutations are prevalent in both *ATP7A* and *ATP7B*, with more than half of the exon-intron boundaries being affected; however, there is no apparent correlation between the specific boundaries affected in each disorder. A particular boundary that shows a disparate representation of splice-site mutations for the two genes is IVS8 in *ATP7A* and the corresponding IVS6 in *ATP7B*. There are seven different splice-site mutations located at this position in the MNK gene, whereas the corresponding *ATP7B* site has only two. Furthermore, *ATP7B* has more splice-site junctions affected than *ATP7A*.

iv. Missense mutations

The most common type of point mutation identified in WND patients is the missense mutation (Figure 2-1D). Despite the widespread distribution in *ATP7B*, more missense variants are concentrated within the exons coding for conserved domains, such as the CPC motif (exon 13), the phosphorylation and ATP-BDs (exons 14–18) and TM helices 3–6 (exons 8, 12, 13). As in WND, the 18 MNK-causing missense mutations are positioned primarily within the exons coding for conserved domains and TM helices.

A comparison of the MNK and WND disease-causing missense mutations revealed only four variants that altered the same amino acids in both protein products: (1) Gly-727 in ATP7A (G727R: exon 10) and Gly-710 in ATP7B (G710R/S/C/T: exon 8) located near TM 3; (2) Gly-1118 in ATP7A (G1118D: exon 17) and Gly-1101 in ATP7B (G1101R: exon 15), which lie within the ATP-BD; (3) Gly-1255 in ATP7A (G1255R: exon 19) and Gly-1221 in ATP7B (G1221E: exon 17) in the ATP-BD; and (4) Ser-1344 in ATP7A (S1344R: exon 21) and Ser-1310 in ATP7B (S1310R: exon 19), which lie just ahead of TM 7. Thus, these amino acid changes identify four residues that may be particularly critical for ATP7A and ATP7B function.

When extending the analysis to include all single basepair substitution mutations, three additional variants were identified that alter the same amino acids in both ATP7A and ATP7B: (1) Arg-795 in ATP7A (R795X: exon 10) and Arg-778 in ATP7B (R778L/G/Q/W: exon 8) in TM 4; (2) Arg-986 in ATP7A (R986X: exon 15) and Arg-969 in ATP7B (R969Q: exon 13) in TM 6; and (3) Glu-1081 in ATP7A (E1081X: exon 16) and Glu-1064 in ATP7B (E1064A/K: exon 14) near the invariant aspartic acid in the P-subdomain and just before the conserved SEHPL motif.

C. Mutation Screening of WND patient genomic DNA

i. Mutation screening of exon 20

Given the relative paucity of mutations at the 3' ends of *ATP7B* and *ATP7B* and our interest in the functional importance of the C-terminus (Chapter 3), the genomic DNA of selected WND patients was examined to search for additional disease-causing mutations in exons 20 and 21 (Figure 2-2A).

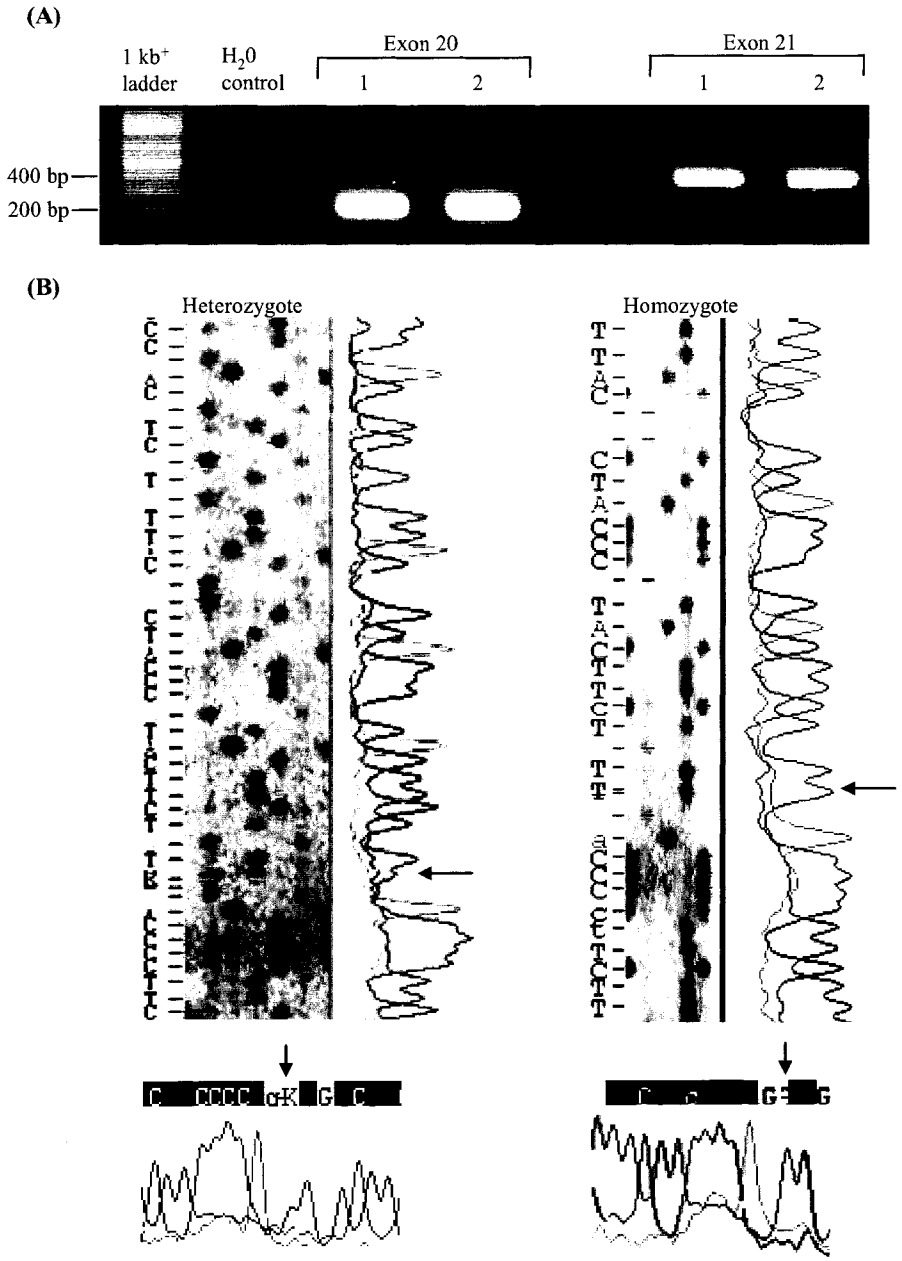

Figure 2-2. Mutation screening of the genomic DNA of WND patients for exon 20 and 21 mutations.

(A) PCR amplification of exons 20 and 21. PCR products were extracted from the agarose gel and sequenced using the automated Li-COR sequencing machine. (B) Examples of the exon 20 G→T transversion mutation. Left sequence, image of the sequencing gel and chromatogram of a WND patient heterozygous for the mutation. Right sequence, image of the sequencing gel and chromatogram of a patient homozygous for the mutation. Arrows identify the DNA sequence change.

In two of the patients, DNA sequence alterations were discovered. In the DNA of an Ukranian patient, a G T transversion at nucleotide 4022 (Gly1341Val) in TM 7 was identified. In a patient of Latvian/Ukranian ancestry, a deletion of a cytosine was detected at nucleotide 4074, leading to a frameshift (Ala1358Ala-fs) in TM 8 and premature termination at codon 1392 (Figure 2-2B). The remaining patient DNAs showed no sequence changes in exon 20.

ii. Mutation screening of exon 21

The genomic DNA of 16 suspected WND patients was screened for possible mutations (Figure 2-2A). More WND patients were not assessed because of difficulties amplifying exon 21, due to either degraded DNA or depletion of the DNA stock before sequencing was completed. No sequence alterations were detected in any of the DNA templates.

IV. DISCUSSION

The study was performed in order to elucidate regions and amino acids of ATP7B important for its function. From the sequence alignments, the central exons of human *ATP7A* and *ATP7B* were found to be more similar than outlying exons, corresponding to the functional domains of P-type ATPases and TM helices. This sequence similarity was evident among the mammalian orthologues. Further, the strong conservation of functional domains was clearly apparent when compared with the orthologous sequences from lower species. Conservation of these domains in species as divergent as bacteria and humans signifies their importance for the function of these heavy-metal P-type ATPases.

From comparing the spectra of MNK and WND disease-causing variants, three aspects have been observed: A) the regions primarily affected were conserved functional domains, B) the spectrum of mutations varied, and C) three areas of interest were identified with a higher prevalence of mutation in one disease in comparison with the other.

A. IMPORTANCE OF THE CONSERVED FUNCTIONAL DOMAINS

An analysis of the sequence variants revealed a bias toward the central exons, likely reflecting the importance of the functional domains and the membrane-spanning regions that are primarily located in the mid-section of the proteins.

i. The ATP-binding domain

Homology modeling of the large extracellular domain between TM 6 and TM 7 of ATP7B, which includes the ATP-BD (P- and N-subdomain) and invariant aspartic acid, was possible because of the strong conservation of this region with other proteins in the P-type ATPase family (Fatemi and Sarkar 2002b; Lutsenko *et al.* 2002). The crystal structure of SERCA1a, a P-type ATPase that transports Ca^{2+}, was used as a template and the 3D structure of ATP7B was modeled. The overall fold of the phosphorylation and ATP-BDs were similar to the Ca-ATPase suggesting conservation in biological activity and thus functional significance. It can be inferred that the residues conferring this topology would be important and variation of these domains would foreseeably result in disease.

ii. Transmembrane domains

TM domains are likewise necessary for the overall tertiary structure of the protein and for cation transport function. The formation of membrane-spanning regions requires hydrophobic amino acids in the TM and positively-charged residues at entry-exit points. Thus, mutation of a critical amino acid may result in an incorrectly folded protein and subsequent degradation. Mutational studies of TM 4 and TM 6 (Forbes and Cox 1998; Bissig *et al.* 2001; Voskoboinik *et al.* 2001a), have indicated that particular residues within these TM helices are crucial for function. TM 6 is an especially critical TM helix since it contains the CPC motif, a motif that is highly conserved in all ATPases responsible for the transport of transition metals. The CPC motif is thought to be part of the intramembrane metal binding site (Bissig *et al.* 2001), and TM 6 itself, is involved in the formation of the channel through which Cu is passed. In fact, TM 6, TM 7 and TM 8 of Cu-ATPases have been shown to correspond to the TM helices in the Ca-ATPase associated with the transduction channel and which contain residues critical for cation transport (Toyoshima *et al.* 2000). In addition, TM 7 may be particularly important for metal specificity as it

contains a two-residue motif (Tyr-Asn) seen in all ATPases involved in Cu transport, but lacking in those that transport zinc or cadmium (Lutsenko *et al.* 2002). Mutation of the conserved tyrosine has been detected in WND patients (Tyr1331Ser), reiterating the significance of the amino acid for the Cu transport function of ATP7B.

iii. The metal-binding sites of the copper-binding domain

Mutations within the conserved heavy metal binding sequences were less prevalent. The limited number of mutations is presumably related to the apparent redundancy of the MBSs, in that not all six are required for the protein to be functional (Forbes *et al.* 1999). Since the bacterial, yeast, worm and plant orthologues all contain fewer than six MBSs and are still capable of Cu transport, this redundancy is expected. Therefore, in-frame sequence changes, such as missense mutations and small in-frame deletions and insertions, may not result in disease and consequently, remain undetected.

iv. Adjoining region between the copper-binding domain and the ATPase core

Exon 8 of the *ATP7A* gene, which is the region between MBS 6 and TM 1, contains many MNK patient mutations (14.3% of all *ATP7A* mutations) and has the highest mutation frequency amongst those in *ATP7A* and all of *ATP7B* (7.65 normalized mutation frequency), mainly due to the number of splice-site mutations. The corresponding exon 6 in *ATP7B* does not show this large percentage of mutations (2.5%) or high mutation frequency (4.44). There are seven MNK splice-site mutations in IVS8, compared with two in *ATP7B*. This suggests that the region may be either highly mutable or the integrity of this boundary is particularly critical. Although a specific function has yet to be assigned, researchers propose that the sequence between MBS 6 and TM 1 is important for protein folding and required to join the CuBD to the ATPase core of the protein (Tumer *et al.* 1999). Studies on the CuBD in ATP7B have shown that the spacing between the last MBS and the first TM helix is critical (Forbes *et al.* 1999), suggesting that this segment in both ATP7A and ATP7B plays an essential structural role necessary for cation transport. Therefore, it is unlikely that the enrichment for *ATP7A* mutations in this exon and IVS is simply due to chance. Since this region appears to be necessary and shows relatively high

amino acid identity between ATP7A and ATP7B, investigation of this sequence in *ATP7B* in WND patients may lead to the identification of causative WND mutations

B. Differences and similarities between the mutation spectra

i. Difference in overall mutation spectra

The WND mutation spectrum was definitely skewed toward a prominence of missense mutations that was not evident among MNK patient mutations. Tümer et al. have previously performed a comprehensive analysis of the mutation spectrum of *ATP7A*, which revealed a nearly equal representation from all four types of point mutations (deletions/insertions/duplications, missense and nonsense mutations and splice-site mutations) (Tumer *et al.* 1999). Our data also showed an equivalent representation from missense, nonsense and splice-site mutations; however, small insertions/duplications and deletions represented a slightly higher percentage of the total number of mutations analyzed. There is no apparent reason for this difference; although, as noted earlier, the MNK gene has more large deletions and the same may be true for the smaller deletions/insertions.

A useful outcome of our comparisons was the identification of regions showing differences between the MNK and WND mutations in the distribution of their disease-causing sequence alterations and in the prevalence for mutation types. Although the differences could have occurred by chance, the disparity seen could reflect regions of functional relevance. When analyzing the normalized mutation frequencies, many of the conserved domains (transduction domain, phosphorylation domain and ATP-BD, as well as TM 1-4 and TM 5, 6) showed lower mutation frequencies in the *ATP7A* gene when compared with the mutation frequency seen with WND patient mutations in the regions. In all of these functional domains, there was a clear predominance of missense mutations in *ATP7B*, which may account for the lack of correspondence with the *ATP7A* mutation spectrum. Since the functional domains show high structural similarity and amino acid identity with other P-type ATPases, certain residues may be essential and it is not improbable for sequence changes to be disease-causing. Therefore, it is likely that additional MNK patient mutations have yet to be identified in these regions.

In both genes, there were fewer mutations seen in the very N- and C-terminal regions. Hence, the genomic DNA of several suspected WND patients was screened for possible mutations in exons 20 and 21 of *ATP7B*.

ii. Four amino acids are similarly affected

Comparison of the *ATP7A* and *ATP7B* mutation spectra identified several residues, in the same sequence position in the two proteins, which were mutated in both MNK and WND patients. The identification of these amino acids was of interest since they presumably identify essential residues, and three of these lie outside of a conserved functional domain. This suggests that critical residues may not be limited to the signature domains of heavy metal P-type ATPases, and additional functional regions within ATP7A and ATP7B may exist and be important for maintaining Cu homeostasis.

iii. *ATP7A* mutations that result in milder disease

Clinical heterogeneity contributes another level of complexity since the milder disease forms and their causative mutations are more difficult to detect. The X-linked inheritance pattern of MNK and its associated allelic disorders facilitates the identification of disease-causing mutations and the determination of phenotypic consequences. In fact, with *ATP7A*, there have been mutations identified in patients with milder forms of MNK, including occipital horn syndrome (OHS) and mild MNK.

There are 35-40 known cases of OHS worldwide; however, mutations in only nine have been elucidated (Moller *et al.* 2000; Dagenais *et al.* 2001). In seven of these, the *ATP7A* mutation leads to aberrant splicing of the transcript (Kaler *et al.* 1994; Das *et al.* 1995; Ronce *et al.* 1997; Qi and Byers 1998; Moller *et al.* 2000; Gu *et al.* 2001). Four of the OHS patient mutations occur at splice-site junctions, and two are missense mutations that do not adversely affect function (Kaler *et al.* 1994; Ronce *et al.* 1997), with one being a deletion of a guanine and the other occurring in the regulatory region of the gene (not plotted in Figure 2-1). *ATP7A* transcript levels as low as two to five percent of normal can result in the milder phenotype rather than classic MNK, and in four of the cases described, low levels of normal transcript have been detected (Das et al. 1995; Gu et al. 2001; Levinson et al. 1996; Møller et al. 2000). Furthermore, sufficient Cu efflux function from a

mutant protein product results in a milder phenotype (Dagenais *et al.* 2001). Such mutations in *ATP7B*, which cause milder disease in *ATP7A*, may not lead to clinical disease in WND compound heterozygote patients. Milder forms of WND have been seen, with those persons affected presenting at later ages of onset. However, patients with late onset disease may remain undiagnosed or may be classified as heterozygotes because the other mutant allele is not identified. Based on the MNK mutation spectrum, it is conceivable that additional WND mutations are present that result in milder disease.

C. Conclusion

WND patient mutation detection is made even more challenging by the large number of possible disease-causing sequence variations and the fact that most WND patients are compound heterozygotes. Our study has highlighted additional regions that must not be missed when screening for patient mutations, regions which are highly conserved between orthologues and with human ATP7A and regions which have a high mutation frequency in the paralogous *ATP7A* gene. The identification of certain amino acids and areas of the protein that are conserved pinpoints important sequences that when altered could plausibly result in disease. The functional domains are clearly essential; however, the identification of mutations outside these domains reiterates the fact that there are other regions and amino acids critical for maintaining Cu homeostasis by ATP7A and ATP7B. Even though this analysis has revealed crucial information regarding the *ATP7B* gene and important conserved regions, any change in the genomic DNA sequence of an affected individual does not necessarily indicate a disease-causing change. Functional studies are still required to determine whether the resultant protein product is defective, leading to a WND phenotype. This study is useful, however, in providing an initial step for the detection of possible disease-causing mutations and for the development of a mutation screening strategy.

CHAPTER 3:
Functional assessment of the carboxy-terminus of the Wilson disease copper-transporting ATPase, ATP7B

Results in this chapter have been published in:

Hsi G, Cullen LM, Glerum DM, and Cox DW. (2004). Functional assessment of the carboxy-terminus of the Wilson disease copper-transporting ATPase, ATP7B. *Genomics* 83(3): 473-481.

I. INTRODUCTION

To date, over 300 disease-causing mutations have been identified in WND patients (http://www.medicalgenetics.med.ualberta.ca/wilson/index.php). The WND mutation spectrum has an overrepresentation of single base pair substitutions leading to missense mutations, with most of the DNA changes in the conserved functional domains and membrane-spanning segments within the centre exons (Chapter 2) (Hsi and Cox 2004). Several assays have been developed to study the consequences of patient mutations on the function of the protein (Hung *et al.* 1997; Forbes and Cox 1998; Iida *et al.* 1998; Payne *et al.* 1998; Forbes *et al.* 1999; Forbes and Cox 2000; Bissig *et al.* 2001; Voskoboinik *et al.* 2001a; Tsivkovskii *et al.* 2002). Despite these functional assays, mutation studies have been limited to a select few mutations identified in WND patients and confined to the functional domains that are conserved in heavy metal P-type ATPases. Therefore, several regions of the gene remain to be evaluated and our current understanding of the effects of different WND patient mutations on the function of ATP7B is still inconclusive.

A basepair substitution is considered likely to be disease-causing if it is not found on at least 50 normal chromosomes, if no other mutations can be detected, if the substituted amino acid is conserved in functionally related proteins, or if the amino acid substitution is non-conservative. However, it is still difficult to determine whether a sequence change is a disease-causing missense mutation or a rare normal variant not yet identified on a normal chromosome, especially when the amino acid change is conservative and/or the residue is not conserved in homologous proteins. Thus, reliable functional assessment is always desirable.

Our laboratory has designed a yeast functional assay to specifically analyze the capacity of ATP7B variants to transport Cu through the membrane and deliver it to the Cu-dependent apo-Cp (Forbes and Cox 1998). This yeast assay has been a valuable tool as an indirect assay for examining the Cu delivery function of ATP7B variants. Our laboratory has successfully used the system to study the effect of mutations and deletions within the Cu-binding motifs of ATP7B (Forbes *et al.* 1999), and to assess the degree to which disease

mutations found in the membrane-spanning segments of ATP7B affect protein function (Forbes and Cox 1998).

In this chapter, complementation of yeast mutant for *CCC2* was used to study the role of the C-terminus of ATP7B in maintaining Cu homeostasis. This region contains a 93-amino acid cytoplasmic tail that has not been studied previously nor analyzed extensively for its functional significance. As described in chapter 2 (Hsi and Cox 2004), the C-terminus has few sequence alterations suggesting either that the C-terminus is less important for function, or that disease-causing mutations have not been identified. Our mutation screening of exons 20 and 21 in several WND patients did not reveal any additional sequence changes (Chapter 2); however, sequence variations have been detected in WND patients, so at least some sequences in the 3' coding region are important for proper function of ATP7B within the cell and for Cu homeostasis. Furthermore, it is likely that only key amino acids residues in this cytoplasmic tail are critical.

II. MATERIALS AND METHODS

A. COMPUTER ANALYSES

A standard protein-protein BLAST analysis of the NCBI non-redundant database was completed (http://www.ncbi.nlm.nih.gov/BLAST/) to perform sequence comparisons of the 93 amino acid C-terminus of ATP7B (NP_000044) with its orthologues and with the paraloguous human ATP7A protein (NP_000043).

A web-based application, SOSUI (http://sosui.proteome.bio.tuat.ac.jp/sosuiframe0.html), which discriminates between membrane and soluble proteins and predicts TM helices for membrane proteins, was used to model the protein variants. The program uses four physicochemical parameters, including the hydrophobicity of the amino acid sequence, the amphiphilicity index of polar side chains, amino acid charges and the length of the amino acid sequence being analyzed (Hirokawa *et al.* 1998).

B. ATP7B cDNA CONSTRUCTS

The full length 4.395-kb coding region of *ATP7B* was previously constructed in our laboratory from total human liver RNA by a former graduate student (Dr. John R. Forbes) (Forbes and Cox 1998). The liver RNA was used as a template for reverse transcription to create the first cDNA strand, which was then used as the template for polymerase chain reaction (PCR) amplification of five overlapping fragments containing the entire coding region of *ATP7B*. The five primer pairs were chosen such that unique restriction sites were present near the ends of each cDNA fragment, facilitating construction of the full length cDNA. A 5'-*Bam*H1 site was added to the PCR primer sequence immediately preceding the initiating ATG codon, for use in cloning into expression vectors. The PCR products were adenylated and cloned into T/A cloning vectors (pGEM-T vectors, Promega; and pCR2.1, Invitrogen). Each of the five fragments was sequenced according to manufacturer's protocol (USB Corporation) to ensure sequence fidelity. The five fragments were ligated together, and the final cDNA construct was cloned into a pUC19 vector using the 5'-*Bam*H1 site and a 3'-*Sal*1site from the polylinker of the Promega T/A vector. This plasmid stock was used as the source of full-length *ATP7B* cDNA for all subsequent experiments and is also referred to as the unmanipulated cDNA.

To create point mutations within the cDNA, site-directed mutagenesis (QuikChange, Stratagene) of the *ATP7B* full-length cDNA (described above) was performed. Two complementary oligonucleotide primers bearing the desired codon changes were synthesized for each mutation. Primers were designed so that approximately ten bases of matched normal sequence flanked the mutated codon. The mutagenic primers used are listed in Table 3-1. The site-directed mutagenesis was carried out as follows: 20 ng of *ATP7B* cDNA was used as template with 500-750 ng of each mutagenic primer, 2.5 units of *Pfu* polymerase, 2.5 mM of each dATP, dCTP, dGTP and dTTP in the manufacturer's buffer to a total volume of 50 μL. The reaction mixtures were temperature cycled as follows: 95°C for 1 min as an initial denaturation step, followed by twenty cycles of 30 s at 95°C for denaturation, 1 min at 55°C for primer annealing, 17 min at 68°C for polymerase extension.

Table 3-1. Primers used for the generation of *ATP7B* mutant variants.

Variant	Forward Primer	Reverse Primer
Pro1379Ser	GCTATAAGAAG**T**CTGACCTGGAG	CTCCAGGTCAG**A**CTTCTTATAGC
4195 C	CTGACGGCATCC^AGGTCAGTG	CACTGACCT^**GG**ATGCCGTCAG
Thr1434Met	GTCCTCCCTGA**T**GTCCGACAAGC	GCTTGTCGGAC**A**TCAGGGAGGAC
Lys1437Lys	CGTCCGACAA**A**CCATCTCGGC	GCCGAGATGG**T**TTGTCGGACG
4117	GT***GGCTAG***CATTCACCTTTCC	CTAGGTCGAC**CTA**CTGCAGGGATGAGAGCACCAC
4126	GT***GGCTAG***CATTCACCTTTCC	CTAGGTCGAC**CTA**GCACTTGAGCTGCAGGG
4213	GT***GGCTAG***CATTCACCTTTCC	CTAGGTCGAC**CTA**TATGTGCACACTGACC
4360	GT***GGCTAG***CATTCACCTTTCC	CTAGGTCGAC**CTA**AGACCACTTGTCCCCATCATCG
LLL>ALL	GACAAGTGGTCT**GCT**CTCCTGAATGGC	GCCATTCAGGAG**AGC**AGACCACTTGTC
LLL>AAL	GACAAGTGGTCT**GCTGCC**CTGAATGGC	GCCATTCA**GGCAGC**AGACCACTTGTC
LLL>AAA	GGTCT**GCTGCCGCG**AATGGCAGGG	CCCTGCCATT**CGCGGCAGC**AGACC
D>A	GACGATGATGGGG**C**CAAGTGGTCTCTG	CAGAGACCACTTG**G**CCCCATCATCGTC
W-M hybrid (Xho 1 site)	GAAGGATTTTT***CTCGAG***CTCTT	CCCTAATATAA***GAGCTC***GAGAA
W-M hybrid (Nhe 1 site)	GGATGTAGTG***GCTAGC***ATTGACTTATC	GATAAGTCAAT***GCTAGC***CACTACATCC

Bold and underlined, nucleotide substitutions. ^, nucleotide deletion. Bold, stop codon. Bold and italicized, engineered restriction enzyme site.

Following the temperature cycling procedure, 20 units of the methylation sensitive restriction enzyme *Dpn*1 was added to the reaction mixture and incubated for approximately 2 hr at 37°C to destroy the template plasmid. The *Dpn*1-digested DNA was transformed into chemically competent DH5 *E. coli* cells according to manufacturer's protocol (Invitrogen) and selected on solid Luria Broth medium supplemented with 100 μg/mL carbenicillin (Sigma). Plasmid DNA was isolated from individual mutated colonies (Qiagen), and sequenced across the mutation sites to confirm the presence of the desired mutations, according to manufacturer's protocol (Thermosequenase, USB Corporation). Mutant cDNA fragments, encompassing the region between unique restriction sites in the *ATP7B* sequence and surrounding the desired mutation, were sequenced to ensure that no secondary mutations occurred during mutagenesis. The correct mutated fragments were liberated from the mutant plasmid by restriction enzyme digestion and were agarose gel purified and ligated back into a complementarily prepared, unmanipulated cDNA to create the full-length mutant constructs in pUC19 vectors.

To create the 3' deletion constructs, synthetic oligonucleotides containing stop codons at desired positions were used in PCR amplications of a fragment of the full-length *ATP7B* cDNA. The forward primer of each primer pair used in the PCR reaction included a natural restriction site found in the *ATP7B* coding region. The primer pairs used for mutagenesis are listed in Table 3-1. PCR amplification was carried out as follows. The reaction mix consisted of reaction buffer, 2 mM each of dATP, dCTP, dTTP and dGTP nucleotides, 1 mM magnesium chloride, 100 ng of each primer, 0.1-0.5 units of Taq (Sigma), and template DNA in a total volume of 25-50 μL. The template DNA was amplified as follows: 2 min at 94°C, followed by 30 cycles of 30 s of 94°C denaturation, 30 s of 58°C primer annealing, and 30-45 s of 72°C extension. The PCR was completed with a final extension at 72°C for 5 min and then held at 4°C. The PCR products were separated on an agarose gel, gel purified (Qiagen), and cloned into T/A cloning vectors (pGEM-T vectors, Promega; and pCR2.1, Invitrogen), cycle-sequenced using the LongRead IR automated sequencing system (Li-COR) to ensure presence of the desired deletion and absence of secondary mutations. Correct, deleted fragments were removed from the T/A cloning vectors by restriction enzyme digestion and agarose gel purified, and then ligated back into

a complementarily prepared, unmanipulated *ATP7B* cDNA to create the deletion constructs in pUC19 vectors.

The 3' coding end of the *ATP7A* cDNA was constructed from total human lymphoblast RNA derived from a human lymphoblast cell culture. The RNA was used as a template for reverse transcription, with oligo-d(T) primers and Superscript II reverse transcriptase to prime the first strand cDNA (Invitrogen). PCR primers were used to amplify the last approximately 1300 nucleotides of *ATP7A*. The PCR product was ligated into a PCR2.1 T/A cloning vector (Invitrogen). A reverse primer containing an *Xho*I restriction site was used to engineer this enzyme site into the 3' end (Table 3-1). Site-directed mutagenesis was also used to engineer in an *Nhe*1 site at the 5' end of the fragment to facilitate the generation of an in-frame *ATP7A/ATP7B* hybrid (Table 3-1). The *ATP7A* fragment was digested with *Nhe*1 and *Xho*1, gel purified, and ligated to an unmanipulated *ATP7B*/pG4 construct digested with *Nhe*1 and *Sal*1 enzymes to create an *ATP7B* cDNA with its 3' end replaced with the 3' of the *ATP7A* cDNA (W-M hybrid).

C. YEAST STRAINS

The wild-type yeast strain used was the protease-deficient *S. cerevisiae* strain BJ2168 (*MAT***a** *pep4-3 prc1-407 prb-1122 ura3-52 trp1 leu2*) (Zubenko *et al.* 1980) originally provided by Dr. Morrie Manolson at The Hospital for Sick Children, Toronto. A protease-deficient strain was used to minimize potential proteolysis during procedures, such as the oxidase assay, in which samples are not heated prior to electrophoresis.

The *ccc2* and *fet3* mutant yeast strains were created by homologous recombination. The *fet3* mutant strain, which lacks a functional *FET3*, was made previously by transforming a gene disruption plasmid (p fet3) into BJ2168 wild-type yeast (Forbes and Cox 1998). The *ccc2* mutant strain was similarly made using the E5-URA3.4 gene disruption plasmid. E5-URA3.4 contains 1.1-kb of the *URA3* gene flanked by a total of 685-bp of the yeast *CCC2* gene sequence (c.2104_2430 and c.2431_2728). Prior to transformation into BJ2168, E5-URA3.4 was linearized by digestion with *Bam*H1 and *Not*1. The ~1.8-kb linearized plasmid was gel purified (Qiagen), and then transformed into BJ2168 yeast. Integrations were selected on synthetic dextrose (SD) medium, made from 0.17% yeast nitrogen base

without glucose or ammonium sulphate (Bio-101), supplemented with 2% glucose, 0.5% ammonium sulphate, and all amino acids except uracil (Kaiser *et al.* 1994). SD medium was solidified for plating transformants by adding 2% Bacto-agar (Difco) to the liquid SD medium. Single transformant colonies were isolated and streaked again onto the -Ura selective medium. These transformants were checked for *URA3* gene integration into the yeast genome by PCR using primers matching the *CCC2* sequence flanking *URA3* in the plasmid (E5-URA3.4F: 5'-GAAAGCGAATACGTGTT GG-3' and E5-URA3.4R: 5'-GAGATCACATTTGCCTGTGG-3'). Integration would result in a PCR product 1.5-kb in length, rather than a 378-bp PCR product. All yeast transformations were performed using a modified lithium acetate method (Elble 1992; Kaiser *et al.* 1994).

D. YEAST EXPRESSION CONSTRUCTS

For high level *ATP7B* expression in yeast, cDNAs were released from pUC19 vectors by *Bam*H1 and *Sal*1 restriction enzyme digest sites, the product gel-purified, and then ligated into a multicopy 2 replication origin vector pG3 (Schena *et al.* 1991) obtained from Dr. Morrie Manolson at The Hospital for Sick Children, Toronto. The pG3 vector uses a strong, constitutive glyceraldehyde-3-phosphate dehydrogenase (GAPDH) promoter, a phosphoglycerate kinase (PGK) terminator and polyadenylation sequence, and a tryptophan selectable marker.

The integrating vector pG4 was previously derived from pG3 for single copy expression of *ATP7B* in yeast (Forbes and Cox 1998). A fragment of the pG3 vector containing the 2μ origin of replication was removed by digesting with *Eco*R1. The resulting fragments were electrophoresed to isolate the product lacking the yeast origin of replication, which was extracted from the agarose gel and purified (Qiagen), and then ligated to form pG4. *ATP7B* cDNAs were cloned into pG4 vectors as for pG3.

Yeast expression constructs were transformed into yeast and selection was based on tryptophan/uracil prototrophy as the pG3/pG4 vectors contained the wild-type *TRP* gene and the yeast *ccc2* mutants were created by disruption of *CCC2* with *URA3*. Single colonies were re-streaked onto selective medium to ensure clonality and clones were

checked monthly for trytophan/uracil prototrophy to confirm that revertants were not present.

To increase the efficiency of transformation into yeast cells, the pG4 constructs were first linearized by digestion with *Xba*1 and then gel purified prior to transformation. This linearization targeted the integration of the plasmid to the yeast *trp1* locus. Genomic DNA from the yeast strains containing pG4 constructs was isolated as described in Current Protocols (Ausubel *et al.* 1998). The genomic DNA was analyzed by Southern blotting to confirm that the constructs were correctly integrated in single copies. Five μg of genomic DNA was restriction enzyme digested with *Bam*H1 since there is a single *Bam*H1 restriction enzyme site within the expression construct. The digested DNA was electrophoresed for approximately 500 V·hr on a 0.6% agarose gel. Southern hybridization was performed using alkaline transfer from the gels onto Hybond-N+ membrane as described by the manufacturer (Amersham Pharmacia Biotech). In general, after electrophoresis, the gel was incubated in 0.25 M HCl for 30 min, followed by a 30 min incubation in denaturation solution (0.4 M NaOH). After rinsing quickly with distilled water, the DNA was transferred overnight to Hybond-N+ membrane in 0.4 M NaOH solution. After transfer, the membrane was pre-hybridized in Church and Gilbert hybridization solution (Church and Gilbert 1984) (0.34 M Na_2HPO_4, 0.16 M NaH_2PO_4, 7% SDS, 1% BSA) for one hour at 65°C. *ATP7B* cDNA was labeled with ^{32}P-dCTP (Amersham) by random priming using a T7 Quickprime kit according to manufacturer's protocol (Amersham). The Southern blot was probed overnight at 65°C in hybridization solution. After hybridization, the membrane was washed with varying concentrations of a salt solution/detergent (standard sodium citrate, SSC and sodium dodecyl sulphate, SDS) at different temperatures to reduce the background signal. Generally, the blot was washed for 5 min at room temperature with 2 x SSC, 0.1% SDS, followed by a 15-30 min wash at 65°C with 2 x SSC, 0.1% SDS, 30 min at 65°C with 0.5 x SSC, 0.1% SDS, and a final 30-45 min wash at 65°C with 0.1 x SSC, 0.1% SDS. The blot was wrapped in Saran-Wrap and exposed to Kodak X-OMAT film. Single copy integrations were identified by the presence of single high molecular weight bands (> 9-kb) that were visible following autoradiography (BioMax MS film, Kodak). If integrated in multiple copies, a band equal

to the combined size of *ATP7B* cDNA and the expression vector was visible (approximately 9-kb band for full-length *ATP7B* constructs) in addition to the high molecular weight band.

Once transformed into yeast, integration of the pG4 constructs were further confirmed by sequencing across the desired mutation site. Yeast genomic DNA was isolated as above, following the method described in Current Protocols (Ausubel *et al.* 1998). PCR amplification across the desired region was performed using a reverse primer in the pG4 vector and an *ATP7B* gene-specific forward primer. The reaction was carried out as follows: approximately 100 ng of genomic DNA was used as template with 50 ng of each oligonucleotide primer, 0.5 units of Taq polymerase (Sigma), 2 mM each of dATP, dCTP, dGTP and dTTP, 1.5 mM magnesium chloride and the manufacturer's buffer in a total volume of 25 μL. The reaction mixtures were temperature cycled as follows: 94°C for 3 min as an initial denaturation step, followed by thirty cycles of 30 s at 94°C for denaturation, 30 s at 56°C for primer annealing, 45 s at 72°C for polymerase extension, and then held at 4°C. The PCR products were gel purified and cycle sequenced using a dye-labeled gene-specific primer according to the manufacturer's protocol (Li-COR).

For yeast transformed with pG3 constructs, plasmid DNA was isolated as described in Current Protocols (Ausubel *et al.* 1998). Yeast cells were pelleted and resuspended in 200 μL of breaking buffer: 10% Triton X-100, 10% SDS, 1.5 M NaCl, 1 M Tris-Base pH 8, 250 mM EDTA pH 8.4. Cells were lysed by vortexing with glass beads (425-600 micron diameter, Sigma) for 3 min. Cellular debris was removed by centrifugation. The yeast plasmid DNA was transformed into DH5 *E. coli* bacterial cells. From the bacteria, plasmid DNA was prepared and sequenced using dye-labeled gene-specific primers according to the manufacturer's protocol (Li-COR) in order to confirm the presence of the desired mutations.

E. YEAST COMPLEMENTATION ASSAY: GROWTH ASSAY

Base assay medium consisted of 0.17% (w/v) yeast nitrogen base lacking Fe, Cu (Bio-101), 50 mM MES buffer pH 6.1 (Sigma), 2% (w/v) glucose, and 0.5% (w/v) ammonium sulphate, and supplemented with all amino acids except tryptophan (Kaiser *et al.* 1994).

Fe-limited medium was base assay medium containing 1 mM ferrozine (Fe specific chelator, Sigma), 50 μM ferrous ammonium sulphate (Sigma), and 1 μM copper sulphate (Sigma). Fe-limited medium was supplemented to make Cu- or Fe-sufficient media. Cu-sufficient medium was base assay medium containing 1 mM ferrozine, 50 μM ferrous ammonium sulphate, and 500 μM copper sulphate. Fe-sufficient medium was base assay medium containing 1 mM ferrozine, 350 μM ferrous ammonium sulphate, and 1 μM copper sulphate.

The growth assay was established previously in our laboratory to quantify the relative ability of ATP7B variants to complement the *ccc2* mutation in yeast (Forbes and Cox 1998; Forbes *et al.* 1999). The growth rates of *ccc2* yeast transformed with *ATP7B* cDNA were measured in Fe-limited medium. The yeast cells were prepared for the growth assay in the following manner: yeast cultures were grown to stationary phase in standard SD medium lacking tryptophan, washed with sterile ice-cold distilled water, resuspended in Fe-limited medium, and then grown overnight to saturation at 30°C. These starter cultures were used to inoculate fresh Fe-limited medium to a cell density of $OD_{600nm} = 0.1$. Growth at 30°C was monitored spectroscopically for 21 hr, with measurements taken at 0, 9, 12, 15, 18 and 21 hr. These experiments were performed in triplicate and growth rates were calculated using the cell density readings measured at the times of 12 and 18 hr, and recorded in OD_{600nm}/hr units.

F. Assay of ferroxidase activity

The Fet3p oxidase assay measures the Fet3 oxidase activity of the yeast transformed with the *ATP7B* cDNA constructs and is based upon a modified version of the assay previously described (Yuan *et al.* 1995). Fet3p oxidase activity depends on the Cu received from Ccc2p for its function, and thus can serve as a sensitive marker for the putative Cu-transporting function of Ccc2p (Yuan *et al.* 1995).

Cells were grown to mid-log phase at 30°C in SD medium lacking tryptophan, Fe and Cu, and supplemented with 50 mM MES buffer pH 6.1 and 0.5 μM $CuSO_4$. Twenty-five mL of yeast culture were washed twice with ice-cold deionized water, followed by a wash with 800 μL of supplemented homogenization buffer (either with $CuSO_4$, or with BCS and

ascorbate), described below. The homogenization buffer consisted of 25 mM HEPES-NaOH pH 7.4, 150 mM NaCl, and a protease inhibitor cocktail of 30 μM leupeptin, 10 μM pepstatin A and 5 μM aprotinin. Yeast membrane proteins were isolated with homogenization buffer supplemented with 50 μM $CuSO_4$ to reconstitute apo-Fet3p *in vitro* during homogenization and to detect total Fet3p, as a positive control. On the other hand, yeast membrane proteins were isolated with homogenization buffer supplemented with 1 mM BCS (Sigma) and 1 mM ascorbic acid (Sigma) to prevent Cu loading of Fet3p *in vitro* during homogenization and to only detect holo Fet3p.

Following the washes, the yeast cell pellets were then resuspended in 200 μL of the same homogenization buffers. Cells were lysed by vortexing with glass beads (425-600 micron diameter, Sigma) for a total of 5 min (10 cycles of 30 s vortex and 1 min on ice). Yeast membranes were recovered by the addition of 800 μL of homogenization buffer (supplemented as described above), and the supernatants were cleared of unbroken cells and heavy organelles by centrifugation for 30 s at 10,000 x g. This step was repeated once. Membranes were collected by centrifugation at 20,000 x g for 30 min and washed with buffer containing 1 mM BCS. The final membrane pellets were made soluble by adding 100 μL of buffer containing 1 mM BCS and 1% enzyme-grade Triton X-100 (Boehringer Mannheim). Insoluble material was removed by a final centrifugation at 20,000 x g for 20 min. The solubilized membrane protein was quantified using the Enhanced Bradford assay (Pierce Chemical).

30 μg of solubilized membrane proteins were dissolved in Laemmli loading buffer (Laemmli 1970) lacking dithiothreitol (DTT) and without heating, and electrophoresed by 7.5% SDS polyacrylamide gel electrophoresis (SDS-PAGE). The PAGE gels were equilibrated for 30 min in 500 mL of oxidase buffer, which contains 100 mM sodium acetate pH 5.7, 10% glycerol, 1 mM sodium azide and 0.05% Triton X-100 (Boehringer Mannheim). This was followed by two additional 15 min incubations in 250 mL of the oxidase buffer. Equilibrated gels were soaked in 20 mL/gel of buffer containing 100 mL sodium acetate pH 5.7, 0.5 mg/mL *p*-phenylenediamine dihydrocholoride substrate (Sigma), and 1 mM sodium azide for one hour in the dark. Bands of oxidase activity were

developed overnight by incubating the gels in the dark between cellophane sheets in a humidified box.

All glassware and glass beads for cell disruption were washed extensively with copper-free 1 M hydrochloric acid (J.T. Baker, "Instra-Analyzed" grade), and well rinsed with deionized water (Milli-Q, Millipore) to eliminate Cu contamination.

G. YEAST PROTEIN PREPARATION

Yeast total cell protein extracts were prepared as follows: homogenization buffer consisted of 25 mM HEPES-NaOH pH 7.4, 150 mM NaCl, 1 mM DTT, and a protease inhibitor cocktail containing 30 μM leupeptin, 10 μM pepstatin A, 5 μM aprotinin and 1 mM EDTA. Cells from 10 mL of stationary culture were washed twice with ice-cold distilled water, followed by a wash with homogenization buffer. The cell pellets were resuspended in 200 μL of homogenization buffer. Cells were broken by vortexing in the presence of acid-washed glass beads (425-600 micron diameter, Sigma) for a total of 5 min (10 cycles of 30 s of vortexing and 1 min on ice). The homogenate was centrifuged for 30 s at either 10,000 x g or 1,000 x g, depending on the *ATP7B* variant, to remove unbroken cells and heavy organelles. Protein content was estimated by the Enhanced Bradford assay (Pierce Chemical).

H. WESTERN BLOTTING

SDS-PAGE was performed using the discontinuous method of Laemmli (Laemmli 1970). Reagents were prepared as described in Current Protocols (Ausubel *et al.* 1998). Yeast cell protein extracts containing ATP7B protein were electrophoresed on 7.5% separating gels. 10 μg of protein extract was mixed with Laemmli loading buffer containing DTT, heated for 5 min at 75°C and separated by 7.5% SDS-PAGE. The polyacrylamide gels were generally electrophoresed in Mini-gel format on the Mini-Protean 2 apparatus (Bio-Rad).

Proteins in unstained SDS-PAGE gels were transferred electrophoretically to nitrocellulose membrane (Sigma) or polyvinylidine difluoride (PVDF) membrane (Bio-Rad) using the Mini-Protean 2 apparatus (Bio-Rad). The yeast protein extracts were transferred for 15 hours at 30 V (450 V·hr) in Towbin buffer (Towbin *et al.* 1979), which contains 15% methanol and 0.01% SDS. Following transfer, the membranes were first checked for

protein by staining with Ponceau S stain (Sigma), and then rinsed in deionized water to remove excess Ponceau S.

Western blotting was performed as follows: membranes were blocked with 5% milk powder in Tris-buffered saline (TBS: 50 mM Tris-HCl pH 7.5, 150 mM NaCl) for 30 min to 1 hr. The membranes were washed twice for 5 min each with TBS-T, TBS containing 0.1% Tween-20 (Fisher Scientific). Two primary antibodies were used: either a rabbit polyclonal antibody against the CuBD of ATP7B (ATP7B.N60) (Forbes and Cox 2000), or a rabbit polyclonal antibody against the C-terminal 10-kDa fragment of ATP7B (anti-ATP7B.C10) (Forbes and Cox 1998; Forbes *et al.* 1999). The membranes were incubated with primary antibodies in TBS-T with 5% milk powder for 3 hr at a dilution of 1:17,000. Following primary antibody incubation, the membranes were quickly rinsed twice with TBS-T and then washed 3 times, with shaking, for 5 min each in TBS-T buffer. Secondary antibodies were horseradish peroxidase conjugated goat anti-rabbit antibodies (Pierce Chemical) incubated for approximately 1 hr in TBS-T with 5% milk powder at a dilution of 1:25,000. The membranes were quickly rinsed three times with TBS-T, and then washed 4 times, with shaking, for 5 min each in TBS-T buffer. Bound antibodies were detected by enhanced chemiluminescence using Supersignal substrate (Pierce Chemical, Rockford, IL, USA). The chemiluminescence was visualized by exposure to autoradiography film (Fuji).

III. RESULTS

A. Analysis of the conservation of the C-terminus of ATP7B

Comparisons of the 93-amino acid C-terminal region of ATP7B with its orthologues revealed high sequence conservation between human ATP7B and the orthologous mouse, rat and sheep ATP7B, with amino acid identities of 84, 83 and 82%, respectively. The conservation between human ATP7A and ATP7B was lower with an overall amino acid identity of 56% (Figure 3-1).

The sequence alignments identified a conserved tri-leucine motif, at a position similar to the di-leucine motif in ATP7A, which is involved in ATP7A retrieval from the PM to the TGN (Petris *et al.* 1998; Francis *et al.* 1999).

Figure 3-1. Amino acid alignment between human ATP7B and its homologues.

An amino acid alignment of the 93 amino acid C-terminus of human ATP7B with the C-termini of mouse (*Mus musculus*) Atp7b, rat (*Rattus norvegicus*) Atp7b, sheep (*Ovis aries*) ATP7B and human ATP7A. The alignment was generated by the ClustalW program (http://www.ebi.ac.uk/clustalw/) and shaded with the Boxshade program (http://www.ch/embnet.org/software/BOX_form.html). Identical residues are shaded in black and conservative replacements are shaded in gray. The asterisks (*) mark the WND patient missense mutations examined in this study.

The conservation of select amino acid residues in the C-terminal region, as well as the presence of a potential targeting motif suggests that parts of this region may be functionally important.

B. Mutant constructs used for the analysis of the C-terminus

A set of 3' mutant constructs were generated which corresponded to sequence alterations identified in the 3' coding region of DNA from WND patients (Figure 3-2). These include: 1) a missense mutation, Pro1379Ser, corresponding to c.4135C>T (Cox *et al.* 2005); 2) a deletion mutation, c.4195delC, which removes a cytosine and results in a frameshift and premature truncation of the protein product six amino acids downstream (Majumdar *et al.* 2000); 3) a missense mutation, Thr1434Met, corresponding to c.4301C>T (Loudianos *et al.* 1999); and 4) c.4311G>A, which does not affect the amino acid sequence (Lys1437Lys) and was detected in a chromosome that already had an additional mutation identified as disease-causing (Loudianos *et al.* 1999).

A set of deletions were also generated to identify specific regions of the C-terminus with potential functional importance. The deletion labeled 4117 represents an engineered sequence alteration at nucleotide position 4117 that incorporates a stop codon at amino acid position 1373, resulting in a deletion of the entire C-terminus of the protein. The deletion begins at the junction between the last TM segment (TM 8) and the soluble C-terminus. To examine whether retention of a small number of amino acids after the predicted eighth TM domain would affect Cu transport function, the deletion 4126 was synthesized by replacing the amino acid at position 1376 with a stop codon. This left three amino acids following the last amino acid residue of TM 8. At the DNA level, the 4126 construct deletes all of the nucleotides of the entire last exon (exon 21).

The deletion 4213 was generated to correspond to the premature truncation seen with the WND patient mutation 4195 C. 4213 was created by substituting the glycine residue at amino acid position 1405 (DNA sequence change at nucleotide position 4213) with a stop codon, truncating the protein by 60 amino acid residues.

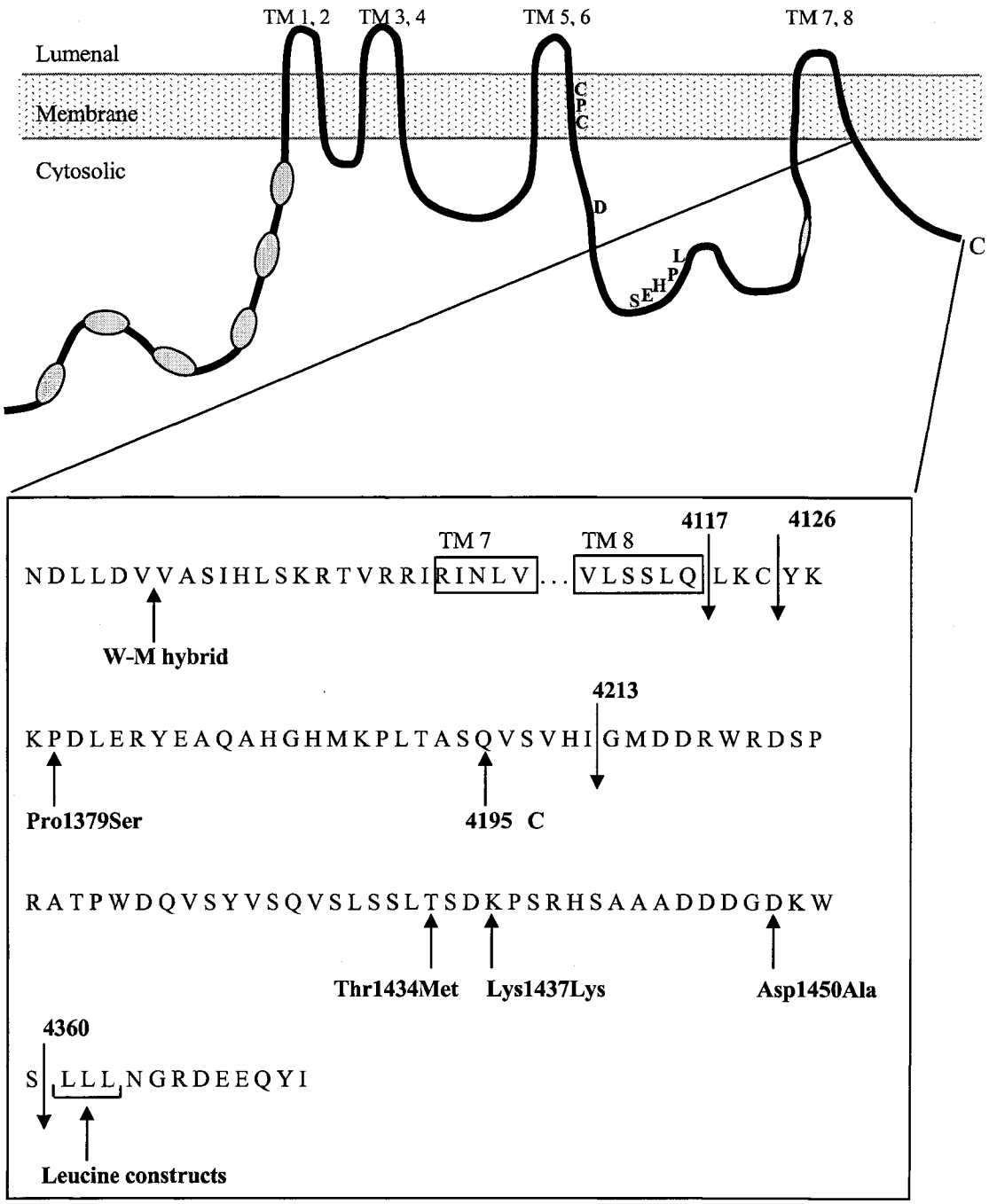

Figure 3-2. Amino acid position of ATP7B variant constructs.

The ATP7B constructs are shown on the amino acid sequence of the C-terminus of ATP7B. Arrows pointing downwards indicate the deletion constructs generated. Arrows pointing upwards specify the other site-directed mutations introduced. Boxes labeled "TM 7" and "TM 8" represent sections of the seventh and eighth transmembrane domains of ATP7B, respectively.

4360, which is not a patient mutation, was designed to delete the last 12 amino acids from the protein product by replacing the amino acid at position 1454 with a stop codon (DNA change at nucleotide position 4360).

A series of point mutations was created to sequentially change the leucine residues to alanine residues within the conserved tri-leucine motif. A total of three leucine-alanine *ATP7B* variants were generated and examined for their functional competence: 1) LLL>ALL (p.Leu1454Ala), 2) LLL>AAL (p.Leu1454Ala, Leu1455Ala), 3) LLL>AAA (p.Leu1454Ala, Leu1455Ala, Leu1456Ala). The aspartic acid located at codon position 1450, four amino acid residues upstream of the tri-leucine, was also mutated to an alanine, D>A (p.Asp1450Ala). Residues surrounding conserved leucine motifs, in particular acidic residues found four to five amino acids upstream of leucine motifs, have been demonstrated to be important for the correct trafficking of proteins within the secretory pathway.

To determine if there was a difference in Cu transport between the 3' coding ends of *ATP7B* and *ATP7A*, the paralogous MNK gene, the 3' region of *ATP7B* was substituted with the 3' region of *ATP7A*. The *ATP7A/ATP7B* hybrid included the first 3920 nucleotides (c.1_c.3920) of the *ATP7B* gene, and continued with the 3' end of the *ATP7A* gene beginning at nucleotide position 4023 (c.4023_c.4500). The Nhe 1 site was at *ATP7A* nucleotide position 4027, just prior to TM 7. The biochemical Fet3p oxidase assay was used to evaluate the copper transport function of this *ATP7B* variant (W-M hybrid).

C. Assessment of expression of the ATP7B variants in *ccc2* mutant yeast

In order to identify whether the *ATP7B* variants had an effect on ATP7B Cu transport function, these constructs were transformed into a *ccc2* null mutant and the strains were analyzed for their ability to complement the high-affinity Fe-uptake deficiency phenotype of the mutant. All yeast strains demonstrated genomic stability and had neither secondary mutations nor rearrangements within the gene. Growth in SD medium was also normal for all yeast strains analyzed in this study.

Prior to performing the functional studies, expression of the *ATP7B* variant constructs within the heterologous yeast system was verified. Membrane proteins from *ccc2* mutant yeast transformed with *ATP7B* constructs were extracted, and the preparations were analyzed by Western blotting for ATP7B expression (Figure 3-3).

All *ATP7B* constructs containing WND patient mutations (Pro1379Ser, 4195 C, Thr1434Met and Lys1437Lys) showed expression in the *ccc2* mutant yeast (Figure 3-3A). The altered mobility of 4195 C reflects the production of a prematurely truncated protein product. The deletion constructs 4213 and 4360 were expressed in the *ccc2* mutant yeast and also showed altered mobility (Figure 3-3B). This was expected given that part of the protein is removed by the sequence alteration and the product is shorter in length. *ccc2* mutant yeast transformed with *ATP7B* variants that had sequence changes affecting the leucine motif, including LLL>ALL, LLL>AAL, LLL>AAA, and D>A, all demonstrated normal expression (Figure 3-3C).

The 4117 and 4126 deletion constructs that remove significant portions of the C-terminus, were of exceptional interest. As a standard for our membrane protein preparations, a final 10,000 x g centrifugation was generally performed to isolate solubilized membrane proteins while excluding heavier organellar membrane fractions. The supernatant from this centrifugation would thus include the TGN fraction, where the *ATP7B* variants were expected to be expressed (Hung *et al.* 1997; Payne *et al.* 1998; Schaefer *et al.* 1999a; Suzuki and Gitlin 1999; Forbes and Cox 2000). Under this standard procedure, there was a lack of expression of the variant 4117 and the variant 4126 was only weakly detectable (Figure 3-3B). To determine whether these protein products were being mislocalized to other membrane fractions, the protocol was modified by performing the final centrifugation at 1,000 x g rather than the usual 10,000 x g. Under these conditions, 4117 had a weakly detectable band, which was still greatly reduced compared with normal ATP7B expression in *ccc2* mutant yeast. This protocol modification did not result in greatly increased levels of detectable ATP7B expression in the yeast transformed with 4126 (Figure 3-3B).

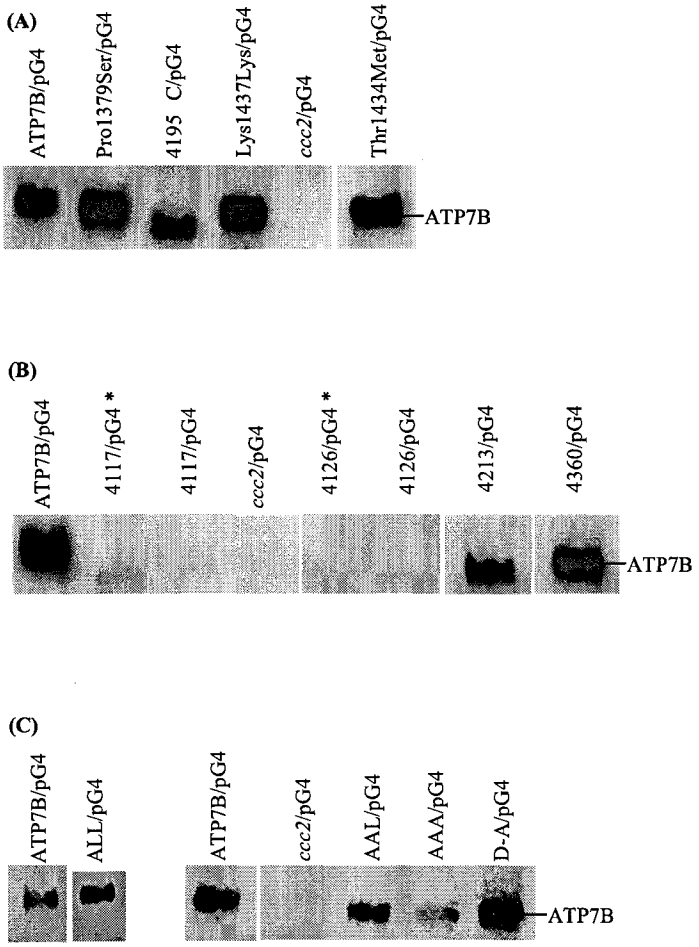

Figure 3-3. Expression of *ATP7B* constructs in *ccc2* mutant yeast.

All ATP7B variant single-copy plasmids were transformed into *ccc2* mutant yeast and membrane protein preparations of the transformants were obtained. ATP7B expression was analyzed by western blotting. Analysis of 10μg of yeast protein extract was performed by enhanced chemiluminescence using an affinity-purified rabbit polyclonal antibody against the N-terminal Cu-binding domain of ATP7B ("anti-ATP7B.N60"). (A) Expression of WND patient mutation constructs in *ccc2* mutant yeast. (B) Expression of deletion constructs in *ccc2* mutant yeast. The asterisks (*) indicate those protein preparations performed with a final centrifugation spin of 1,000 x g before isolation of the protein supernatant. (C) Expression of leucine variants and aspartic acid acid variant in *ccc2* mutant yeast. ATP7B/pG4: *ccc2* mutant expressing wild-type human ATP7B; *ccc2*/pG4: *ccc2* mutant transformed with vector only.

D. ASSESSMENT OF COPPER TRANSPORT FUNCTION BY THE GROWTH ASSAY

To determine whether the difference in protein levels seen with the ATP7B variants affected Cu transport function, the ability of the yeast strains to functionally complement the *ccc2* mutation in the yeast was assessed. The growth rates of the ATP7B variants in Fe-limited medium were measured and compared with the growth rates of *ccc2* mutant yeast expressing wild-type ATP7B. Growth occurred at an approximately equal rate to the parent strain with wild-type *CCC2* (Figure 3-4).

The strain expressing a mutant lacking the entire C-terminus (4117 variant) was completely unable to grow in Fe-limited medium (Table 3-2, Figure 3-5A). In contrast, the deletion that involves removal of all but three amino acids of the C-terminus (4126) showed some growth under the Fe-limited conditions and thus partially complemented the *ccc2* mutant phenotype. The growth rate of this ATP7B deletion variant was 0.13 OD_{600nm}/hr, which represented 45% of the wild-type growth rate (Table 3-2, Figure 3-5A).

The other deletion constructs, 4213 and 4360, were able to complement the yeast mutation (Table 3-2, Figure 3-5A). The average growth rate of the deletion variant 4213 was 91% growth compared with that of wild-type ATP7B-expressing *ccc2* yeast. The deletion variant 4360 grew at 90% of the growth rate of *ccc2* mutant yeast transformed with wild-type human ATP7B.

All three putative WND disease-causing missense variants demonstrated full complementation of the yeast *ccc2* Fe-deficient phenotype. The average growth rates of Pro1379Ser, 4195 C and Thr1434Met correspond to 100, 93 and 98% of the growth conferred by wild-type ATP7B, respectively (Table 3-2, Figure 3-5B). The neutral sequence alteration, Lys1437Lys, showed an average growth rate of 81% of that of wild-type ATP7B-expressing *ccc2* mutant yeast growth (Table 3-2, Figure 3-5B). All *ccc2* mutants expressing ATP7B variants demonstrated comparable growth rates in SD medium, which is not Fe-limited, indicating that these strains are only compromised in their Cu transport ability under low Fe conditions.

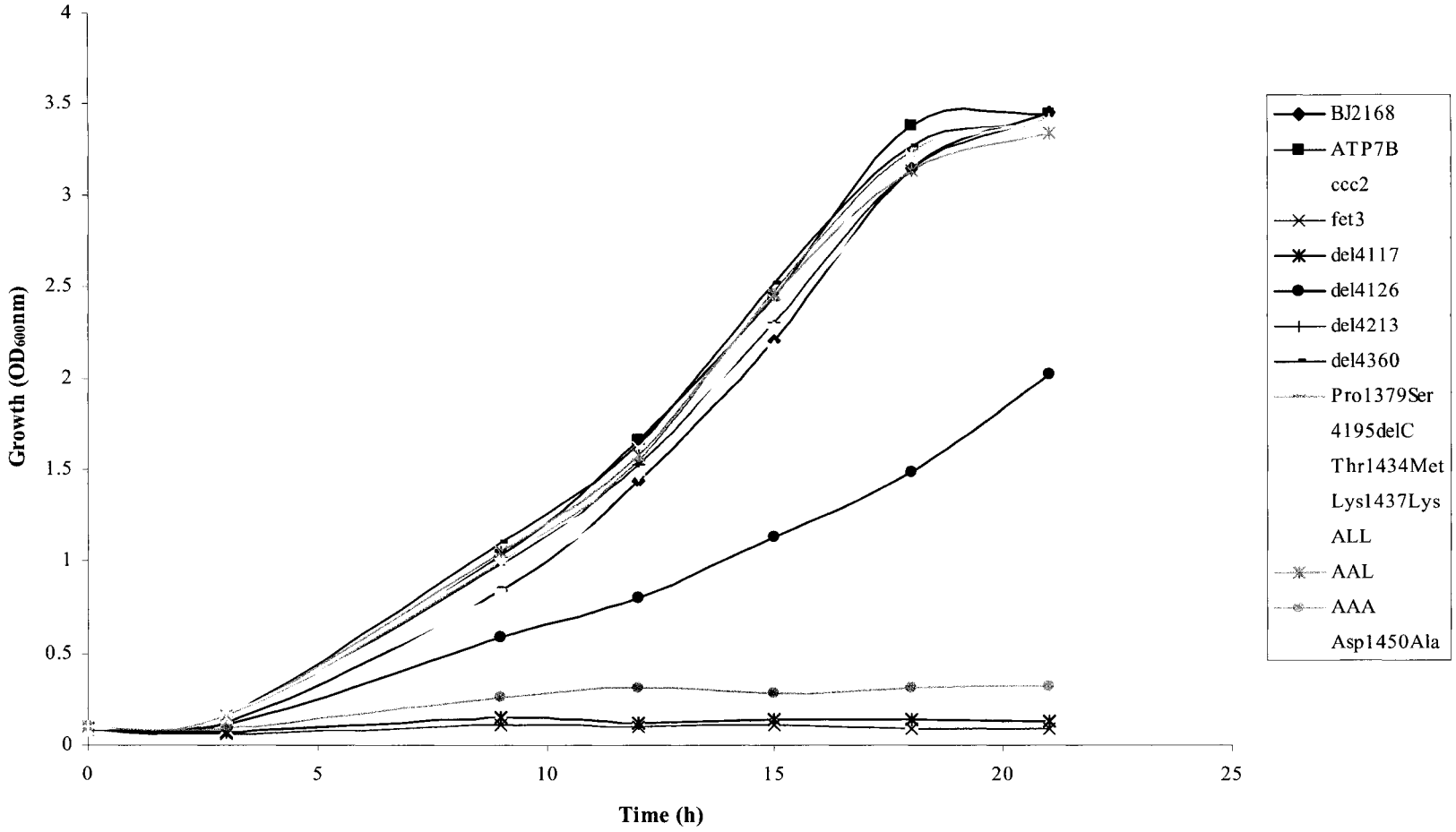

Figure 3-4. Growth of *ccc2* transformed yeast strains in liquid culture.

Representative growth of yeast strains in iron-limited media over 24 hours at 30°C. The legend on the right indicates the yeast strains analyzed. This growth assay was performed as described in the text. The datum depicted represents the values of one experiment. At least three liquid growth assays were completed for each yeast strain studied.

Table 3-2. Growth rates of *ccc2* mutant yeast expressing *ATP7B* variants.

Variant[a]	Average Growth Rate ± SE[f] (OD_{600nm}/hr)	% Growth of wild-type ATP7B	Cu Incorporation into apo-Fet3p	Ability to complement
WT yeast[b]	0.26 ± 0.015	93	Yes	-
ATP7B/pG4[c]	0.28 ± 0.005	100	Yes	Yes
ccc2/pG4[d]	0 ± 0.001	0	No	No
fet3/pG4[e]	0 ± 0.004	0	No	-
4117/pG4	0 ± 0.007	0	No	No
4126/pG4	0.13 ± 0.006	45	Reduced	Partial
4213/pG4	0.26 ± 0.006	91	Slightly impaired	Slightly impaired
4360/pG4	0.25 ± 0.012	90	Yes	Yes
Pro1379Ser/pG4	0.28 ± 0.005	100	Yes	Yes
4195 C/pG4	0.26 ± 0.017	93	Slightly impaired	Slightly impaired
Thr1434Met/pG4	0.28 ± 0.017	98	Yes	Yes
Lys1437Lys/pG4	0.23 ± 0.008	81	Yes	Yes
ALL/pG4	0.26 ± 0.016	92	Yes	Yes
AAL/pG4	0.27 ± 0.018	96	Yes	Yes
AAA/pG4	0 ± 0.001	0	No	No
D-A/pG4	0.26 ± 0.020	92	Yes	Yes
W-M/pG4	-	-	Yes	Yes

[a]*ccc2* mutant yeast transformed with ATP7B variant-expressing plasmids, unless indicated. [b]WT yeast: BJ2168; [c]ATP7B/pG4: *ccc2* mutant yeast transformed with wild-type ATP7B; [d]*ccc2*: *ccc2* mutant yeast transformed with vector; [e]*fet3*: *fet3* mutant transformed with vector. [f]SE: one standard error of the mean.

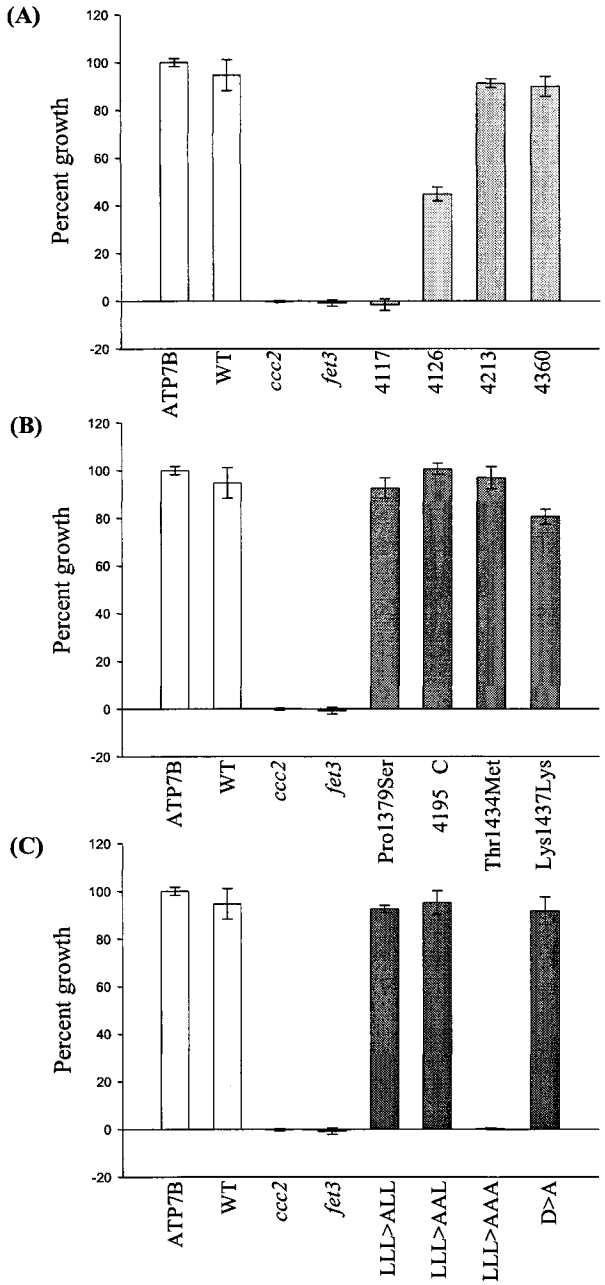

Figure 3-5. Comparison of growth rates of ATP7B variants in iron-limited media.

A comparison of the growth of all variant-expressing yeast strains with wild-type ATP7B-expressing yeast. Wild-type ATP7B growth set at 100%. Standard error of the mean is indicated by the bars. (A) Growth rates of deletion constructs compared with wild-type ATP7B. (B) Growth rates of WND mutant constructs based on patient mutations. (C) Growth rates of leucine mutant constructs and the aspartic acid variant. ATP7B: *ccc2* mutant yeast expressing wild-type ATP7B; WT: BJ2168; *ccc2*: *ccc2* mutant yeast transformed with vector only; *fet3*: *fet3* yeast transformed with vector only; all others represent *ccc2* mutant yeast expressing the ATP7B variant constructs.

Mutant yeast expressing the human *ATP7B* variants LLL>ALL, LLL>AAL and D>A demonstrated full complementation of the *ccc2* Fe-deficient phenotype. The average growth rates for these yeast transformants were 93, 95 and 92% of the wild-type ATP7B-expressing yeast growth rate, respectively (Table 3-2, Figure 3-5C). The *ATP7B* mutation LLL>AAA, however, did not complement the mutant phenotype in the *ccc2* yeast. The yeast expressing this variant had an average growth rate of 0.25% compared with the growth conferred by wild-type ATP7B (Table 3-2, Figure 3-5C).

E. Assessment of copper transport function by the Fet3p oxidase assay

Gel-based ferroxidase assays were also performed to provide biochemical evidence for complementation of the *ccc2* yeast by human ATP7B. The levels of holo-Fet3p, representing *in vivo* Cu incorporation, were compared with total-Fet3p, which represents both holo-Fet3p and apo-Fet3p that is reconstituted with Cu *in vitro*. Little difference between holo- and total-Fet3p activities is seen with wild-type yeast and yeast expressing normal ATP7B, indicative of little or no excess apo-Fet3p production and normal Cu transport function. Since Fet3p expression is induced when high-affinity Fe uptake is reduced or absent (Askwith *et al.* 1994), a higher level of total-Fet3p oxidase activity compared with holo-Fet3p, signifies an impairment of Cu transport.

The Fet3p oxidase assay was performed on all ATP7B variant-expressing yeast (Figure 3-6). This biochemical assay yielded more sensitive results, identifying additional variants with compromised Cu transport activity. Although the growth assay results showed near wild-type growth, the 4213-expressing yeast (Figure 3-6A) and 4195 C-expressing yeast (Figure 3-6B) demonstrated a reduced amount of holo-Fet3p activity when compared with total-Fet3p oxidase activity. This indicated impairment of *in vivo* Cu delivery to apo-Fet3p by these ATP7B variants. The 4360-expressing yeast (Figure 3-6A) and all other WND patient mutation constructs (Figure 3-6B) showed little variation between the levels of holo- and total-Fet3p activities, illustrating their abilities to bypass the yeast *ccc2* mutant phenotype and provide Fet3p with its requisite Cu.

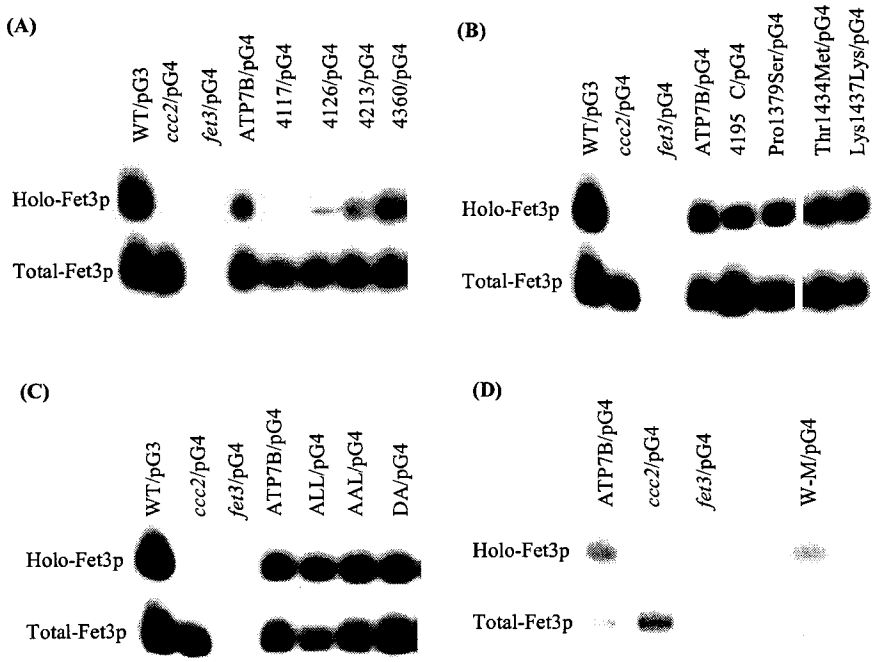

Figure 3-6. Fet3p oxidase assay.

Holo-Fet3p represents protein preparations isolated in the presence of copper chelator (BCS) and reducing agent (ascorbic acid) to prevent adventitious copper loading into apo-Fet3p *in vitro*. Total-Fet3p represents protein preparations done in the presence of copper sulphate to measure the total amount of Fet3p in the cell (apo- and holo-Fet3p) since any apo-Fet3p would be loaded with copper *in vitro*. Yeast strains are as in figure 4. (A) Fet3p oxidase assay performed on yeast expressing deletion constructs. (B) Fet3p oxidase assay performed on yeast expressing WND patient mutation constructs. (C) Fet3p oxidase assay performed on yeast expressing ALL, AAL and DA mutant constructs. (D) Fet3p oxidase assay performed on yeast expressing the *ATP7B/ATP7A* hybrid, W-M.

The *ccc2* yeast expressing the LLL>ALL, LLL>AAL, and D>A, and W-M hybrid variants also showed small differences between the holo- and total-Fet3p activity levels, when comparing the wild-type human *ATP7B*-expressing *ccc2* yeast (Figures 3-6C and 3-6D, respectively). LLL>AAA was unable to sustain growth in the induction medium used to grow the yeast to mid-log phase; therefore, the level of Fet3p oxidase activity in these yeast transformants was unmeasurable. Given that there was limited complementation of the Fe-deficient phenotype, the level of holo-Fet3p activity could be assumed to be negligible.

The yeast expressing the deletion constructs 4117 and 4126, in accordance with their impaired growth and severely reduced steady state levels of protein, had compromised Cu transport to apo-Fet3p (Figure 3-6A). There was no evidence of holo-Fet3p activity with the 4117 deletion variant, which was expected from the near undetectable levels of ATP7B with this mutant. The 4126 yeast strain had only a trace amount of holo-Fet3p activity compared with the high level of total-Fet3p activity, which correlates well with the reduced amount of stable protein present in the *ccc2* yeast. Surprisingly, the level of holo-Fet3p activity detected did not correlate with the approximately 50% of wild-type ATP7B growth rate suggesting that only a fraction of the total-Fet3p needs to be active for complementation in the growth assay.

F. Prediction of transmembrane topology using a computer modeling program

The western blot results revealed an almost complete lack of detectable ATP7B with the deletion variant 4117, suggesting that the sequence alteration of *ATP7B* may affect the folding of the protein and lead to incorrect transmembrane topology. The addition of only three amino acids (4126 construct) to the putative end of TM 8 appears to aid in the ability of ATP7B to fold and correctly insert into the TGN membrane, the cellular location for Cu transport from Ccc2p to Fet3p, since this variant showed growth and transport of Cu into apo-Fet3p. Furthermore, the retention of 32 amino acids, as seen with the 4213 deletion construct, leads to the expression of normal levels of ATP7B in *ccc2* mutant yeast.

The membrane topology of the deletion variants as well as full-length ATP7B was modeled with the web-based SOSUI system. For the full-length ATP7B amino acid sequence, the

SOSUI tool predicted transmembrane domains seven and eight, as expected from previous reports (Fatemi and Sarkar 2002b). On the contrary, the deletion of the entire C-terminal tail sequence (4117 variant) removed the last TM segment from the computer model. The addition of only three amino acids (Leu-Cys-Leu) with the 4126 deletion variant resulted in a predicted topology with all the membrane-spanning regions intact.

IV. DISCUSSION

To date, five presumed WND patient mutations have been identified in the C-terminal region of ATP7B. The presence of these mutations in WND patients implies that sequence alterations within this region can have an effect on protein function, underscoring the importance of the cytosolic tail of ATP7B. The similarities between the yeast and human copper transport pathways have been exploited to examine the function of C-terminal variants. The yeast system is specifically designed to evaluate only one aspect of ATP7B function, namely Cu transport. This assay does not delineate the capacity of the mutants to traffick within the hepatocyte.

Western blot analysis of the *ccc2* yeast expressing the deletion variants 4117 and 4126 revealed that these C-terminal deletions affect the expression levels of ATP7B in the mutant yeast. By varying the centrifugation speeds during protein isolation, a detectable amount of the 4117 variant is found in a fraction distinct from that of wild-type ATP7B. This suggests that the 4117 deletion construct is mislocalized in the *ccc2* yeast. The 4126 variant showed protein expression in both subcellular fractions, albeit at a reduced intensity. The general reduction in expression levels of both these deletion variants may result from instability at the RNA level or increased proteolysis of an unstable protein product. Alternatively, the lower expression of the 4117- and 4126-expressing yeast may be due to an aggregation of the proteins or an inability of these ATP7B variants to fold into their correct conformations, leading to proteasome-mediated degradation (Brodsky and McCracken 1999; Bross *et al.* 1999). In fact, some WND patient mutations are known to cause misfolding and aggregation of the mutant ATP7B, with subsequent degradation in the cytosol (Harada *et al.* 2001).

The web-based modeling program, SOSUI, was used to analyze whether the membrane topology would be affected by the deletions. The SOSUI modeling results strongly suggested that the lack of expression of the 4117 deletion construct in the yeast is due to incorrect TM topology. Deletion of the entire C-terminal tail likely disrupts the stability of the last TM segment, resulting in an improperly folded protein that is unable to transport copper. The addition of three amino acids following the end of the predicted TM 8 apparently rectifies the problem of incorrect membrane formation. Therefore, when only seven of the eight TM domains are present, a non-functional protein product is likely the result.

The 4117- and 4126-expressing yeast strains were the only *ATP7B* deletion variants showing severely reduced growth in Fe-limited medium when compared with wild-type ATP7B-expressing yeast. This is consistent with the expression data. Amongst the other *ATP7B* variants studied, only the *ccc2* yeast transformed with LLL>AAA showed negligible complementation in the Fe-deficient conditions. Considering the normal variation in growth routinely seen amongst identical yeast strains with replicate experiments, all other ATP7B variants analyzed were considered to have growth rates near normal.

The Fet3p oxidase assay was a more sensitive method of determining Cu transport ability, allowing verification of our complementation results and the identification of mutants that cause only a partial impairment in function that cannot be delineated with the growth assay. With the ATP7B variants analyzed in this study, the biochemical evidence obtained from the Fet3p assay supported the growth assay results, with the yeast transformed with the deletion constructs 4117 and 4126 demonstrating significant differences between the holo- and total-Fet3p activities. In addition, two ATP7B variants, 4213 and 4195 C, were shown to have a slight impairment in their ability to incorporate Cu into apo-Fet3p. The other patient mutations, Pro1379Ser and Thr1434Met, functionally complemented the *ccc2* mutant yeast in both the growth and Fet3 assays. The W-M hybrid construct as well as the mutations surrounding the leucine motif, with the exception of LLL>AAA, showed sufficient ability to deliver Cu to apo-Fet3p. These sequence alterations may, however, affect some other aspect of ATP7B function that is not measured in our system.

The yeast assay does not reflect any effects that the mutations may have on the regulation of the ability of the variants to transport Cu in varying Cu conditions. There is the possibility that certain residues within the C-terminus of ATP7B may be involved in interacting with a regulatory protein that activates or inhibits the Cu transport function of ATP7B. This is the case with the sarco(endo)plasmic reticulum Ca^{2+}-ATPases (SERCAs), which are regulated by phospholamban (Tada and Kadoma 1989; Simmerman and Jones 1998) and sarcolipin (Odermatt *et al.* 1998; Asahi *et al.* 2002). Both of these proteins can bind SERCA alone or jointly to inhibit the transport of Ca^{2+} from the sarcoplasm to the lumen of muscle cells by SERCA (Asahi *et al.* 2003; MacLennan *et al.* 2003). Phospholamban and sarcolipin interact and inhibit the activity of SERCA under low, but not high, Ca^{2+} concentrations by lowering the apparent affinity of SERCA for Ca^{2+}.

The yeast assay also does not address the issue of subcellular trafficking, so the constructs that displayed normal function in the yeast assay may be unable to traffick within the human hepatocyte, as previously shown for the variant Gly943Ser (Forbes and Cox 2000). Just as the Cu transport function requires correct localization within the TGN, the excretory function necessitates ATP7B localization near the bile canalicular membrane. To facilitate its dual role within the hepatocyte, ATP7B undergoes Cu-dependent localization; under Cu stimulation, ATP7B redistributes to an undefined vesicular compartment for its excretory role and recycles back to the TGN once excess Cu is removed (Hung *et al.* 1997; Payne *et al.* 1998; Schaefer *et al.* 1999a; Suzuki and Gitlin 1999; Forbes and Cox 2000; Roelofsen *et al.* 2000; La Fontaine *et al.* 2001). A disruption in trafficking would thus impair the ability of ATP7B to remove Cu and result in a WND phenotype.

The leucine motif present within the C-terminus of ATP7B is a known targeting signal responsible for the intracellular localization of a number of secretory pathway proteins (Trowbridge *et al.* 1993). This is conserved among ATP7B orthologues and is also found in the paralogous protein ATP7A. The di-leucine motif within the C-terminus of ATP7A has been demonstrated to be responsible for the recycling of ATP7A from the plasma membrane in response to Cu depletion (Petris *et al.* 1998; Francis *et al.* 1999). The results from the deletion studies appear to illustrate that the motif is not necessary for the Cu transport function of ATP7B. Specifically, the 4360 deletion variant, which removes the

amino acids from just before the leucine motif to the end of the protein sequence, functionally complements the *ccc2* mutant phenotype. Further, the lack of detectable Cu transport with the 4117 variant is likely due to its instability rather than the removal of the leucine residues, since the other deletion constructs are still able to deliver copper to apo-Fet3p. The deletion variants also reflected improved Cu transport function with the retention of successively more amino acids; thus, from these results, it seems that it is not the removal of a critical sequence but rather an increase in the stability of the end of the protein, which is the crucial factor. If a particular amino acid residue or motif were necessary for Cu transport, one would expect an all-or-nothing effect with the deletion constructs.

The difficulty with this explanation, however, is the LLL>AAA results, where yeast expressing this mutant construct were unable to grow in Fe-limited medium. Studies focused on trafficking signals have demonstrated that the context in which the di-leucine motif exists often influences the ability of the protein to be localized correctly within the cell (Pond *et al.* 1995; Kang *et al.* 1998; Setaluri 2000; Johnson *et al.* 2001). It is thus possible that the mutation of the leucines to alanines is more disruptive to the cytosolic C-terminal portion than deletion of 11 amino acid residues. Thus, the lack of functional complementation in the yeast system may only be a secondary consequence of a problem of structure. The data also indicated that both Leu1455 and Leu1456 or all three leucines (Leu1454_Leu1456) must be mutated for the severe effect on Cu transport ability. Three additional mutations have been generated to examine the importance of each leucine in detail: 1) LLL>LAL (Leu1455Ala), 2) LLL>LLA (Leu1456Ala), and 3) LLL>LAA (Leu1455Ala, Leu1456Ala). Another possible explanation for the apparent discrepancy in results between the deletion variant 4360 and the leucine variant LLL>AAA, may be that the yeast system does not reflect the actual defect of the LLL>AAA-expressing yeast, given that the real effect of the mutation is likely in the localization of ATP7B within the mammalian hepatocyte.

Both ATP7B and ATP7A undergo Cu-dependent trafficking; however, their destinations under high Cu conditions differ in non-polarized mammalian cells. Although the two are localized in the TGN in low Cu environments, ATP7A relocalizes to the plasma membrane

in the presence of high levels of Cu (Petris *et al.* 1996), and ATP7B moves to a vesicular compartment (Payne *et al.* 1998; Forbes and Cox 2000). Thus, the difference in sequence between ATP7A and ATP7B could dictate a difference in localization in non-polarized cells instead of a difference in the provision of Cu to Cu-dependent enzymes, which occurs in the TGN. As shown by the more sensitive Fet3p oxidase assay, the W-M hybrid in fact does complement the Fe-deficient phenotype and is able transport Cu to apo-Fet3p in yeast.

Our results have demonstrated that a portion of the C-terminus of ATP7B appears to be important for protein stability, likely required for formation of a TM segment. The growth assay detects those ATP7B variants that have a pronounced defect in Cu incorporation into apo-Fet3p, whereas the oxidase assay can also identify ATP7B variants with partial impairment in function. Further studies are necessary to examine the intracellular localization of the ATP7B variants reported here, particularly those that have demonstrated normal Cu delivery to apo-Fet3p.

CHAPTER 4:
Assessment of the copper transport capacity of functional sub-domain mutants in a yeast model system

Dr. Matthew M. Chen (University of Alberta) contributed to the generation of mutant constructs and in the examination of the variants in the yeast system.

Dr. Lara M. Cullen (University of Alberta) contributed to the assessment of function of the variants through Western blot analysis, and by performing the complementation and Fet3p oxidase assays.

Dr. Gina Macintyre (University of Alberta) contributed to this chapter by generating a molecular model of the ATP-binding domain of ATP7B

I. INTRODUCTION

Understanding the effect of mutations in *ATP7B* is critical for determining the phenotypic consequences associated with a particular mutation and for dissecting the functional regions of the protein. This has been a challenge given the more than 260 different WND mutations that have been identified (http://www.medicalgenetics.med. ualberta.ca /wilson/index.php – accessed May 2005) (Cox and Moore 2002; Hsi and Cox 2004).

There is limited functional data available on reported patient mutations; thus a sequence alteration in the DNA of a patient is not necessarily a WND-causing mutation. For a reliable diagnosis of WND, the ability to discriminate between disease-causing mutations and rare normal variants is critical. This differentiation can often be uncertain, especially if the amino acid substitution is conservative or the change is at a residue that is not highly conserved in Cu-transporting P-type ATPases.

In this chapter, the yeast functional assay was used to assess the Cu transport activity of 11 *ATP7B* missense variants that were originally identified in WND patients. These sequence alterations are located either within the CuBD in the N-terminus or within the ATP-BD. The specific roles of different amino acids in both of these functional domains are relatively unknown, and the effects of WND patient mutations on the Cu transport function in these regions have not been comprehensively addressed.

The CuBD is interesting in that there may be redundancy in the MBSs and a single missense mutation in one MBS may not significantly affect function. However, as highlighted in Chapter 1, several reports indicate that these Cu-binding sites may not be entirely redundant and may act co-operatively in a particular structure. Studying mutations in this domain may help to clarify the role of certain amino acids and the importance of specific regions of the CuBD.

The ATP-BD was intriguing, given the abundance of WND mutations in the region. Furthermore, the ATP-BD as a whole plays a critical role in the catalytic cycle of ATP7B and the translocation of Cu across the membrane; thus it was of interest to identify the residues that are important for acyl-phosphorylation and the catalytic activity of the protein.

Functional analysis of these variants in terms of their Cu transport activity will thus increase our current knowledge of the essential amino acid residues and regions in the P-type Cu-transporting ATPases, and a valuable step in understanding the molecular mechanisms underlying WND. Furthermore, functional assessment of the mutations will aid in molecular diagnosis of the disease and elucidate potential genotype-phenotype correlations.

II. MATERIALS AND METHODS

A. MISSENSE VARIANTS ANALYZED

Eleven *ATP7B* missense variants, originally identified in WND patients, were examined (Figure 4-1, Table 4-1). Eight of the ATP7B variants lie within the nucleotide-binding and phosphorylation regions of the ATP-BD of the protein: Arg1041Trp (Loudianos *et al.* 1998b), Glu1064Lys (Figus *et al.* 1995), Leu1083Phe (Kim *et al.* 1998), Val1106Asp (Waldenstrom *et al.* 1996), Ala1140Val (Figus *et al.* 1995), Met1169Val (Loudianos *et al.* 1999), Ala1183Thr (Loudianos *et al.* 1998b), and Gly1186Ser (Yamaguchi *et al.* 1998). Three of the ATP7B variants studied lie within the amino-terminal CuBD: Tyr532His (Cox *et al.* 2005), Gly626Ala (Figus *et al.* 1995), and Asp642His (Loudianos *et al.* 1998b).

One hundred control chromosomes, of similar ethnic origin, were tested for all, except for the Gly1186Ser variant (54 control chromosomes) and Tyr532His, Val1106Asp, and Ala1140Val (none reported). For those variants tested in controls, the sequence changes were not found on the normal chromosomes. Other mutations have been described at some of the amino acid positions, possibly indicating the functional importance of the residue (Table 4-1). Conservation of the amino acid at each mutation site was examined by comparison of ATP7B orthologous sequences for mouse, rat, sheep and human, and for the related human MNK Cu transporter, ATP7A, using standard NCBI protein-protein BLAST analysis of the non-redundant database (http://www.ncbi.nlm.nih.gov/BLAST/).

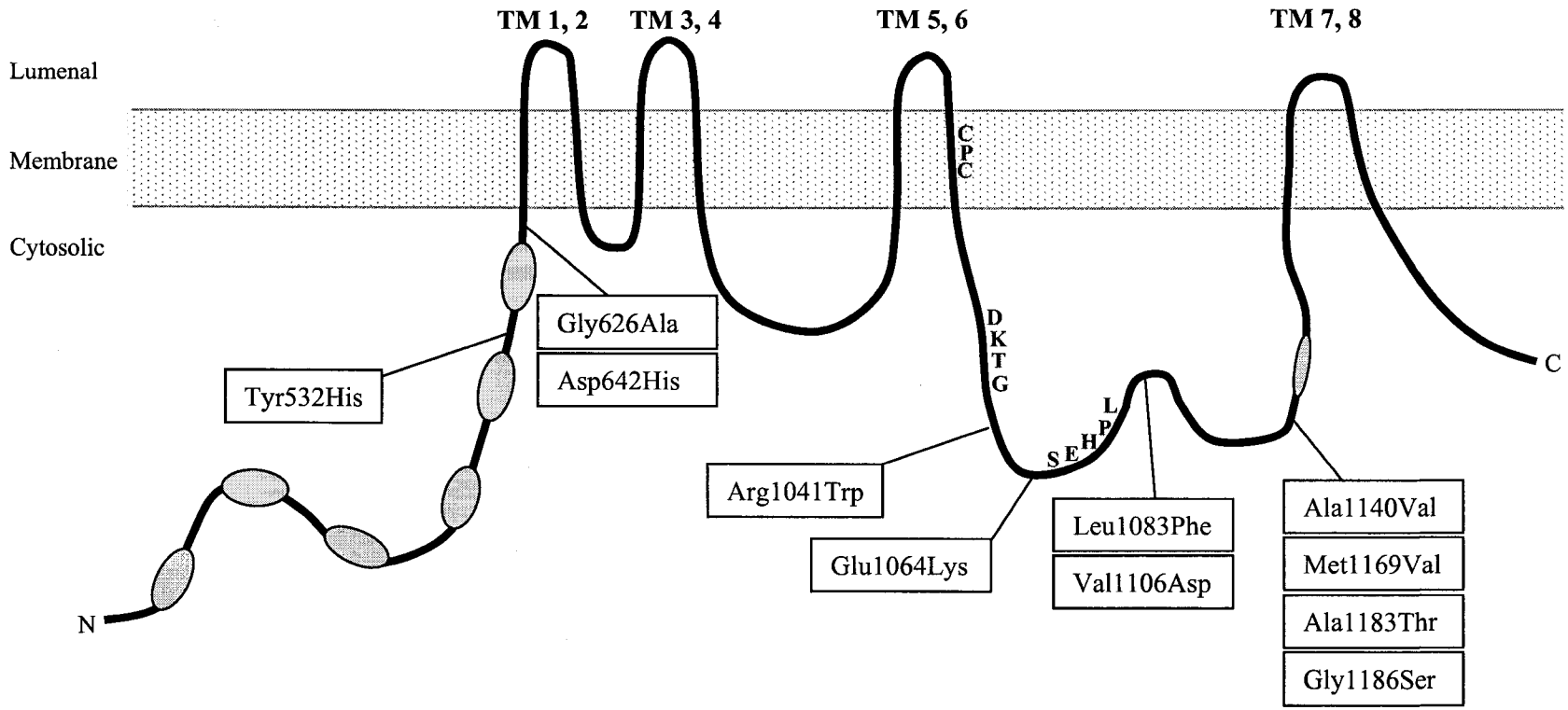

Figure 4-1. Position of the copper-binding domain and ATP-binding domain variants.

The relative location of the ATP7B constructs is depicted on the two-dimensional diagram of the WND Cu-transporting P-type ATPase. The conserved sequences and domains are represented as in Figure 1-3.

Table 4-1. ATP7B missense variants evaluated for copper transport activity in yeast.

Mutation	Exon	Location	Amino acid conservation[a]	Previously reported designation[c]	References for mutations studied	Additional mutations[b]	References for additional mutations
Tyr532His	4	MBS5 - MBS6	1	WND mutation	(Cox et al. 2005)	none reported	--
Gly626Ala	6	MBS6 - TM1	1	WND mutation	(Figus et al. 1996)	none reported	--
Asp642His	6	MBS6 - TM1	1	WND mutation	(Loudianos et al. 1998)	none reported	--
Arg1041Trp	14	ATP-BD	2	WND mutation	(Loudianos et al. 1998)	Arg1041Pro	(Loudianos et al. 1999)
Glu1064Lys	14	ATP-BD	1	WND mutation	(Figus et al. 1996)	Glu1064Ala	(Shah et al. 1997)
Leu1083Phe	15	ATP-BD	1	WND mutation	(Kim et al. 1998)	none reported	--
Val1106Asp	15	ATP-BD	1	WND mutation	(Waldenstrom et al. 1996)	none reported	--
Ala1140Val	16	ATP-BD	3	Normal variant	(Figus et al. 1996)	none reported	--
Met1169Val	16	ATP-BD	1	WND mutation	(Loudianos et al. 1999)	Met1169Thr	(Loudianos et al. 1999)
Ala1183Thr	16	ATP-BD	1	WND mutation	(Loudianos et al. 1998)	Ala1183Gly	(Loudianos et al. 1998)
Gly1186Ser	16	ATP-BD	2	WND mutation	(Yamaguchi et al. 1998)	Gly1186Cys	(Shah et al. 1997)

[a]1 – conservation with human ATP7A and other species; 2 – with other species, not human ATP7A; 3 – not conserved. Aligned in Figure 4-1. [b]Additional mutations at same amino acid position.

Alignment of the sequences was done using the multi-align function in BCM search launcher (http://searchlauncher.bcm.tmc.edu/multi-align/multi-align.html) (Figure 4-2).

B. YEAST STRAINS

The protease-deficient *S. cerevisiae* strain BJ2168 (MATa pep4-3 prc1-407 prb1-1122 ura3-52 trp1 leu2) was used as the wild-type yeast control (Zubenko *et al.* 1980). Mutant strains *ccc2* and *fet3*, which lack functional *CCC2* and *FET3* genes, were derived from the BJ2168 parental yeast strain. The yeast strains are described in detail in Chapter 3, and have been previously described (Forbes and Cox 1998).

C. ATP7B EXPRESSION CONSTRUCTS

The full-length wild-type and mutant *ATP7B* cDNAs were constructed and cloned as described in Chapter 3. Cloned *ATP7B* cDNAs carrying the desired missense mutations were created using synthetic oligonucleotides containing the desired nucleotide changes and the QuikChange site-directed mutagenesis kit (Stratagene) (Table 4-2). DNA fragments were generated from the mutated plasmids by PCR and sequenced using the automated Li-COR sequencer to ensure that the fragments did not contain any random sequence changes. The PCR products were then ligated into the yeast multicopy vector, pG3 (Schena *et al.* 1991), and the single-copy derivative, pG4 (Forbes and Cox 1998).

The ATP7B expression constructs (pG3 and pG4 constructs) were transformed into *ccc2* yeast using a modified lithium acetate method (Elble 1992), and tryptophan auxotrophy was used to select transformants. Genomic DNA was extracted from all pG4 transformants, digested with *Bam*H1, and analyzed by Southern blot hybridization to confirm single-copy integration of the plasmid. The same methods used in Chapter 3 were used in studying this set of ATP7B variants.

D. YEAST PROTEIN PREPARATION AND WESTERN BLOTTING

Yeast cells were grown at 30°C for 48 hours in SD medium with all amino acids except tryptophan. Protein extracts from the yeast mutant strains were prepared as described in Chapter 3, and quantified using the enhanced Bradford assay (Pierce Chemical).

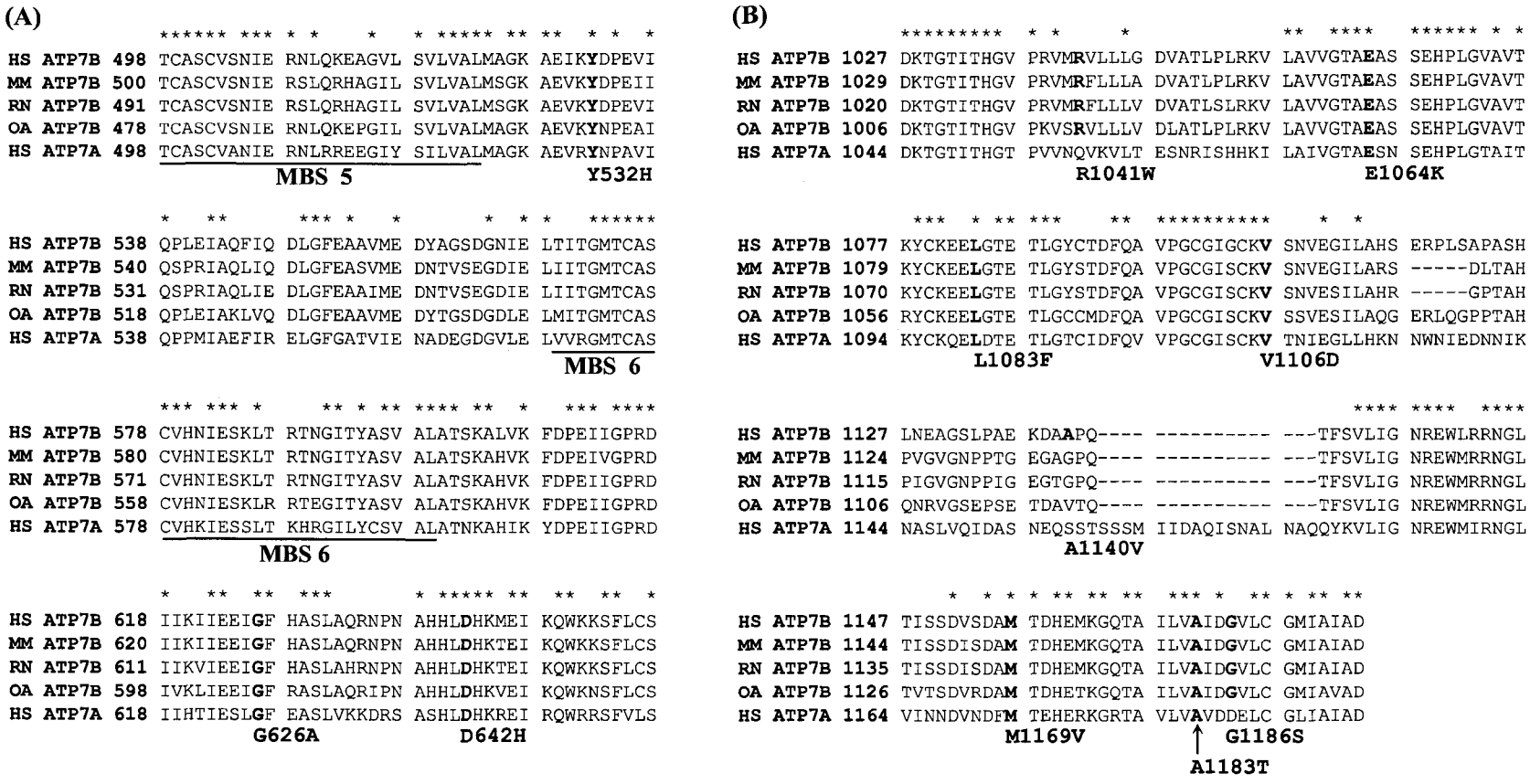

Figure 4-2. Amino acid alignment of regions of human ATP7B with its orthologues.

Amino acid alignment of portions of (A) the copper-binding domain, and (B) the ATP-binding domain of ATP7B from human (HS), mouse (MM), rat (RN), sheep (OA) and human ATP7A. Single-letter amino acid codes are used for the sequence and ATP7B variants tested. Fully conserved residues are marked with an * above the sequence. Positions of the ATP7B variants are indicated below the sequence.

Table 4-2. Oligonucleotides used for site-directed mutagenesis.

Mutation	Forward Primer	Reverse Primer
Tyr532His	5'-GCAGAGATCAAG**C**ATGACCCAGAGG-3'	5'-CCTCTGGGTCAT**G**CTTGATCTCTGC-3'
Gly626Ala	5'-GAGGAAATTG**C**CTTTCATGCTTCCC-3'	5'-GGGAAGCATGAAAG**G**CAATTTCCTC-3'
Asp642His	5'-GCTCATCACTTG**C**ACCACAAGATGG-3'	5'-CCATCTTGTGGT**G**CAAGTGATGAGC-3'
Arg1041Trp	5'-CAGGGTCATG**T**GGGTGCTCCTGC-3'	5'-GCAGGAGCACCC**A**CATGACCCTG-3'
Glu1064Lys	5'-GGGGACTGCG**A**AGGCCAGCAGTG-3'	5'-CACTGCTGGCCT**T**CGCAGTCCCC-3'
Leu1083Phe	5'-GTAAAGAGGAA**T**TTGGAACAGAGACC-3'	5'-GGTCTCTGTTCCAA**A**TTCCTCTTTAC-3'
Val1106Asp	5'-GGTGCAAAG**A**CAGCAACGTGGAAGG-3'	5'-CCTTCCACGTTGCTG**T**CTTTGCACC-3'
Ala1140Val	5'-GAAAAAGATGCAG**T**CCCCCAGACCTTC-3'	5'-GAAGGTCTGGGGG**A**CTGCATCTTTTTC-3'
Met1169Val	5'-CAGTGACGCT**G**TGACAGACCACGAG-3'	5'-CTCGTGGTCTGTCA**C**AGCGTCACTG-3'
Ala1183Thr	5'-CCATCCTGGTG**A**CTATTGACGGTG-3'	5'-CACCGTCAATAG**T**CACCAGGATGG-3'
Gly11864Ser	5'-GGCTATTGAC**A**GTGTGCTCTGTGG-3'	5'-CCACAGAGCACAC**T**GTCAATAGCC-3'

Bold and underlined nucleotidesdemarcate those nucleotides altered through site-directed mutagenesis.

Twenty μg of each protein sample was electrophoresed on a 7.5% polyacrylamide gel and transferred to PVDF membrane. Expression of ATP7B from both pG3 and pG4 transformants was confirmed by Western blotting using a polyclonal antibody against the C-terminal 10 kDa fragment of ATP7B (anti-ATP7B.C10), as outlined in Chapter 3. Bound antibody was detected by enhanced chemiluminescence using Supersignal substrate (Pierce Chemical).

E. COMPLEMENTATION ASSAY

Multicopy (pG3) and single-copy (pG4) transformed strains were tested for their capacity to complement the *ccc2* phenotype using a plating assay. The same assay media described in Chapter 3 (base assay, Fe-limited, Fe-supplemented, and Cu-supplemented media) were used in this study. Solid medium for the plating assay was made using 2% Bacto agar (Difco). Cells were prepared for the plating assay as follows: stationary yeast cultures grown in standard SD liquid media lacking tryptophan were washed with sterile ice-cold distilled water, resuspended in liquid Fe-limited medium then grown to saturation overnight. For each strain, the cultures were diluted to an optical density of OD_{600nm}=0.1 in 1 mL of sterile deionized water, and 5 μL of each cell suspension was streaked on Fe-limited media. Growth of the mutant strains was compared with that of *ccc2* yeast transformed with normal ATP7B. Cell viability was confirmed by streaking 5 μL of each cell suspension on Fe-supplemented and Cu-supplemented media. All plates were grown for 48 hours at 30°C and then photographed.

The Cu transport activity of single-copy (pG4) transformed strains was also evaluated in liquid culture using growth curve analysis, as described in Chapter 3. The mean growth rate of each mutant strain was calculated from at least three independent experiments, and compared with the growth of *ccc2* yeast transformed with wild-type *ATP7B* cDNA.

F. TEMPERATURE ASSAY

The Cu transport activity of single-copy (pG4) transformed strains was further examined under higher growth temperatures. The yeast strains were grown as per the plating assay, and the Fe-limited cultures diluted to an optical density of OD_{600nm}=0.1 in Fe-limited medium lacking tryptophan. For each yeast strain, the cell suspensions were further diluted

1:1, 1:10, 1:25 and 1:50, and 2.5 μL of each diluted cell suspension was spotted onto Fe-limited, Fe-supplemented and Cu-supplemented media. This system of diluting and spotting onto plates using a multi-channel pipette was done to reduce the quantity of reagents and hands-on time required for the assay. All plates were grown for approximately 68 hrs at 35°C and then photographed. Three clones of each ATP7B variant were spotted in triplicate.

G. Fet3p Oxidase assay

The Fet3p oxidase assay indirectly evaluates the capacity of yeast strains to deliver Cu to Fet3p. As described in Chapter 3, the Fet3p assay is more sensitive than the growth assay as it can discriminate smaller variations in Cu transport (Chapter 3) (Hsi *et al.* 2004). The amount of apo-Fet3p (Cu-free) present was estimated by comparing total Fet3p and holo-Fet3p (Cu-bound) levels. Total Fet3p oxidase activity is determined by homogenization of yeast in buffer containing Cu (50mM $CuSO_4$), to reconstitute Fet3p activity *in vitro* (+Cu). Holo-Fet3p activity is determined by homogenization in buffer containing the Cu chelator, bathocuproine disulfonate, BCS (1 mM BCS) and the reducing agent ascorbate, to measure activity of Fet3p loaded with Cu *in vivo* (-Cu).

Protein was prepared from the yeast strains, and Fet3p oxidase activity present in the different strains was measured. The assay is outlined in detail in Chapter 3.

H. Molecular modeling of ATP7B

To assess possible effects of ATP7B missense variants upon functionally important regions of ATP7B, a molecular model of the ATP7B region containing the phosphorylation (P)- and nucleotide-binding (N)-subdomains of the ATP-BD and TM 6 and TM 7 was generated using the high-resolution crystal structure of the Ca^{2+}-ATPase SERCA1a (Protein Data Bank accession number 1iwoA) in the calcium-bound E2-conformation (Toyoshima *et al.* 2000). SWISS-MODEL and DEEP-VIEW (Guex and Peitsch 1997) were used to align and model various segments of the ATP7B amino acid sequence, including Trp-712 to Gly-943, Tyr-952 to Gln-1004, Asn-1005 to Ala-1065, Ser-1066 to Val-1109, Val-1182 to Lys-1238, Val-1239 to Ile-1348. Non-conserved loop regions were

not included. This alignment is a modification of those previously described (Fatemi and Sarkar 2002b; Tsivkovskii *et al.* 2003).

III. RESULTS

A. Assessment of expression of ATP7B missense variants in *ccc2* yeast

The expression of ATP7B from all pG3 and pG4 transformed mutant strains was confirmed by Western blotting using anti-ATP7B.C10 as the primary antibody. All multicopy (pG3) transformed mutant strains showed expression of ATP7B equivalent to that of the strain transformed with wild-type ATP7B, except for Glu1064Lys, which showed only weak expression (Figure 4-3A), and Val1106Asp (Figure 4-3B), for which expression was consistently absent despite testing of multiple transformants. In order to determine whether the ATP7B variant proteins, Glu1064Lys and Val1106Asp, were being expressed but unrecoverable using the standard protocol for protein extraction, protein was prepared using a centrifugation speed of 1,000 x g instead of 10,000 x g for the removal of cellular debris. The protein extracts prepared with the lower centrifugation speed showed expression of Glu1064Lys (data not shown) and Val1106Asp (Figure 4-3B) in contrast to those prepared with the 10,000 x g spin. This suggested that these mutant proteins are mislocalized, perhaps due to aggregation, as the lower centrifugation step would recover heavier organellar membrane fractions not present with the standard procedure.

All single-copy (pG4) transformed strains showed ATP7B expression, with the exception of Glu1064Lys and Val1106Asp (data not shown). This was consistent with our observations in the ATP7B pG3 transformed strains.

B. Assessment of copper transport function by the yeast complementation assay

All 11 *ATP7B* missense variants were initially tested for their capacity to complement the yeast *ccc2* phenotype in pG3 and pG4 transformed strains by plating equal numbers of cells on Fe-limited, Fe-supplemented and Cu-supplemented plates (Figure 4-4). No difference in results was observed between the pG3 transformed strains and the pG4 transformed strains for all of the missense variants examined.

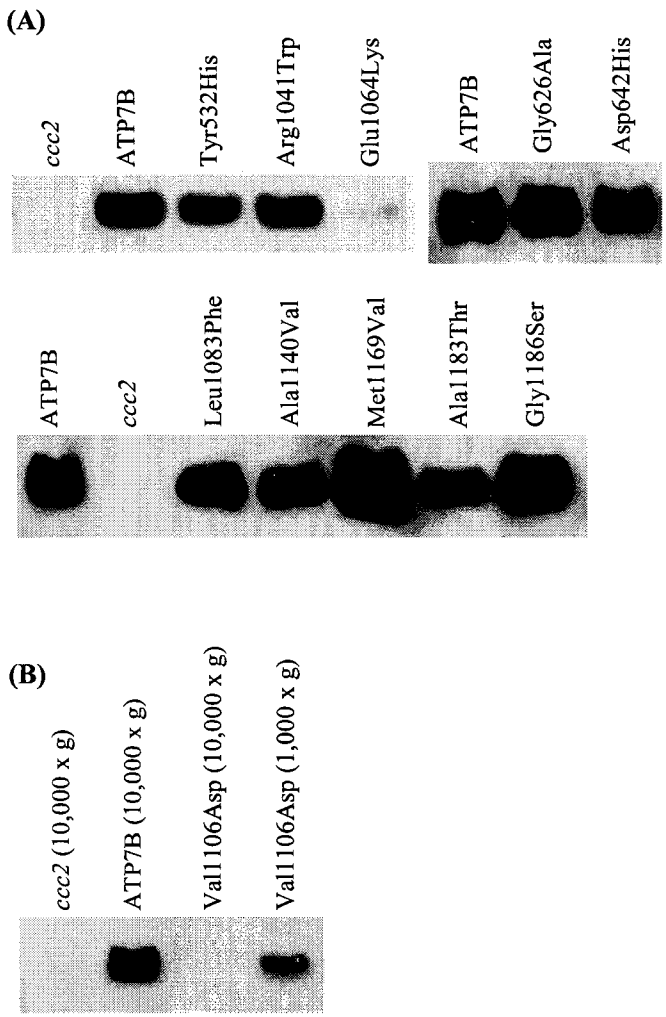

Figure 4-3. Detection of expression of ATP7B variants in *ccc2* mutant yeast by Western blot.

(A) Western blot of ATP7B variants in *ccc2* yeast using 20 μg total yeast protein from multicopy transformants and the polyclonal antibody anti-ATP7B.C10. Strains are indicated by mutation. *ccc2* yeast transformed with empty vector (*ccc2*) and with wild-type *ATP7B* (ATP7B) were included as controls. (B) Val1106Asp expression in *ccc2* yeast. Western blot of ATP7B and Val1106Asp multicopy strains using 20 g total yeast protein extract prepared with either 10,000 x g centrifugation or 1,000 x g centrifugation.

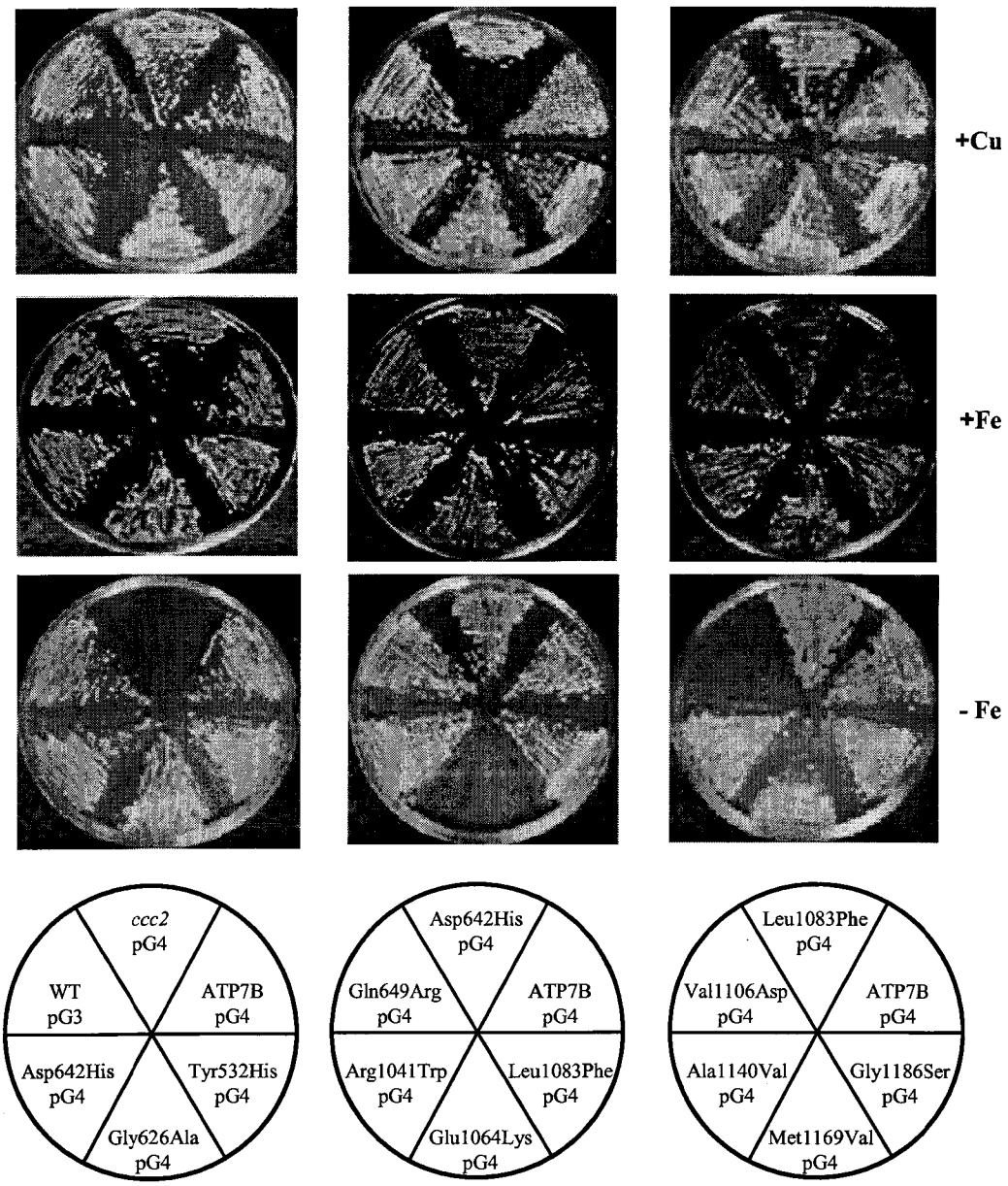

Figure 4-4. Plating assay to assess complementation of *ccc2* yeast by single-copy ATP7B variants.

Complementation of *ccc2* mutant yeast by single copy *ATP7B* variants. Yeast strains transformed with *ATP7B* variants were plated on iron-limited media (- Fe) to evaluate their ability to complement the *ccc2* phenotype. Equal numbers of cells were plated on iron-supplemented (+Fe) and copper-supplemented (+Cu) media as controls for cell viability. ATP7B variant strains are indicated in the legend by mutation. Wild-type (WT pG3) and *ccc2* transformed with either wild-type *ATP7B* cDNA (ATP7B pG4) or empty vector (*ccc2* pG4) are included as controls. Gln649Arg was not confirmed as a mutation in a WND patient and was not characterized further.

Nine of the variants tested (Tyr532His, Gly626Ala, Asp642His, Arg1041Trp, Leu1083Phe, Ala1140Val, Met1169Val, Ala1183Thr and Gly1186Ser) were able to fully complement the *ccc2* yeast phenotype, as demonstrated by growth equivalent to the wild-type ATP7B strain under Fe-limited conditions. Two missense variants, Glu1064Lys and Val1106Asp, were unable to complement the *ccc2* phenotype. This observation was consistent with the Western blot data where both variant proteins demonstrated subcellular mislocalization.

Since the single-copy transformed strains complemented the *ccc2* phenotype to the same degree as the multicopy strains in the plating assay, analysis of growth in liquid culture was performed using only pG4 transformants (Figure 4-5, Table 4-3). The growth rates of ATP7B missense variants were compared with that of the wild-type ATP7B-transformed strain between 12 and 18 hr (Table 4-3, Figure 4-6). Seven variants (Tyr532His, Gly626Ala, Asp642His, Arg1041Trp, Ala1140Val, Ala1183Thr, Gly1186Ser) grew at a rate similar to that of the wild-type ATP7B-transformed strain under Fe-limited conditions; the variants Leu1083Phe and Met1169Val, however, showed slight growth impairment. The Glu1064Lys and Val1106Asp yeast strains demonstrated severe defects in growth, indicating almost complete lack of Cu transport (Table 4-3).

C. Assessment of copper transport activity under a higher growth temperature

The temperature assay was initially tried at the human physiological temperature of 37°C; however, the yeast strains (pG4 transformants), including yeast transformed with wild-type ATP7B, showed only sparse growth at this higher temperature (data not shown). Thus, the assay was done at the lower temperature of 35°C. The cell suspensions were also spotted onto Fe-limited, Fe-supplemented and Cu-supplemented plates, and grown at 30°C for 48 hours as a control. The growth results were similar to those seen with the plating assay. A previous WND mutation that showed temperature sensitivity, Met769Val (Forbes and Cox 1998), was used as a positive control, and showed reduced growth at 35°C under Fe-limited conditions as compared with its growth at 30°C and the growth of wild-type ATP7B-transformed yeast grown at 35°C. The increased growth temperature did not reveal additional variants unable to functionally complement the *ccc2* yeast phenotype.

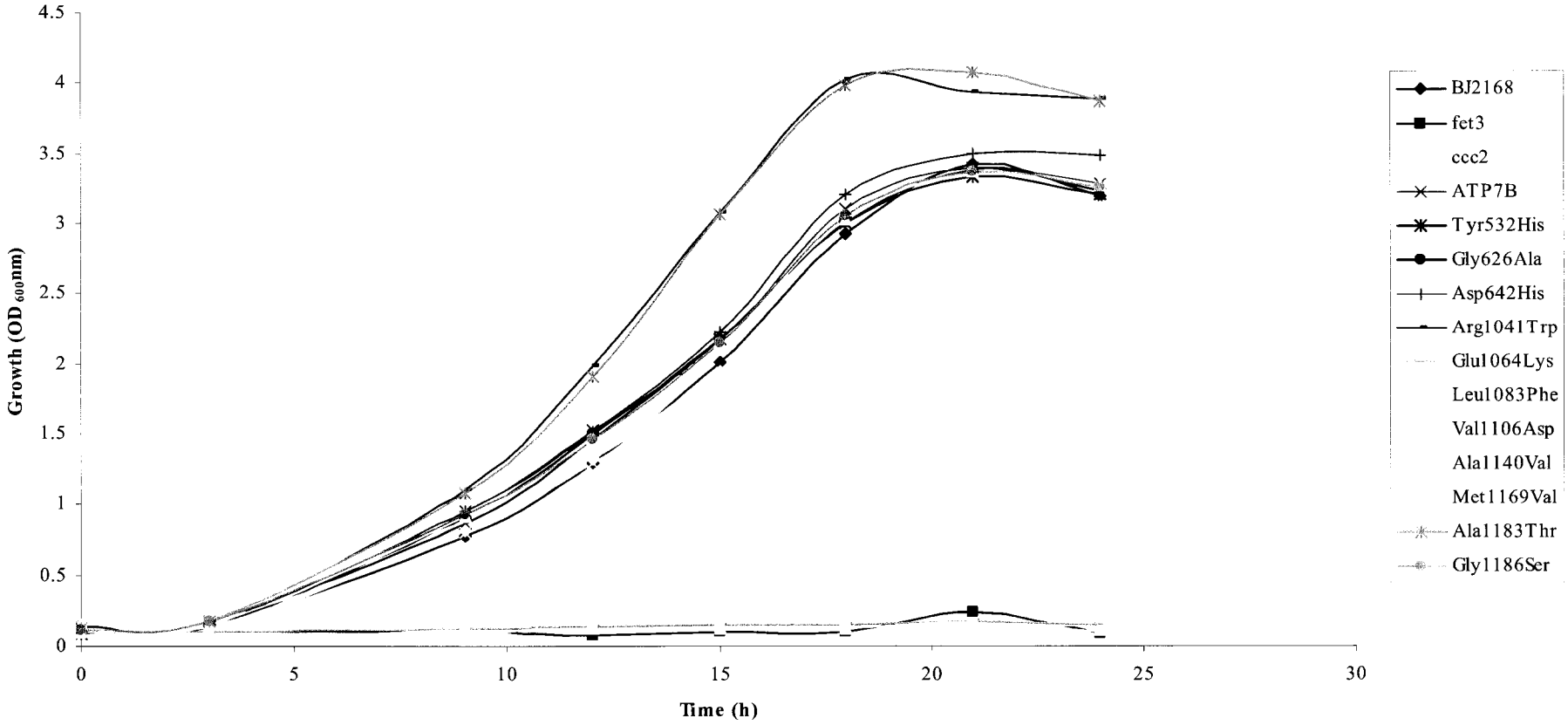

Figure 4-5. Growth of *ccc2* transformed yeast strains in liquid culture.

Representative growth of yeast strains in iron-limited media over 24 hours at 30°C. The legend on the right indicates the yeast strains analyzed. This growth assay was performed as described in the text. The datum depicted represents the values of one experiment. At least three liquid growth assays were completed for each yeast strain studied.

Table 4-3. Liquid assay growth rates of *ccc2* yeast transformed with ATP7B missense variants in single-copy.

Strain	Plating assay: *ccc2* complementation[a]	Growth rate (OD_{600nm}/hr)[b]	Growth rate as % of normal ATP7B[c]	Fet3p Activity	Mutation status
BJ2168	Yes	0.260±0.018	92		
fet3	No	0	0		
ccc2	No	0.0002±0.002	0.07		
ATP7B	Yes	0.283±0.006	100		
Tyr532His	Yes	0.270±0.013	96	Normal	Inconclusive
Gly626Ala	Yes	0.266±0.01	94	Normal	Inconclusive
Asp642His	Yes	0.291±0.005	103	Normal	Inconclusive
Arg1041Trp	Yes	0.327±0.008	116	Normal	Inconclusive
Glu1064Lys	No	0.005±0.006	2	None	WND mutation
Leu1083Phe	Yes	0.222±0.012	79	Impaired	WND mutation
Val1106Asp	No	0.002±0.002	0.8	None	WND mutation
Ala1140Val	Yes	0.279±0.013	99	Normal	Normal variant (see text)
Met1169Val	Yes	0.231±0.032	82	Impaired	WND mutation
Ala1183Thr	Yes	0.302±0.021	107	Normal	Inconclusive
Gly1864Ser	Yes	0.293±0.008	98	Normal	Inconclusive

[a]Complementation results done at 30°C and at 35°C. [b]Measured in Fe-limited media at 30°C between 12 and 18 hours of growth (mean of at 3 independent trials). [c]*ccc2* yeast strain transformed with wild-type ATP7B was set at 100% growth.

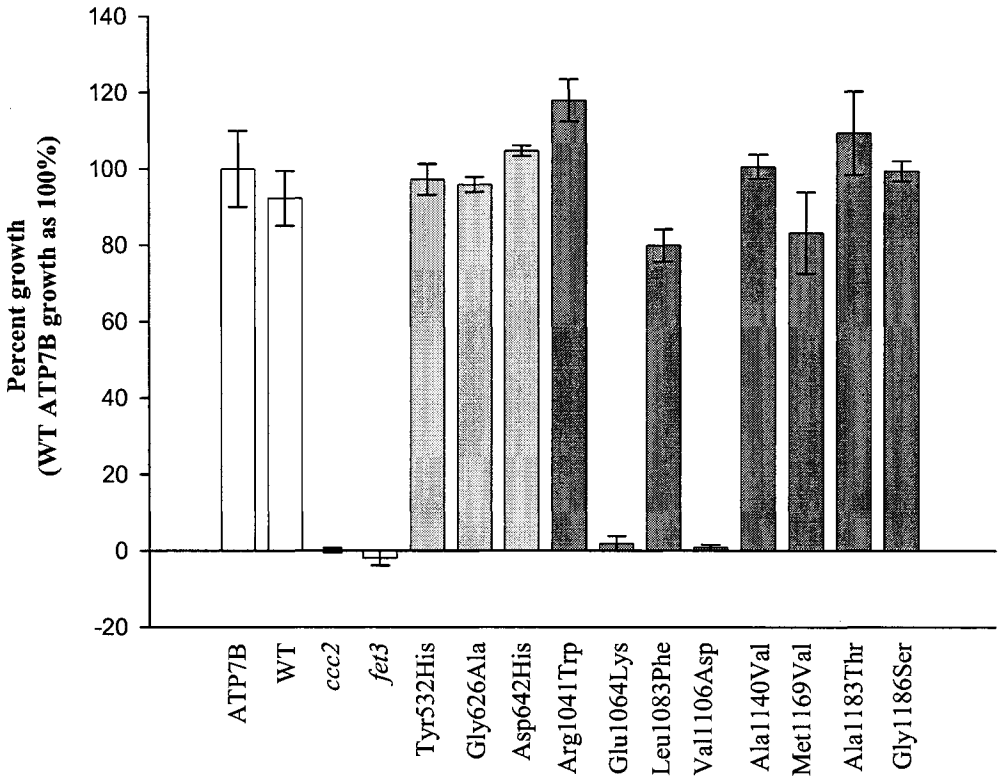

Figure 4-6. Growth rates in Fe-limited media of *ccc2* yeast transformed with single-copy ATP7B variants.

Growth rates of single-copy ATP7B variants in liquid media expressed as a percentage (+/- SE) of the growth rate of wild-type ATP7B. Growth rates were measured between 12 and 18 hours while the yeast were in exponential growth. Rates shown are the mean of at least three independent experiments.

The most severe defects in growth were consistently seen with the Glu1064Lys- and Val1106Asp-transformed yeast strains. The Leu1083Phe strains showed slightly reduced growth when compared with the wild-type ATP7B-transformed strain and the parental yeast strain BJ2168. All other strains demonstrated growth similar to that of the wild-type ATP7B-transformed strain and the BJ2168 yeast strain (data not shown).

D. Assessment of copper transport function by the Fet3p oxidase assay

Fet3p was a suitable marker enzyme to use for analyzing the Cu transport activity of these ATP7B variants since Fet3p oxidase activity is dependent on the amount of Cu delivered to it by Ccc2p, the yeast orthologue of ATP7B. Under normal circumstances, Fet3p is present in the yeast cell as holo-Fet3p (Cu-loaded), and only trace amounts of apo-Fet3p (Cu-free) exists. An impairment of Ccc2p activity results in a greater percentage of the Fet3p present in the apo-Fet3p form.

Fet3p oxidase activity was measured in *ccc2* mutant yeast transformed with ATP7B variants in single-copy. Wild-type yeast (BJ2168 strain) and *ccc2* yeast transformed with wild-type ATP7B showed similar amounts of holo-Fet3p and total-Fet3p activity (Figure 4-7). This indicated that the majority of the Fet3p present in the strains had Cu incorporated into the ferroxidase proteins. The Glu1064Lys- and Val1106Asp-transformed yeast strains showed no evidence of holo-Fet3p activity, demonstrating that these mutations completely eliminate the ability of the protein to transport Cu. These findings were consistent with the complementation assay results, in which Glu1064Lys and Val1106Asp were unable to rescue the *ccc2* yeast phenotype in either single or multicopy strains. The Leu1083Phe and Met1169Val strains showed a decrease in holo-Fet3p activity compared with total-Fet3p activity, suggesting that these mutations interfere with Cu transport, albeit to a lesser extent than Glu1064Lys and Val1106Asp (Figure 4-7). Tyr532His-, Gly626Ala-, Asp642His-, Ala1183Thr- and Gly1186Ser-transformed yeast strains showed similar levels of holo-Fet3p and total-Fet3p activity, indicating that these ATP7B variants retain normal Cu transport activity in this system (Figure 4-7).

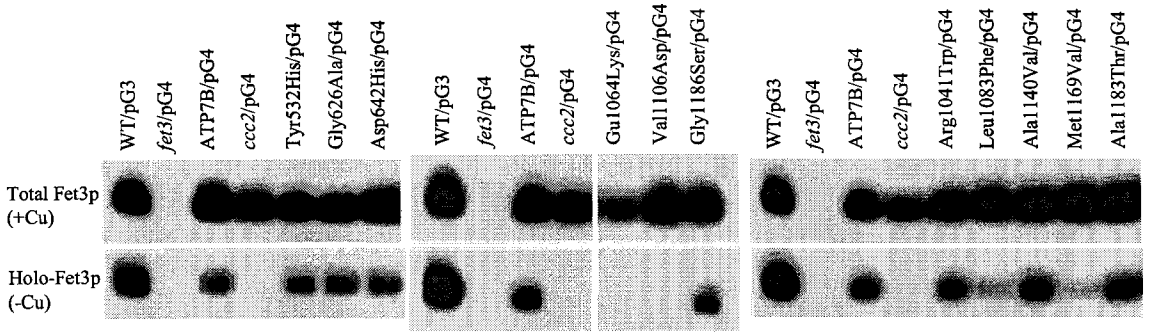

Figure 4-7. Fet3p oxidase activity of *ccc2* yeast transformed with single-copy *ATP7B* variants.

Cu transport activity of single-copy yeast strains was indirectly measured by evaluating their capacity to deliver copper to Fet3p. The bands in the photograph are bands of oxidized substrate (*p*-phenylenediamine dihydrochloride) developed overnight in the dark, and indicate Fet3p oxidase activity. The brightness of the band correlates with active, Cu-loaded Fet3p present in the 30 μg of protein sample loaded. Strains are labeled as per other figures.

E. Effects of ATP7B missense mutations predicted by homology modeling

A protein structure model of the ATP-BD of ATP7B, which consists of a P-subdomain and an N-subdomain, was generated based upon the crystal structure of the Ca^{2+}-ATPase, SERCA1a. The predicted positions of the missense variants located within the ATP-BD are indicated (Figure 4-8). In the model, Glu-1064, which is close to the $SEH^{1069}PL$ motif, assumed a position near the P-subdomain of the protein. Glu1064Lys, Leu1083Phe and Val1106Asp substitutions were predicted to alter hydrogen-bonding based upon their location within the model. The amino acid residues Arg-1041, Ala-1183, and Gly-1186 were situated within the N-subdomain of ATP7B in the protein model, and did not appear to be in positions directly interacting with amino acids residing in either the P-subdomain or the transduction domain.

The amino acid residues Ala-1140 and Met-1169 could not be placed on the model as they lie within a loop region that shows little amino acid conservation with SERCA1a. A structural model was not generated for the N-terminal CuBD of ATP7B as there was no available crystal structure on which to derive a model.

IV. DISCUSSION

The ability of selected ATP7B variants to complement the high-affinity Fe uptake deficiency phenotype of *ccc2* mutant yeast was evaluated. All eleven variants were originally identified as sequence alterations on chromosomes from WND patients, and none had been previously proven to be disease-causing variants by functional analysis. To classify mutations as disease-causing, the amino acid substitution must be shown to result in an aberrant or nonfunctional protein product. The yeast assay used in our laboratory measures the capacity of ATP7B variants to transport Cu across the membrane and transfer it to apo-Fet3p, the yeast orthologue of apo-Cp; therefore, mutant proteins unable to complement the *ccc2* yeast mutant are functionally impaired and likely to be the cause of the WND phenotype in the patient. Results are summarized in Table 4-4.

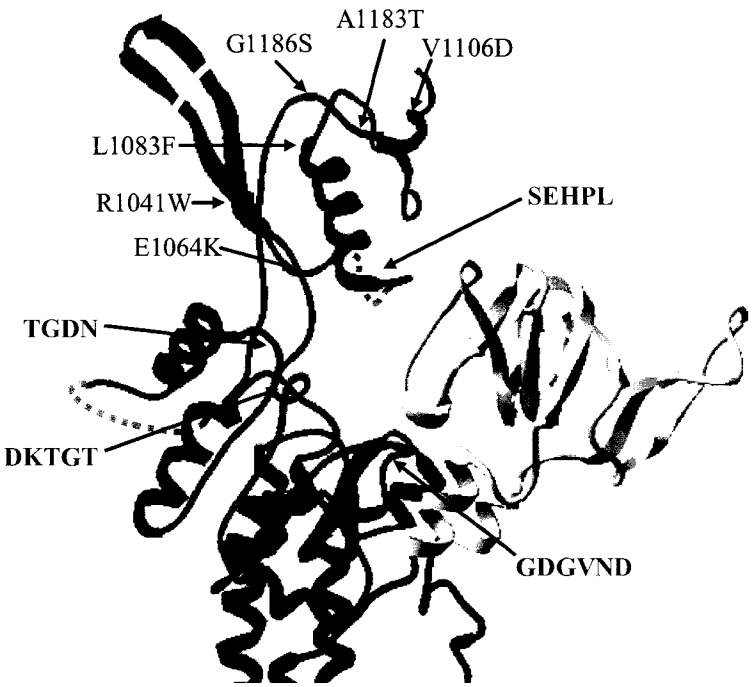

Figure 4-8. ATP-binding domain, including the phosphorylation and nucleotide-binding subdomains, of ATP7B.

Molecular model derived from a homology modeling analysis of ATP7B using SERCA1a (1iwoA) as the template structure. ATP-BD (green) with functionally important regions (red) highlighted, including the P-subdomain (DKTG and GDGVDN), TGDN and SEH^{1069}PL. The transduction domain (yellow) and part of the transmembrane domain (blue) are also shown. Six of the eight ATP7B variants within the ATP-BD that were studied are labeled (black). Broken lines indicate adjacent residues. A non-conserved region within the ATP-BD (approximately to scale) was added manually (light grey). The transmembrane regions (blue) were removed from the model. The single-letter amino acid codes are used for simplicity.
(Molecular model was produced by Dr. Gina Macintyre).

Table 4-4. Summary of functional data obtained for ATP7B mutant variants characterized in this chapter.

Mutation	Yeast functional data	Molecular modeling data	Data from other studies	Functional designation
Tyr532His	Normal Cu transport	--	Mutation in *A. thaliana* RAN1 gene in similar region	Normal variant or mislocalized
Gly626Ala	Normal Cu transport	--	High mutation region in *ATP7A*	Normal variant or mislocalized
Asp642His	Normal Cu transport	--	High mutation region in *ATP7A*	Normal variant or mislocalized
Arg1041Trp	Normal Cu transport	No change	Arg1041Pro - additional mutation	Normal variant or mislocalized
Glu1064Lys	No Cu transport - aberrant expression	Possible affect on structure	Affect on ATP-binding	Disease-causing mutation
Leu1083Phe	Reduced Cu transport	Possible affect on structure	--	Disease-causing mutation
Val1106Asp	No Cu transport - aberrant expression	Possible affect on structure	Cys1104Phe - affect on protein folding	Disease-causing mutation
Ala1140Val	Normal Cu transport	--	Normal variant	Normal variant
Met1169Val	Reduced Cu transport	--	Met1169Thr - additional mutation	Disease-causing mutation
Ala1183Thr	Normal Cu transport	No change	Ala1183Gly - additional mutation	Normal variant or mislocalized
Gly11864Ser	Normal Cu transport	No change	Gly1186Cys - additional mutation	Normal variant or mislocalized

A. IDENTIFICATION OF FOUR AMINO ACIDS CRITICAL FOR COPPER TRANSPORT

In this study, four missense mutations (Glu1064Lys, Val1106Asp, Leu1083Phe and Met1169Val) were confirmed as disease-causing mutations using the yeast functional assay. Two of the variants, Glu1064Lys and Val1106Asp, showed marked impairment in all components of the assay: the plating assay, liquid growth assay, temperature assay and Fet3p oxidase assay. The other two, Leu1083Phe and Met1169Val, showed both moderate growth reduction and impairment of Fet3p oxidase activity, indicating that these amino acid substitutions affect the Cu transport capacity of ATP7B.

All four of the sequence changes considered disease-causing lie within clusters of several conserved amino acids and are situated in the region encompassing the P- and N-subdomains of the ATP-BD. To further characterize the consequences of these mutations, a molecular model of ATP7B was derived, based on the Ca^{2+}-ATPase, SERCA1a. In this 3D molecular model, Glu1064Lys, Val1106Asp and Leu1083Phe fall within the N-subdomain of ATP7B (residues Val-1036 to Asp-1196). Given their spatial locations, the mutations were predicted to affect hydrogen-bonding or the shape of the subdomain, thus possibly influencing the capacity of the variant proteins to bind ATP, which would support our functional data. In addition to their significant positions, all four amino acid substitutions change the size, charge and/or hydrophobicity of the replaced residue. The Glu-1064 and Met-1169 residues also have other WND patient mutations reported at their amino acid positions (Table 4-1) (Shah *et al.* 1997; Loudianos *et al.* 1999). In light of all the data, it is apparent that these four variants are disease-causing mutations, with Glu1064Lys and Val1106Asp having the most pronounced effect.

A recent study has also demonstrated the importance of the Glu-1064 and Val-1106 residues (Morgan *et al.* 2004). The effect of four WND mutations (Glu1064Ala, His1069Glu, Cys1104Phe, and Arg1151His) on protein folding and nucleotide binding was examined, and a molecular model of the ATP-BD was produced based upon the E1 conformation of the Ca^{2+}-ATPase. Although mutation of the Glu-1064 residue did have an affect on the catalytic function of the protein, the conclusions from their study are inconsistent with ours. Substitution of Glu-1064 with alanine did not alter the secondary

structure of the protein, as in our study; instead, the mutation had a profound effect on nucleotide-binding, with the variant losing the ability to bind ATP entirely (Morgan *et al.* 2004). This result was similar to that in studies performed on the bacterial Zn^{2+}-transporting P-type ATPase ZntA, where the Glu470Ala mutation, which corresponds to the Glu1064Ala mutation, demonstrated severe disruption of enzyme function and a reduced ability to bind ATP (Okkeri and Haltia 1999; Okkeri *et al.* 2004). The involvement of Glu-1064 in ATP-binding is consistent with the location of the residue, immediately proximal to the adenosine moiety of ATP in the predicted model (Lutsenko *et al.* 2002; Efremov *et al.* 2004; Morgan *et al.* 2004).

Our data suggest that mutation of Glu-1064 may cause conformational changes and/or proteolytic degradation of a misfolded protein product, as demonstrated by the altered expression of Glu1064Lys and the placement of the residue on the theoretical model. However, it is also possible that the functional consequences of the Glu1064Lys mutation are due to a loss in ATP-binding ability, as our yeast model system is not capable of assessing this aspect of ATP7B Cu transport function. An inability to bind ATP and transport Cu may result in faster turnover of the mutant protein product; however, this has yet to be determined. Furthermore, it is likely that even minor, subtle changes in folding may be sufficient to decrease protein stability and result in degradation or altered expression in a cell. Nevertheless, the different studies, including ours, demonstrate the importance of this residue in the Cu transport function of ATP7B.

This is also the situation with Val-1106, where additional studies have supported our finding that this residue is necessary for function. The Cys1104Phe mutation, which is near the Val1106Asp mutation in our study, has been shown to affect the folding of the N-subdomain but not the ability of the variant protein to bind ATP (Morgan *et al.* 2004). Replacement of the Cys-1104 with alanine, a less bulky residue, was tolerated and the variant had a secondary structure similar to the wild-type N-subdomain. Therefore, it is the larger phenylalanine residue causing the disruption in the fold of the domain, suggesting that the amino acids in this region of ATP7B are critical for the proper overall structure of the ATP-BD. It is possible that replacement of Val-1106 with the aspartic acid residue also disrupts the fold of the protein and the Cu transport function of ATP7B. Furthermore, the

Val-1106 residue is located within the glycine motif (Gly-1099 to Val-1106) identified in ZntA to be central for the formation of the nucleotide binding site (Okkeri *et al.* 2004).

Although Leu1083Phe and Met1169Val show only subtle reductions in their Cu transport activity, it is possible that these mutations cause disease in patients harbouring the sequence changes. The effect of these mutations may be especially adverse when in combination with a mutant allele that has a more severe effect on function. His1069Gln is the most common mutation in the European population and is regarded as a disease-causing mutation; yet, in the yeast assay, this mutation is capable of partially restoring *ccc2* yeast function (Iida *et al.* 1998), exhibiting only a modest reduction (~40%) in Cu transport when compared with *ccc2* yeast transformed with wild-type ATP7B (Cox, unpublished). A study completed in our laboratory on a number of WND patient mutations also identified mutant proteins that were able to partially complement the yeast phenotype yet deemed to be disease-causing (Forbes and Cox 1998). This implies that even slight reductions in ATP7B activity will result in WND, corroborating our conclusion of Leu1083Phe and Met1169Val as disease-causing changes.

The remaining four variants within the ATP-BD (Ala1140Val, Gly1186Ser, Arg1041Trp and Ala1183T) exhibited normal Cu transport in the yeast functional assay. Ala1140Val was regarded to be a normal variant as it is not conserved amongst all four species compared, and the replacement of Ala-1140 with valine has been previously considered a normal polymorphism (Figus *et al.* 1995; Thomas *et al.* 1995; Waldenstrom *et al.* 1996).

Whether the other three ATP-BD variants are rare normal variants or disease-causing cannot be definitively concluded based on the current functional data. By using homology modeling and assessing the characteristics of the substituted amino acids, insight can be gained as to whether they may affect protein function. These substitutions were not predicted to change the protein structure in our molecular model; nevertheless, additional changes have been reported in these amino acid positions (Table 4-1) (Shah *et al.* 1997; Loudianos *et al.* 1998b; Loudianos *et al.* 1999), suggesting that these specific residues may be critical for some aspect of ATP7B function. The Arg-1041 (Arg1041Trp) and Ala-1183 (Ala1183Thr) residues are also replaced by amino acids of different size, charge and/or hydrophobicity, which may affect intra- and intermolecular bonding capabilities of the

variant proteins. From the liquid growth assay, Arg1041Trp and Ala1183Thr also appeared to complement the *ccc2* phenotype better than wild-type human ATP7B. It is unknown whether this would contribute to the pathogenesis of WND in patients.

B. The N-terminal amino acids are not essential for copper transport

All three of the CuBD missense variants were able to functionally complement the *ccc2* yeast Fe-deficient phenotype. This was not surprising as there are no missense mutations reported in the CuBD of the MNK gene, *ATP7A* (Chapter 2, Figure 2-1), and it is believed that there is redundancy among the six N-terminal copper-binding sites. The bacterial and yeast orthologues of ATP7B have one or two MBSs, implying that not all six in the human protein are necessary for function. In fact, previous experiments using the yeast complementation assay have demonstrated that only the fifth or sixth MBS (MBS 5 or MBS 6) is necessary and sufficient for ATP7B Cu transport function (Forbes *et al.* 1999; Cater *et al.* 2004). Either MBS 5 or MBS 6, along with the first 63 amino acids of the N-terminus, are also necessary and sufficient for Cu-dependent trafficking (Cater *et al.* 2004; Guo *et al.* 2005). It is unknown whether the entire sequence surrounding the fifth and sixth MBSs is required, or only the conserved Cu-binding motifs are essential; nonetheless, the data indicate that portions of the N-terminus are dispensable for ATP7B function.

The CuBD variants studied are localized between MBS 5 and MBS 6 (one variant) and MBS 6 and TM 1 (two variants), but none are found within the conserved Cu-binding motifs. The Tyr532His substitution occurs in a region where a missense mutation has been identified in the orthologous *Arabidopsis thaliana* RAN1 gene (equivalent to amino acid position 528 in human ATP7B) (Hirayama *et al.* 1999). Although this suggests that the region between MBS5 and MBS6 may be necessary for function, it has not been determined whether the tyrosine residue at position 532 is itself critical. The two variants between MBS 6 and TM 1, Gly626Ala and Asp642His, are located within clusters of several conserved amino acids, and the substituted amino acids differ in size, charge and hydrophobicity. Furthermore, several different mutations between MBS 6 and TM 1 have been reported in MNK patients (Das *et al.* 1994; Ronce *et al.* 1997; Tumer *et al.* 1997; Gu *et al.* 2001; Hahn *et al.* 2001). This region has been proposed to be important for ATP7A/ATP7B protein folding and for the interaction of the CuBD with the ATPase core

of the protein (Forbes *et al.* 1999; Tumer *et al.* 1999). Thus, these sequence variants may have an effect on ATP7B structure and function by altering the flexibility of this adjoining region and the overall structure of the N-terminus.

C. Conclusion

Many missense mutations have been reported in the literature and are listed in the WND database without functional assessment. The data in this chapter has expanded our understanding of additional sequence changes in *ATP7B* for their abilities to transport Cu and their putative characterizations as disease-causing or possible rare normal variants (Table 4-4). Through the use of a yeast functional assay and molecular modeling, four mutations have been successfully classified as disease-causing: Glu1064Lys, Val1106Asp, Leu1083Phe and Met1169Val.

CHAPTER 5:
Development of an immunofluorescence method for analyzing the subcellular localization of ATP7B mutant proteins

I. INTRODUCTION

The work in this thesis has used complementation of *ccc2* mutant yeast as an assay to assess the functional capability of WND patient mutations and other ATP7B variants within the cytosolic C-terminal tail (Chapter 3) (Hsi *et al.* 2004), ATP-BD and CuBD (Chapter 4) (Cullen *et al.* 2005) of human ATP7B. The assay was useful for determining whether the WND patient mutations contributed to manifestation of the disease and for understanding the role of particular regions of the protein in the provision of Cu to apo-Fet3p. However, the yeast assay evaluates only transport function, and a sequence alteration with no effect on Cu transport may still be detrimental to the required trafficking function of ATP7B.

ATP7B-mediated Cu homeostasis not only relies upon the Cu transport activity of ATP7B, but also depends upon the correct intracellular localization of the protein within the hepatocyte. As discussed in Chapter 1, the localization of ATP7B is critical for executing its dual functional role in the cell; its biosynthetic role of delivering copper to apo-Cp within the TGN (Yamada *et al.* 1993; Murata *et al.* 1995; Terada *et al.* 1998), and its excretory role of transporting excess Cu out of the cell from an undefined vesicular compartment (Schilsky *et al.* 1994; Terada *et al.* 1999). To accomplish these two crucial roles, ATP7B demonstrates Cu-induced re-distribution in response to changing Cu conditions (Hung *et al.* 1997; Schaefer *et al.* 1999a; Roelofsen *et al.* 2000).

Studies on WND patient mutations have in fact demonstrated that the localization of mutant proteins could contribute to the pathogenesis of the disease, with some variants mislocalized to the endoplasmic reticulum or throughout the cytoplasm (Hung *et al.* 1997; Payne *et al.* 1998; Forbes and Cox 2000; Huster *et al.* 2003), and others unable to traffick in Cu-rich environments (Hung *et al.* 1997; Forbes and Cox 2000; La Fontaine *et al.* 2001).

As described in Chapter 1, various methods have been used to study the intracellular localization of ATP7B and its variants (Hung *et al.* 1997; Schaefer *et al.* 1999a; Forbes and Cox 2000; Harada *et al.* 2000a; Harada *et al.* 2000b; Roelofsen *et al.* 2000; Harada *et al.* 2001; Harada *et al.* 2003; Huster *et al.* 2003; Petris *et al.* 2003; Cater *et al.* 2004; Harada *et al.* 2005). Our laboratory has previously focused on localization within the mammalian

CHO cell line, using indirect immunofluorescence with multiple antibodies to detect the subcellular distribution of ATP7B variants (Forbes and Cox 2000).

The goal of this chapter was to develop an immunofluorescence method in the laboratory for studying the subcellular localization of multiple ATP7B variants in different Cu environments, and possibly in a more biologically relevant cell type, such as a hepatic cell line. Given the number of variants studied in previous chapters and the many additional mutations that could be analyzed, the aim was to set up a higher throughput system for examining the variants, compared with our current system, by limiting the use of antibodies for detection. A more efficient system would allow the assessment of several cell lines to determine whether the distribution of ATP7B depends on the particular cell type. Furthermore, a method to detect real-time Cu-dependent trafficking, to possibly follow the exocytic and endocytic pathways followed by ATP7B, was desirable. To achieve this goal, GFP-tagged constructs were generated, as this would permit immediate visualization under fluorescence. Experiments were designed around the use of these constructs and creating a system for more accurate intracellular localization of the variant proteins.

II. MATERIALS AND METHODS

A. GENERATION OF ATP7B FUSION CONSTRUCTS

For immunofluorescence studies in mammalian cells, *ATP7B* cDNA variants (Chapter 3) were cloned into the expression vector, phrGFP-N1 from Stratagene, for expression of the constructs in mammalian cells. The vector phrGFP-N1 places the GFP tag at the N-terminus of the protein. The cDNAs were ligated into the vector so that the GFP tag was fused in-frame with the *ATP7B* cDNAs, and the translational termination codon of *ATP7B* was used to stop translation of the fusion construct. In addition to the mutants studied in Chapter 3, variants from previous work in our laboratory (CysProCys/Ser, Asp765Asn, Gly943Ser, and Leu776Val) were also cloned into the phrGFP-N1 vector (Forbes and Cox 1998). Asp-765 and Leu-776 are located in TM 4 of ATP7B, Gly-943 in TM 5, and Cys-Pro-Cys in TM 6.

The full-length wild-type *ATP7B* cDNA, cloned into pUC19 vector, was previously constructed in the laboratory by Dr. John R. Forbes. ATP7B mutant variants were generated from the full-length *ATP7B* cDNA as outlined in Chapter 3, and cloned into phrGFP-N1 vectors.

Correct *ATP7B* cDNAs were removed from pUC19 vectors by digesting with *Bam*H1 and *Sal*1 restriction enzymes, agarose gel purified, and then ligated back into a phrGFP-N1 vector complementarily prepared by digesting with *Bgl*II and *Sal*1 restriction enzymes. Expression plasmids were isolated from 100 mL cultures of bacteria grown in LB medium containing 100 μg/mL carbenicillin using ion exchange chromatography (Qiagen Midi Prep kit, Qiagen), according to the manufacturer's protocol. Some expression plasmids were isolated from 100 mL cultures of bacteria grown in LB containing 100 μg/mL carbenicillin using ion exchange chromatography and an endotoxin-free method (Qiagen Endotoxin-free Maxi Prep kit, Qiagen), according to manufacturer's protocol.

B. CELL CULTURE

Cell lines used in this study were the following: CHO cells; African green monkey kidney, COS-7 cells (gift from Dr. Chris Bleakley, University of Alberta and from Dr. Rachel Wevrick, University of Alberta); human embryonic kidney (HEK293) cells (gift from Dr. R. Wevrick, University of Alberta); HepG2 cells and Huh7 cells. The CHO, HepG2 and Huh7 cell lines were originally obtained from the American Type Cell Culture (ATCC) resource. Cells were maintained in either Dulbecco's Modified Eagle Medium (DMEM) or Alpha Modified Eagle Medium (-MEM) supplemented with 10% fetal bovine serum (FBS; Gibco), and 100 U/mL each of penicillin and streptomycin (Invitrogen/Life Technologies). To polarize HepG2 cells, cells were grown in DMEM + GlutaMAX Medium (Invitrogen/Life Technologies), which contains L-glutamine in a stabilized form so that it does not degrade in storage or during incubation. All cell lines were grown in tissue culture incubators set at 37°C with a 5% carbon dioxide atmosphere.

C. ANTIBODIES AND SUBCELLULAR MARKERS

Various organelle markers were used in this study to detect subcellular structures. For the analysis of transfected cells in real-time, Living Colors Subcellular Localization Vectors

from BD Biosciences (Clontech) were initially attempted to demarcate the endoplasmic reticulum (ER), the Golgi apparatus and the plasma membrane: pECFP-ER, pECFP-Golgi, pECFP-mem, respectively. These vectors contained specific proteins fused to the GFP color variant, enhanced cyan fluorescent protein (ECFP), which fluoresces cyan when excited. CHO cells were transiently transfected with both an *ATP7B-GFP* fusion construct and an ECFP-subcellular localization vector. These were visualized using the confocal microscope with the assistance of Dr. Xuejun Sun and Gerry Baron (Cell Imaging Facility, University of Alberta).

Lysotracker, ER tracker and Lectin GS-IIA organellar stains from Molecular Probes were also tried for real-time analysis to detect the lysosomes, ER and TGN, respectively, for co-localization. CHO cells were transiently transfected with wild-type *ATP7B-GFP* fusion constructs. Following overnight growth in the transfection mixture, 1 μM ER tracker, 1μM Lysotracker or 50 μg/mL Lectin GS-IIA were added to the wells and incubated at 37°C for one hour to detect the ER, lysosomes and TGN, respectively. These were visualized using the confocal microscope with the assistance of Dr. Ing-Swie Goping (University of Alberta).

Different antibodies were also used for co-localization experiments with ATP7B variants. Mouse monoclonal anti- -adaptin (AP-1) antibody recognizes the Golgi adaptor complex AP-1, and appears to be largely confined to the TGN (Sigma). An antibody produced in mouse against the multidrug resistance-associated protein 2 (anti-MRP2) was used to show the apical membrane of polarized HepG2 cells (Sigma-Aldrich). Mouse monoclonal anti-Golgi 58K Protein antibody was used as a general Golgi apparatus marker, as the protein Golgi 58K/formiminotransferase cyclodeaminase is a peripheral membrane protein exposed on the cytoplasmic face of the Golgi (Sigma). DAPI (4', 6-Diamidino-2-phenylindole), which stains double-stranded DNA and fluoresces blue when excited, was used to highlight the nucleus in transfected cells (Roche).

To assess the possibility of performing live cell imaging, a trial experiment was performed on a chamber that housed *ATP7B-GFP*-transfected CHO cells to visualize the distribution of the wild-type ATP7B fusion construct in real-time. 200 μM of $CuCl_2$ was added to the chamber and visualized using a water immersion lens and an environment chamber that

maintained the pH and temperature of the dish. The localization of the ATP7B-GFP signal was tracked over 30 min to follow the trafficking of the protein from the TGN to cytoplasmic vesicles.

D. TRANSIENT TRANSFECTION OF CELL LINES

One day prior to transfection, cells were seeded at 2.5 x 10^5 cells/mL in 2 mL of medium with 10% FBS onto sterile glass coverslips (10 mM diameter, Fisher Scientific) contained in six-well tissue culture plates. Cells were grown overnight to approximately 90% confluence. Before transfection, the growth medium was removed and cells washed with phosphate-buffered saline (PBS). 10 x PBS consisted of 11.5 g Na_2HPO_4, 2 g KH_2PO_4, 80 g NaCl and 2 g KCl in distilled water to a total volume of 1 L.

Cells were transfected using Lipofectamine 2000 reagent (LF), according to manufacturer's protocol (Invitrogen). Transfections were generally carried out in 6-well plates with either 2 μg DNA or 4 μg DNA per transfection sample, at a ratio of 1 μg DNA: 2.5 μL LF. For each transfection sample, the DNA-LF complexes were prepared as follows: the appropriate volume of LF was diluted in Opti-MEM I Reduced Serum Medium (Invitrogen) to a total volume of 250 μL, mixed gently and incubated for at most 5 min. The appropriate volume of DNA was diluted in Opti-MEM I Reduced Serum Medium to a total volume of 250 μL, mixed gently and then combined with the diluted LF reagent to a total volume of 500 μL. The DNA-LF complexes were mixed gently and left to incubate for 20-30 min at room temperature. After incubation, the 500 μL of DNA-LF mixture was added in a drop-wise fashion to each well containing cells and medium, while swirling or gently rocking the plate. The cells were incubated with the transfection mixture overnight.

Twenty-one to twenty-four hours following the addition of the transfection mixture, the medium was removed from the wells and the cells were rinsed twice with PBS; on occasion, however, the medium was removed following six hours of incubation in the transfection mixture if the cells appeared unhealthy at that time. Standard medium (DMEM or -MEM) with 10% FBS was added back to the PBS-washed cells, and the medium was either left unsupplemented, supplemented with $CuCl_2$ or $CuSO_4$ (generally 250 μM), or supplemented with 100 μM bathocuproine disulfonate, BCS (Sigma). The

cells were incubated for a further 2-4 or 12 hr in the supplemented or unsupplemented medium prior to immunofluorescence. Different incubation times, as per the Roelofsen *et al.* study, were used to assess whether varied times would affect localization (Roelofsen *et al.* 2000).

The transfection reagent Fugene 6 (Roche) was also used for transient transfections of Huh7 cells and HepG2 cells. The protocal was similar to that used with LF. Transfections were done following overnight growth of the cells when the cells were at 80-90% confluency. Cells were washed twice with 1 x PBS. Fugene 6 was added directly to 100 μL of serum-free media, and tapped gently. DNA was then added to the Fugene 6 transfection mixture. Different Fugene 6 (μL)-to-DNA (μg) ratios were used, 3:2, 3:1 or 6:1, depending on the cell type. The Fugene:DNA mixtures were incubated for approximately 45 min at room temperature and then added drop-wise to the cells and incubated overnight at 37°C in tissue culture incubators. The cells were then treated as described above.

E. Preparation of slides for immunofluorescence microscopy

Following the incubations, the cells attached to coverslips were washed twice on a shaker for 5 min each with 1 x PBS, either at room temperature or warmer, and then fixed for 15 min at 4°C with 4% paraformaldehyde made in PBS at pH 7.2-7.4. To permeabilize the cells, fixed cells were incubated three times on a shaker for 5 min each with PBS and 0.05% Triton X-100 (Triton X-100, membrane grade, Boehringer Mannheim) (PBS-X) at room temperature. Permeable cells were blocked for 15 min at room temperature on a shaker with PBS-X and 5% BSA (PBS-X/BSA).

Cells were incubated with primary antibodies for 1 hour at room temperature in PBS-X/BSA. To detect the Golgi apparatus, anti-Golgi 58K antibodies were used at a dilution of 1:200 in PBS-X/BSA. To detect the TGN, anti-AP-1 antibodies were used at a dilution of 1:500 in PBS-X/BSA. To show polarization of HepG2 cells and to detect the apical membrane, anti-MRP2 antibodies were used at a dilution of 1:1000 in PBS-X/BSA. Affinity-purified rabbit anti-ATP7B.N60 and anti-ATP7B.C10 primary antibodies against

human ATP7B were used at a dilution of 1:100 in PBS-X/BSA to detect ATP7B normal and mutant constructs, in those experiments that used *ATP7B/pCDNA* constructs.

After the primary antibody incubations, cells were rinsed three times for 5 min each with PBS-X on a shaker. Secondary antibodies were added for 1 hour in the dark at room temperature in PBS-X/BSA using a 1:1000 dilution. For the mouse primary antibodies, a goat anti-mouse secondary antibody conjugated to Alexa Fluor 594, which emits fluorescence in the red spectrum (Molecular Probes) was used. For the rabbit primary antibodies, a goat anti-rabbit mouse secondary antibody conjugated to either Alexa Fluor 594 or Alexa Fluor 488, which emits fluorescence in the green spectrum (Molecular Probes, gift from Dr. R. Wevrick) were used. Following secondary antibody incubation, cells were washed three times for 5 min each with PBS-X at room temperature in the dark on a shaker. Cells were then stained with DAPI (Roche), by incubating the cells in 200 ng/mL DAPI diluted in 1x PBS for 10 min in the dark at room temperature on a shaker. After DAPI staining, the cells were washed twice for 5 min each with PBS-X at room temperature on a shaker.

Coverslips were mounted on slides using ProLong mounting medium and ProLong antifade reagent (Molecular Probes), according to manufacturer's protocol. Slides were dried in the dark overnight on a flat surface, and stored at 4°C in a slide box.

F. Fluorescent and Confocal Microscopy

Most of the microscopy was performed on a Leica DMRE fluorescent microscope with filters for FITC, rhodamine, or DAPI, using either a 40x or 100x oil-immersion objective lens. Images were obtained and saved using Northern Elite software (Empix Imaging Inc.).

The laser scanning confocal microscope in the cell imaging facility of the Department of Oncology (Cross Cancer Institute, University of Alberta) was also used for microscopy work. The facility houses a Zeiss LSM510 confocal microscope consisting of 4 lasers with multiple laser lines from UV to far red (351 nm, 364 nm, 458 nm, 488 nm, 543 nm and 633 nm) for excitation of fluorophores. Images were saved and analyzed using the Zeiss LSM Image Browser software.

G. Isolation of whole cell lysates for Western blots

Cell cultures were grown in 100 mm diameter petri dishes in DMEM + 10% FBS to confluency. Growth medium was removed and cells washed with 10 mL of ice-cold 1 x PBS. Cells were extracted from the plates by scraping with a rubber cell scraper in 3 mL of ice-cold 1 x PBS, and the cells were collected in pre-chilled 50 mL conical tubes. The scraping and collection of cells was repeated once, and then cells were spun down at 4,000 rpm for 4 min at 4°C and the supernatant discarded. Cell pellets were resuspended in 1 mL of ice-cold 1 x PBS, transferred into a pre-chilled 1.5-ml microfuge tube, and re-pelleted using a microfuge at 4,500 x g for 4 min at 4°C. The supernatant was discarded and cell pellets resuspended in Nuclear Lysis Buffer, which consisted of the following: 20 mM HEPES buffer, 20% glycerol, 500 mM NaCl, 1.5 mM $MgCl_2$, 0.2 mM EDTA, 0.1% Triton X-100, 1 mM DTT and a protease inhibitor cocktail for mammalian tissues (Sigma).

Cell lysates were quantified for protein content using the Bradford Assay. Thirty μg of protein was used in a Western blot (for protocol see Chapter 3). The nitrocellulose membrane, with the transferred protein, was incubated with a 1:200 dilution of mouse anti-AP-1 primary antibody, followed by a 1:10,000 dilution of sheep anti-mouse secondary antibody conjugated to horseradish peroxidase (Pierce Chemical, gift from Dr. R. Wevrick). Bound antibodies were detected by enhanced chemiluminescence using Supersignal substrate (Pierce Chemical, Rockford, IL, USA), and visualized by exposure to autoradiography film (Fuji), as described in Chapter 3.

III. RESULTS

A. ATP7B cDNAs tagged with Green Fluorescent Protein

GFP-tagged constructs were created to enable live-cell imaging of ATP7B trafficking and to limit the use of antibodies. Wild-type and mutant *ATP7B* cDNAs generated and used in the yeast assay (Chapter 3) were tagged with GFP at the N-terminus. The wild-type *ATP7B-GFP* fusion construct was initially tested for correct localization under high Cu conditions (+Cu; 200 μM $CuCl_2$) and low Cu conditions (-Cu; 100 μM BCS) by transfecting into CHO cells. Vector only controls were simultaneously done and showed

non-specific green fluorescence throughout the cells. The slides were independently verified by others and the overall distribution pattern of ATP7B-GFP expression appeared to correlate with their respective Cu conditions (data not shown).

B. Live cell imaging techniques

i. Living Colors Subcellular Localization vectors

Living Colors Subcellular Localization (LCSL) vectors have cDNA sequences encoding proteins that localize specifically to the ER (pECFP-ER), TGN (pECFP-Golgi) or plasma membrane (pECFP-mem), fused to the sequence encoding the cyan fluorescent protein (CFP). Thus, co-localization of ATP7B-GFP with these vectors in mammalian cells allows a relatively easy way of detecting ATP7B localization in real-time.

CHO cells, which have supported ATP7B trafficking in our laboratory (Forbes and Cox 2000), were double-transfected with the wild-type *ATP7B-GFP* fusion construct and one of the LCSL vectors. The double transfections were analyzed using the confocal microscope. The absorption and emission spectra of the two fluorescent proteins were too close to be distinguished with the available laser lights (data not shown). GFP absorbs light at a wavelength of 475 nm and emits light at 505 nm, whereas CFP absorbs at 458 nm and emits at 489 nm. The filters available with the Leica fluorescent microscope were also unable to differentiate between the two fluorophores.

ii. Lysotracker, ER tracker and Lectin GS-IIA from Molecular Probes

Fluorescent stains from Molecular Probes are available to demarcate several organelle structures. ER-Tracker Blue-White DPX is a highly selective and photostable stain for the ER in live cells. Lysotracker Red, a fluorescent acidotropic probe, is effective at labeling and tracing acidic organelles in live cells at low concentrations. Lectin GS-IIA from *Griffonia simplicifolia* is a lectin that has a high affinity for *N*-acetyl-D-glucosaminyl (GlcNAc) residues of glycoproteins. The Golgi apparatus, in particular the intermediate-to-trans Golgi, is the site of *N*-acetylglucosaminyltransferase activity, and thus, conjugates of lectin GS-IIA would be of value in assessing TGN localization. These fluorescent stains appeared to be ideal for our purposes of performing live-cell imaging.

A preliminary experiment to track the movement of wild-type ATP7B-GFP over 30 min did not reveal trafficking of ATP7B-GFP from the TGN to vesicular structures. The ER tracker defined the endoplasmic reticulum well and showed that there was no co-localization with the ATP7B-GFP signal in a low Cu environment. Lysotracker and Lectin GS-IIA showed non-specific staining and were not useful as organellar markers under the conditions used. The costs associated with the probes prevented comprehensive troubleshooting and studies using these markers were not continued.

C. Fixed cell localization studies of GFP-tagged constructs in CHO cells

CHO cells were transfected with *ATP7B* fusion constructs and fixed in order to assess the localization of our GFP tagged constructs under these conditions. The studies were performed without organelle markers, as well as with an antibody for detecting the TGN (anti-TGN38 antibody) or an antibody for detecting the cis/medial-Golgi (anti-GM130 antibody) to aid in verifying the localization of the expressed constructs.

i. Localization of ATP7B-GFP without the use of an organelle marker

A series of transfections in CHO cells were done with wild-type and mutant *ATP7B-GFP* fusion constructs to determine whether -Cu and +Cu conditions could be differentiated, and whether mislocalized or trafficking-defective mutants could be identified.

A global view of the slides did imply subtle differences between the elevated and reduced Cu conditions, and some cells did localize in the expected distribution pattern (Figure 5-1A). CHO cells were also transfected with previously characterized ATP7B variants (CysProCys/Ser, Asp765Asn, Gly943Ser, Leu776Val) to analyze whether similar results could be obtained with GFP-tagged versions of the constructs and using our conditions (Figure 5-1C to 5-1F). The transfected cells were categorized as TGN-localized, localized to vesicular structures, overexpressed, or showing localization in both the TGN and vesicles (Table 5-1). The -Cu and +Cu conditions were essentially indistinguishable from one another, indicating that further troubleshooting of the conditions would be required or that the GFP tag was influencing the ability of the variants to localize correctly.

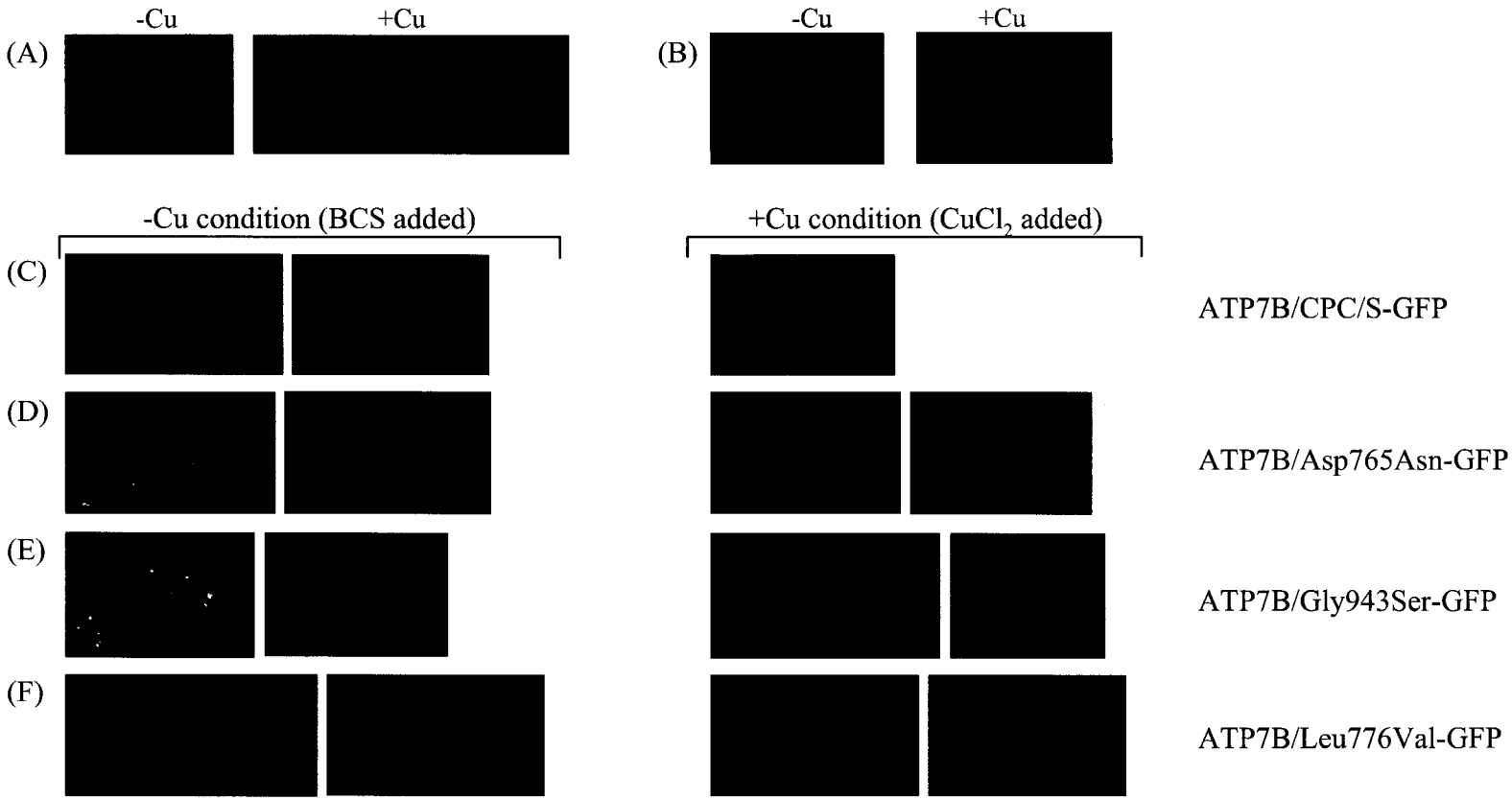

Figure 5-1. Confocal images of transient transfections of CHO cells under low and high copper conditions.

(A) CHO cell transfections with *ATP7B-GFP* constructs (40x lens). ATP7B-GFP was detected using a 488 nm laser, and DAPI stain with a 364 nm laser. -Cu condition, 100 μM BCS for 3 hours; +Cu condition, 200 μM $CuSO_4$ for 3 hours. (B) CHO cell transfections with *ATP7B-pCDNA* expression constructs (40x lens). ATP7B was detected using an antibody against the N-terminus of ATP7B and a 633 nm laser. DAPI stain was visualized using a 364 nm laser. -Cu condition, 100 μM BCS for 3 hours; +Cu condition, 250 μM $CuSO_4$ for 3 hours. (C-F) as per (A), except transfected with mutant *ATP7B-GFP* constructs and no DAPI stain was used. -Cu condition, 100 μM BCS for 3 hours; +Cu condition, 250 μM $CuCl_2$ for 3 hours.

Table 5-1. Categorization of wild-type and mutant ATP7B-GFP in CHO cells under low and high copper conditions.

Variant	-Cu	+Cu	Golgi		Vesicular		Golgi/Vesicular		Overexpressed		Totals	Trafficking results	
			Cells (No.)	Cells (%)	Cells (No.)	Cells (%)	Cells (No.)	Cells (%)	Cells (No.)	Cells (%)		Expected	Observed
Wild-type			35	56.5	10	16.1	15	24.2	2	0.03	62	Golgi	Golgi
Wild-type			38	44.2	24	27.9	22	25.6	2	0.02	86	Vesicular	Golgi
Wild-type			18	38.3	17	36.2	10	21.3	2	4.3	47	Vesicular	Inconclusive
CPC/S			28	45.9	17	27.9	9	14.8	7	11.5	61	Golgi	Golgi
CPC/S			21	50	4	9.5	13	31	4	9.5	42	Golgi	Golgi
CPC/S			17	28.3	17	28.3	15	25	11	18.3	60	Golgi	Inconclusive
CPC/S			30	55.6	12	22.2	8	14.8	4	7.4	54	Golgi	Golgi
Asp765Asn			25	41	15	24.6	18	29.5	3	4.9	61	ER	Golgi
Asp765Asn			24	35.8	27	40.3	16	23.9	0	0	67	ER	Inconclusive
Asp765Asn			13	29.5	20	45.5	10	22.7	1	0.02	44	ER/vesicular	Vesicular
Asp765Asn			13	22	23	39	20	33.9	1	0.02	59	ER/vesicular	Vesicular
Gly943Ser			28	30.4	30	32.6	34	37	0	0	92	Golgi/ER	Inconclusive
Gly943Ser			33	44.6	20	27	19	25.7	2	0.03	74	Golgi/ER	Golgi
Gly943Ser			18	27.7	22	33.8	19	29.2	6	0.09	65	Golgi/ER	Inconclusive
Leu776Val			15	25	21	35	24	40	0	0	60	ER	Vesicular
Leu776Val			36	42.4	30	35.3	19	22.4	0	0	85	ER	Golgi
Leu776Val			28	30.4	37	40.2	27	29.3	0	0	92	ER/vesicular	Vesicular
Leu776Val			18	29.5	22	36.1	19	31.1	2	0.03	61	ER/vesicular	Inconclusive

In spite of optimization to accentuate the distinction between the -Cu and +Cu conditions, the localization of the proteins remained difficult without an organellar marker. Different Cu concentrations (20, 50, 100, 150, 200, or 250 μM of $CuCl_2$), BCS concentrations (50 or 100 μM of BCS) and lengths of incubation times in BCS or Cu (3 or 12 hours) were tried, in accordance with published results (Roelofsen *et al.* 2000).

ii. Use of the anti-TGN38 and anti-GM130 antibodies as organelle markers

A primary antibody against a TGN resident protein, TGN38, was used to facilitate the subcellular localization of ATP7B-GFP. Wild-type ATP7B-GFP-transfected CHO cells were fixed, and localization was analyzed using a sheep anti-rat TGN38 primary antibody (Serotec) and a mouse anti-sheep secondary antibody conjugated to Texas Red (assisted by Ms. Christine Franz, Dr. Bleakley, University of Alberta). The anti-TGN38 primary antibody did not show cross-reactivity in the CHO cell line.

A mouse primary antibody against a cis/medial Golgi protein, GM130, was also used on wild-type ATP7B-GFP-transfected CHO cell lines. The GM130 antibody did not co-localize with ATP7B-GFP, and was not useful in further delineating the localization of our construct. The fusion construct also did not co-localize with calnexin, a marker for the ER (data not shown).

D. Fixed cell localization of ATP7B/pCDNA constructs in CHO cells

To analyze whether the GFP tag was causing aberrant localization results, CHO cells were transfected with an ATP7B/pCDNA construct, which has been previously used and shown to localize correctly and traffick under +Cu conditions (Forbes and Cox 2000). For detecting ATP7B expression, the primary antibody against the N-terminus of human ATP7B worked better than the C-terminus antibody. These preliminary results were comparable to that seen with the GFP constructs. An overall snapshot of the slides indicated differences and cells representing the expected expression of ATP7B could be identified (Figure 5-1B); however, the distinction would not be certain enough for assessing the required trafficking function of different ATP7B variants.

E. Fixed cell localization studies of ATP7B-GFP fusion constructs in hepatic cell lines

i. Localization studies in Huh7 cells using anti-AP-1 and anti-Golgi 58K antibodies

The human hepatoma cell line, Huh7, has been previously transfected with *ATP7B-GFP* constructs, and has demonstrated Cu-dependent localization of wild-type ATP7B (Huster *et al.* 2003). The more biologically relevant hepatic cell line would also be a more accurate representation of ATP7B expression in human hepatocytes.

Experiments with Huh7 used the mouse monoclonal anti- -adaptin (AP-1) primary antibody, which recognizes the Golgi adaptor complex AP-1, for TGN identification. AP-1 is primarily localized to the TGN and has been used in other ATP7B localization studies (Hung *et al.* 1997; Yang *et al.* 1997; Schaefer *et al.* 1999b). A Western blot was performed on cell lysates from CHO cells, COS-7 cells, HEK293 cells, Huh7 cells and HepG2 cells to determine the cross-reactivity of the TGN antibody with AP-1 in these cell lines. A sheep anti-mouse secondary antibody conjugated to horseradish peroxidase was used for detection, and showed expression of AP-1 in all cell lines, except in the CHO cell line (Figure 5-2).

Transfection efficiencies of Huh7 cells were typically low, between 10-30%. With the Leica fluorescence microscope, the ATP7B-GFP signal showed limited overlap with the anti-AP-1 TGN marker (Figure 5-3A), and not all ATP7B-GFP-expressing cells demonstrated this co-localization under low Cu conditions. ATP7B-GFP appeared to redistribute in response to elevated Cu in some cells (Figure 5-3B).

To find a marker to overlap with ATP7B-GFP expression, the monoclonal anti-Golgi 58K primary antibody (Sigma), a general Golgi apparatus marker, and goat anti-mouse secondary antibody conjugated to Alexa Fluor 594 (gift from Dr. R. Wevrick) were used; however, the anti-Golgi 58K and ATP7B-GFP signals did not appear to co-localize well in basal Cu conditions either. As expected, anti-Golgi 58K was not as tight to the nucleus as the anti-AP-1 primary antibody (Figure 5-3C and 5-3D).

Incubation in 200 μM $CuCl_2$ for 2-4 hours appeared to result in an overall more punctate staining than under basal conditions (Figure 5-3E and 5-3F).

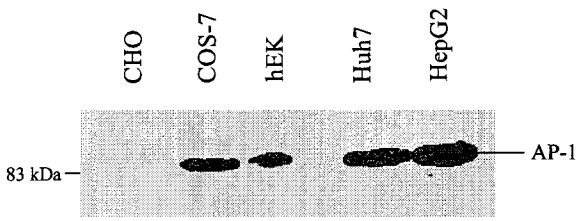

Figure 5-2. Western blot analysis of AP-1 expression in mammalian cell lines.

Untransfected mammalian cell lines were cultured to confluency and then lysed to prepare whole cell lysates. Lysates (15 μg) were analyzed by SDS/PAGE and transferred to a nitrocellulose membrane. AP-1 protein was detected by using mouse monoclonal anti-AP-1 antibody (1:300 dilution) and sheep anti-mouse secondary antibody conjugated to horseradish peroxidase (1:10,000 dilution).

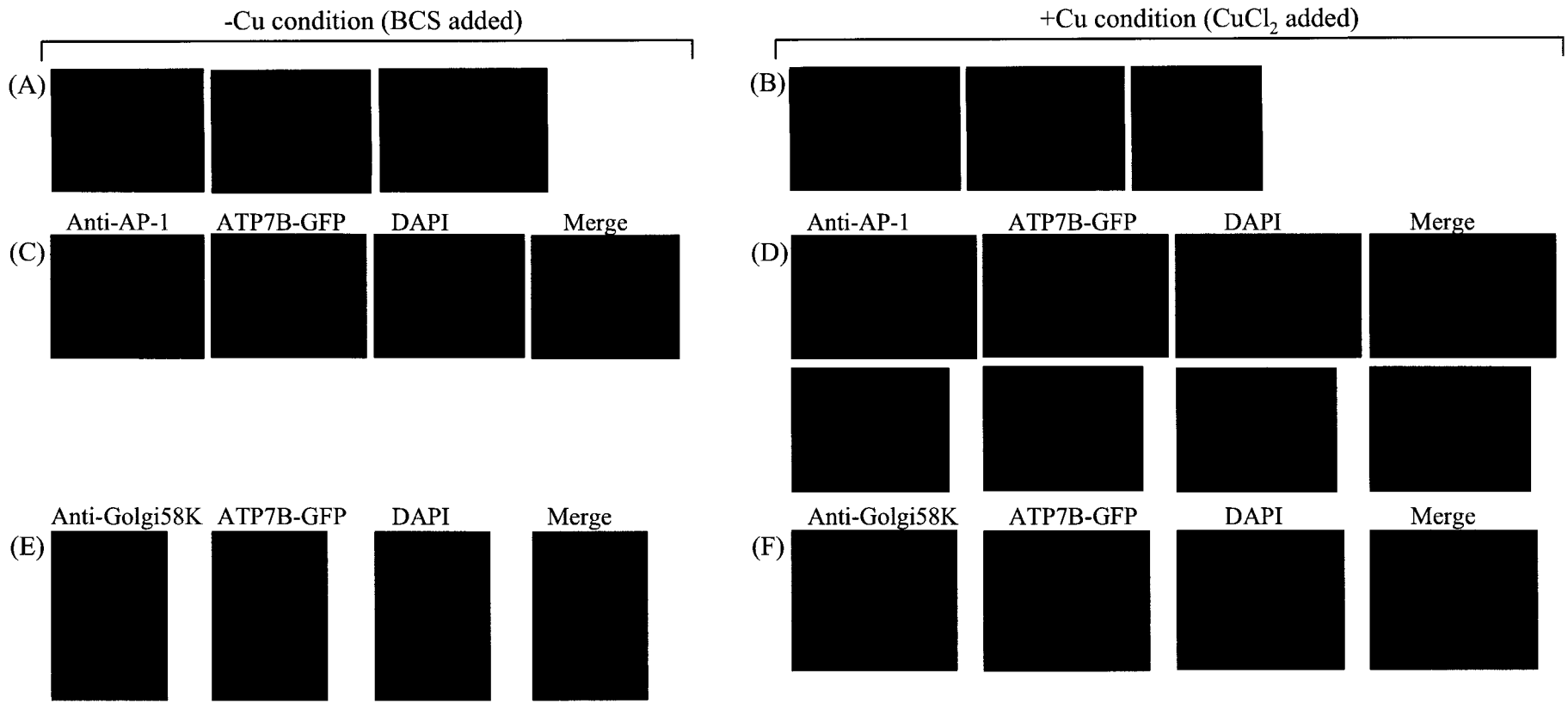

Figure 5-3. Transient transfection of Huh7 cells with *ATP7B-GFP* expression constructs under low and high copper conditions. (A) and (B) Confocal images of transfections. ATP7B-GFP; detected using a 488 nm laser on the Zeiss laser scanning confocal microscope and a 40x objective lens. DAPI stain; visualized using a 364 nm laser. (C) and (D) Fluorescent microscope images using a 100x oil immersion lens. Anti-AP-1; used to detect the TGN and visualized using a rhodamine filter. ATP7B-GFP; detected using a FITC filter cube. Nucleus; recognized using a DAPI filter cube. Merged images done using the Northern Eclipse software. (E) and (F) as per (C) and (D), except anti-Golgi 58K was used to detect the Golgi. -Cu, incubation with 100 μM BCS for approximately 3 hours; +Cu, incubation with 250 μM $CuCl_2$ for approximately 3 hours.

Under closer scrutiny, however, it was difficult to be convinced of trafficking as there were still a significant number of cells showing Golgi-localization under the elevated Cu condition and localization in many of the transfected cells could not be positively determined.

ii. Localization studies in HepG2 cells using anti-AP-1 and anti-MRP2 antibodies

HepG2 cells have also been previously used in subcellular localization of ATP7B (Hung *et al.* 1997; Yang *et al.* 1997; Lutsenko and Cooper 1998). Polarized hepatic cells are particularly biologically relevant, as ATP7B has been shown to specifically traffick to the apical membrane rather than the basolateral membrane under high Cu conditions (Roelofsen *et al.* 2000; Guo *et al.* 2005). The HepG2 cells were difficult to propagate in a monolayer since the cells preferred to grow in multilayer clusters, rather than in a single layer. The cells could be grown as a relatively confluent monolayer by seeding lightly, washing off the larger piled cells and growing over a longer period, yet the transfection efficiencies were still low (between 5-20%) and the cells rarely looked healthy upon transfection. The transfection efficiency of the HepG2 cells was moderately improved by using less LF transfection reagent with DMEM serum-free medium, and by changing the transfection medium six hours following the addition of the transfection reagent.

The anti-AP-1 antibody worked well in defining the TGN in the HepG2 cells and the anti-MRP2 primary antibody was useful in identifying the apical membrane of the polarized cells (Figure 5-4A). The anti-AP-1 signal appeared to co-localize with the GFP signal under low Cu conditions in a few cells (Figure 5-4B), but no overlap of signals was seen with the anti-MRP2 antibody under high Cu conditions (Figure 5-4C).

Similar to Huh7, ATP7B-GFP expression was punctate and diffuse in staining in high Cu when compared with the low Cu environment (BCS added); however, a comparison between the two conditions revealed only subtle differences and Cu-induced redistribution could not be confirmed. Despite different Cu concentrations (50, 100 or 200 μM $CuCl_2$/$CuSO_4$) and incubation times (2, 4 or 12 hour incubations in Cu or BCS) to optimize trafficking of the fusion constructs, the distinction between the two conditions remained ambiguous.

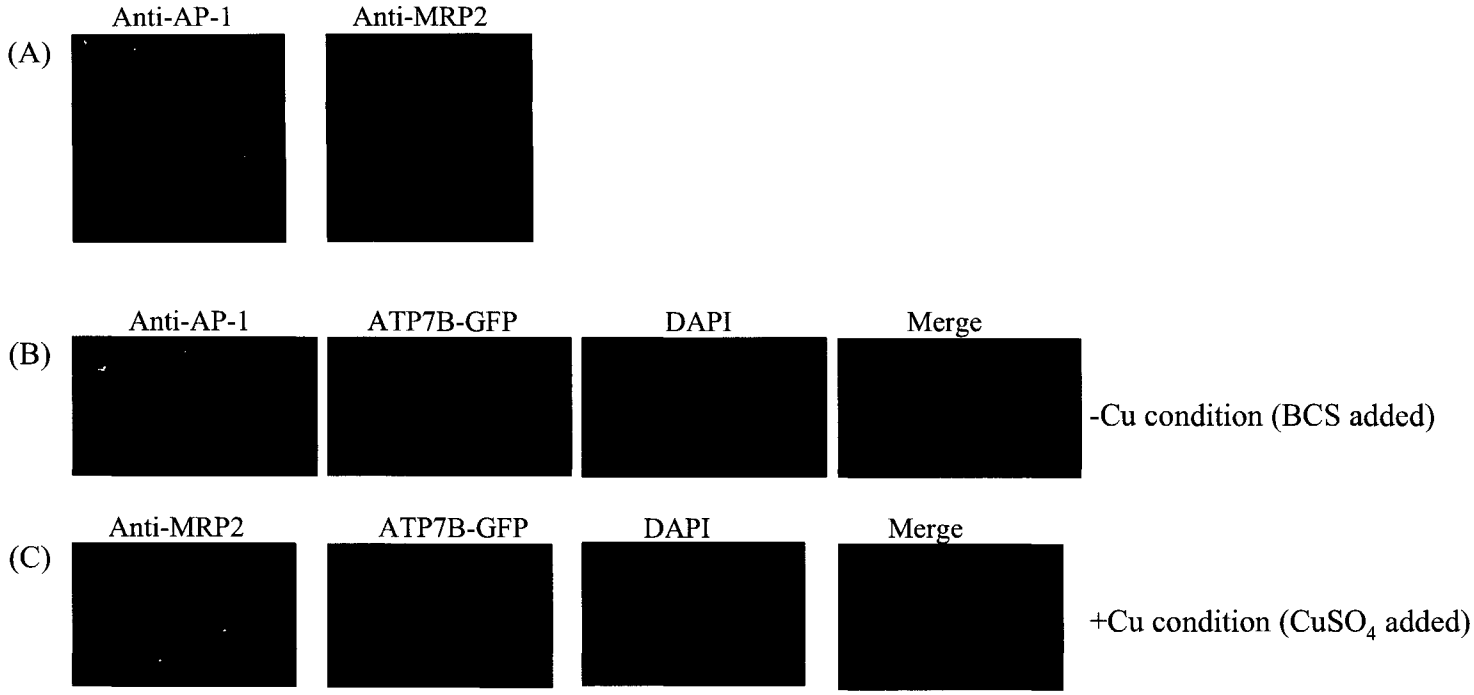

Figure 5-4. Fluorescent images of HepG2 cells.

(A) Images depicting anti-AP-1 and anti-MRP2 detection of the TGN and apical membrane of HepG2 cells, respectively. AP-1 and MRP2 were visualized using the rhodamine filter cube, and the nucleus was visualized using the DAPI filter cube. Images shown are merged images. Microscopy was performed using a 40x lens with oil immersion. (B) Images of transient transfections of HepG2 cells with *ATP7B-GFP* expression constructs under low Cu conditions (100 μM BCS for 12 hours). Anti-AP-1 was used to detect the TGN and was visualized using a rhodamine filter. ATP7B-GFP was detected using a FITC filter cube, and the nucleus was visualized using a DAPI filter cube. Images were merged using Northern Eclipse software. (C) as per (B), except under high Cu conditions (200 μM $CuSO_4$ for 4 hours), and using anti-MRP2 antibody to detect the apical membrane instead of a TGN antibody. Microscopy of (B) and (C) were performed using a 100x lens with oil immersion.

IV. DISCUSSION

The experiments in this chapter were designed to improve upon the current methods used in our laboratory for analyzing the Cu-dependent distribution of wild-type and mutant ATP7B proteins. In particular, a more high-throughput system for examining subcellular localization in a biologically relevant cell line was preferred. To this end, several steps have been examined for their utility in assessing the required trafficking function of ATP7B variants, including: 1) the creation of *ATP7B* cDNAs tagged at their N-terminus with the naturally fluorescent protein GFP to avoid the use of antibodies; 2) the use of techniques for live-cell imaging of ATP7B-GFP within a cell; 3) the analysis of localization in fixed ATP7B-GFP-transfected CHO cells; and 4) the analysis of hepatic cell lines (Huh7 and HepG2) for their use in examining subcellular distribution of ATP7B-GFP constructs. The cell lines and markers used are summarized in Table 5-2.

A. LIVE-CELL IMAGING TECHNIQUES

Live-cell imaging would circumvent the need for cell fixation and indirect immunofluorescence, and would also facilitate the determination of the pathway assumed by ATP7B while moving through the cell. Both the LCSL vectors and fluorescent stains as organellar markers would enable live-cell imaging of transfected mammalian cells.

The cyan fluorescence of the LCSL vector constructs, however, could not be differentiated from the green fluorescence of our fusion proteins. A possible alternative would be to subclone the specific proteins in the LCSL vectors into a different vector, such as a DsRed-type vector (e.g. Clontech), which would create a fusion construct emitting red fluorescence when excited, and thus be distinguishable from green fluorescence (emission wavelength of 505 nm). Likewise, the *ATP7B* cDNAs could be cloned into a different vector to generate fusion constructs which fluoresce in a color distinct from cyan.

The Molecular Probe stains could have been particularly useful, yet the results were inadequate to justify further investigation as the cost of these fluorescent probes far outweighed the potential benefits of the system and extensive troubleshooting could not be rationalized. Due to the limited success of both the LCSL vectors and the Molecular Probe stains, we directed our efforts toward fixed cell studies.

Table 5-2. Summary of cell lines and organelle markers used in the analysis of ATP7B-GFP subcellular localization.

Cell line	Fixed/Live	Organelle Marker	Target	Marker Result	Localization Result
CHO cells	Live cell imaging	*Clontech - LCSL vectors*			--
		pECFP-ER	ER	indistinguishable from GFP	--
		pECFP-Golgi	TGN	indistinguishable from GFP	--
		pECFP-mem	plasma membrane	indistinguishable from GFP	--
CHO cells	Live cell imaging	*Molecular Probes*			no trafficking in real-time
		ER-tracker	ER	no co-localization	--
		Lysotracker red	acidic organelles	non-specific staining	--
		Lectin GS-IIA	TGN	non-specific staining	--
CHO cells	Fixed	no organelle marker	--	--	too ambiguous - only subtle differences
		anti-AP-1 antibody	TGN	no cross-reactivity	--
		anti-TGN38 antibody	TGN	no cross-reactivity	--
		anti-GM130 antibody	cis/medial-Golgi	no co-localization	--
Huh7 cells	Fixed	anti-AP-1 antibody	TGN	limited overlap	appeared to traffic in high Cu, but too ambiguous for use as an assay
		anti-Golgi 58K antibody	general Golgi	limited overlap	
HepG2 cells	Fixed	anti-AP-1 antibody	TGN	some co-localization	appeared to traffic in high Cu, but too ambiguous for use as an assay
		anti-MRP2 antibody	apical membrane	no overlap	

B. The complexities of using fixed ATP7B-GFP-transfected CHO cells for localization studies

Cu-dependent localization studies of ATP7B-GFP were performed in CHO cells since they have been well received amongst researchers analyzing the subcellular distribution of ATP7B and the related protein ATP7A. CHO cells propagate easily as a monolayer and the morphology of the cells permits the discernment of distinct organelles and movement from the TGN to vesicular compartments. Furthermore, wild-type ATP7B cloned in a pCDNA expression vector has been successfully transfected in CHO cells and has shown the appropriate localization results in our laboratory (Forbes and Cox 2000).

The examination of ATP7B-GFP-transfected CHO cells for localization within -Cu and +Cu conditions was ambiguous without the use of an antibody against a TGN-resident protein. ATP7B-GFP expression indicative of TGN localization under low Cu and expression reminiscent of vesicular localization under high Cu were identifiable; however, the distinction between these two conditions was not definitive. Since ATP7B continuously cycles between the TGN and a vesicular compartment (Hung *et al.* 1997; Schaefer *et al.* 1999a), not all transfected cells will show punctate staining in response to Cu. Nevertheless, the difference between the two conditions must be sufficient enough for use as an assay for assessing mutant variants. The weight of the localization results would be improved with the use of an antibody to the TGN and co-localization studies.

i. TGN marker for co-localization studies in CHO cells

An ideal TGN marker would show co-localization with the wild-type ATP7B-GFP construct in low Cu conditions, and movement of ATP7B-GFP away from the TGN marker into vesicular structures in high Cu conditions. Since the localization of ATP7B-GFP was difficult without a TGN marker, it seems that an appropriate organellar marker is necessary to aid in examining the trafficking ability of ATP7B variants.

The inability of the rat anti-TGN38 antibody to cross-react in the CHO cell line was unfortunate given its localization within the TGN. Other studies have used an antibody against Golgi 58K, a general Golgi marker, in CHO cells and this protein has shown

significant overlap with wild-type ATP7B (Forbes and Cox 2000); therefore, the use of this Golgi marker could be valuable for future studies.

C. Establishing hepatic cell lines for use in immunofluorescence studies

The study of the localization of ATP7B and ATP7B variants was proposed to be best performed in a biologically relevant cell line, such that the conclusions drawn from the experiments would be more applicable. Thus, although CHO cells have had a positive history in the research community, experiments were designed to establish an immunofluorescent protocol using a human hepatic cell line.

i. Localization studies in the Huh7 cell line

The Huh7 cell line is an adherent hepatoma cell line that grows in a monolayer with a discernible cell body. ATP7B results in Huh7 cells to-date have been inconsistent, with some studies demonstrating ATP7B-GFP residence within late endosomes (Harada *et al.* 2000a; Harada *et al.* 2000b; Harada *et al.* 2001; Harada *et al.* 2005) and a lack of trafficking in response to higher levels of Cu (Harada *et al.* 2000a; Harada *et al.* 2005); and other studies showing ATP7B-GFP localization within the TGN in the presence of Cu chelator (100 μM BCS) and Cu-dependent trafficking into a more diffuse vesicular distribution in the presence of elevated Cu (200 μM $CuSO_4$) (Huster *et al.* 2003). Given these differences in results and since Huh7 cells are so amenable to localization studies, our ATP7B-GFP construct was examined in the Huh7 cell line. Huh7 cells possibly do not support the correct localization of ATP7B like other cell lines which have been conducive to ATP7B trafficking, perhaps due to the lack of a necessary factor (Harada *et al.* 2000a).

The TGN marker AP-1 and ATP7B-GFP fluorescent signals did not overlap, possibly supporting the theory that ATP7B does not localize within the TGN in Huh7 cells. However, given the complexity of the mammalian cell, it is possible that AP-1 and ATP7B are localized in different TGN buds. In fact, it has been shown that the TGN is composed of different lipid microdomains, and that ATP7B is associated with a particular lipid microdomain in the TGN and remains associated with the same microdomain following transport to the bile canalicular surface (Slimane *et al.* 2003). These results indicated a lipid-raft mediated transport of ATP7B from the TGN, rather than a clathrin-dependent

mechanism, in which AP-1 is involved. This correlates with the ATP7A studies that have identified a novel membrane traffic route from the TGN to the cell surface (Cobbold *et al.* 2002), independent of clathrin-coated vesicles (Cobbold *et al.* 2003). Therefore, it is plausible that the transport pathway of ATP7B is likewise novel and that a different adaptor protein, such as AP-4, which is not enriched in clathrin-coated vesicles (Robinson 2004), facilitates the trafficking of ATP7B.

Furthermore, both the endocytic (cell surface to TGN) and exocytic pathways (TGN to cell surface) may involve trafficking through endosomal compartments. Thus, localization in the TGN versus localization in endosomes could possibly be difficult to separate, and the inconsistent results seen with Huh7 cells may not be that contradictory. Overexpression of ATP7B-GFP also appears to result in the detection of GFP in puncta throughout the cell under low Cu conditions and no change in distribution in elevated Cu conditions (Guo *et al.* 2005), which would explain the late endosomal localization seen in some studies. Stable transfections would alleviate overexpression of ATP7B-GFP in Huh7 cells, and the use of an organelle marker for co-localization and the right Cu conditions to accentuate the differences between the low and high Cu conditions would permit the use of this cell line as an assay.

ii. Localization studies in the HepG2 cell line

Due to the possible inconsistencies with Huh7 cells, the HepG2 cell line, a liver hepatoblastoma line that expresses endogenous protein, was also transiently transfected. The endogenous protein shows distinct TGN localization in steady state conditions with considerable overlap with AP-1, as well as redistribution to a cytoplasmic vesicular compartment upon addition of 200 μM $CuSO_4$ for 2 hours (Hung *et al.* 1997). HepG2 cells can be polarized and thus are more biologically relevant for analyzing the apical localization of ATP7B (Roelofsen *et al.* 2000). The vacuolar appearance and difficulty of culturing HepG2 cells, however, made the transfection efficiencies low and the distinction between the +Cu and -Cu conditions difficult.

The co-localization of ATP7B-GFP with AP-1 in some cells was promising. The increased Cu conditions promoted a more punctate staining pattern in some cells, however, the GFP

signal did not show overlap with the apical marker, MRP2. This could possibly be due to the level of extracellular Cu, in that the concentration of Cu or the length of incubation in the supplemented medium was not sufficient to induce robust trafficking to the apical membrane. Additional troubleshooting may improve the number of trafficking-positive cells under the high Cu conditions and ensure a tighter TGN localization under low Cu conditions.

D. Limitations of our cell studies and the future direction of trafficking studies

The most prominent concern with all the experiments has been the use of GFP as a tag. Our problems with distinguishing between localization under -Cu and +Cu conditions may stem from having such a large tag at the N-terminus of the ATP7B cDNA. The tag could possibly disrupt ATP7B protein folding at the N-terminus and/or conceal a necessary signal for localization and trafficking. Since the first 63 amino acids of the N-terminus are important for trafficking (Cater *et al.* 2004; Guo *et al.* 2005), the presence of the GFP tag at the N-terminus may be problematic. Although not all metal-binding sites in the N-terminal Cu-binding domain are necessary for localization, a disruption of the fold of the N-terminus could influence the necessary factors in the requisite metal binding sites (MBS 5 or MBS 6) and likely impede correct subcellular distribution.

The difficulties encountered with our trafficking studies may be due to the limitations of using cultured cells, such as possible effects of overexpression of the protein on its localization (Guo *et al.* 2005), a potential lack of proper targeting and trafficking components in host cells in a case of heterologous expression, and suboptimal transfection ratios. Stable transfections, instead of transient transfections, may improve the vigour of our transfected cells and reduce overexpression; however, a method that allows the testing of a large number of variants in a relatively quick and easy fashion is preferable. Our studies indicate that designing such a system is difficult, with many aspects to consider, especially given the use of a biological system and a pathway that is complex and depends upon other cellular factors and components.

The recommendations that stem from this chapter include: 1) initial testing of ATP7B/pCDNA constructs in cell lines to determine appropriate Cu conditions; 2) the

preferable use of a more biologically relevant cell line, such as polarized HepG2 cells, or the rat-human hybrid WIF-B hepatic cell line that has been used for trafficking studies (Guo *et al.* 2005); 3) the necessity of appropriate organelle markers for co-localization; 4) testing ATP7B tagged with GFP at the C-terminus and N-terminus if live-cell imaging is to be used; and 5) creating stable cell lines for more accurate examination. In its current state, our assay for assessing the required trafficking function of ATP7B variants is not sufficient for determining the effect of a mutation and the possible consequences for an individual having such a sequence change in their DNA. However, the identification of cells that demonstrated the expected distribution patterns indicates the potential of our assay; thus, further studies are warranted.

CHAPTER 6:
Discussion

The study of the function of ATP7B and its relation to the Cu metabolism disorder, WND, has not wavered since the discovery of the gene in 1993. At the time this thesis was initiated, the role of ATP7B in the Cu transport pathway, especially within the hepatocyte, was just being revealed. Assays were being developed to investigate the significance of ATP7B in balancing the essentiality and toxicity of the metal ion. As the predicted protein product was determined to belong to the conserved family of P-type ATPases, it was expected that certain signature functional domains would likely be essential for the function of ATP7B. Accordingly, studies have focused in on these specific regions of the protein to define their roles in the overall function of ATP7B.

Analyzing the significance of different regions and amino acid residues of the WND protein is important, and thus intriguing, for several reasons. First, it serves to further characterize the biological role of the entire protein in Cu homeostasis. Understanding why specific domains are essential aids in our understanding of the overarching biochemical and physiological function of ATP7B and its role in health and disease. Second, studying isolated regions and explicit patient mutations identifies certain amino acids and domains critical for function, which is useful in the diagnosis of WND and the mutation detection procedure. Given the large number of mutations identified in WND patients and the cost of molecular diagnosis, an efficient screening process is useful. The third reason, which is related to the second, is that the analysis of specific WND mutations is beneficial in distinguishing between true disease-causing mutations and those that are rare normal variants. This is especially imperative with WND since early treatment of the disease is crucial for preventing irreversible liver damage. Fourth, the characterization of essential regions in ATP7B is valuable in elucidating the significance of these domains in related proteins and in possibly identifying the function of unknown protein products with similar amino acid sequences.

The evaluation of mutant ATP7B variants, in particular, has been crucial over the past few years in exposing important amino acids and regions of the protein. In the process, our understanding of the role of ATP7B in Cu homeostasis and our knowledge of mammalian Cu homeostasis pathways has been expanded. The general aim of this thesis has been to further characterize the ATP7B protein by studying the mutation spectrum and several

mutant variants for their functional capability. By performing such experiments, our goal was to elucidate additional amino acids and regions important for maintaining Cu homeostasis within the cell and mammalian system. Various resources were used, including the mutation spectra of both WND and MNK, a well-developed yeast functional assay, and an immunofluorescence procedure for examining intracellular localization.

The comparison of the mutation spectra of the *ATP7A* and *ATP7B* genes in Chapter 2 of this thesis illustrated that the conserved functional domains found in the Cu transporters were the sites of a majority of the missense mutations. However, mutations were not limited to conserved domains and it is evident that the list of mutations thus far identified in WND patients is not exhaustive. This was apparent from our comparison with the *ATP7A* mutation spectrum, which highlighted additional regions in the *ATP7B* gene to investigate for other disease-causing sequence alterations. From the mutation spectrum analysis, regions were selected for further examination using the yeast functional assay. The three areas chosen for study were based on different criteria: (i) the cytosolic C-terminus, which has no identified conserved functional domains and a limited number of WND and MNK patient mutations identified; (ii) the ATP-BD, a conserved domain with a plethora of WND and MNK mutations; and (iii) a segment of the N-terminal CuBD thought to be important given the *ATP7A* mutation spectrum.

I. ROLE OF THE CYTOSOLIC C-TERMINUS

The major hypothesis with respect to the importance of the cytosolic C-terminal tail is that this part of the protein is necessary for the Cu transport function and/or Cu-dependent localization of ATP7B. This prediction has stemmed mainly from the identification of patient mutations within the region and from studies performed in the related protein ATP7A. There are di-leucine motifs (tri-leucine in ATP7B) in the C-termini of both ATP7A and ATP7B, which have been shown to be important for endocytic signaling in a number of secretory proteins. This role in signaling has been demonstrated with ATP7A, where the di-leucine motif is necessary for internalization from the PM. The C-terminus may also be critical for interacting with another protein essential for its Cu transport

function, for Cu-dependent distribution, or for regulation. Thus, the goal of the work in the section of the thesis on the C-terminus (Chapter 3) was to determine which sequences in the cytosolic tail are important for ATP7B function.

A. Requirement for the cytosolic C-terminal tail in correct folding of ATP7B

The cytosolic C-terminus of ATP7B was examined for its contribution to Cu transport. Mutant variants which altered or deleted portions of this protein were generated and analyzed using the yeast functional assay. Although many have acknowledged that the main role of this region would be in intracellular localization, it was possible that the Cu transport function of the variants would likewise be affected, especially given the link between the Cu transport function of ATP7B and the ability of the protein to traffick (Strausak *et al.* 1999; Voskoboinik *et al.* 1999; La Fontaine *et al.* 2001; Petris *et al.* 2002).

From the analysis performed in Chapter 3, it is evident that the role of the C-terminus in Cu transport is not direct; rather, it is necessary for the overall structural integrity of the protein, being integral for the formation of the correct TM topology. A deletion of the entire cytosolic tail (4117) destabilized the last TM domain, producing aberrant expression in the yeast cell. By affecting the TM topology, the deletion likely disrupted the proper folding or processing of the protein product in the ER, causing: (i) aggregation and/or accumulation of the protein within the ER, which elicits a cellular unfolded protein response that attempts to orchestrate the correct folding of the protein; (ii) possible degradation by proteases within the lysosome; or (iii) degradation through the ER quality control machinery, which recognizes terminally misfolded or incompletely folded proteins and efficiently removes them from the secretory pathway by "retro-translocating" the proteins to the cytoplasm for proteasome-mediated degradation (Brodsky and McCracken 1999; Chevet *et al.* 2001). Aggregation within the ER and/or ER-associated protein degradation via the proteasome would explain the low expression levels on Western blots and the mislocalization to a membrane protein fraction distinct from wild-type ATP7B, resulting in lack of Cu transport activity.

This explanation was further confirmed by the finding that the addition of just three additional amino acids (4126) allowed the last TM domain to traverse the membrane,

resulting in measurable Cu transport activity. The three amino acids could be necessary for Cu transport activity; however, they are not sufficient for full Cu transport function. The more likely explanation would be that the three amino acids stabilized the protein product sufficiently for it to be expressed and function in Cu transport. The data from the other deletion variants that retain more of the C-terminal sequence (4213 and 4360) affirm this hypothesis. These deletion variants were expressed at normal levels on Western blot and demonstrated wild-type levels of Cu transport activity in the yeast assay, suggesting that structural stability of the C-terminus was required for full Cu transport function, instead of a critical sequence.

i. Future directions

To substantiate our findings, it is necessary to demonstrate the intracellular localization of the deletion variants and verify their mislocalization compared with wild-type ATP7B localization in the yeast *ccc2* mutants. One method would be the performance of subcellular fractionization of the yeast cells transformed with the mutant constructs.

Studies have also used immunofluorescence techniques for intracellular localization in yeast. In fact, the intracellular localization of Ccc2p has been shown to be restricted to a late- or post-Golgi compartment in *S. cerevisiae* (Yuan *et al.* 1997), and the manganese SOD protein has been localized to intracellular vesicles rather than the PM by immunofluorescence microscopy (Luk and Culotta 2001). More recent studies have indicated that, despite the size of the yeast cell, more precise localization is possible in the *S. cerevisiae* strain. For example, vacuolar and ER localization has been illustrated (Unno *et al.* 2005), as well as a distinction between Golgi/endosomal localization and localization within a prevacuolar endosomal compartment (Johnston *et al.* 2005). Studies on the Cu transport pathway in the yeast strain, *Schizosaccharomyces pombe*, has further elucidated the possibilities of intracellular localization within yeast by establishing vacuolar (Bellemare *et al.* 2002) and cytosolic (Laliberte *et al.* 2004) expression of proteins involved in Cu metabolism. Therefore, immunofluorescence microscopy of these deletion variants is a feasible method for corroborating the data presented in this thesis.

In addition to the localization studies, it would be interesting to determine whether the three additional amino acids in the 4126 variant play a more direct role in the Cu transport function of ATP7B, rather than only a structural role. The amino acids could each be mutated and evaluated for their Cu transport ability in the yeast assay.

It was surprising to find that the other WND patient mutations had normal or near normal Cu transport capability; however, as indicated throughout this thesis, these variants could affect the ability of the proteins to traffick or localize correctly, or could affect some aspect of ATP7B function that is not revealed using the yeast functional assay.

Another role for the C-terminus could be in the protein kinase-dependent phosphorylation of ATP7B, as it contains several potential serine residues that could be phosphorylated and possibly be associated with re-distribution under conditions of elevated extracellular Cu (Vanderwerf *et al.* 2001; Vanderwerf and Lutsenko 2002). Furthermore, it has been shown that part of the cytosolic C-terminus (Ser-796 to Tyr-1384) is important for the basal phosphorylation of ATP7B under low levels of Cu. As this phosphorylation has been connected to the response of the protein to varying Cu environments and the intracellular distribution of ATP7B, these C-terminal mutant variants could be assessed for phosphorylation and their resultant localization in +Cu and -Cu environments.

As discussed in Chapter 3, the C-terminus of ATP7B may also interact with a regulatory protein that inhibits or activates the Cu transport function of the protein, as demonstrated with the sarco(endo)plasmic reticulum Ca^{2+}-ATPases (SERCAs). With SERCA, two inhibitory proteins, phospholamban (Tada and Kadoma 1989; Simmerman and Jones 1998) and sarcolipin (Odermatt *et al.* 1998; Asahi *et al.* 2002), bind the ATPase alone or in combination, at low Ca^{2+} concentrations to lower the apparent affinity of SERCA. Such regulation may also occur with ATP7B, and studies should be aimed at identifying proteins that interact with and regulate ATP7B function, possibly by associating with the cytosolic C-terminus.

B. Role of the di-leucine motif

It is unknown whether the leucine motif in the C-terminus of ATP7B is itself directly important for ATP7B Cu transport function. Deletion of the 11 C-terminal-most amino

acids of ATP7B (4360), which includes all three leucines, does not affect the Cu transport function of the protein; whereas, mutation of all three leucines to alanines (LLL>AAA) abolished the ability of the variant to grow in Fe-limited medium (Chapter 3). Thus, it appeared from the complementation assay, that the mutation of the leucines was more detrimental to the function of the protein than deletion of the motif and amino acids C-terminal to the motif.

There are a few scenarios which could explain the affect of the alanine mutation construct (LLL>AAA) in the yeast complementation assay: (i) the presence of the alanines, rather than the leucines, could upset the secondary structure of the protein by interacting or disrupting interactions with other regions of the protein, and thus disable the Cu transport function of the variant; (ii) by creating an abnormal structure, the mutation could expose a signal that is normally unavailable to the cytoplasmic machinery, which may disrupt Cu transport function or result in the aberrant trafficking of the protein to another intracellular location that precludes Cu transport; or (iii) the mutation could shield a sequence or amino acid critical for Cu transport function or some other aspect of ATP7B function. Therefore, the lack of functional complementation in the yeast system may be a secondary consequence of a problem in structure and the relative exposure of signal sequences or amino acids, instead of the leucine residues having a direct role in Cu transport. The 4360 construct, on the other hand, could retain such a sequence and thus be capable of complementing the Fe-deficient phenotype of the *ccc2* mutant yeast.

In certain sequence contexts, the leucine residues have been shown to be part of a larger targeting motif, and other surrounding amino acids are critical for correct localization within the cell and thus correct function of the protein (Pond *et al.* 1995; Kang *et al.* 1998; Setaluri 2000; Johnson *et al.* 2001). As the leucine residues are part of a larger secondary structure recognized by intracellular machinery, the alteration of the leucines to alanines may be more disruptive than the deletion of the entire targeting motif.

i. Future directions

The research conducted in this thesis has not revealed the exact contribution of the leucine motif to ATP7B function. The leucine residues may be critical amino acids for Cu

transport or may in fact be a key targeting motif in the sequence context of ATP7B and necessary for the retrieval of the protein back to the TGN from vesicular compartments or the apical membrane in polarized cells.

From the studies performed in Chapter 3, it is clear that all three leucines or the two distal leucines or at least the distal-most leucine must be mutated for Cu transport to be compromised. Additional mutations of the leucine motif have been generated (p.LLL>LAL, LLL>LLA, LLL>LAA) to determine whether mutation of only the distal-most leucine is sufficient to result in full abrogation of Cu transport ability. In addition, the localization of the leucine mutant variants should be evaluated in mammalian cells.

The leucine residues are likely involved in the correct localization of ATP7B, especially since a di-leucine motif in the same sequence position in ATP7A is critical for the internalization of ATP7A from the PM. The di-leucine motif is generally recognized by adaptor proteins (APs), which bind sorting motifs in the cytoplasmic domains of membrane proteins that traffick within the cell, and assist in the direct transport of these proteins to their target membranes. The type of di-leucine motif present in ATP7A and ATP7B has been shown to bind to AP complexes *in vitro*. AP-1 and AP-2 are both highly enriched in purified clathrin-coated vesicles, and localize to the TGN/endosomes and the plasma membrane, respectively; on the other hand, AP-3 and AP-4 appear to function independently of clathrin, and localize to the endosome and TGN, respectively (Robinson 2004). Since the endocytic pathway followed by ATP7A has been shown to be clathrin-independent, it is unknown whether the internalization of ATP7A from the PM is associated and depends upon an interaction with AP-2.

Recent evidence might suggest a role for the clathrin-independent AP-3 in the correct intracellular sorting of ATP7B. Di-leucine-based signals in the cytoplasmic domains of certain membrane proteins are required for binding to AP-3 and delivery to lysosomes or lysosome-related storage granules from the TGN/endosomes (Honing *et al.* 1998; Odorizzi *et al.* 1998; Setaluri 2000). Thus, the di-leucine motif in ATP7B may play a similar role in exocytic trafficking, delivering the protein to a specific target organelle in the cytosol using AP-3 as the adaptor protein. Studies demonstrating an interaction or a lack of an

interaction with these APs would clarify the trafficking pathways followed by ATP7A and ATP7B, and define the role of the di-leucine motifs.

A tyrosine-based targeting motif YXX (is a large hydrophobic amino acid residue) is also present in the cytoplasmic C-termini of both ATP7A and ATP7B. The di-leucine motif in ATP7A has been shown to be sufficient for the internalization of the protein from the PM; however many membrane proteins have multiple targeting signals, with some being secondary or present for alternative paths to target organelles (Setaluri 2000). Further investigations are necessary to define the role, if any, of the tyrosine motif in the localization and trafficking of ATP7B.

II. STUDIES OF THE ATP-BINDING DOMAIN

The ATP-BD in P-type ATPases is critical for the catalytic cycle of the transporters and consequently, the overall Cu transport function of the human Cu transporters. The work in this thesis on the ATP-BD was done in the yeast assay based on the hypothesis that mutations within this region would affect the Cu transport ability of the variants because of the involvement of this functional domain in binding ATP and forming a catalytic phosphorylated intermediate. Our aim was to identify whether certain amino acids are especially critical by studying select WND patient mutations. Simultaneously, these studies would be instrumental in determining whether the sequence changes identified in WND patients are disease-causing or rare normal variants that have no affect on protein function.

A. CRITICAL AMINO ACID RESIDUES WITHIN THE ATP-BINDING DOMAIN

Four amino acid residues within the ATP-BD of ATP7B are necessary for full Cu transport activity in the yeast functional assay. This confirmed the importance of this domain in the function of ATP7B as a Cu transporter and indicated that certain amino acids are more crucial than others in this region.

The Glu1064Lys and Val1106Asp missense mutations were the most informative ATP7B mutant variants studied in Chapter 4. Both showed reduced and mislocalized expression in

ccc2 yeast and negligible Cu transport activity in the yeast assay, which could be attributed to their critical spatial positions within the N-subdomain of the ATP-BD and consequential disruption of the catalytic cycle when mutated. Based on molecular modeling experiments described in this thesis, as well as work from other laboratories (Lutsenko *et al.* 2002; Tsivkovskii *et al.* 2003; Efremov *et al.* 2004; Morgan *et al.* 2004), Glu-1064 and Val-1106 both occupy positions within the domain that are central to nucleotide binding. Glu-1064 is located near the P-subdomain of the ATP-BD in our model, suggesting a possible role for this residue in directing the -phosphate of ATP toward the catalytic aspartate. As suggested from our experimental data, mutation of both Glu-1064 and Val-1106 impede the expression of these mutant constructs in *ccc2* yeast. From other studies, the mutation of Glu-1064 appeared to directly influence the ability of the domain to bind ATP, which may result in disruption in structure and/or reduced and altered expression of the protein; mutation of Val-1106 appeared to specifically impede the correct conformation of the N-subdomain resulting in reduced binding of ATP. Although these theories have yet to be confirmed experimentally, the data combined how the mutation of one critical amino acid can impair Cu transport function, either through ATP-binding and hydrolysis and/or aberrant expression of a misfolded protein.

Mutation of Leu1083Phe and Met1169Val also resulted in a distinct defect in Cu delivery to apo-Fet3p in the Fet3p assay, and a reduced ability to complement Fe-deficient growth. Both mutant variants showed normal expression in the *ccc2* mutant yeast. The Leu1083Phe mutation in the model indicated that the leucine residue may have a crucial role in intramolecular H-bonding in the N-subdomain, mutation of which could affect the ability of the domain to bind ATP and phosphorylate the catalytic aspartate. Although the Met-1169 could not be placed on the molecular model, an additional patient mutation has been reported at this methionine residue, and the Met1169Val substitution was a substantial amino acid change likely affecting the secondary structure of the ATP-BD. The results from these variants also revealed the advantages of using the Fet3p assay, in that it was a more sensitive assay and could likely recognize more variants with less severe consequences.

i. Future Directions

Although four amino acids were found to be critical for Cu transport, there were three additional WND patient mutations studied that did not show defects in Cu transport function: Gly1186Ser, Arg1041Trp and Ala1183Thr (Chapter 4). These ATP-BD variants should be assessed for their localization and Cu-induced trafficking capability in mammalian cells.

The next step for the four variants shown to be Cu translocation-defective (Glu1064Lys, Leu1083Phe, Val1106Asp, Met1169Val) is the identification of the specific defect affecting the function of these mutant variants. Although the end consequence is an impairment in Cu transport, these mutations may affect the affinity of the ATP-BD for ATP, the ability of ATP to bind the N-subdomain, or the correct positioning of ATP within the N-subdomain for transfer of the -phosphate to the catalytic aspartate.

To fully comprehend the mechanism of Cu translocation by ATP7A, researchers have designed phosphorylation assays to measure the transient phosphorylation of ATP7A and its Cu dependence using isolated membrane vesicles from yeast cells and incubation with -^{32}P-ATP (Voskoboinik *et al.* 2001b; Petris *et al.* 2002). The catalytic activity of ATP7A has also been assessed using an *in vitro* ^{64}Cu-translocation assay and membrane vesicles isolated from mammalian cells, where various concentrations of ATP are added with ^{64}Cu to calculate the rate of ATP-driven Cu translocation (Voskoboinik *et al.* 1998; Voskoboinik *et al.* 1999; Voskoboinik *et al.* 2003b).

ATP7B-enriched membranes have also been isolated from mammalian cells expressing ATP7B and analyzed using the ^{64}Cu-translocation assay (Voskoboinik *et al.* 2001a). This analysis has been improved by isolating membrane fractions from insect cells infected with recombinant ATP7B baculovirus, permitting more robust expression of ATP7B and direct and quantitative examination of the catalytic properties of the protein using phosphorylation assays (Tsivkovskii *et al.* 2002). General analyses of nucleotide binding by the ATP-BD and the conformational changes associated with such binding have also been performed (Tsivkovskii *et al.* 2001). Therefore, it is possible to evaluate these

properties with the ATP-BD mutants characterized in this thesis to explicitly delineate the affect of the sequence change on protein function.

III. THE COPPER-BINDING DOMAIN MUTANT VARIANTS

Three WND patient mutations in the CuBD of ATP7B were also investigated for their ability to complement the Fe-deficient phenotype of the *ccc2* mutant yeast. Two of the variants are located between MBS 6 and TM 1 (Gly626Ala and Asp642His), a region which holds many MNK patient mutations and has been deemed important for the interaction between the N-terminal CuBD and the ATPase core. According to our mutation spectrum of *ATP7B* in Chapter 2, four WND patient missense mutations are located in this linker region. The other CuBD variant studied in Chapter 4 is located between MBS 5 and MBS 6. All three of these CuBD variants showed Cu transport activity in the yeast functional assay.

MBS 5 and MBS 6 are particularly important for the function of ATP7B, as either of these MBSs is necessary and sufficient for Cu transport (Forbes *et al.* 1999; Cater *et al.* 2004), and either, along with the first N-terminal 63 amino acids, is necessary and sufficient for Cu-dependent trafficking (Cater *et al.* 2004; Guo *et al.* 2005). The entire N-terminal CuBD has been shown to interact with the recently discovered protein COMMD1, which is proposed to be involved in the biliary excretion of Cu (Tao *et al.* 2003).

Some affect on Cu transport function was expected; however, all three of the variants demonstrated normal Cu transport activity in the assay. No model of the entire CuBD is available to allow determination of the effect of the mutations on intramolecular H-bonding or the structure and folding of the domain. The structures of ATP7A MBS 2 and MBS 4 have been determined (Gitschier *et al.* 1998; Jones *et al.* 2003) and could be used to generate structural models of isolated ATP7B MBSs; however, this would not reveal any effects the mutations may have on the overall fold of the N-terminal CuBD or their effects on the interaction between the CuBD and the ATP-BD.

Given that the N-terminus of ATP7B interacts with COMMD1 and has also been shown to be necessary for Cu-induced redistribution, these CuBD mutant variants must be examined for their ability to traffick in response to increased levels of Cu and to excrete excess Cu. Studies with the LEC rat model may be used to test the ability of the mutant variants to participate in biliary Cu excretion. Infusion of recombinant adenovirus expressing ATP7B into the LEC rat has been demonstrated to restore biliary Cu efflux (Terada *et al.* 1999). LEC rats could be infected with recombinant adenovirus ATP7B expression variants and measurements of Cu contents in the hepatic lysosomal fraction and in the bile of the rats after ATP7B introduction could indicate the ability of the variants to excrete excess Cu.

IV. FUTURE DIRECTIONS WITH THE YEAST FUNCTIONAL ASSAY

Preliminary experiments have been initiated in our laboratory to improve upon the utility of the yeast complementation assay. The liquid growth assays (Chapter 3 and 4) and the plating assays (Chapter 4) were laborious, involved many hands-on hours, and required copious amounts of yeast components. Although there are limitations of the yeast assay that cannot be rectified, several steps can be taken to minimize the amounts of materials used and to generate a higher throughput assay.

The laboratory has been designing a new system for performing the liquid growth assay as a method for measuring the Cu transport activity of mutant variants. Preliminary steps have been taken to decrease the necessary volumes used in culturing the yeast cells, which has allowed the assay to be conducted in 96-well plates. The 96-well plate format would facilitate the use of an automated plate reader and incubator such that the actual bench work required would be extremely limited. This design would further permit the screening of multiple Cu and growth conditions to thoroughly examine the mutant variants for their complementation of the *ccc2* phenotype.

The Fet3p assay has proven to be more sensitive than the plating and liquid growth assays (Chapters 3 and 4). To improve the Fet3p assay, a dilution method could be devised to obtain thinner bands of oxidase activity and make subtle changes more noticeable and identifiable. Furthermore, a liquid method for analyzing the holo-Fet3p activity present has

been considered to replace the laborious process of pouring and running gels and developing the bands of oxidase activity (Macintyre *et al.* 2004). This method would entail a spectrophotometric assay, which may involve adding our membrane protein samples to a Fet3p substrate (e.g. paraphenylenediamine dihydrochloride) and measuring oxidation by taking readings at an optical density of 610 nm. An oxidation rate could be measured by taking readings at different time intervals, which may reveal mutants that have a slower rate in transferring Cu to apo-Fet3p. This type of procedure would be more quantitative and thus could be more informative by identifying those mutants that are only slightly impaired in their Cu transport function.

V. FUTURE DIRECTIONS WITH THE ANALYSIS OF ATP7B TRAFFICKING

The experiments performed with delineating the localization of ATP7B variants in mammalian cells in this thesis have demonstrated the difficulties of working within a biological system and have proven the complexities of the Cu-induced distribution of ATP7B.

The question that stemmed from our studies is whether ATP7B trafficks from its basal steady state localization under elevated Cu conditions. The consensus in the literature tends to be that ATP7B is localized within the TGN and redistributes to cytoplasmic vesicular compartments or the apical membrane in polarized cells when in a high Cu environment. However, given that there have been conflicting reports, the distribution of ATP7B within the cell may not be that simplistic, which likely complicates the studies performed in evaluating ATP7B location.

In vivo experiments in the laboratory setting also introduce several confounding effects which can lead to varying results: (i) the cell type used and possible intracellular factors that may not be present and are necessary for correct localization or trafficking; (ii) the different Cu conditions used; (iii) different incubation times in the presence of Cu chelator or added Cu; (iv) the ATP7B expression construct used in the transfections; (v) the organellar markers used for co-localization experiments; and/or (vi) the "trained" eye analyzing the results and the methods used to record the results.

A. Improvements to the assay as a result of this thesis

The research in Chapter 5 showed potential; however, additional experiments are required for the localization studies to be convincing. Our difficulties lay mainly in finding the right combination of cell type, Cu condition, incubation time, and organelle marker to define the TGN.

Although a system amenable to live-cell imaging and not entailing an antibody to ATP7B was desired, future experiments would be best initiated with ATP7B-pCDNA constructs instead of continuing with our GFP fusion constructs. The GFP tag did not appear to be causing a significant problem; however, it is preferable to continue initially with the least number of components that may confound the results. Future experiments requiring the ATP7B-GFP constructs for live cell imaging should include the incorporation of the GFP tag at both the N- and C-termini of wild-type ATP7B and the assessment of localization and trafficking. Furthermore, cloning the ATP7B-GFP constructs into pG4 yeast expression vectors would be useful for determining whether the GFP variants are functional and could complement the phenotype since a variant unable to transport Cu would most likely be unable to redistribute and respond to increased levels of extracellular Cu. The key to this assay will be finding the Cu conditions that accentuate the different distribution patterns previously observed in low and high Cu environments. This would be facilitated by the use of an organelle marker for the TGN.

Some studies have also used stable transfections of mammalian cells (Cater *et al.* 2004), which may be a consideration, to limit overexpression of constructs and minimize mislocalization that results from overexpression (Guo *et al.* 2005). The down-side of using stable transfectants is the time necessary to create the cell lines, which would hinder the higher throughput study of mutant variants.

B. Is ATP7B localized to the trans-Golgi network?

Based on our data, conclusive results require the use of a TGN marker. Finding an appropriate TGN marker and a cell line in which the antibody cross-reacts have been difficult. Furthermore, the limited overlap between the expression of the Golgi markers and ATP7B-GFP under low Cu conditions has been surprising. As mentioned in Chapter

1, there are distinct lipid microdomains at the TGN. ATP7B has been shown to associate with a specific subset and remains associated with this same subset when at the apical bile canalicular membrane (Slimane *et al.* 2003). It is possible that the TGN markers used are not localized in the same microdomains, and thus do not fully overlap with the ATP7B expression seen in the mammalian cells.

In addition, studies of ATP7A suggest that there may be a distinct pool of the Cu transporter that resides in the proximity of the PM under basal Cu conditions and rapidly recycles to the PM under elevated Cu levels (Pase *et al.* 2004). This results in efficient efflux of Cu under such conditions, and also indicates that this pool of ATP7A does not recycle to the TGN and remains near the PM. Therefore, it was not surprising to have found a significant portion of our ATP7B-GFP fusion products in a more vesicular pattern even when Cu levels were low. A different pool of ATP7A was also shown to traffick from the TGN to the PM (Pase *et al.* 2004), implying that some ATP7A remains associated with the TGN even under high Cu levels. This supports our results where the addition of Cu did not reveal movement of all ATP7B-GFP to cytoplasmic vesicular compartments, making it difficult to evaluate trafficking. These findings are useful in interpreting our data and for assessing future studies. It appears that the distinction between the +Cu and -Cu conditions will not be obvious and clear-cut, and more discriminatory conditions for the maximum effect will have to be determined for the cell lines used.

VI. CONCLUSION

The general goal of this thesis was to characterize regions in ATP7B critical for the function of the protein within the hepatocyte by using different methods for evaluation.

(1) A comparative analysis of the WND and MNK patient mutations was performed since the genes responsible for the diseases were similar in structure and encoded proteins which have been shown to function in Cu efflux and belong to the same protein family. The hypothesis was that this type of analysis would underscore any differences and similarities in the point mutations seen and the regions or amino acids affected, resulting in the identification of important areas in ATP7B and directing attention to regions not

considered previously. The comparison study provided valuable information and was used in selecting the regions of interest for functional assessment.

(2) The cytosolic C-terminus was examined based on the limited number of patient mutations in the region, the limited knowledge of this cytosolic tail, and the presence of a possible targeting signal. The hypothesis was that this region was important for protein function. Cu transport studies revealed that this 93-amino acid cytosolic region is essential for the integrity of the last TM domain and correct conformation of the protein product. The leucine sequence may play a role in trafficking, but studies specifically directed toward determining this are necessary.

(3) The ATP-binding domain (ATP-BD) is a critical portion of the P-type ATPase family of proteins, and in both ATP7A and ATP7B, this domain contains a significant number of patient mutations and has been shown to be essential for the catalytic activity of the proteins. The hypothesis was that several essential amino acids would be revealed by assessing the Cu transport function of WND patient mutations. Our studies in Chapter 4 of this thesis indicate that at least four residues within the ATP-BD are necessary for function, mutation of which would result in the WND phenotype. Thus, the analysis also confirmed the disease-causing status of these *ATP7B* sequence alterations previously identified in patients.

(4) Based on previous work on the function of the N-terminal Cu-binding domain (CuBD) and the considerable number of mutations identified in exon 8 of the *ATP7A* gene that encodes part of the CuBD, this region was assessed for its Cu transport function. The hypothesis was that specific residues within this domain, particularly between MBS 5 and TM 1, would be critical for the function of ATP7B in Cu homeostasis. The three mutant variants analysed for Cu transport were not defective, suggesting that some residues within this domain are dispensable for function, or that they are involved in trafficking.

(5) A significant aspect of ATP7B function is its trafficking within the cell. Given its role in the delivery of Cu to a secretory protein and its role in the excretion of excess Cu via bile, the ability of ATP7B to respond to different Cu environments and localize correctly is crucial. An assay to examine Cu-induced distribution is, therefore, important. This thesis

was aimed at developing a method more suited to large-scale functional analysis of mutant variants. The work in Chapter 5 has confirmed the complexities of the localization of ATP7B and has laid the groundwork for future studies. The cell type, organellar marker, ATP7B construct, and different Cu and incubation conditions employed in the experiments are critical for obtaining the reproducible and reliable results that are required for analyzing the functional consequences of mutations identified in WND patients.

I have achieved the goal of identifying the C-terminal region and amino acids within the ATP-BD as critical for ATP7B Cu transport function, and select amino acids in the CuBD as expendable. In doing so, I have also critically evaluated the utility of the techniques available in the laboratory for assessing function and have provided the preliminary steps for improving the assays and various methods that could be engaged in future evaluations.

REFERENCES

ALA A, BORJIGIN J, ROCHWARGER A, and SCHILSKY M. (2005). Wilson disease in septuagenarian siblings: Raising the bar for diagnosis. *Hepatology* 41(3): 668-670.

ALCONADA A, BAUER U, and HOFLACK B. (1996). A tyrosine-based motif and a casein kinase II phosphorylation site regulate the intracellular trafficking of the varicella-zoster virus glycoprotein I, a protein localized in the *trans*-Golgi network. *EMBO J* 15(22): 6096-6110.

AMBROSINI L and MERCER JF. (1999). Defective copper-induced trafficking and localization of the Menkes protein in patients with mild and copper-treated classical Menkes disease. *Hum Mol Genet* 8(8): 1547-1555.

ASAHI M, KURZYDLOWSKI K, TADA M, and MACLENNAN DH. (2002). Sarcolipin inhibits polymerization of phospholamban to induce superinhibition of sarco(endo)plasmic reticulum Ca^{2+}-ATPases (SERCAs). *J Biol Chem* 277(30): 26725-26728.

ASAHI M, SUGITA Y, KURZYDLOWSKI K, DE LEON S, TADA M *et al.* (2003). Sarcolipin regulates sarco(endo)plasmic reticulum Ca^{2+}-ATPase (SERCA) by binding to transmembrane helices alone or in association with phospholamban. *Proc Natl Acad Sci U S A* 100(9): 5040-5045.

ASKWITH C, EIDE D, VAN HO A, BERNARD PS, LI L *et al.* (1994). The *FET3* gene of *S. cerevisiae* encodes a multicopper oxidase required for ferrous iron uptake. *Cell* 76(2): 403-410.

AUSUBEL FM, BRENT R, KINGSTON RE, MOORE DD, SEIDMAN JG *et al.* (1998). Current Protocols in Molecular Biology. in (ed., pp. 1.0.1-A.5.45. John Wiley and Sons, Inc., New York.

BECK J, ENDERS H, SCHLIEPHACKE M, BUCHWALD-SAAL M, and TÜMER Z. (1994). X;1 translocation in a female Menkes patient: characterization by fluorescence *in situ* hybridization. *Clin Genet* 46(4): 295-298.

BELLEMARE DR, SHANER L, MORANO KA, BEAUDOIN J, LANGLOIS R *et al.* (2002). Ctr6, a vacuolar membrane copper transporter in *Schizosaccharomyces pombe*. *J Biol Chem* 277(48): 46676-46686.

BIASIO W, CHANG T, MCINTOSH CJ, and MCDONALD FJ. (2004). Identification of Murr1 as a regulator of the human delta epithelial sodium channel. *J Biol Chem* 279(7): 5429-5434.

BISSIG KD, WUNDERLI-YE H, DUDA PW, and SOLIOZ M. (2001). Structure-function analysis of purified *Enterococcus hirae* CopB copper ATPase: effect of Menkes/Wilson disease mutation homologues. *Biochem J* 357(Pt 1): 217-223.

BORJIGIN J, PAYNE AS, DENG J, LI X, WANG MM *et al.* (1999). A novel pineal night-specific ATPase encoded by the Wilson disease gene. *J Neurosci* 19(3): 1018-1026.

BORM B, MØLLER LB, HAUSSER I, EMEIS M, BAERLOCHER K *et al.* (2004). Variable clinical expression of an identical mutation in the *ATP7A* gene for Menkes disease/occipital horn syndrome in three affected males in a single family. *J Pediatr* 145(1): 119-121.

BOS K, WRAIGHT C, and STANLEY KK. (1993). TGN38 is maintained in the *trans*-Golgi network by a tyrosine-containing motif in the cytoplasmic domain. *EMBO J* 12(5): 2219-2228.

BOWCOCK AM, FARRER LA, CAVALLI-SFORZA LL, HEBERT JM, KIDD KK *et al.* (1987). Mapping the Wilson disease locus to a cluster of linked polymorphic markers on chromosome 13. *Am J Hum Genet* 41(1): 27-35.

BOWCOCK AM, FARRER LA, HEBERT JM, AGGER M, STERNLIEB I *et al.* (1988). Eight closely linked loci place the Wilson disease locus within 13q14-q21. *Am J Hum Genet* 43(5): 664-674.

BREWER GJ and YUZBASIYAN-GURKAN V. (1992). Wilson disease. *Medicine (Baltimore)* 71(3): 139-164.

BRODSKY JL and MCCRACKEN AA. (1999). ER protein quality control and proteasome-mediated protein degradation. *Semin Cell Dev Biol* 10(5): 507-513.

BROSS P, CORYDON TJ, ANDRESEN BS, JORGENSEN MM, BOLUND L *et al.* (1999). Protein misfolding and degradation in genetic diseases. *Hum Mutat* 14(3): 186-198.

BUCCI C, PARTON RG, MATHER IH, STUNNENBERG H, SIMONS K *et al.* (1992). The small GTPase Rab5 functions as a regulatory factor in the early endocytic pathway. *Cell* 70(5): 715-728.

BUIAKOVA OI, XU J, LUTSENKO S, ZEITLIN S, DAS K *et al.* (1999). Null mutation of the murine *ATP7B* (Wilson disease) gene results in intracellular copper accumulation and late-onset hepatic nodular transformation. *Hum Mol Genet* 8(9): 1665-1671.

BULL PC, THOMAS GR, ROMMENS JM, FORBES JR, and COX DW. (1993). The Wilson disease gene is a putative copper transporting P-type ATPase similar to the Menkes gene. *Nat Genet* 5(4): 327-337.

BULL PC and COX DW. (1994). Wilson disease and Menkes disease: new handles on heavy-metal transport. *Trends Genet* 10(7): 246-252.

BURSTEIN E, GANESH L, DICK RD, VAN DE SLUIS B, WILKINSON JC *et al.* (2004). A novel role for XIAP in copper homeostasis through regulation of MURR1. *EMBO J* 23(1): 244-254.

BYERS PH, SIEGEL RC, HOLBROOK KA, NARAYANAN AS, BORNSTEIN P *et al.* (1980). X-linked cutis laxa: defective cross-link formation in collagen due to decreased lysyl oxidase activity. *N Engl J Med* 303(2): 61-65.

CARR HS and WINGE DR. (2003). Assembly of cytochrome-*c*-oxidase within the mitochondrion. *Acc Chem Res* 36(5): 309-316.

CARTWRIGHT GE, GUBLER CJ, BUSH JA, and WINTROBE MM. (1956). Studies of copper metabolism. XVII. Further observations on the anemia of copper deficiency in swine. *Blood* 11(2): 143-153.

CATER MA, FORBES J, LA FONTAINE S, COX D, and MERCER JF. (2004). Intracellular trafficking of the human Wilson protein: the role of the six N-terminal metal-binding sites. *Biochem J* 380(Pt 3): 805-813.

CAUZA E, MAIER-DOBERSBERGER T, POLLI C, KASERER K, KRAMER L *et al.* (1997). Screening for Wilson's disease in patients with liver diseases by serum ceruloplasmin. *J Hepatol* 27(2): 358-362.

CECCHI C, BIASOTTO M, TOSI M, and AVNER P. (1997). The mottled mouse as a model for human Menkes disease: identification of mutations in the *Atp7a* gene. *Hum Mol Genet* 6(5): 829.

CHELLY J, TÜMER Z, TONNESEN T, PETTERSON A, ISHIKAWA-BRUSH Y *et al.* (1993). Isolation of a candidate gene for Menkes disease that encodes a potential heavy metal binding protein. *Nat Genet* 3(1): 14-19.

CHEVET E, CAMERON PH, PELLETIER MF, THOMAS DY, and BERGERON JJ. (2001). The endoplasmic reticulum: integration of protein folding, quality control, signaling and degradation. *Curr Opin Struct Biol* 11(1): 120-124.

CHUANG LM, WU HP, JANG MH, WANG TR, SUE WC *et al.* (1996). High frequency of two mutations in codon 778 in exon 8 of the *ATP7B* gene in Taiwanese families with Wilson disease. *J Med Genet* 33(6): 521-523.

CHURCH GM and GILBERT W. (1984). Genomic sequencing. *Proc Natl Acad Sci U S A* 81(7): 1991-1995.

COBBOLD C, PONNAMBALAM S, FRANCIS MJ, and MONACO AP. (2002). Novel membrane traffic steps regulate the exocytosis of the Menkes disease ATPase. *Hum Mol Genet* 11(23): 2855-2866.

COBBOLD C, COVENTRY J, PONNAMBALAM S, and MONACO AP. (2003). The Menkes disease ATPase (ATP7A) is internalized via a Rac1-regulated, clathrin- and caveolae-independent pathway. *Hum Mol Genet* 12(13): 1523-1533.

COBBOLD C, COVENTRY J, PONNAMBALAM S, and MONACO AP. (2004). Actin and microtubule regulation of *trans*-Golgi network architecture, and copper-dependent protein transport to the cell surface. *Mol Membr Biol* 21(1): 59-66.

CORONADO V, NANJI M, and COX DW. (2001). The Jackson toxic milk mouse as a model for copper loading. *Mamm Genome* 12(10): 793-795.

CORONADO VA, DAMARAJU D, KOHIJOKI R, and COX DW. (2003). New haplotypes in the Bedlington terrier indicate complexity in copper toxicosis. *Mamm Genome* 14(7): 483-491.

CORVERA S, CHAWLA A, CHAKRABARTI R, JOLY M, BUXTON J *et al.* (1994). A double leucine within the GLUT4 glucose transporter COOH-terminal domain functions as an endocytosis signal. *J Cell Biol* 126(6): 1625.

COX DW. (1996). Molecular advances in Wilson disease. *Prog Liver Dis* 14(245-264.

COX DW and MOORE SD. (2002). Copper transporting P-type ATPases and human disease. *J Bioenerg Biomembr* 34(5): 333-338.

COX DW, PRAT L, WALSHE JM, HEATHCOTE J, and GAFFNEY D. (2005). Twenty-four novel mutations in Wilson disease patients of predominantly European ancestry. *Hum Mutat* 26(3): 280.

COYLE P, PHILCOX JC, CAREY LC, and ROFE AM. (2002). Metallothionein: the multipurpose protein. *Cell Mol Life Sci* 59(4): 627-647.

CULLEN LM, HSI G, MACINTYRE G, CHEN MM, GLERUM DM *et al.* (2005). Mutations in the ATP-binding domain of the Wilson disease protein, ATP7B, affect copper transport in a yeast model system. *Submitted*:

CULOTTA VC, KLOMP LW, STRAIN J, CASARENO RL, KREMS B *et al.* (1997). The copper chaperone for superoxide dismutase. *J Biol Chem* 272(38): 23469-23472.

CUMINGS JN. (1948). The copper and iron content of bran and liver in the normal and in hepato-lenticular degeneration. *Brain* 71(410-415.

CUNLIFFE P, REED V, and BOYD Y. (2001). Intragenic deletions at *Atp7a* in mouse models for Menkes disease. *Genomics* 74(2): 155-162.

CZLONKOWSKA A, RODO M, GAJDA J, PLOOS VAN AMSTEL HK, JUYN J *et al.* (1997). Very high frequency of the His1069Gln mutation in Polish Wilson disease patients. *J Neurol* 244(9): 591-592.

DAGENAIS SL, ADAM AN, INNIS JW, and GLOVER TW. (2001). A novel frameshift mutation in exon 23 of *ATP7A* (*MNK*) results in occipital horn syndrome and not in Menkes disease. *Am J Hum Genet* 69(2): 420-427.

DAMERON CT and HARRISON MD. (1998). Mechanisms for protection against copper toxicity. *Am J Clin Nutr* 67(5 Suppl): 1091S-1097S.

DANCIS A, HAILE D, YUAN DS, and KLAUSNER RD. (1994a). The *Saccharomyces cerevisiae* copper transport protein (Ctr1p). Biochemical characterization, regulation by copper, and physiologic role in copper uptake. *J Biol Chem* 269(41): 25660-25667.

DANCIS A, YUAN DS, HAILE D, ASKWITH C, EIDE D *et al.* (1994b). Molecular characterization of a copper transport protein in *S. cerevisiae*: an unexpected role for copper in iron transport. *Cell* 76(2): 393-402.

DANKS DM, CAMPBELL PE, STEVENS BJ, MAYNE V, and CARTWRIGHT E. (1972). Menkes's kinky hair syndrome. An inherited defect in copper absorption with widespread effects. *Pediatrics* 50(2): 188-201.

DANKS DM, CARTWRIGHT E, STEVENS BJ, and TOWNLEY RR. (1973). Menkes' kinky hair disease: further definition of the defect in copper transport. *Science* 179(78): 1140-1142.

DANKS DM, CAMAKARIS J, HERD S, MANN JR, and PHILLIPS M. (1983). Copper transport in Menkes' disease. in *Biological Aspects of Metals and Metal-Related Diseases* (ed. Sarkar B), pp. 133-146. Raven Press, New York.

DANKS DM. (1988). The mild form of Menkes disease: progress report on the original case. *Am J Med Genet* 30(3): 859-864.

DAS S, LEVINSON B, WHITNEY S, VULPE C, PACKMAN S *et al.* (1994). Diverse mutations in patients with Menkes disease often lead to exon skipping. *Am J Hum Genet* 55(5): 883-889.

DAS S, LEVINSON B, VULPE C, WHITNEY S, GITSCHIER J *et al.* (1995). Similar splicing mutations of the Menkes/mottled copper-transporting ATPase gene in occipital horn syndrome and the blotchy mouse. *Am J Hum Genet* 56(3): 570-576.

DE SILVA DM, ASKWITH CC, EIDE D, and KAPLAN J. (1995). The *FET3* gene product required for high affinity iron transport in yeast is a cell surface ferroxidase. *J Biol Chem* 270(3): 1098-1101.

DEMIRKIRAN M, JANKOVIC J, LEWIS RA, and COX DW. (1996). Neurologic presentation of Wilson disease without Kayser-Fleischer rings. *Neurology* 46(4): 1040-1043.

DENING TR and BERRIOS GE. (1989). Wilson's disease. Psychiatric symptoms in 195 cases. *Arch Gen Psychiatry* 46(12): 1126-1134.

DIDONATO M, NARINDRASORASAK S, FORBES JR, COX DW, and SARKAR B. (1997). Expression, purification, and metal binding properties of the N-terminal domain from the Wilson disease putative copper-transporting ATPase (ATP7B). *J Biol Chem* 272(52): 33279-33282.

DIDONATO M, HSU HF, NARINDRASORASAK S, QUE L, JR., and SARKAR B. (2000). Copper-induced conformational changes in the N-terminal domain of the Wilson disease copper-transporting ATPase. *Biochemistry* 39(7): 1890-1896.

DIERICK HA, AMBROSINI L, SPENCER J, GLOVER TW, and MERCER JF. (1995). Molecular structure of the Menkes disease gene (*ATP7A*). *Genomics* 28(3): 462-469.

DIERICK HA, ADAM AN, ESCARA-WILKE JF, and GLOVER TW. (1997). Immunocytochemical localization of the Menkes copper transport protein (ATP7A) to the *trans*-Golgi network. *Hum Mol Genet* 6(3): 409-416.

DITTRICH E, ROSE-JOHN S, GERHARTZ C, MULLBERG J, STOYAN T *et al.* (1994). Identification of a region within the cytoplasmic domain of the interleukin-6 (IL-6) signal transducer gp130 important for ligand-induced endocytosis of the IL-6 receptor. *J Biol Chem* 269(29): 19014-19020.

DITTRICH E, HAFT CR, MUYS L, HEINRICH PC, and GRAEVE L. (1996). A di-leucine motif and an upstream serine in the interleukin-6 (IL-6) signal transducer gp130 mediate ligand-induced endocytosis and down-regulation of the IL-6 receptor. *J Biol Chem* 271(10): 5487-5494.

DURAND F, BERNUAU J, GIOSTRA E, MENTHA G, SHOUVAL D *et al.* (2001). Wilson's disease with severe hepatic insufficiency: beneficial effects of early administration of D-penicillamine. *Gut* 48(6): 849-852.

EFREMOV RG, KOSINSKY YA, NOLDE DE, TSIVKOVSKII R, ARSENIEV AS *et al.* (2004). Molecular modelling of the nucleotide-binding domain of Wilson's disease protein: location of the ATP-binding site, domain dynamics and potential effects of the major disease mutations. *Biochem J* 382(Pt 1): 293-305.

ELBLE R. (1992). A simple and efficient procedure for transformation of yeasts. *Biotechniques* 13(1): 18-20.

FAN Y, YU L, JIANG Y, XU Y, YANG R *et al.* (2000). Identification of a mutation hotspot in exon 8 of Wilson disease gene by cycle sequencing. *Chin Med J (Engl)* 113(2): 172-174.

FATEMI N and SARKAR B. (2002a). Molecular mechanism of copper transport in Wilson disease. *Environ Health Perspect* 110 Suppl 5(695-698.

FATEMI N and SARKAR B. (2002b). Structural and functional insights of Wilson disease copper-transporting ATPase. *J Bioenerg Biomembr* 34(5): 339-349.

FENG Y, PRESS B, and WANDINGER-NESS A. (1995). Rab 7: an important regulator of late endocytic membrane traffic. *J Cell Biol* 131(6 Pt 1): 1435-1452.

FERENCI P, CACA K, LOUDIANOS G, MIELI-VERGANI G, TANNER S *et al.* (2003). Diagnosis and phenotypic classification of Wilson disease. *Liver Int* 23(3): 139-142.

FERENCI P. (2004a). Pathophysiology and clinical features of Wilson disease. *Metab Brain Dis* 19(3-4): 229-239.

FERENCI P. (2004b). Review article: diagnosis and current therapy of Wilson's disease. *Aliment Pharmacol Ther* 19(2): 157-165.

FIELD LS, LUK E, and CULOTTA VC. (2002). Copper chaperones: personal escorts for metal ions. *J Bioenerg Biomembr* 34(5): 373-379.

FIGUS A, ANGIUS A, LOUDIANOS G, BERTINI C, DESSI V *et al.* (1995). Molecular pathology and haplotype analysis of Wilson disease in Mediterranean populations. *Am J Hum Genet* 57(6): 1318-1324.

FIRNEISZ G, LAKATOS PL, SZALAY F, POLLI C, GLANT TT *et al.* (2002). Common mutations of *ATP7B* in Wilson disease patients from Hungary. *Am J Med Genet* 108(1): 23-28.

FLEISCHER B. (1903). Zwei weitere Falle von grunliche Verfarbung der Kornea. *Klin Mbl Augenheilk* 41(489-491.

FLEISCHER B. (1912). Ueber einer der "Pseudosclerose" nahestehende bisher unbekannte Krankheit (gekennzeichnet durch Tremor, psychische Stoerungen, braeunlicke Pigmentierung bestimmter Gewebe, insbesondere Such der Hornhauptperipherie, Lebercirrhose). *Deutsch Z Nerven Heilk* 44(179-201.

FORBES JR and COX DW. (1998). Functional characterization of missense mutations in *ATP7B*: Wilson disease mutation or normal variant? *Am J Hum Genet* 63(6): 1663-1674.

FORBES JR, HSI G, and COX DW. (1999). Role of the copper-binding domain in the copper transport function of ATP7B, the P-type ATPase defective in Wilson disease. *J Biol Chem* 274(18): 12408-12413.

FORBES JR and COX DW. (2000). Copper-dependent trafficking of Wilson disease mutant ATP7B proteins. *Hum Mol Genet* 9(13): 1927-1935.

FRANCIS MJ, JONES EE, LEVY ER, PONNAMBALAM S, CHELLY J *et al.* (1998). A Golgi localization signal identified in the Menkes recombinant protein. *Hum Mol Genet* 7(8): 1245-1252.

FRANCIS MJ, JONES EE, LEVY ER, MARTIN RL, PONNAMBALAM S *et al.* (1999). Identification of a di-leucine motif within the C terminus domain of the Menkes disease protein that mediates endocytosis from the plasma membrane. *J Cell Sci* 112 (Pt 11)(1721-1732.

FRIEDEN E and OSAKI S. (1974). Ferroxidases and ferrireductases: their role in iron metabolism. *Adv Exp Med Biol* 48(0): 235-265.

FROMMER DJ. (1981). Urinary copper excretion and hepatic copper concentrations in liver disease. *Digestion* 21(4): 169-178.

GAFFNEY D, FELL GS, and O'REILLY DS. (2000). ACP Best Practice No 163. Wilson's disease: acute and presymptomatic laboratory diagnosis and monitoring. *J Clin Pathol* 53(11): 807-812.

GANESH L, BURSTEIN E, GUHA-NIYOGI A, LOUDER MK, MASCOLA JR *et al.* (2003). The gene product Murr1 restricts HIV-1 replication in resting $CD4^+$ lymphocytes. *Nature* 426(6968): 853-857.

GARIPPA RJ, JOHNSON A, PARK J, PETRUSH RL, and MCGRAW TE. (1996). The carboxyl terminus of GLUT4 contains a serine-leucine-leucine sequence that functions as a potent internalization motif in Chinese hamster ovary cells. *J Biol Chem* 271(34): 20660-20668.

GAXIOLA RA, YUAN DS, KLAUSNER RD, and FINK GR. (1998). The yeast CLC chloride channel functions in cation homeostasis. *Proc Natl Acad Sci U S A* 95(7): 4046-4050.

GIBBS K and WALSHE JM. (1979). A study of the caeruloplasmin concentrations found in 75 patients with Wilson's disease, their kinships and various control groups. *Q J Med* 48(191): 447-463.

GITSCHIER J, MOFFAT B, REILLY D, WOOD WI, and FAIRBROTHER WJ. (1998). Solution structure of the fourth metal-binding domain from the Menkes copper-transporting ATPase. *Nat Struct Biol* 5(1): 47-54.

GOODYER ID, JONES EE, MONACO AP, and FRANCIS MJ. (1999). Characterization of the Menkes protein copper-binding domains and their role in copper-induced protein relocalization. *Hum Mol Genet* 8(8): 1473-1478.

GOW PJ, SMALLWOOD RA, ANGUS PW, SMITH AL, WALL AJ *et al.* (2000). Diagnosis of Wilson's disease: an experience over three decades. *Gut* 46(3): 415-419.

GREENOUGH M, PASE L, VOSKOBOINIK I, PETRIS MJ, O'BRIEN AW *et al.* (2004). Signals regulating trafficking of Menkes (MNK; ATP7A) copper-translocating P-type ATPase in polarized MDCK cells. *Am J Physiol Cell Physiol* 287(5): C1463-1471.

GRIMES A, HEARN CJ, LOCKHART P, NEWGREEN DF, and MERCER JF. (1997). Molecular basis of the *brindled* mouse mutant (Mo(*br*)): a murine model of Menkes disease. *Hum Mol Genet* 6(7): 1037-1042.

GROSS C, KELLEHER M, IYER VR, BROWN PO, and WINGE DR. (2000). Identification of the copper regulon in *Saccharomyces cerevisiae* by DNA microarrays. *J Biol Chem* 275(41): 32310-32316.

GROSS JB, JR., MYERS BM, KOST LJ, KUNTZ SM, and LARUSSO NF. (1989). Biliary copper excretion by hepatocyte lysosomes in the rat. Major excretory pathway in experimental copper overload. *J Clin Invest* 83(1): 30-39.

GROVER WD and SCRUTTON MC. (1975). Copper infusion therapy in trichopoliodystrophy. *J Pediatr* 86(2): 216-220.

GU YH, KODAMA H, MURATA Y, MOCHIZUKI D, YANAGAWA Y *et al.* (2001). *ATP7A* gene mutations in 16 patients with Menkes disease and a patient with occipital horn syndrome. *Am J Med Genet* 99(3): 217-222.

GU YH, KODAMA H, DU SL, GU QJ, SUN HJ *et al.* (2003). Mutation spectrum and polymorphisms in *ATP7B* identified on direct sequencing of all exons in Chinese Han and Hui ethnic patients with Wilson's disease. *Clin Genet* 64(6): 479-484.

GUEX N and PEITSCH MC. (1997). SWISS-MODEL and the Swiss-PdbViewer: an environment for comparative protein modeling. *Electrophoresis* 18(15): 2714-2723.

GUO Y, NYASAE L, BRAITERMAN LT, and HUBBARD AL. (2005). NH_2-terminal signals in ATP7B Cu-ATPase mediate its Cu-dependent anterograde traffic in polarized hepatic cells. *Am J Physiol Gastrointest Liver Physiol* 289(5): G904-916.

GUPTA A, AIKATH D, NEOGI R, DATTA S, BASU K *et al.* (2005). Molecular pathogenesis of Wilson disease: haplotype analysis, detection of prevalent mutations and genotype-phenotype correlation in Indian patients. *Hum Genet*: 1-9.

HAHN S, CHO K, RYU K, KIM J, PAI K *et al.* (2001). Identification of four novel mutations in classical Menkes disease and successful prenatal DNA diagnosis. *Mol Genet Metab* 73(1): 86-90.

HALLIWELL B and GUTTERIDGE JM. (1984). Oxygen toxicity, oxygen radicals, transition metals and disease. *Biochem J* 219(1): 1-14.

HALLIWELL B and GUTTERIDGE JM. (1990). Role of free radicals and catalytic metal ions in human disease: an overview. *Methods Enzymol* 186(1-85.

HAMER DH. (1986). Metallothionein. *Annu Rev Biochem* 55(913-951.

HAMZA I, FAISST A, PROHASKA J, CHEN J, GRUSS P *et al.* (2001). The metallochaperone Atox1 plays a critical role in perinatal copper homeostasis. *Proc Natl Acad Sci U S A* 98(12): 6848-6852.

HAMZA I, PROHASKA J, and GITLIN JD. (2003). Essential role for Atox1 in the copper-mediated intracellular trafficking of the Menkes ATPase. *Proc Natl Acad Sci U S A* 100(3): 1215-1220.

HARADA M, SAKISAKA S, YOSHITAKE M, SHAKADOH S, GONDOH K *et al.* (1993). Biliary copper excretion in acutely and chronically copper-loaded rats. *Hepatology* 17(1): 111-117.

HARADA M, SAKISAKA S, KAWAGUCHI T, KIMURA R, TANIGUCHI E *et al.* (2000a). Copper does not alter the intracellular distribution of ATP7B, a copper-transporting ATPase. *Biochem Biophys Res Commun* 275(3): 871-876.

HARADA M, SAKISAKA S, TERADA K, KIMURA R, KAWAGUCHI T *et al.* (2000b). Role of ATP7B in biliary copper excretion in a human hepatoma cell line and normal rat hepatocytes. *Gastroenterology* 118(5): 921-928.

HARADA M, SAKISAKA S, TERADA K, KIMURA R, KAWAGUCHI T *et al.* (2001). A mutation of the Wilson disease protein, ATP7B, is degraded in the proteasomes and forms protein aggregates. *Gastroenterology* 120(4): 967-974.

HARADA M, KUMEMURA H, SAKISAKA S, SHISHIDO S, TANIGUCHI E *et al.* (2003). Wilson disease protein ATP7B is localized in the late endosomes in a polarized human hepatocyte cell line. *Int J Mol Med* 11(3): 293-298.

HARADA M, KAWAGUCHI T, KUMEMURA H, TERADA K, NINOMIYA H *et al.* (2005). The Wilson disease protein ATP7B resides in the late endosomes with Rab7 and the Niemann-Pick C1 protein. *Am J Pathol* 166(2): 499-510.

HARRIS ED. (2000). Cellular copper transport and metabolism. *Annu Rev Nutr* 20(291-310.

HARRISON MD and DAMERON CT. (1999). Molecular mechanisms of copper metabolism and the role of the Menkes disease protein. *J Biochem Mol Toxicol* 13(2): 93-106.

HARRISON MD, JONES CE, and DAMERON CT. (1999). Copper chaperones: function, structure and copper-binding properties. *J Biol Inorg Chem* 4(2): 145-153.

HILL GM, BREWER GJ, PRASAD AS, HYDRICK CR, and HARTMANN DE. (1987). Treatment of Wilson's disease with zinc. I. Oral zinc therapy regimens. *Hepatology* 7(3): 522-528.

HIRAYAMA T, KIEBER JJ, HIRAYAMA N, KOGAN M, GUZMAN P *et al.* (1999). RESPONSIVE-TO-ANTAGONIST1, a Menkes/Wilson disease-related copper transporter, is required for ethylene signaling in Arabidopsis. *Cell* 97(3): 383-393.

HIROKAWA T, BOON-CHIENG S, and MITAKU S. (1998). SOSUI: classification and secondary structure prediction system for membrane proteins. *Bioinformatics* 14(4): 378-379.

HIRST J and ROBINSON MS. (1998). Clathrin and adaptors. *Biochim Biophys Acta* 1404(1-2): 173-193.

HONING S, SANDOVAL IV, and VON FIGURA K. (1998). A di-leucine-based motif in the cytoplasmic tail of LIMP-II and tyrosinase mediates selective binding of AP-3. *EMBO J* 17(5): 1304-1314.

HOOGENRAAD TU, VAN HATTUM J, and VAN DEN HAMER CJ. (1987). Management of Wilson's disease with zinc sulphate. Experience in a series of 27 patients. *J Neurol Sci* 77(2-3): 137-146.

HORN N. (1976). Copper incorporation studies on cultured cells for prenatal diagnosis of Menkes' disease. *Lancet* 1(7970): 1156-1158.

HORN N and JENSEN OA. (1980). Menkes syndrome: subcellular distribution of copper determined by an ultrastructural histochemical technique. *Ultrastruct Pathol* 1(2): 237-242.

HOUWEN RH, VAN HATTUM J, and HOOGENRAAD TU. (1993). Wilson disease. *Neth J Med* 43(1-2): 26-37.

HOUWEN RH, JUYN J, HOOGENRAAD TU, PLOOS VAN AMSTEL JK, and BERGER R. (1995). H714Q mutation in Wilson disease is associated with late, neurological presentation. *J Med Genet* 32(6): 480-482.

HOWELL JM and MERCER JF. (1994). The pathology and trace element status of the toxic milk mutant mouse. *J Comp Pathol* 110(1): 37-47.

HSI G and COX DW. (2004). A comparison of the mutation spectra of Menkes disease and Wilson disease. *Hum Genet* 114(2): 165-172.

HSI G, CULLEN LM, GLERUM DM, and COX DW. (2004). Functional assessment of the carboxy-terminus of the Wilson disease copper-transporting ATPase, ATP7B. *Genomics* 83(3): 473-481.

HUNG AY and SHENG M. (2002). PDZ domains: structural modules for protein complex assembly. *J Biol Chem* 277(8): 5699-5702.

HUNG IH, SUZUKI M, YAMAGUCHI Y, YUAN DS, KLAUSNER RD *et al.* (1997). Biochemical characterization of the Wilson disease protein and functional expression in the yeast *Saccharomyces cerevisiae*. *J Biol Chem* 272(34): 21461-21466.

HUNG IH, CASARENO RL, LABESSE G, MATHEWS FS, and GITLIN JD. (1998). HAH1 is a copper-binding protein with distinct amino acid residues mediating copper homeostasis and antioxidant defense. *J Biol Chem* 273(3): 1749-1754.

HUSTER D, HOPPERT M, LUTSENKO S, ZINKE J, LEHMANN C *et al.* (2003). Defective cellular localization of mutant ATP7B in Wilson's disease patients and hepatoma cell lines. *Gastroenterology* 124(2): 335-345.

HUSTER D and LUTSENKO S. (2003). The distinct roles of the N-terminal copper-binding sites in regulation of catalytic activity of the Wilson's disease protein. *J Biol Chem* 278(34): 32212-32218.

HYUN C, LAVULO LT, and FILIPPICH LJ. (2004). Evaluation of haplotypes associated with copper toxicosis in Bedlington Terriers in Australia. *Am J Vet Res* 65(11): 1573-1579.

IIDA M, TERADA K, SAMBONGI Y, WAKABAYASHI T, MIURA N *et al.* (1998). Analysis of functional domains of Wilson disease protein (ATP7B) in *Saccharomyces cerevisiae*. *FEBS Lett* 428(3): 281-285.

ISHIDA S, LEE J, THIELE DJ, and HERSKOWITZ I. (2002). Uptake of the anticancer drug cisplatin mediated by the copper transporter Ctr1 in yeast and mammals. *Proc Natl Acad Sci U S A* 99(22): 14298-14302.

JOHNSON AO, LAMPSON MA, and MCGRAW TE. (2001). A di-leucine sequence and a cluster of acidic amino acids are required for dynamic retention in the endosomal recycling compartment of fibroblasts. *Mol Biol Cell* 12(2): 367-381.

JOHNSON GF, STERNLIEB I, TWEDT DC, GRUSHOFF PS, and SCHEINBERG I. (1980). Inheritance of copper toxicosis in Bedlington terriers. *Am J Vet Res* 41(11): 1865-1866.

JOHNSTON HD, FOOTE C, SANTEFORD A, and NOTHWEHR SF. (2005). Golgi-to-late endosome trafficking of the yeast pheromone processing enzyme Ste13p is regulated by a phosphorylation site in its cytosolic domain. *Mol Biol Cell* 16(3): 1456-1468.

JONES CE, DALY NL, COBINE PA, CRAIK DJ, and DAMERON CT. (2003). Structure and metal binding studies of the second copper binding domain of the Menkes ATPase. *J Struct Biol* 143(3): 209-218.

KAISER C, MICHAELIS S, and MITCHELL A. (1994). *Methods in yeast genetics: A Cold Spring Harbor Laboratory course manual.* Cold Spring Harbor Laboratory Press, Cold Spring Harbor, New York.

KALER SG, GALLO LK, PROUD VK, PERCY AK, MARK Y *et al.* (1994). Occipital horn syndrome and a mild Menkes phenotype associated with splice site mutations at the *MNK* locus. *Nat Genet* 8(2): 195-202.

KALER SG, BUIST NR, HOLMES CS, GOLDSTEIN DS, MILLER RC *et al.* (1995). Early copper therapy in classic Menkes disease patients with a novel splicing mutation. *Ann Neurol* 38(6): 921-928.

KALER SG. (1998a). Metabolic and molecular bases of Menkes disease and occipital horn syndrome. *Pediatr Dev Pathol* 1(1): 85-98.

KALER SG. (1998b). Diagnosis and therapy of Menkes syndrome, a genetic form of copper deficiency. *Am J Clin Nutr* 67(5 Suppl): 1029S-1034S.

KANG S, LIANG L, PARKER CD, and COLLAWN JF. (1998). Structural requirements for major histocompatibility complex class II invariant chain endocytosis and lysosomal targeting. *J Biol Chem* 273(32): 20644-20652.

KANZAKI A, TOI M, NEAMATI N, MIYASHITA H, OUBU M *et al.* (2002). Copper-transporting P-type adenosine triphosphatase (ATP7B) is expressed in human breast carcinoma. *Jpn J Cancer Res* 93(1): 70-77.

KAPUR S, HIGGINS JV, DELP K, and ROGERS B. (1987). Menkes syndrome in a girl with X-autosome translocation. *Am J Med Genet* 26(2): 503-510.

KATANO K, KONDO A, SAFAEI R, HOLZER A, SAMIMI G *et al.* (2002). Acquisition of resistance to cisplatin is accompanied by changes in the cellular pharmacology of copper. *Cancer Res* 62(22): 6559-6565.

KATANO K, SAFAEI R, SAMIMI G, HOLZER A, ROCHDI M *et al.* (2003). The copper export pump ATP7B modulates the cellular pharmacology of carboplatin in ovarian carcinoma cells. *Mol Pharmacol* 64(2): 466-473.

KAYSER B. (1902). Ueber einen Fall von angeborener grunlicher Verfarbung der Kornea. *Klin Mbl Augenheilk* 40(22-25.

KIM BE, SMITH K, MEAGHER CK, and PETRIS MJ. (2002). A conditional mutation affecting localization of the Menkes disease copper ATPase. Suppression by copper supplementation. *J Biol Chem* 277(46): 44079-44084.

KIM BE, SMITH K, and PETRIS MJ. (2003). A copper treatable Menkes disease mutation associated with defective trafficking of a functional Menkes copper ATPase. *J Med Genet* 40(4): 290-295.

KIM EK, YOO OJ, SONG KY, YOO HW, CHOI SY *et al.* (1998). Identification of three novel mutations and a high frequency of the Arg778Leu mutation in Korean patients with Wilson disease. *Hum Mutat* 11(4): 275-278.

KITZBERGER R, MADL C, and FERENCI P. (2005). Wilson disease. *Metab Brain Dis* 20(4): 295-302.

KLOMP AE, TOPS BB, VAN DENBERG IE, BERGER R, and KLOMP LW. (2002). Biochemical characterization and subcellular localization of human copper transporter 1 (hCTR1). *Biochem J* 364(Pt 2): 497-505.

KLOMP AE, VAN DE SLUIS B, KLOMP LW, and WIJMENGA C. (2003). The ubiquitously expressed MURR1 protein is absent in canine copper toxicosis. *J Hepatol* 39(5): 703-709.

KLOMP LW, LIN SJ, YUAN DS, KLAUSNER RD, CULOTTA VC *et al.* (1997). Identification and functional expression of *HAH1*, a novel human gene involved in copper homeostasis. *J Biol Chem* 272(14): 9221-9226.

KNIGHT SA, LABBE S, KWON LF, KOSMAN DJ, and THIELE DJ. (1996). A widespread transposable element masks expression of a yeast copper transport gene. *Genes Dev* 10(15): 1917-1929.

KODAMA H, MURATA Y, MOCHIZUKI D, and ABE T. (1998). Copper and ceruloplasmin metabolism in the LEC rat, an animal model for Wilson disease. *J Inherit Metab Dis* 21(3): 203-206.

KOLLROS PR, DICK RD, and BREWER GJ. (1991). Correction of cerebrospinal fluid copper in Menkes kinky hair disease. *Pediatr Neurol* 7(4): 305-307.

KOMATSU M, SUMIZAWA T, MUTOH M, CHEN ZS, TERADA K *et al.* (2000). Copper-transporting P-type adenosine triphosphatase (ATP7B) is associated with cisplatin resistance. *Cancer Res* 60(5): 1312-1316.

KREUDER J, OTTEN A, FUDER H, TÜMER Z, TÖNNESEN T *et al.* (1993). Clinical and biochemical consequences of copper-histidine therapy in Menkes disease. *Eur J Pediatr* 152(10): 828-832.

KUSUDA Y, HAMAGUCHI K, MORI T, SHIN R, SEIKE M *et al.* (2000). Novel mutations of the *ATP7B* gene in Japanese patients with Wilson disease. *J Hum Genet* 45(2): 86-91.

LA FONTAINE S, FIRTH SD, LOCKHART PJ, BROOKS H, PARTON RG *et al.* (1998a). Functional analysis and intracellular localization of the human Menkes protein (MNK) stably expressed from a cDNA construct in Chinese hamster ovary cells (CHO-K1). *Hum Mol Genet* 7(8): 1293-1300.

LA FONTAINE S, FIRTH SD, LOCKHART PJ, BROOKS H, CAMAKARIS J *et al.* (1999). Intracellular localization and loss of copper responsiveness of Mnk, the murine homologue of the Menkes protein, in cells from *blotchy* (Mo *blo*) and *brindled* (Mo *br*) mouse mutants. *Hum Mol Genet* 8(6): 1069-1075.

LA FONTAINE S, THEOPHILOS MB, FIRTH SD, GOULD R, PARTON RG *et al.* (2001). Effect of the toxic milk mutation (*tx*) on the function and intracellular localization of Wnd, the murine homologue of the Wilson copper ATPase. *Hum Mol Genet* 10(4): 361-370.

LA FONTAINE SL, FIRTH SD, CAMAKARIS J, ENGLEZOU A, THEOPHILOS MB *et al.* (1998b). Correction of the copper transport defect of Menkes patient fibroblasts by expression of the Menkes and Wilson ATPases. *J Biol Chem* 273(47): 31375-31380.

LAEMMLI UK. (1970). Cleavage of structural proteins during the assembly of the head of bacteriophage T4. *Nature* 227(5259): 680-685.

LALIBERTE J, WHITSON LJ, BEAUDOIN J, HOLLOWAY SP, HART PJ *et al.* (2004). The *Schizosaccharomyces pombe* Pccs protein functions in both copper trafficking and metal detoxification pathways. *J Biol Chem* 279(27): 28744-28755.

LANGNER C and DENK H. (2004). Wilson disease. *Virchows Arch* 445(2): 111-118.

LARIN D, MEKIOS C, DAS K, ROSS B, YANG AS *et al.* (1999). Characterization of the interaction between the Wilson and Menkes disease proteins and the cytoplasmic copper chaperone, HAH1p. *J Biol Chem* 274(40): 28497-28504.

LEE CC, WU JY, TSAI FJ, KODAMA H, ABE T *et al.* (2000). Molecular analysis of Wilson disease in Taiwan: identification of one novel mutation and evidence of haplotype-mutation association. *J Hum Genet* 45(5): 275-279.

LEE GR, NACHT S, LUKENS JN, and CARTWRIGHT GE. (1968). Iron metabolism in copper-deficient swine. *J Clin Invest* 47(9): 2058-2069.

LETOURNEUR F and KLAUSNER RD. (1992). A novel di-leucine motif and a tyrosine-based motif independently mediate lysosomal targeting and endocytosis of CD3 chains. *Cell* 69(7): 1143-1157.

LEVINSON B, CONANT R, SCHNUR R, DAS S, PACKMAN S *et al.* (1996). A repeated element in the regulatory region of the *MNK* gene and its deletion in a patient with occipital horn syndrome. *Hum Mol Genet* 5(11): 1737-1742.

LEVINSON B, PACKMAN S, and GITSCHIER J. (1997). Deletion of the promoter region in the *Atp7a* gene of the mottled *dappled* mouse. *Nat Genet* 16(3): 224-225.

LI L, TOGASHI Y, and TAKEICHI N. (1991). Abnormal copper accumulation in the liver of LEC rats: a rat form of Wilson's disease. in *The LEC Rat, a New Model for Hepatitis and Liver Cancer* (ed. Mori M, Yoshida MC, Takeichi N and Taniguchi N), pp. 122-132. Springer-Verlag, Tokyo.

LI X, CHEN S, WANG Q, ZACK DJ, SNYDER SH *et al.* (1998). A pineal regulatory element (PIRE) mediates transactivation by the pineal/retina-specific transcription factor CRX. *Proc Natl Acad Sci USA* 95(4): 1876-1881.

LIN SJ, PUFAHL RA, DANCIS A, O'HALLORAN TV, and CULOTTA VC. (1997). A role for the *Saccharomyces cerevisiae ATX1* gene in copper trafficking and iron transport. *J Biol Chem* 272(14): 9215-9220.

LIN X, OKUDA T, HOLZER A, and HOWELL SB. (2002). The copper transporter CTR1 regulates cisplatin uptake in *Saccharomyces cerevisiae*. *Mol Pharmacol* 62(5): 1154-1159.

LINDER MC. (1991). *Biochemistry of copper*. Plenum Press, New York.

LINDER MC and HAZEGH-AZAM M. (1996). Copper biochemistry and molecular biology. *Am J Clin Nutr* 63(5): 797S-811S.

LINDER MC, WOOTEN L, CERVEZA P, COTTON S, SHULZE R *et al.* (1998). Copper transport. *Am J Clin Nutr* 67(5 Suppl): 965S-971S.

LIU XQ, ZHANG YF, LIU TT, HSIAO KJ, ZHANG JM *et al.* (2004). Correlation of *ATP7B* genotype with phenotype in Chinese patients with Wilson disease. *World J Gastroenterol* 10(4): 590-593.

LOCKHART PJ and MERCER JF. (2000). Identification of the copper chaperone SAH in *Ovis aries*: expression analysis and *in vitro* interaction of SAH with ATP7B. *Biochim Biophys Acta* 1490(1-2): 11-20.

LOUDIANOS G, DESSI V, ANGIUS A, LOVICU M, LOI A *et al.* (1996). Wilson disease mutations associated with uncommon haplotypes in Mediterranean patients. *Hum Genet* 98(6): 640-642.

LOUDIANOS G, DESSI V, LOVICU M, ANGIUS A, KANAVAKIS E *et al.* (1998a). Haplotype and mutation analysis in Greek patients with Wilson disease. *Eur J Hum Genet* 6(5): 487-491.

LOUDIANOS G, DESSI V, LOVICU M, ANGIUS A, NURCHI A *et al.* (1998b). Further delineation of the molecular pathology of Wilson disease in the Mediterranean population. *Hum Mutat* 12(2): 89-94.

LOUDIANOS G, DESSI V, LOVICU M, ANGIUS A, ALTUNTAS B *et al.* (1999). Mutation analysis in patients of Mediterranean descent with Wilson disease: identification of 19 novel mutations. *J Med Genet* 36(11): 833-836.

LUK E, JENSEN LT, and CULOTTA VC. (2003). The many highways for intracellular trafficking of metals. *J Biol Inorg Chem* 8(8): 803-809.

LUK EE and CULOTTA VC. (2001). Manganese superoxide dismutase in *Saccharomyces cerevisiae* acquires its metal co-factor through a pathway involving the Nramp metal transporter, Smf2p. *J Biol Chem* 276(50): 47556-47562.

LUTSENKO S and KAPLAN JH. (1995). Organization of P-type ATPases: significance of structural diversity. *Biochemistry* 34(48): 15607-15613.

LUTSENKO S, PETRUKHIN K, COOPER MJ, GILLIAM CT, and KAPLAN JH. (1997). N-terminal domains of human copper-transporting adenosine triphosphatases (the Wilson's and Menkes disease proteins) bind copper selectively *in vivo* and *in vitro* with stoichiometry of one copper per metal-binding repeat. *J Biol Chem* 272(30): 18939-18944.

LUTSENKO S and COOPER MJ. (1998). Localization of the Wilson's disease protein product to mitochondria. *Proc Natl Acad Sci U S A* 95(11): 6004-6009.

LUTSENKO S, EFREMOV RG, TSIVKOVSKII R, and WALKER JM. (2002). Human copper-transporting ATPase ATP7B (the Wilson's disease protein): biochemical properties and regulation. *J Bioenerg Biomembr* 34(5): 351-362.

MACINTYRE G, GUTFREUND KS, MARTIN WR, CAMICIOLI R, and COX DW. (2004). Value of an enzymatic assay for the determination of serum ceruloplasmin. *J Lab Clin Med* 144(6): 294-301.

MACLENNAN DH, ASAHI M, and TUPLING AR. (2003). The regulation of SERCA-type pumps by phospholamban and sarcolipin. *Ann N Y Acad Sci* 986(472-480.

MAIER-DOBERSBERGER T, FERENCI P, POLLI C, BALAC P, DIENES HP *et al.* (1997). Detection of the His1069Gln mutation in Wilson disease by rapid polymerase chain reaction. *Ann Intern Med* 127(1): 21-26.

MAJUMDAR R, AL JUMAH M, AL RAJEH S, FRASER M, AL ZABEN A *et al.* (2000). A novel deletion mutation within the carboxyl terminus of the copper-transporting ATPase gene causes Wilson disease. *J Neurol Sci* 179(S 1-2): 140-143.

MAK BS, CHI CS, and TSAI CR. (2002). Menkes gene study in the Chinese population. *J Child Neurol* 17(4): 250-252.

MARGARIT E, BACH V, GOMEZ D, BRUGUERA M, JARA P *et al.* (2005). Mutation analysis of Wilson disease in the Spanish population -- identification of a prevalent substitution and eight novel mutations in the *ATP7B* gene. *Clin Genet* 68(1): 61-68.

MASUDA R, YOSHIDA MC, SASAKI M, DEMPO K, and MORI M. (1988). High susceptibility to hepatocellular carcinoma development in LEC rats with hereditary hepatitis. *Jpn J Cancer Res* 79(7): 828-835.

MAXFIELD AB, HEATON DN, and WINGE DR. (2004). Cox17 is functional when tethered to the mitochondrial inner membrane. *J Biol Chem* 279(7): 5072-5080.

MCDONALD JA, SNITCH P, PAINTER D, HENSLEY W, GALLAGHER ND *et al.* (1992). Striking variability of hepatic copper levels in fulminant hepatic failure. *J Gastroenterol Hepatol* 7(4): 396-398.

MENG Y, MIYOSHI I, HIRABAYASHI M, SU M, MOTOTANI Y *et al.* (2004). Restoration of copper metabolism and rescue of hepatic abnormalities in LEC rats, an animal model of Wilson disease, by expression of human *ATP7B* gene. *Biochim Biophys Acta* 1690(3): 208-219.

MENKES JH, ALTER M, STEIGLEDER GK, WEAKLEY DR, and SUNG JH. (1962). A sex-linked recessive disorder with retardation of growth, peculiar hair, and focal cerebral and cerebellar degeneration. *Pediatrics* 29(764-779.

MERCER JF, LIVINGSTON J, HALL B, PAYNTER JA, BEGY C *et al.* (1993). Isolation of a partial candidate gene for Menkes disease by positional cloning. *Nat Genet* 3(1): 20-25.

MERCER JF, GRIMES A, AMBROSINI L, LOCKHART P, PAYNTER JA *et al.* (1994). Mutations in the murine homologue of the Menkes gene in *dappled* and *blotchy* mice. *Nat Genet* 6(4): 374-378.

MERCER JF. (1998). Menkes syndrome and animal models. *Am J Clin Nutr* 67(5 Suppl): 1022S-1028S.

MERCER JF, BARNES N, STEVENSON J, STRAUSAK D, and LLANOS RM. (2003). Copper-induced trafficking of the Cu-ATPases: a key mechanism for copper homeostasis. *Biometals* 16(1): 175-184.

MICHALCZYK AA, RIEGER J, ALLEN KJ, MERCER JF, and ACKLAND ML. (2000). Defective localization of the Wilson disease protein (ATP7B) in the mammary gland of the toxic milk mouse and the effects of copper supplementation. *Biochem J* 352 Pt 2(565-571.

MIYAJIMA H, NISHIMURA Y, MIZOGUCHI K, SAKAMOTO M, SHIMIZU T *et al.* (1987). Familial apoceruloplasmin deficiency associated with blepharospasm and retinal degeneration. *Neurology* 37(5): 761-767.

MØLLER LB, TÜMER Z, LUND C, PETERSEN C, COLE T *et al.* (2000). Similar splice-site mutations of the *ATP7A* gene lead to different phenotypes: classical Menkes disease or occipital horn syndrome. *Am J Hum Genet* 66(4): 1211-1220.

MØLLER LB, OTT P, LUND C, and HORN N. (2005). Homozygosity for a gross partial gene deletion of the C-terminal end of ATP7B in a Wilson patient with hepatic and no neurological manifestations. *Am J Med Genet A* 138(4): 340-343.

MOORE SD and COX DW. (2002). Expression in mouse kidney of membrane copper transporters Atp7a and Atp7b. *Nephron* 92(3): 629-634.

MORGAN CT, TSIVKOVSKII R, KOSINSKY YA, EFREMOV RG, and LUTSENKO S. (2004). The distinct functional properties of the nucleotide-binding domain of ATP7B, the human copper-transporting ATPase: analysis of the Wilson disease mutations E1064A, H1069Q, R1151H, and C1104F. *J Biol Chem* 279(35): 36363-36371.

MORRISON P, CHUNG KC, and ROSNER MR. (1996). Mutation of di-leucine residues in the juxtamembrane region alters EGF receptor expression. *Biochemistry* 35(46): 14618-14624.

MURATA Y, YAMAKAWA E, IIZUKA T, KODAMA H, ABE T *et al.* (1995). Failure of copper incorporation into ceruloplasmin in the Golgi apparatus of LEC rat hepatocytes. *Biochem Biophys Res Commun* 209(1): 349-355.

MYARI A, HADJILIADIS N, FATEMI N, and SARKAR B. (2004). Copper(I) interaction with model peptides of WD6 and TM6 domains of Wilson ATPase: regulatory and mechanistic implications. *J Inorg Biochem* 98(9): 1483-1494.

NAGANO K, NAKAMURA K, URAKAMI KI, UMEYAMA K, UCHIYAMA H *et al.* (1998). Intracellular distribution of the Wilson's disease gene product (ATPase7B) after *in vitro* and *in vivo* exogenous expression in hepatocytes from the LEC rat, an animal model of Wilson's disease. *Hepatology* 27(3): 799-807.

NAKAYAMA K, KANZAKI A, OGAWA K, MIYAZAKI K, NEAMATI N *et al.* (2002). Copper-transporting P-type adenosine triphosphatase (ATP7B) as a cisplatin based chemoresistance marker in ovarian carcinoma: comparative analysis with expression of MDR1, MRP1, MRP2, LRP and BCRP. *Int J Cancer* 101(5): 488-495.

NANJI MS, NGUYEN VT, KAWASOE JH, INUI K, ENDO F *et al.* (1997). Haplotype and mutation analysis in Japanese patients with Wilson disease. *Am J Hum Genet* 60(6): 1423-1429.

NIELSEN E, SEVERIN F, BACKER JM, HYMAN AA, and ZERIAL M. (1999). Rab5 regulates motility of early endosomes on microtubules. *Nat Cell Biol* 1(6): 376-382.

O'HALLORAN TV and CULOTTA VC. (2000). Metallochaperones, an intracellular shuttle service for metal ions. *J Biol Chem* 275(33): 25057-25060.

ODERMATT A, BECKER S, KHANNA VK, KURZYDLOWSKI K, LEISNER E *et al.* (1998). Sarcolipin regulates the activity of SERCA1, the fast-twitch skeletal muscle sarcoplasmic reticulum Ca^{2+}-ATPase. *J Biol Chem* 273(20): 12360-12369.

ODORIZZI G, COWLES CR, and EMR SD. (1998). The AP-3 complex: a coat of many colours. *Trends Cell Biol* 8(7): 282-288.

OGAWA A, YAMAMOTO S, TAKAYANAGI M, KOGO T, KANAZAWA M *et al.* (1999a). An Ile/Val polymorphism at codon 1464 of the *ATP7A* gene. *J Hum Genet* 44(6): 423-424.

OGAWA A, YAMAMOTO S, TAKAYANAGI M, KOGO T, KANAZAWA M *et al.* (1999b). Identification of three novel mutations in the *MNK* gene in three unrelated Japanese patients with classical Menkes disease. *J Hum Genet* 44(3): 206-209.

OGAWA A, YAMAMOTO S, KANAZAWA M, OGAWA E, TAKAYANAGI M *et al.* (2000). Novel mutation of L718X in the *ATP7A* gene in a Japanese patient with classical Menkes disease, and four novel polymorphisms in the Japanese population. *J Hum Genet* 45(5): 315-317.

OH WJ, KIM EK, PARK KD, HAHN SH, and YOO OJ. (1999). Cloning and characterization of the promoter region of the Wilson disease gene. *Biochem Biophys Res Commun* 259(1): 206-211.

OKADA T, SHIONO Y, HAYASHI H, SATOH H, SAWADA T *et al.* (2000). Mutational analysis of *ATP7B* and genotype-phenotype correlation in Japanese with Wilson's disease. *Hum Mutat* 15(5): 454-462.

OKKERI J and HALTIA T. (1999). Expression and mutagenesis of *ZntA*, a zinc-transporting P-type ATPase from Escherichia coli. *Biochemistry* 38(42): 14109-14116.

OKKERI J, BENCOMO E, PIETILA M, and HALTIA T. (2002). Introducing Wilson disease mutations into the zinc-transporting P-type ATPase of *Escherichia coli*. The mutation P634L in the 'hinge' motif (GDGXNDXP) perturbs the formation of the E2P state. *Eur J Biochem* 269(5): 1579-1586.

OKKERI J, LAAKKONEN L, and HALTIA T. (2004). The nucleotide-binding domain of the Zn^{2+}-transporting P-type ATPase from *Escherichia coli* carries a glycine motif that may be involved in binding of ATP. *Biochem J* 377(Pt 1): 95-105.

OSAKI S, JOHNSON DA, and FRIEDEN E. (1966). The possible significance of the ferrous oxidase activity of ceruloplasmin in normal human serum. *J Biol Chem* 241(12): 2746-2751.

OSAKI S and JOHNSON DA. (1969). Mobilization of liver iron by ferroxidase (ceruloplasmin). *J Biol Chem* 244(20): 5757-5758.

OWEN CA, JR. and HAZELRIG JB. (1966). Metabolism of Cu-64-labeled copper by the isolated rat liver. *Am J Physiol* 210(5): 1059-1064.

OZAWA H, KODAMA H, MURATA Y, TAKASHIMA S, and NOMA S. (2001). Transient temporal lobe changes and a novel mutation in a patient with Menkes disease. *Pediatr Int* 43(4): 437-440.

PALMGREN MG and AXELSEN KB. (1998). Evolution of P-type ATPases. *Biochim Biophys Acta* 1365(1-2): 37-45.

PANAGIOTAKAKI E, TZETIS M, MANOLAKI N, LOUDIANOS G, PAPATHEODOROU A *et al.* (2004). Genotype-phenotype correlations for a wide spectrum of mutations in the Wilson disease gene (*ATP7B*). *Am J Med Genet A* 131(2): 168-173.

PASCALE MC, FRANCESCHELLI S, MOLTEDO O, BELLEUDI F, TORRISI MR *et al.* (2003). Endosomal trafficking of the Menkes copper ATPase ATP7A is mediated by vesicles containing the Rab7 and Rab5 GTPase proteins. *Exp Cell Res* 291(2): 377-385.

PASE L, VOSKOBOINIK I, GREENOUGH M, and CAMAKARIS J. (2004). Copper stimulates trafficking of a distinct pool of the Menkes copper ATPase (ATP7A) to the plasma membrane and diverts it into a rapid recycling pool. *Biochem J* 378(Pt 3): 1031-1037.

PAYNE AS and GITLIN JD. (1998). Functional expression of the Menkes disease protein reveals common biochemical mechanisms among the copper-transporting P-type ATPases. *J Biol Chem* 273(6): 3765-3770.

PAYNE AS, KELLY EJ, and GITLIN JD. (1998). Functional expression of the Wilson disease protein reveals mislocalization and impaired copper-dependent trafficking of the common H1069Q mutation. *Proc Natl Acad Sci U S A* 95(18): 10854-10859.

PENA MM, LEE J, and THIELE DJ. (1999). A delicate balance: homeostatic control of copper uptake and distribution. *J Nutr* 129(7): 1251-1260.

PETRIS MJ, MERCER JF, CULVENOR JG, LOCKHART P, GLEESON PA *et al.* (1996). Ligand-regulated transport of the Menkes copper P-type ATPase efflux pump from the Golgi apparatus to the plasma membrane: a novel mechanism of regulated trafficking. *EMBO J* 15(22): 6084-6095.

PETRIS MJ, CAMAKARIS J, GREENOUGH M, LAFONTAINE S, and MERCER JF. (1998). A C-terminal di-leucine is required for localization of the Menkes protein in the *trans*-Golgi network. *Hum Mol Genet* 7(13): 2063-2071.

PETRIS MJ and MERCER JF. (1999). The Menkes protein (ATP7A; MNK) cycles via the plasma membrane both in basal and elevated extracellular copper using a C-terminal di-leucine endocytic signal. *Hum Mol Genet* 8(11): 2107-2115.

PETRIS MJ, VOSKOBOINIK I, CATER M, SMITH K, KIM BE *et al.* (2002). Copper-regulated trafficking of the Menkes disease copper ATPase is associated with formation of a phosphorylated catalytic intermediate. *J Biol Chem* 277(48): 46736-46742.

PETRIS MJ, SMITH K, LEE J, and THIELE DJ. (2003). Copper-stimulated endocytosis and degradation of the human copper transporter, hCtr1. *J Biol Chem* 278(11): 9639-9646.

PETRUKHIN K, LUTSENKO S, CHERNOV I, ROSS BM, KAPLAN JH *et al.* (1994). Characterization of the Wilson disease gene encoding a P-type copper transporting ATPase: genomic organization, alternative splicing, and structure/function predictions. *Hum Mol Genet* 3(9): 1647-1656.

POND L, KUHN LA, TEYTON L, SCHUTZE MP, TAINER JA *et al.* (1995). A role for acidic residues in di-leucine motif-based targeting to the endocytic pathway. *J Biol Chem* 270(34): 19989-19997.

POULSEN L, HORN N, HEILSTRUP H, LUND C, TUMER Z *et al.* (2002). X-linked recessive Menkes disease: identification of partial gene deletions in affected males. *Clin Genet* 62(6): 449-457.

PROHASKA JR and GYBINA AA. (2004). Intracellular copper transport in mammals. *J Nutr* 134(5): 1003-1006.

PROUD VK, MUSSELL HG, KALER SG, YOUNG DW, and PERCY AK. (1996). Distinctive Menkes disease variant with occipital horns: delineation of natural history and clinical phenotype. *Am J Med Genet* 65(1): 44-51.

PUFAHL RA, SINGER CP, PEARISO KL, LIN SJ, SCHMIDT PJ *et al.* (1997). Metal ion chaperone function of the soluble Cu(I) receptor Atx1. *Science* 278(5339): 853-856.

QI M and BYERS PH. (1998). Constitutive skipping of alternatively spliced exon 10 in the *ATP7A* gene abolishes Golgi localization of the menkes protein and produces the occipital horn syndrome. *Hum Mol Genet* 7(3): 465-469.

RAE TD, SCHMIDT PJ, PUFAHL RA, CULOTTA VC, and O'HALLORAN TV. (1999). Undetectable intracellular free copper: the requirement of a copper chaperone for superoxide dismutase. *Science* 284(5415): 805-808.

RALLE M, LUTSENKO S, and BLACKBURN NJ. (2004). Copper transfer to the N-terminal domain of the Wilson disease protein (ATP7B): X-ray absorption spectroscopy of reconstituted and chaperone-loaded metal binding domains and their interaction with exogenous ligands. *J Inorg Biochem* 98(5): 765-774.

RAUCH H. (1983). Toxic milk, a new mutation affecting cooper metabolism in the mouse. *J Hered* 74(3): 141-144.

RAUCH H and WELLS AJ. (1995). The toxic milk mutation, *tx*, which results in a condition resembling Wilson disease in humans, is linked to mouse chromosome 8. *Genomics* 29(2): 551-552.

REAVES BJ, BANTING G, and LUZIO JP. (1998). Lumenal and transmembrane domains play a role in sorting type I membrane proteins on endocytic pathways. *Mol Biol Cell* 9(5): 1107-1122.

REED V, WILLIAMSON P, BULL PC, COX DW, and BOYD Y. (1995). Mapping of the mouse homologue of the Wilson disease gene to mouse chromosome 8. *Genomics* 28(3): 573-575.

REED V and BOYD Y. (1997). Mutation analysis provides additional proof that *mottled* is the mouse homologue of Menkes' disease. *Hum Mol Genet* 6(3): 417-423.

RIORDAN SM and WILLIAMS R. (2001). The Wilson's disease gene and phenotypic diversity. *J Hepatol* 34(1): 165-171.

ROBERTS EA and COX DW. (1998). Wilson disease. *Bailliere's Clinical Gastroenterology* 12(2): 237-256.

ROBERTS EA and SCHILSKY ML. (2003). A practice guideline on Wilson disease. *Hepatology* 37(6): 1475-1492.

ROBINSON MS. (1994). The role of clathrin, adaptors and dynamin in endocytosis. *Curr Opin Cell Biol* 6(4): 538-544.

ROBINSON MS and BONIFACINO JS. (2001). Adaptor-related proteins. *Curr Opin Cell Biol* 13(4): 444-453.

ROBINSON MS. (2004). Adaptable adaptors for coated vesicles. *Trends Cell Biol* 14(4): 167-174.

ROELOFSEN H, WOLTERS H, VAN LUYN MJ, MIURA N, KUIPERS F *et al.* (2000). Copper-induced apical trafficking of ATP7B in polarized hepatoma cells provides a mechanism for biliary copper excretion. *Gastroenterology* 119(3): 782-793.

RONCE N, MOIZARD MP, ROBB L, TOUTAIN A, VILLARD L *et al.* (1997). A C2055T transition in exon 8 of the *ATP7A* gene is associated with exon skipping in an occipital horn syndrome family. *Am J Hum Genet* 61(1): 233-238.

ROSENZWEIG AC and O'HALLORAN TV. (2000). Structure and chemistry of the copper chaperone proteins. *Curr Opin Chem Biol* 4(2): 140-147.

ROST B. (1999). Twilight zone of protein sequence alignments. *Protein Eng* 12(2): 85-94.

SAFAEI R, HOLZER AK, KATANO K, SAMIMI G, and HOWELL SB. (2004a). The role of copper transporters in the development of resistance to Pt drugs. *J Inorg Biochem* 98(10): 1607-1613.

SAFAEI R, KATANO K, SAMIMI G, NAERDEMANN W, STEVENSON JL *et al.* (2004b). Cross-resistance to cisplatin in cells with acquired resistance to copper. *Cancer Chemother Pharmacol* 53(3): 239-246.

SAFAEI R and HOWELL SB. (2005). Copper transporters regulate the cellular pharmacology and sensitivity to Pt drugs. *Crit Rev Oncol Hematol* 53(1): 13-23.

SAMIMI G, KATANO K, HOLZER AK, SAFAEI R, and HOWELL SB. (2004a). Modulation of the cellular pharmacology of cisplatin and its analogs by the copper exporters ATP7A and ATP7B. *Mol Pharmacol* 66(1): 25-32.

SAMIMI G, SAFAEI R, KATANO K, HOLZER AK, ROCHDI M *et al.* (2004b). Increased expression of the copper efflux transporter ATP7A mediates resistance to cisplatin, carboplatin, and oxaliplatin in ovarian cancer cells. *Clin Cancer Res* 10(14): 4661-4669.

SANCHEZ-ALBISUA I, GARDE T, HIERRO L, CAMARENA C, FRAUCA E *et al.* (1999). A high index of suspicion: the key to an early diagnosis of Wilson's disease in childhood. *J Pediatr Gastroenterol Nutr* 28(2): 186-190.

SAQI MA, RUSSELL RB, and STERNBERG MJ. (1998). Misleading local sequence alignments: implications for comparative protein modelling. *Protein Eng* 11(8): 627-630.

SARKAR B, LINGERTAT-WALSH K, and CLARKE JT. (1993). Copper-histidine therapy for Menkes disease. *J Pediatr* 123(5): 828-830.

SARKAR B. (2000). Copper transport and its defect in Wilson disease: characterization of the copper-binding domain of Wilson disease ATPase. *J Inorg Biochem* 79(1-4): 187-191.

SATO M and GITLIN JD. (1991). Mechanisms of copper incorporation during the biosynthesis of human ceruloplasmin. *J Biol Chem* 266(8): 5128-5134.

SCARBOROUGH GA. (1999). Structure and function of the P-type ATPases. *Curr Opin Cell Biol* 11(4): 517-522.

SCHAEFER M, HOPKINS RG, FAILLA ML, and GITLIN JD. (1999a). Hepatocyte-specific localization and copper-dependent trafficking of the Wilson's disease protein in the liver. *Am J Physiol* 276(3 Pt 1): G639-646.

SCHAEFER M, ROELOFSEN H, WOLTERS H, HOFMANN WJ, MULLER M *et al.* (1999b). Localization of the Wilson's disease protein in human liver. *Gastroenterology* 117(6): 1380-1385.

SCHAFER W, STROH A, BERGHOFER S, SEILER J, VEY M *et al.* (1995). Two independent targeting signals in the cytoplasmic domain determine *trans*-Golgi network localization and endosomal trafficking of the proprotein convertase furin. *EMBO J* 14(11): 2424-2435.

SCHENA M, PICARD D, and YAMAMOTO KR. (1991). Vectors for constitutive and inducible gene expression in yeast. *Methods Enzymol* 194(389-398.

SCHILSKY ML, BLANK RR, CZAJA MJ, ZERN MA, SCHEINBERG IH *et al.* (1989). Hepatocellular copper toxicity and its attenuation by zinc. *J Clin Invest* 84(5): 1562-1568.

SCHILSKY ML. (1994). Identification of the Wilson's disease gene: clues for disease pathogenesis and the potential for molecular diagnosis. *Hepatology* 20(2): 529-533.

SCHILSKY ML, STOCKERT RJ, and STERNLIEB I. (1994). Pleiotropic effect of LEC mutation: a rodent model of Wilson's disease. *Am J Physiol* 266(5 Pt 1): G907-913.

SCHILSKY ML. (2002). Diagnosis and treatment of Wilson's disease. *Pediatr Transplant* 6(1): 15-19.

SETALURI V. (2000). Sorting and targeting of melanosomal membrane proteins: signals, pathways, and mechanisms. *Pigment Cell Res* 13(3): 128-134.

SHAH AB, CHERNOV I, ZHANG HT, ROSS BM, DAS K *et al.* (1997). Identification and analysis of mutations in the Wilson disease gene (*ATP7B*): population frequencies, genotype-phenotype correlation, and functional analyses. *Am J Hum Genet* 61(2): 317-328.

SHAW CF, 3RD, SAVAS MM, and PETERING DH. (1991). Ligand substitution and sulfhydryl reactivity of metallothionein. *Methods Enzymol* 205(401-414.

SHIM H and HARRIS ZL. (2003). Genetic defects in copper metabolism. *J Nutr* 133(5 Suppl 1): 1527S-1531S.

SHIMIZU N, NAKAZONO H, TAKESHITA Y, IKEDA C, FUJII H *et al.* (1999). Molecular analysis and diagnosis in Japanese patients with Wilson's disease. *Pediatr Int* 41(4): 409-413.

SIMMERMAN HK and JONES LR. (1998). Phospholamban: protein structure, mechanism of action, and role in cardiac function. *Physiol Rev* 78(4): 921-947.

SIMPSON F, PEDEN AA, CHRISTOPOULOU L, and ROBINSON MS. (1997). Characterization of the adaptor-related protein complex, AP-3. *J Cell Biol* 137(4): 835-845.

SLIMANE TA, TRUGNAN G, VAN ISC, and HOEKSTRA D. (2003). Raft-mediated trafficking of apical resident proteins occurs in both direct and transcytotic pathways in polarized hepatic cells: role of distinct lipid microdomains. *Mol Biol Cell* 14(2): 611-624.

SOLIOZ M and VULPE C. (1996). CPx-type ATPases: a class of P-type ATPases that pump heavy metals. *Trends Biochem Sci* 21(7): 237-241.

SOLIOZ M. (1998). Copper homeostasis of CPX-type ATPases, the subclass of heavy metal P-type ATPases. *Advances in Molecular and Cell Biology* 23A(167-203.

STAPELBROEK JM, BOLLEN CW, VAN AMSTEL JK, VAN ERPECUM KJ, VAN HATTUM J *et al.* (2004). The H1069Q mutation in *ATP7B* is associated with late and neurologic presentation in Wilson disease: results of a meta-analysis. *J Hepatol* 41(5): 758-763.

STEINDL P, FERENCI P, DIENES HP, GRIMM G, PABINGER I *et al.* (1997). Wilson's disease in patients presenting with liver disease: a diagnostic challenge. *Gastroenterology* 113(1): 212-218.

STEPHENSON SE, DUBACH D, LIM CM, MERCER JF, and LA FONTAINE S. (2005). A single PDZ domain protein interacts with the Menkes copper ATPase, ATP7A. A new protein implicated in copper homeostasis. *J Biol Chem* 280(39): 33270-33279.

STRAUSAK D, LA FONTAINE S, HILL J, FIRTH SD, LOCKHART PJ *et al.* (1999). The role of GMXCXXC metal binding sites in the copper-induced redistribution of the Menkes protein. *J Biol Chem* 274(16): 11170-11177.

SU LC, RAVANSHAD S, OWEN CA, JR., MCCALL JT, ZOLLMAN PE *et al.* (1982). A comparison of copper-loading disease in Bedlington terriers and Wilson's disease in humans. *Am J Physiol* 243(3): G226-230.

SUZUKI M and GITLIN JD. (1999). Intracellular localization of the Menkes and Wilson's disease proteins and their role in intracellular copper transport. *Pediatr Int* 41(4): 436-442.

TADA M and KADOMA M. (1989). Regulation of the Ca^{2+} pump ATPase by cAMP-dependent phosphorylation of phospholamban. *Bioessays* 10(5): 157-163.

TAKESHITA Y, SHIMIZU N, YAMAGUCHI Y, NAKAZONO H, SAITOU M *et al.* (2002). Two families with Wilson disease in which siblings showed different phenotypes. *J Hum Genet* 47(10): 543-547.

TAN PK, WAITES C, LIU Y, KRANTZ DE, and EDWARDS RH. (1998). A leucine-based motif mediates the endocytosis of vesicular monoamine and acetylcholine transporters. *J Biol Chem* 273(28): 17351-17360.

TANZI RE, PETRUKHIN K, CHERNOV I, PELLEQUER JL, WASCO W *et al.* (1993). The Wilson disease gene is a copper transporting ATPase with homology to the Menkes disease gene. *Nat Genet* 5(4): 344-350.

TAO TY, LIU F, KLOMP L, WIJMENGA C, and GITLIN JD. (2003). The copper toxicosis gene product Murr1 directly interacts with the Wilson disease protein. *J Biol Chem* 278(43): 41593-41596.

TAPIERO H, TOWNSEND DM, and TEW KD. (2003). Trace elements in human physiology and pathology. Copper. *Biomed Pharmacother* 57(9): 386-398.

TARNACKA B, GROMADZKA G, RODO M, MIERZEJEWSKI P, and CZLOONKOWSKA A. (2000). Frequency of His1069Gln and Gly1267Lys mutations in Polish Wilson's disease population. *Eur J Neurol* 7(5): 495-498.

TERADA K, KAWARADA Y, MIURA N, YASUI O, KOYAMA K *et al.* (1995). Copper incorporation into ceruloplasmin in rat livers. *Biochim Biophys Acta* 1270(1): 58-62.

TERADA K, NAKAKO T, YANG XL, IIDA M, AIBA N *et al.* (1998). Restoration of holoceruloplasmin synthesis in LEC rat after infusion of recombinant adenovirus bearing WND cDNA. *J Biol Chem* 273(3): 1815-1820.

TERADA K, AIBA N, YANG XL, IIDA M, NAKAI M *et al.* (1999). Biliary excretion of copper in LEC rat after introduction of copper transporting P-type ATPase, ATP7B. *FEBS Lett* 448(1): 53-56.

THEOPHILOS MB, COX DW, and MERCER JF. (1996). The toxic milk mouse is a murine model of Wilson disease. *Hum Mol Genet* 5(10): 1619-1624.

THOMAS GR, FORBES JR, ROBERTS EA, WALSHE JM, and COX DW. (1995). The Wilson disease gene: spectrum of mutations and their consequences. *Nat Genet* 9(2): 210-217.

TODOROV T, SAVOV A, JELEV H, PANTELEEVA E, KONSTANTINOVA D *et al.* (2005). Spectrum of mutations in the Wilson disease gene (*ATP7B*) in the Bulgarian population. *Clin Genet* 68(5): 474-476.

TOWBIN H, STAEHELIN T, and GORDON J. (1979). Electrophoretic transfer of proteins from polyacrylamide gels to nitrocellulose sheets: procedure and some applications. *Proc Natl Acad Sci U S A* 76(9): 4350-4354.

TOYOSHIMA C, NAKASAKO M, NOMURA H, and OGAWA H. (2000). Crystal structure of the calcium pump of sarcoplasmic reticulum at 2.6 Å resolution. *Nature* 405(6787): 647-655.

TOYOSHIMA C and NOMURA H. (2002). Structural changes in the calcium pump accompanying the dissociation of calcium. *Nature* 418(6898): 605-611.

TROWBRIDGE IS, COLLAWN JF, and HOPKINS CR. (1993). Signal-dependent membrane protein trafficking in the endocytic pathway. *Annu Rev Cell Biol* 9(129-161.

TSAI CH, TSAI FJ, WU JY, CHANG JG, LEE CC *et al.* (1998). Mutation analysis of Wilson disease in Taiwan and description of six new mutations. *Hum Mutat* 12(6): 370-376.

TSIVKOVSKII R, MACARTHUR BC, and LUTSENKO S. (2001). The Lys1010-Lys1325 fragment of the Wilson's disease protein binds nucleotides and interacts with the N-terminal domain of this protein in a copper-dependent manner. *J Biol Chem* 276(3): 2234-2242.

TSIVKOVSKII R, EISSES JF, KAPLAN JH, and LUTSENKO S. (2002). Functional properties of the copper-transporting ATPase ATP7B (the Wilson's disease protein) expressed in insect cells. *J Biol Chem* 277(2): 976-983.

TSIVKOVSKII R, EFREMOV RG, and LUTSENKO S. (2003). The role of the invariant His-1069 in folding and function of the Wilson's disease protein, the human copper-transporting ATPase ATP7B. *J Biol Chem* 278(15): 13302-13308.

TÜMER Z, TOMMERUP N, TÖNNESEN T, KREUDER J, CRAIG IW *et al.* (1992). Mapping of the Menkes locus to Xq13.3 distal to the X-inactivation center by an intrachromosomal insertion of the segment Xq13.3-q21.2. *Hum Genet* 88(6): 668-672.

TÜMER Z, TÖNNESEN T, BOHMANN J, MARG W, and HORN N. (1994a). First trimester prenatal diagnosis of Menkes disease by DNA analysis. *J Med Genet* 31(8): 615-617.

TÜMER Z, TÖNNESEN T, and HORN N. (1994b). Detection of genetic defects in Menkes disease by direct mutation analysis and its implications in carrier diagnosis. *J Inherit Metab Dis* 17(3): 267-270.

TÜMER Z, VURAL B, TÖNNESEN T, CHELLY J, MONACO AP *et al.* (1995). Characterization of the exon structure of the Menkes disease gene using vectorette PCR. *Genomics* 26(3): 437-442.

TÜMER Z, HORN N, TÖNNESEN T, CHRISTODOULOU J, CLARKE JT *et al.* (1996). Early copper-histidine treatment for Menkes disease. *Nat Genet* 12(1): 11-13.

TÜMER Z and HORN N. (1997). Menkes disease: recent advances and new aspects. *J Med Genet* 34(4): 265-274.

TÜMER Z, LUND C, TOLSHAVE J, VURAL B, TÖNNESEN T *et al.* (1997). Identification of point mutations in 41 unrelated patients affected with Menkes disease. *Am J Hum Genet* 60(1): 63-71.

TÜMER Z, MØLLER LB, and HORN N. (1999). Mutation spectrum of *ATP7A*, the gene defective in Menkes disease. *Adv Exp Med Biol* 448(83-95.

TÜMER Z, MØLLER LB, and HORN N. (2003). Screening of 383 unrelated patients affected with Menkes disease and finding of 57 gross deletions in *ATP7A*. *Hum Mutat* 22(6): 457-464.

TÜMER Z, HORN N, TÖNNESEN T, CHRISTODOULOU J, CLARKE JT *et al.* (2004). Gene symbol: *ATP7A*. Disease: Menkes disease. *Hum Genet* 114(6): 606.

TWEDT DC, STERNLIEB I, and GILBERTSON SR. (1979). Clinical, morphologic, and chemical studies on copper toxicosis of Bedlington Terriers. *J Am Vet Med Assoc* 175(3): 269-275.

UAUY R, OLIVARES M, and GONZALEZ M. (1998). Essentiality of copper in humans. *Am J Clin Nutr* 67(5 Suppl): 952S-959S.

UNNO K, JUVVADI PR, NAKAJIMA H, SHIRAHIGE K, and KITAMOTO K. (2005). Identification and characterization of rns4/vps32 mutation in the RNase T1 expression-sensitive strain of *Saccharomyces cerevisiae*: Evidence for altered ambient response resulting in transportation of the secretory protein to vacuoles. *FEMS Yeast Res* 5(9): 801-812.

VAN DE SLUIS B, KOLE S, VAN WOLFEREN M, HOLMES NG, PEARSON PL *et al.* (2000). Refined genetic and comparative physical mapping of the canine copper toxicosis locus. *Mamm Genome* 11(6): 455-460.

VAN DE SLUIS B, ROTHUIZEN J, PEARSON PL, VAN OOST BA, and WIJMENGA C. (2002). Identification of a new copper metabolism gene by positional cloning in a purebred dog population. *Hum Mol Genet* 11(2): 165-173.

VAN DE SLUIS BJ, BREEN M, NANJI M, VAN WOLFEREN M, DE JONG P *et al.* (1999). Genetic mapping of the copper toxicosis locus in Bedlington terriers to dog chromosome 10, in a region syntenic to human chromosome region 2p13-p16. *Hum Mol Genet* 8(3): 501-507.

VANDERWERF SM, COOPER MJ, STETSENKO IV, and LUTSENKO S. (2001). Copper specifically regulates intracellular phosphorylation of the Wilson's disease protein, a human copper-transporting ATPase. *J Biol Chem* 276(39): 36289-36294.

VANDERWERF SM and LUTSENKO S. (2002). The Wilson's disease protein expressed in Sf9 cells is phosphorylated. *Biochem Soc Trans* 30(4): 739-741.

VERHEY KJ and BIRNBAUM MJ. (1994). A Leu-Leu sequence is essential for COOH-terminal targeting signal of GLUT4 glucose transporter in fibroblasts. *J Biol Chem* 269(4): 2353-2356.

VOORHEES P, DEIGNAN E, VAN DONSELAAR E, HUMPHREY J, MARKS MS *et al.* (1995). An acidic sequence within the cytoplasmic domain of furin functions as a determinant of *trans*-Golgi network localization and internalization from the cell surface. *EMBO J* 14(20): 4961-4975.

VOSKOBOINIK I, BROOKS H, SMITH S, SHEN P, and CAMAKARIS J. (1998). ATP-dependent copper transport by the Menkes protein in membrane vesicles isolated from cultured Chinese hamster ovary cells. *FEBS Lett* 435(2-3): 178-182.

VOSKOBOINIK I, STRAUSAK D, GREENOUGH M, BROOKS H, PETRIS M *et al.* (1999). Functional analysis of the N-terminal CXXC metal-binding motifs in the human Menkes copper-transporting P-type ATPase expressed in cultured mammalian cells. *J Biol Chem* 274(31): 22008-22012.

VOSKOBOINIK I, GREENOUGH M, LA FONTAINE S, MERCER JF, and CAMAKARIS J. (2001a). Functional studies on the Wilson copper P-type ATPase and toxic milk mouse mutant. *Biochem Biophys Res Commun* 281(4): 966-970.

VOSKOBOINIK I, MAR J, STRAUSAK D, and CAMAKARIS J. (2001b). The regulation of catalytic activity of the menkes copper-translocating P-type ATPase. Role of high affinity copper-binding sites. *J Biol Chem* 276(30): 28620-28627.

VOSKOBOINIK I and CAMAKARIS J. (2002). Menkes copper-translocating P-type ATPase (ATP7A): biochemical and cell biology properties, and role in Menkes disease. *J Bioenerg Biomembr* 34(5): 363-371.

VOSKOBOINIK I, FERNANDO R, VELDHUIS N, HANNAN KM, MARMY-CONUS N *et al.* (2003a). Protein kinase-dependent phosphorylation of the Menkes copper P-type ATPase. *Biochem Biophys Res Commun* 303(1): 337-342.

VOSKOBOINIK I, MAR J, and CAMAKARIS J. (2003b). Mutational analysis of the Menkes copper P-type ATPase (*ATP7A*). *Biochem Biophys Res Commun* 301(2): 488-494.

VRABELOVA S, LETOCHA O, BORSKY M, and KOZAK L. (2005). Mutation analysis of the *ATP7B* gene and genotype/phenotype correlation in 227 patients with Wilson disease. *Mol Genet Metab* 86(1-2): 277-285.

VULPE C, LEVINSON B, WHITNEY S, PACKMAN S, and GITSCHIER J. (1993). Isolation of a candidate gene for Menkes disease and evidence that it encodes a copper-transporting ATPase. *Nat Genet* 3(1): 7-13.

WALDENSTROM E, LAGERKVIST A, DAHLMAN T, WESTERMARK K, and LANDEGREN U. (1996). Efficient detection of mutations in Wilson disease by manifold sequencing. *Genomics* 37(3): 303-309.

WALKER JM, TSIVKOVSKII R, and LUTSENKO S. (2002). Metallochaperone Atox1 transfers copper to the NH_2-terminal domain of the Wilson's disease protein and regulates its catalytic activity. *J Biol Chem* 277(31): 27953-27959.

WALKER JM, HUSTER D, RALLE M, MORGAN CT, BLACKBURN NJ *et al.* (2004). The N-terminal metal-binding site 2 of the Wilson's disease protein plays a key role in the transfer of copper from Atox1. *J Biol Chem* 279(15): 15376-15384.

WALSHE JM. (1956). Penicillamine, a new oral therapy for Wilson's disease. *Am J Med* 21(4): 487-495.

WALSHE JM. (1984). Treatment of Wilson's disease with zinc sulphate. *Br Med J (Clin Res Ed)* 289(6444): 558-559.

WALSHE JM. (2005). Hepatic Wilson's Disease: Initial Treatment and Long-term Management. *Curr Treat Options Gastroenterol* 8(6): 467-472.

WANG E, PENNINGTON JG, GOLDENRING JR, HUNZIKER W, and DUNN KW. (2001). Brefeldin A rapidly disrupts plasma membrane polarity by blocking polar sorting in common endosomes of MDCK cells. *J Cell Sci* 114(Pt 18): 3309-3321.

WATANABE A and SHIMIZU N. (2005). Identification of three novel mutations in Japanese patients with Menkes disease and mutation screening by denaturing high performance liquid chromatography. *Pediatr Int* 47(1): 1-6.

WERNIMONT AK, HUFFMAN DL, LAMB AL, O'HALLORAN TV, and ROSENZWEIG AC. (2000). Structural basis for copper transfer by the metallochaperone for the Menkes/Wilson disease proteins. *Nat Struct Biol* 7(9): 766-771.

WIJMENGA C and KLOMP LW. (2004). Molecular regulation of copper excretion in the liver. *Proc Nutr Soc* 63(1): 31-39.

WILSON SAK. (1912). Progressive lenticular degeneration. A familial nervous disease associated with cirrhosis of the liver. *Brain* 34(295-507.

WU J, FORBES JR, CHEN HS, and COX DW. (1994). The LEC rat has a deletion in the copper transporting ATPase gene homologous to the Wilson disease gene. *Nat Genet* 7(4): 541-545.

WU Z, WANG N, MURONG S, and LIN M. (2000). Identification and analysis of mutations of the Wilson disease gene in Chinese population. *Chin Med J (Engl)* 113(1): 40-43.

WU ZY, WANG N, LIN MT, FANG L, MURONG SX *et al.* (2001). Mutation analysis and the correlation between genotype and phenotype of Arg778Leu mutation in chinese patients with Wilson disease. *Arch Neurol* 58(6): 971-976.

XU P, LIANG X, JANKOVIC J, and LE W. (2001). Identification of a high frequency of mutation at exon 8 of the *ATP7B* gene in a Chinese population with Wilson disease by fluorescent PCR. *Arch Neurol* 58(11): 1879-1882.

YAMADA T, AGUI T, SUZUKI Y, SATO M, and MATSUMOTO K. (1993). Inhibition of the copper incorporation into ceruloplasmin leads to the deficiency in serum ceruloplasmin activity in Long-Evans cinnamon mutant rat. *J Biol Chem* 268(12): 8965-8971.

YAMAGUCHI A, MATSUURA A, ARASHIMA S, KIKUCHI Y, and KIKUCHI K. (1998). Mutations of *ATP7B* gene in Wilson disease in Japan: identification of nine mutations and lack of clear founder effect in a Japanese population. *Hum Mutat* Suppl 1(S320-322.

YAMAGUCHI Y, HEINY ME, SUZUKI M, and GITLIN JD. (1996). Biochemical characterization and intracellular localization of the Menkes disease protein. *Proc Natl Acad Sci U S A* 93(24): 14030-14035.

YANG XL, MIURA N, KAWARADA Y, TERADA K, PETRUKHIN K *et al.* (1997). Two forms of Wilson disease protein produced by alternative splicing are localized in distinct cellular compartments. *Biochem J* 326 (Pt 3)(897-902.

YOO HW. (2002). Identification of novel mutations and the three most common mutations in the human *ATP7B* gene of Korean patients with Wilson disease. *Genet Med* 4(6 Suppl): 43S-48S.

YOSHIDA MC, MASUDA R, SASAKI M, TAKEICHI N, KOBAYASHI H *et al.* (1987). New mutation causing hereditary hepatitis in the laboratory rat. *J Hered* 78(6): 361-365.

YOSHIMIZU T, OMOTE H, WAKABAYASHI T, SAMBONGI Y, and FUTAI M. (1998). Essential Cys-Pro-Cys motif of *Caenorhabditis elegans* copper transport ATPase. *Biosci Biotechnol Biochem* 62(6): 1258-1260.

YUAN DS, STEARMAN R, DANCIS A, DUNN T, BEELER T *et al.* (1995). The Menkes/Wilson disease gene homologue in yeast provides copper to a ceruloplasmin-like oxidase required for iron uptake. *Proc Natl Acad Sci U S A* 92(7): 2632-2636.

YUAN DS, DANCIS A, and KLAUSNER RD. (1997). Restriction of copper export in *Saccharomyces cerevisiae* to a late Golgi or post-Golgi compartment in the secretory pathway. *J Biol Chem* 272(41): 25787-25793.

YUCE A, KOCAK N, OZEN H, and GURAKAN F. (1999). Wilson's disease patients with normal ceruloplasmin levels. *Turk J Pediatr* 41(1): 99-102.

YUZBASIYAN-GURKAN V, BREWER GJ, BOERWINKLE E, and VENTA PJ. (1988). Linkage of the Wilson disease gene to chromosome 13 in North-American pedigrees. *Am J Hum Genet* 42(6): 825-829.

ZHOU B and GITSCHIER J. (1997). *hCTR1*: a human gene for copper uptake identified by complementation in yeast. *Proc Natl Acad Sci U S A* 94(14): 7481-7486.

ZUBENKO GS, MITCHELL AP, and JONES EW. (1980). Mapping of the proteinase b structural gene *PRB1*, in *Saccharomyces cerevisiae* and identification of nonsense alleles within the locus. *Genetics* 96(1): 137-146.

APPENDICES

I. APPENDIX A. Sequence alignments for comparison.

A. ALIGNMENT OF HUMAN ATP7A AND HUMAN ATP7B

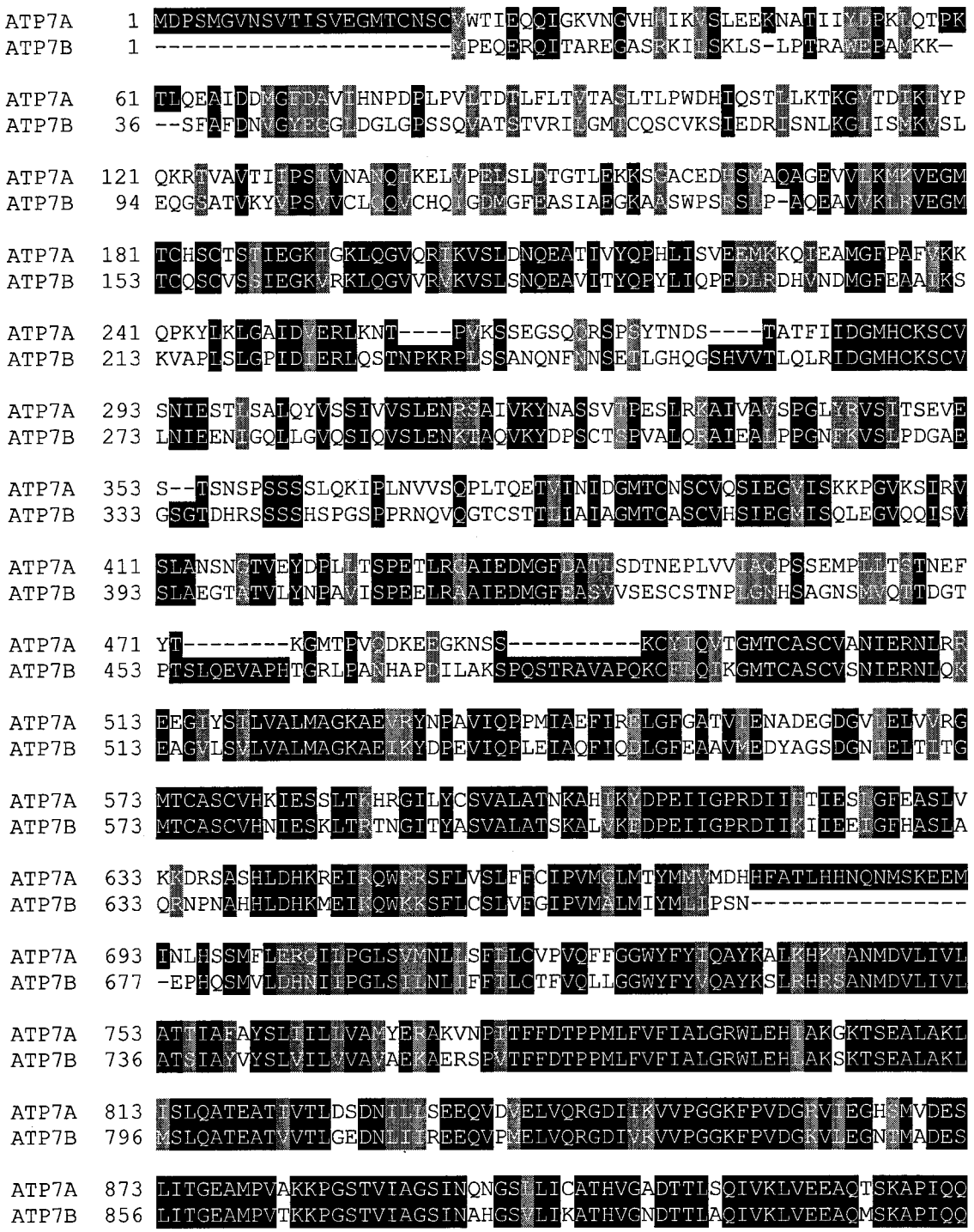

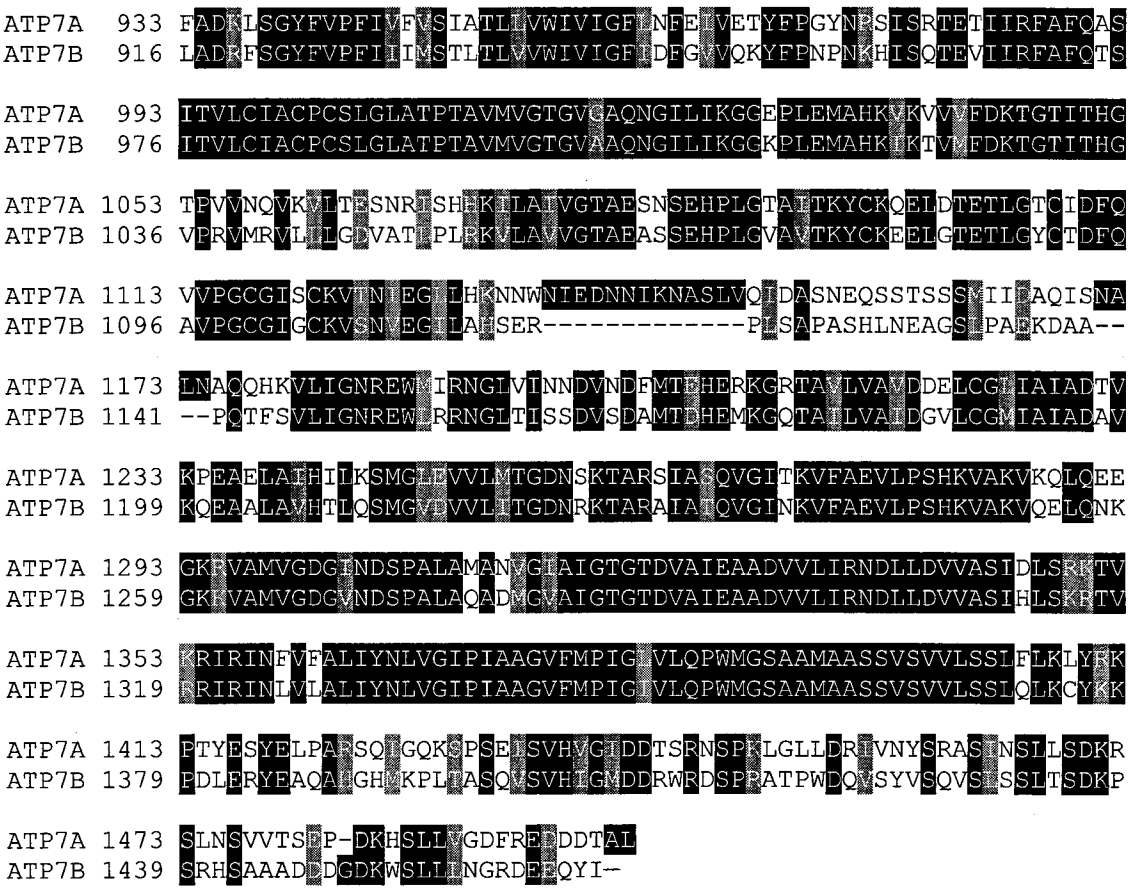

B. HUMAN ATP7B ALIGNED WITH ITS ORTHOLOGUES

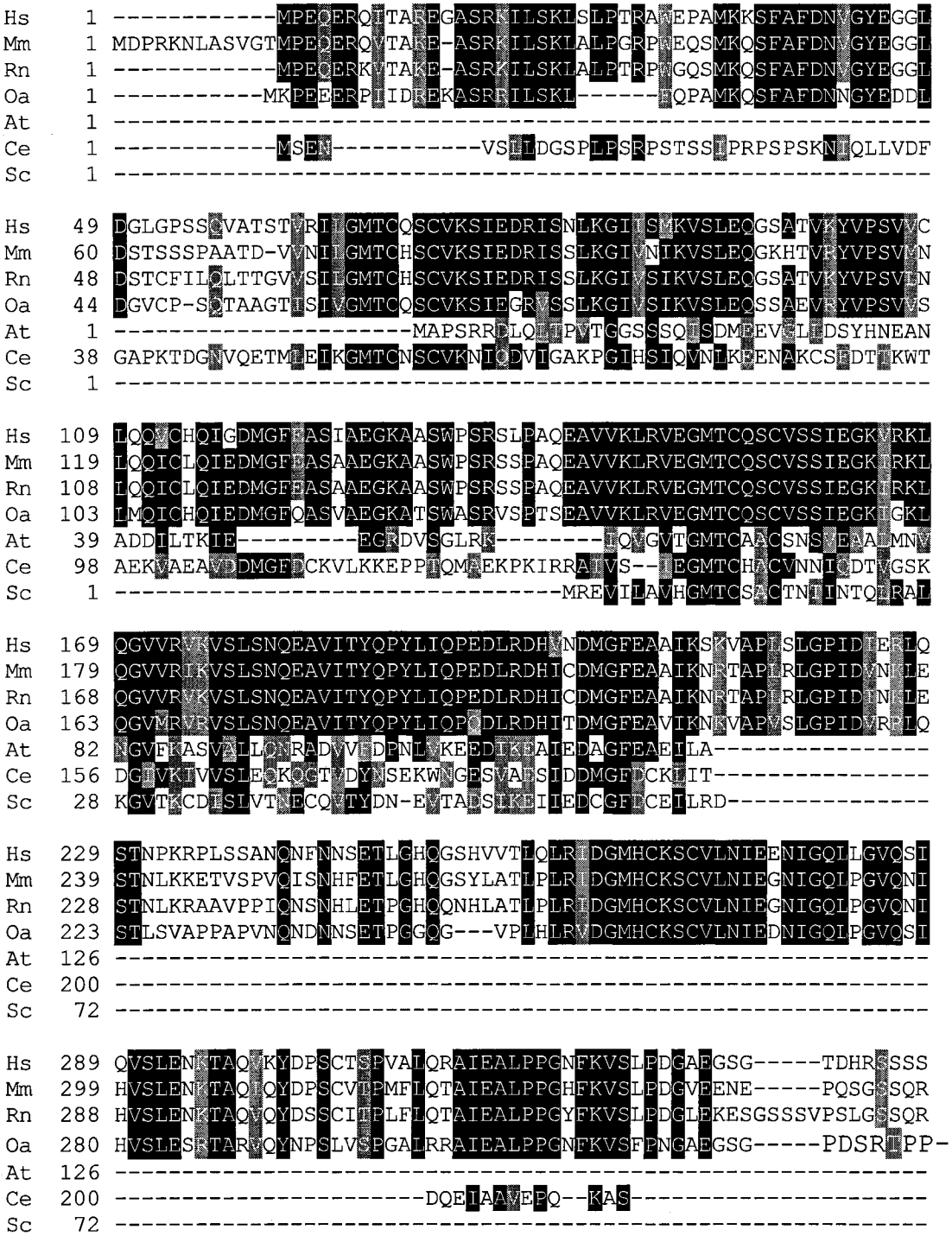

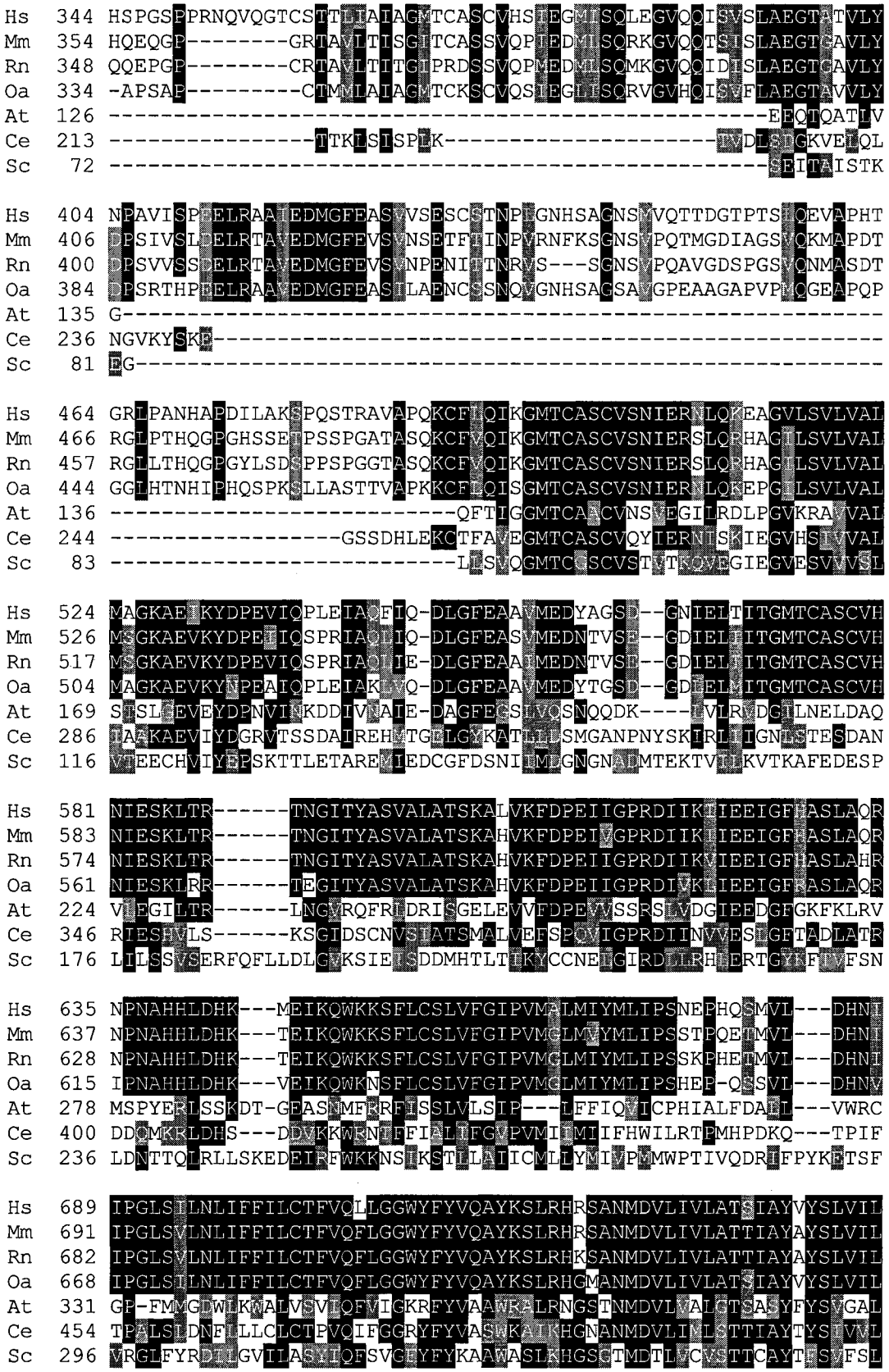

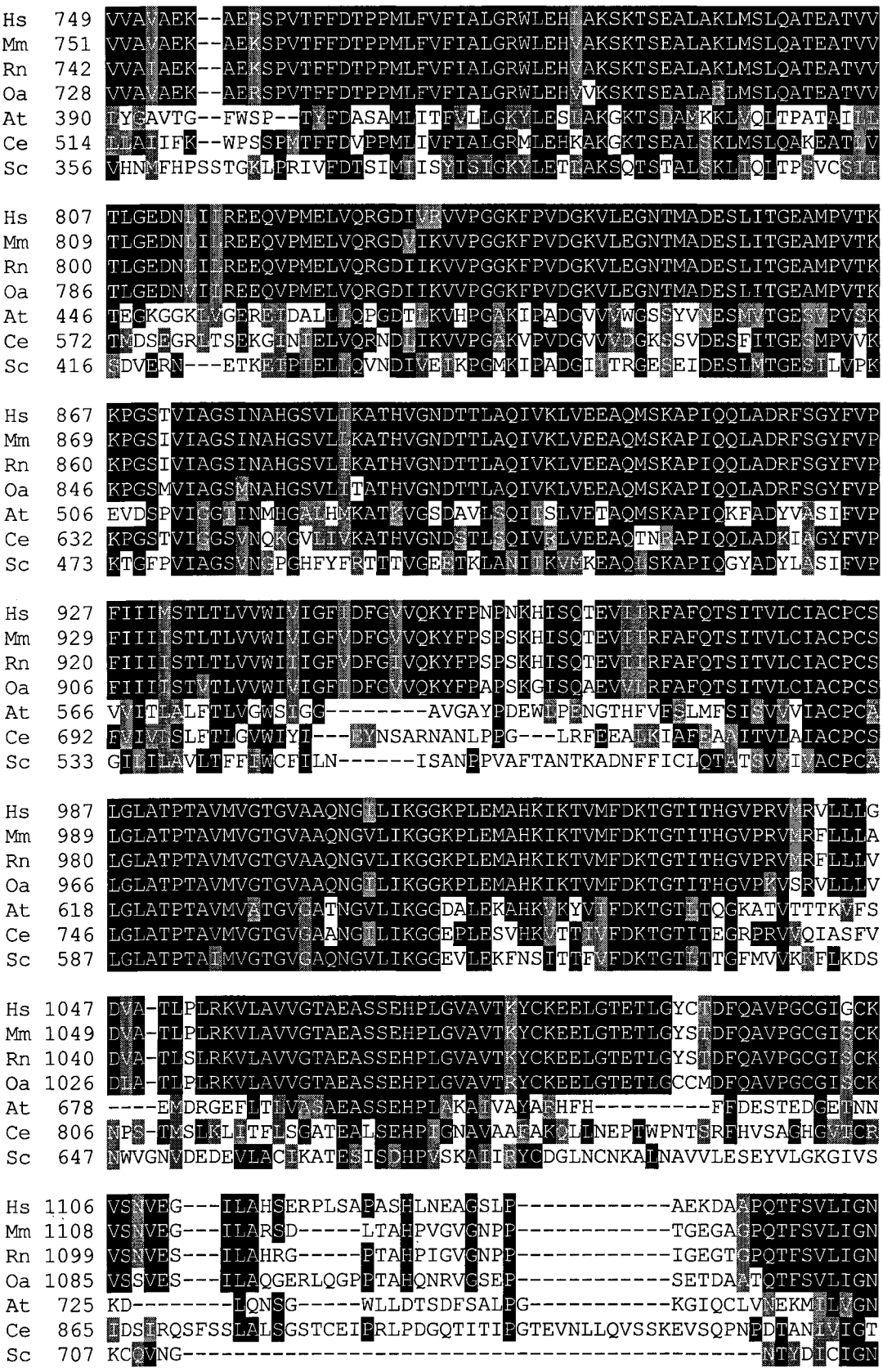

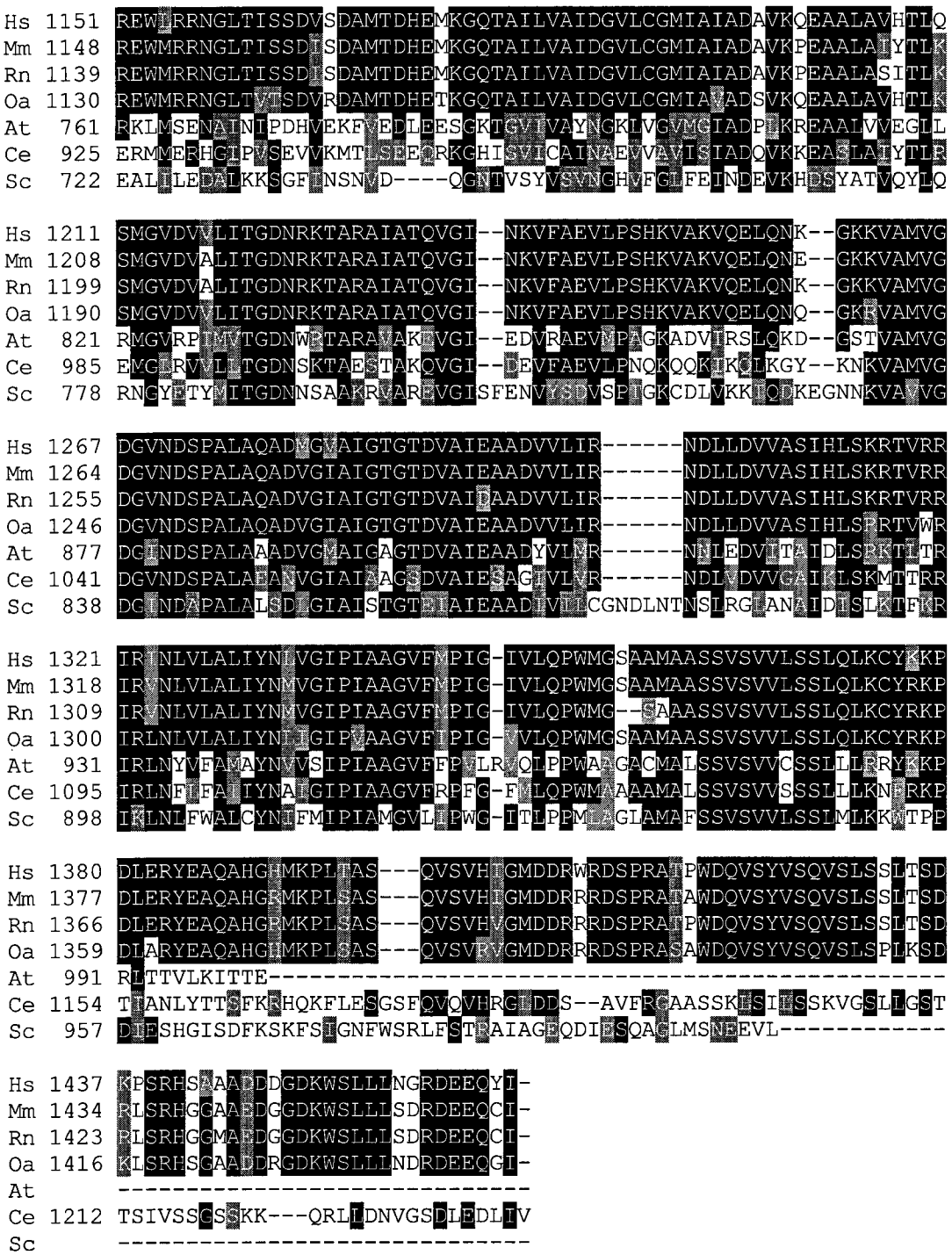

C. HUMAN ATP7A ALIGNED WITH ITS ORTHOLOGUES

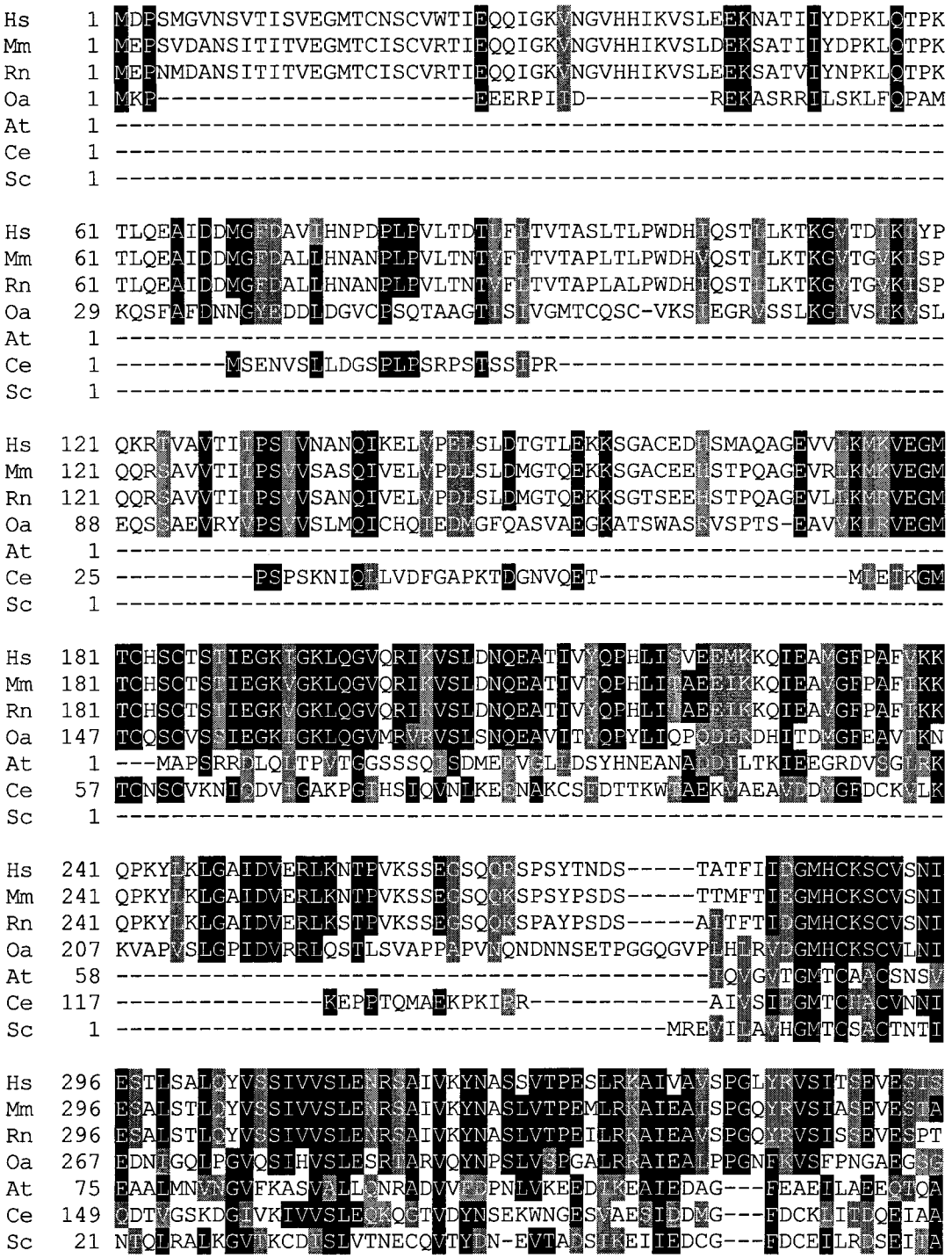

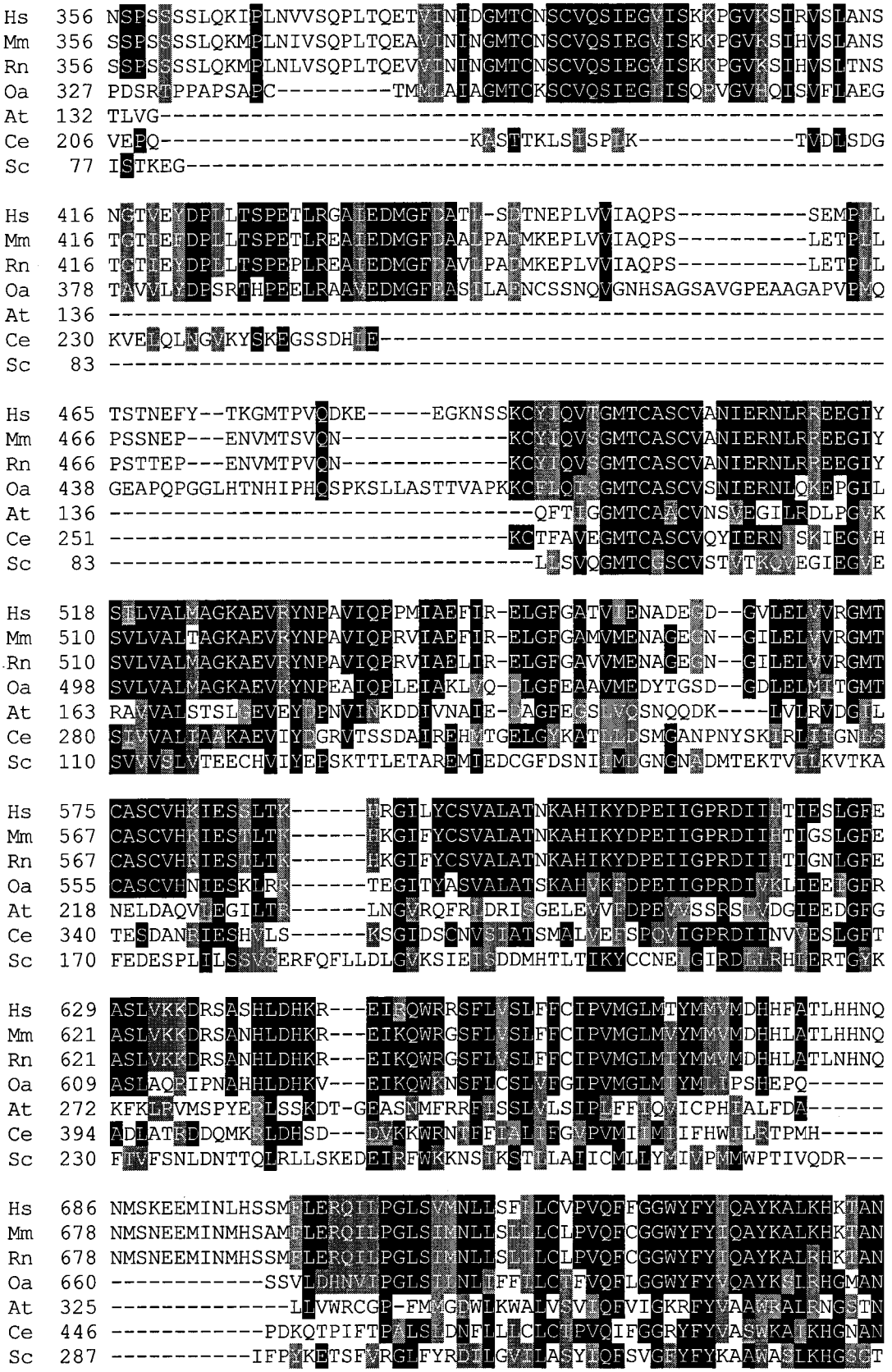

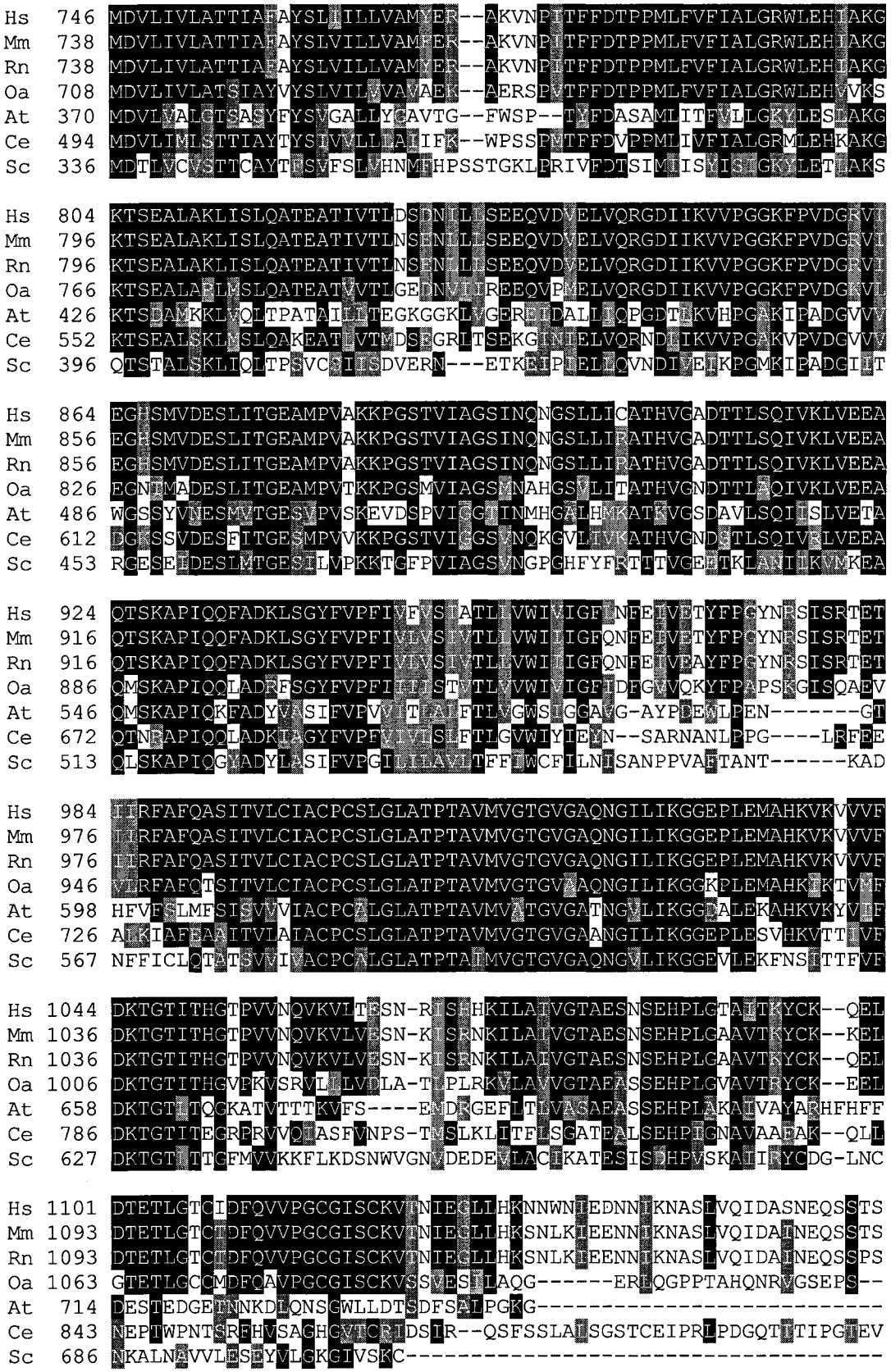

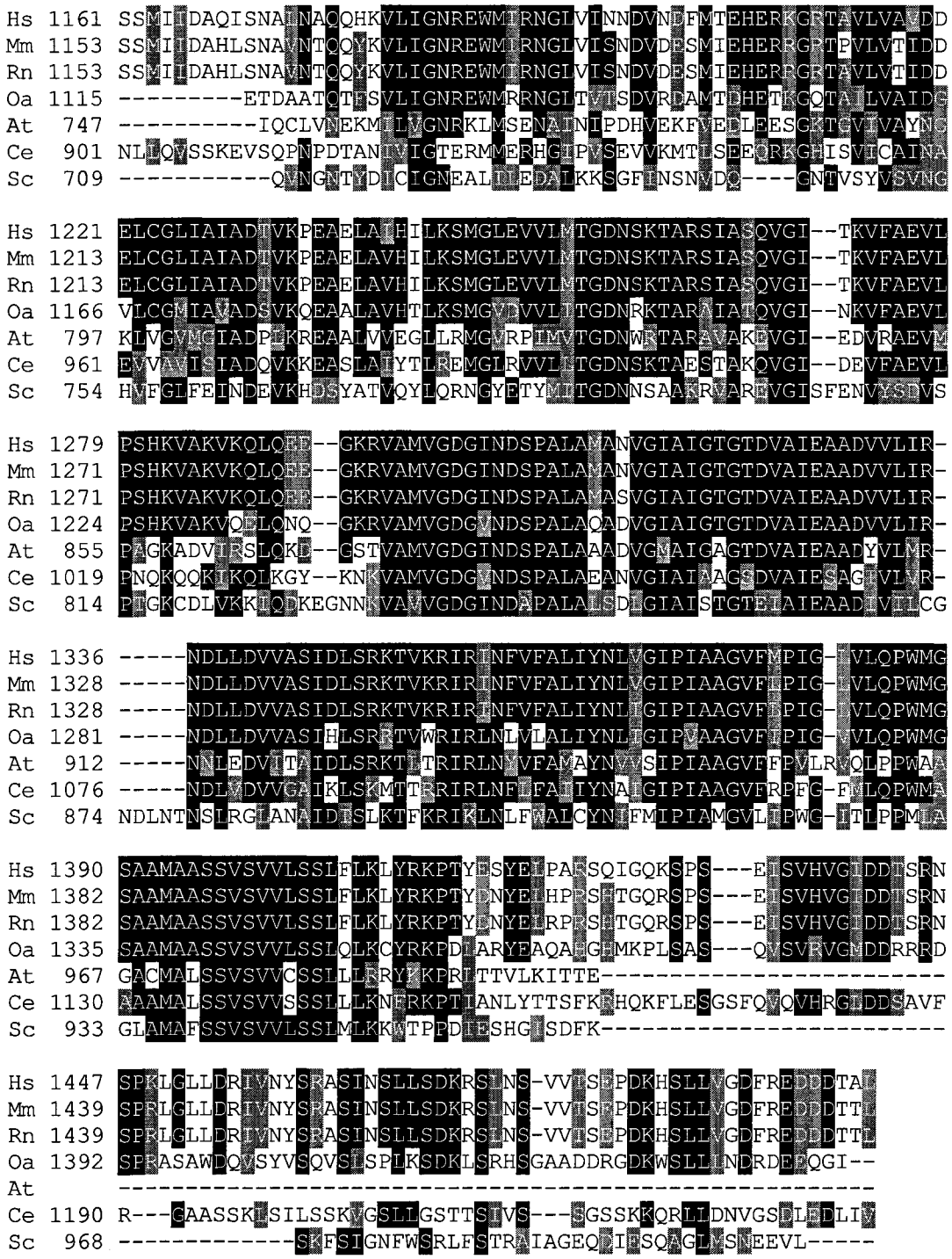

II. APPENDIX B. *ATP7A* mutation database.

EXON	NT (cDNA)	CODON	TYPE		DIS	SEQUENCE	REGION OF PROTEIN[a]	REF[b]
			(nucleotide)	(protein)				
5'UTR	~403del98		deletion		OHS		5'UTR	15
3	c.499C>T	Gln167X	substitution	nonsense	MNK	**C**AA>**T**AA	MBS 2	5
3	c.526_529dupAAAG	Val177-fs	duplication	frameshift	MNK	ins**AAAG**	MBS 2	28
4	c.653_657delATCTT	His218His-fs	deletion	frameshift	MNK	C**ATCTT**AT	MBS 2-3	5
4	c.658_662delATCTC	Ile220Ser-fs	deletion	frameshift	MNK	del**ATCTC**	MBS 2-3	5
4	c.890delG	Ser297Ile-fs	deletion	frameshift	MNK	GAA^A**G**TACT	MBS 3	27
4	c.1029dupA	Tyr343X	duplication	termination	MNK	CTA^TAT>CTATA**A**T	MBS 3-4	19
4	c.1135delA	Thr379Leu-fs	deletion	frameshift	MNK	CAA^GAA**A**CT	MBS 4	28
4	c.1225C>T	Arg409X	substitution	nonsense	MNK	**C**GA-**T**GA	MBS 4	28
4	c.1234delC	Leu412Leu-fs	deletion	frameshift	MNK	TCC^**C**TT	MBS 4	28
5	c.1460C>A	Ser487X	substitution	nonsense	MNK	T**C**A>T**A**A	MBS 5	7
6	c.1585G>T	Glu529X	substitution	nonsense	MNK	**G**AA>**T**AA	MBS 5-6	7
IVS6	c.1707+1g>a		substitution	splice-donor	MNK	GTT**g**taag>GTT**a**taag		18
IVS6	c.1707+5g>a		substitution	splice-donor	MNK	GTTgtaa**g**>GTTgtaa**a**		18
IVS6	c.1707+6del4		deletion	splice-donor	OHS	GTTgtaag**taag**		7,18
7	c.1734C>A	Cys578X	substitution	nonsense	MNK	TG**C**>TG**A**	MBS 6	28
7	c.1748_1749delAG	Glu583Val-fs	deletion	frameshift	MNK	ATA^G**AG**^TCT	MBS 6	5
7	c.1770_1771delAG	Arg590Arg-fs	deletion	frameshift	MNK	CAC^AG**AG**GG	MBS 6	28
7	c.1780dupT	Tyr594Leu-fs	duplication	frameshift	MNK	CTA^TAC>CTA^T**T**AC	MBS 6 - TM 1	28
7	c.1819delT	Ile606Ile-fs	deletion	frameshift	MNK	CAT^AT**T**AAA	MBS 6 - TM 1	28
IVS7	c.1870-1g>c		substitution	splice-acceptor	MNK	a**g**AGC>a**c**AGC		28
IVS7	c.1869+41c>t		substitution	splice-acceptor		same as C2055T		23

8	c.1885_1886insA	Ala629Asp-fs	insertion	frameshift	MNK	GAA^GCT>GAA^G**A**CT	MBS 6 - TM 1	7
8	c.1885G>C	Ala629Pro	substitution	missense	MNK	**G**CT>**C**CT	MBS 6 - TM 1	28
8	c.1910C>G	Ser637X	substitution	nonsense	MNK	T**C**A>T**G**A	MBS 6 - TM 1	28
8	c.1910C>T	Ser637Leu	substitution	missense	OHS	T**C**A>T**T**A	MBS 6 - TM 1	23
8	c.1933C>T	Arg645X	substitution	nonsense	MNK	**C**GA>**T**GA	MBS 6 - TM 1	5
8	c.1936G>T	Glu646X	substitution	nonsense	MNK	**G**AA>**T**AA	MBS 6 - TM 1	8
IVS8	c.1946+1g>c		substitution	splice-donor	MNK	ACA**g**ta>ACA**c**ta		28
IVS8	c.1946+2t>c		substitution	splice-donor	MNK	ACAg**t**a>ACAg**c**a		5
IVS8	c.1946+2_+3del		deletion	splice-donor	MNK	ACAg**ta**agt		28
IVS8	c.1946+5g>a		substitution	splice-donor	MNK	ACAgtaa**g**>ACAgtaa**a**		28
IVS8	c.1946+5g>c		substitution	splice-donor	MNK	ACAgtaa**g**>ACAgtaa**c**		28
IVS8	c.1946+6t>g		substitution	splice-donor	MNK	ACAgtaag**t**>ACAgtaa**g**		28
IVS8	c.1947-1_-5dup		duplication	splice-acceptor	MNK	ataagAT>ataag**ataag**AT		5,28
9	c.2058delA	Asn686Lys-fs	deletion	frameshift	MNK	AAT^CAAA**A**C	TM 1 - TM 2	28
9	c.2068G>T	Glu690X	substitution	nonsense	MNK	**G**AA>**T**AA	TM 1 - TM 2	28
9	c.2117T>G	Leu706Arg	substitution	missense	MNK	C**T**T>C**G**T	TM 2	8
9	c.2153T>A	Leu718X	substitution	nonsense	MNK	T**T**A>T**A**A	TM 2	20
9	c.2172G>T	Gln724His	substitution	missense	MNK	CA**G**>CA**T**	TM 2	10
IVS9	c.2172+5g>c		substitution	splice-donor	MNK			19
10	c.2179G>A	Gly727Arg	substitution	missense	MNK	**G**GA>**A**GA	TM 2	28
10	c.2203_2204insA	Ala735Asp-fs	insertion	frameshift	MNK	CAG^GCT>CAGG**A**CT	TM 2 - TM 3	28
10	c.2284_2285delTT	Leu762-fs	deletion	frameshift	MNK	TAC^TCT**TT**G	TM 3	28
10	c.2314_2317delAGAG	Arg771Pro-fs	deletion	frameshift	MNK	GAG**AGAG**CC	TM 3 - TM 4	7
10	c.2337_2350del	Thr779-fs	deletion	frameshift	MNK	CCT^ATTAC**TTTCTTTGACACAC**CCCCT	TM 4	28
10	c.2383C>T	Arg795X	substitution	nonsense	MNK	**C**GA>**T**GA	TM 4	28
IVS10	c.2406+3a>t		substitution	splice-donor	OHS	gt**a**aagt>gt**t**aagt		22
11	c.2446C>T	Gln816X	substitution	nonsense	MNK	**C**AA>**T**AA	TD	17
11	c.2497A>G	Ser833Gly	substitution	missense	OHS	**A**GT>**G**GT	TD	9

12	c.2508delA	Gln836Gln-fs	deletion	frameshift	MNK	GAA^CA**A**GTG	TD	27
12	c.2618T>G	Leu873Arg	substitution	missense	MNK	C**T**C>C**G**C	TD	19
IVS12	c.2627-2a>g		substitution	splice-acceptor	MNK	**a**gGGG>**g**gGGG		28
13	c.2686C>T	Gln896X	substitution	nonsense	MNK	**C**AG>**T**AG	TD	28
13	c.2770C>T	Gln924X	substitution	nonsense	MNK	**C**AA>**T**AA	TD	28
14	c.2867G>A	Trp956X	substitution	nonsense	MNK	T**G**G>T**A**G	TM 5	28
14	c.2888delA	Asn963Ile-fs	deletion	frameshift	MNK	TTT^CTGA**A**TTTT	TM 5	28
IVS14	c.2917-4a>g		substitution	splice-acceptor	OHS			6
15	c.2938delC	Arg980Glu-fs	deletion	frameshift	MNK	ATC^TCC**C**GAACA	TM 5 - TM 6	28
15	c.2938C>T	Arg980X	substitution	nonsense	MNK	TCC^**C**GA	TM 5 - TM 6	7
15	c.2956C>T	Arg986X	substitution	nonsense	MNK	**C**GA>**T**GA	TM 6	21
15	c.3017T>C	Leu1006Pro	substitution	missense	MNK	C**T**G>C**C**G	TM 6	28
15	c.3056G>A	Gly1019Asp	substitution	missense	MNK	G**G**T>G**A**T	TM 6	28
15	c.3074_3075dupTA	Ile1026X	duplication	termination	MNK	ATACTA**TA**ATA	TM 6	7
16	c.3241G>T	Glu1081X	substitution	nonsense	MNK	**G**AA>**T**AA	PD - SEHPL	28
16	c.32450dupA	Asn1083Lys-fs	insertion	frameshift	MNK	AGTAAC>AGTAA**A**C	PD - SEHPL	28
16	c.3293_3294delAG	Gln1098Arg-fs	deletion	frameshift	MNK	AAAC**AG**GTAC	SEHPL - ATP	7
17	c.3353G>A	Gly1118Asp	substitution	missense	MNK	G**G**T>G**A**T	ATP	8
17	c.3493delT	Ile1164Ile-fs	deletion	frameshift	MNK	TCC^ATGAT**T**ATT	ATP	28
IVS17	c.3511+5g>a		substitution	splice-donor	mild			6,16
19	c.3682delC	Ala1227-fs	deletion	frameshift	MNK	ATAGC**C**	ATP	17
19	c.3706delA	Glu1235-fs	deletion	frameshift	MNK	AAG^CCTGA**A**GCA	ATP	28
19	c.3763G>A	Gly1255Arg	substitution	missense	MNK	**G**GA>**A**GA	ATP	8
20	c.3883delA	Lys1294Asn-fs	deletion	frameshift	MNK	GAG^GGGAA**A**	ATP	28
20	c.3904G>A	Gly1302Arg	substitution	missense	MNK	**G**GA>**A**GA	ATP	5
20	c.4005delG	Arg1335-fs	deletion	frameshift	MNK	ATA^AG**G**AAT	ATP	7
IVS20	c.4006-2a>g		substitution	splice-acceptor	MNK	**a**gAA>**g**gAA		5

21	c.4032T>A	Ser1344Arg	substitution	missense	MNK	AG**T**>AG**A**	ATP	7
21	c.4033A>T	Ile1345Phe	substitution	missense	MNK	**A**TT>**T**TT	ATP	7
21	c.4085C>T	Ala1362Val	substitution	missense	MNK	G**C**T>G**T**T	TM 7	1
IVS21	c.4123+3a>t		substitution	splice-donor	MNK			9
22	c.4132dupA	Met1378Asn-fs	duplication	frameshift	MNK	TTT^A**A**TG	TM 7	1
22	c.4141_4150del	Gly1381Cys-fs	deletion	frameshift	MNK	CCC^ATT**GGTTTGGTTT**TGCA	TM 7	28
22	c.4198_4199delGT	Val1400-fs	deletion	frameshift	MNK	GTT^TCT**GT**AGTA	TM 8	28
22/IVS22	c.4208del15, c.4226+1_+19del	Leu1402-fs	deletion	splice-donor	MNK	**TCTTCTCTCTTAAACTgtaagtatgatagcttttg**	3'-COOH	7
IVS22			substitution	splice-donor	MNK	ACT**g**t>ACT**g**c		28
23	c.4352delG	Gly1451Val-fs	deletion	frameshift	OHS	AAA^CTGG**G**TT	3'-COOH	4

[a]MBS: metal-binding site; TM: transmembrane helix; TD: transduction domain; PD: phosphorylation domain; SEHPL: conserved SEHPL motif; ATP: nucleotide-binding domain

[b]Full references listed below

References	
1	Ambrosini L, Mercer JFB (1999) Defective copper-induced trafficking and localization of the Menkes protein in patients with mild and copper-treated classical Menkes disease. Hum Mol Genet 8: 1547-1555.
2	Barton NW, Dambrosia JM, Barranger JA (1983) Menkes' kinky hair syndrome: report of a case in a female infant. Neurology 33 (Suppl 2), 154.
3	Beck J, Enders H, Schliephacke M, Buchwald-Saal M, Tumer Z (1994) X;1 translocation in a female Menkes patient: characterization by FISH. Clin Genet 46: 295-298.
4	Dagenais SL, Adam AN, Innis JW and Glover TW (2001) A novel frameshift mutation in exon 23 of ATP7A results in occipital horn syndrome and not in Menkes disease. Am J Hum Genet 69: 420-427.
5	Das S, Levinson B, Whitney S, Vulpe C, Packman S, Gitschier J (1994) Diverse mutations in patients with Menkes disease often lead to exon skipping. Am J Hum Genet 55: 883-889.
6	Das S, Levinson B, Vulpe C, Whitney S, Gitschier J, Packman S (1995) Similar splicing mutations of the Menkes/mottled copper-transporting ATPase gene in occipital horn syndrome and the blotchy mouse. Am J Hum Genet 56: 570-576.
7	Gu YH, Kodam H, Murata Y, Mochizuki D, Tanagawa Y, Ushijima H, Shiba T, Lee CC (2001) ATP7A gene mutations in 16 patients with Menkes disease and a patients with occipital horn syndrome. Am J Med Genet 99:217-222.
8	Hahn S, Cho K, Ryu K, Kim J, Pai K, Kim M, Park H, Yoo O. (2001) Identification of four novel mutations in classical Menkes diseas and successful prenatal DNA diagnosis. Molecular Genetics and Metabolism 73: 86-90.
9	Kaler SG, Gallo LK, Proud VK, Percy AK, Mark Y, Segal NA, Goldstein DS, Holmes CS, Gahl WA (1994) Occipital horn syndrome and a mild Menkes phenotype associated with splice site mutations at the MNK locus. Nat Genet 8: 195-202.
10	Kaler SG, Buist NRM, Holmes CS, Goldstein DS, Miller RC, Gahl WA (1995) Early copper therapy in classic Menkes disease patients with a novel splicing mutation. Ann Neurol 38: 921-928.
11	Kaler SG, Das S, Levinson B, Goldstein DS, Holmes CS, Patronas NJ, Packman S, Gahl WA 1996) Successful early copper therapy in Menkes disease associated with a mutant transcript containing a small in-frame deletion. Biochemical and Molecular Medicine 57: 37-46.
12	Kapur S, Higgins JV, Delp K, Rogers B (1987) Menkes syndrome in a girl with X-autosome translocation. Am J Med Genet 26: 503-510.
13	Levinson B, Packman S, Gitschier J (1997) Mutation analysis of mottled pewter. Mouse Genome 95:163-165.
14	Levinson B, Packman S, Gitschier J (1997) Deletion of the promoter region of the Atp7a gene of the mottled dapplied mouse. Nat Genet 16:223-224.

15	Levinson B, Conant R, Schnur R, Das S, Packman S, Gitschier J (1996) A repeated element in the regulatory region of the MNK gene and its deletion in a patients with occipital horn syndrome. Hum Mol Genet 5:1737-1742.
16	Levinson B, Gitschier J, Vulpe C, Whitney S, Yang S, Packman S (1993) Are X-linked cutis laxa and Menkes disease allelic? Nat Genet 3:6.
17	Mak BS, Chi CS and Tsai CR (2002) Menkes gene study in the Chinese population. J Child Neurol 17(4): 250-2.
18	Moller LB, Tumer Z, Lund C, Petersen C, Cole T, Hanusch R, Seidel J, Jensen LR, Horn N (2000) Similar splice-site mutations of the ATP7A gene lead to different phenotypes: classical Menkes disease or occipital horn syndrome. Am J Hum Genet 66:1211-1220.
19	Ogawa A, Yamamoto, S, Takayanagi M, Kogo T, Kanazawa M, Kohno Y. (1999) Identification of the three novel mutations in the MNK gene in three unrelated Japanese patients with classical Menkes disease. J Hum Genet 44:206-209.
20	Ogawa A, Yamamoto S, Kanazawa M, Ogawa E, Takayangi M, Hasegawa S, Kohno Y. (2000) Novel mutation of L718X in the ATP7A gene in a Japanese patients with classical Menkes disease, and four novel polymorphisms in the Japanese population. J Hum Genet 45: 315-317.
21	Ozawa H, Kodama H, Murata Y, Takashima S, Noma S. (2001) Transient temporal lobe changes and a novel mutation in a patient with Menkes disease. Pediatrics International 43: 437-440.
22	Qi M, Byers PH (1998) Constitutive skipping of alternatively spliced exon 10 in ATP7A gene abolishes Golgi localization of the Menkes protein and produces the occipital horn syndrome. Hum Mol Genet 7: 465-469.
23	Ronce N, Moizard MP, Robb L, Toutain A, Villard L, Moraine C (1997) A C2055T transition in exon 8 of the ATP7A gene is associated with exon skipping in an occipital horn syndrome family. Am J Hum Genet 61: 233-238.
24	Tumer Z, Tommerup N, Kreuder J, Craig IW, Horn N (1992) Mapping of the Menkes locus to Xq13.3-q21.2. Hum Genet 88: 668-672.
25	Tumer Z, Tonnesen T, Bohmann J, Marg W, Horn N (1994) First trimester prenatal diagnosis of Menkes disease by DNA analysis. J Med Genet 31:615-517.
26	Tumer Z, Tonnesen T, Horn N. (1994) Detection of genetic defects in Menkes disease by direct mutation analysis and its implication in carrier diagnosis. J Inher Metab Dis 17: 267-270.
27	Tumer Z, Horn N, Tonnesen T, Christodoulou J, Clarke JTR, Sarkar B (1996) Early copper-histidine treatment for Menkes disease. Nat Genet 12: 11-13.
28	Tumer Z, Lund C, Tolshave J, Vural B, Tonnesen T, Horn N. (1997) Identification of point mutations in 41 unrelated patients affected with Menkes disease. Am J Hum Genet 60:63-71.